UNIVERSITY OF CALIFORNIA, MERCED

The role of erosion in soil organic matter and pyrogenic carbon dynamics in fire-prone temperate forests

A dissertation submitted in partial satisfaction of the requirements for the degree Doctor of Philosophy

in

Environmental Systems

by

Rebecca Brianne Abney

Committee in charge:

Asmeret Asefaw Berhe, Chair
Stephen C. Hart
Marilyn L. Fogel
Jonathan Sanderman

2017

The Dissertation of Rebecca Brianne Abney is approved, and it is acceptable in quality and form for publication on microfilm and electronically:

Asmeret Asefaw Berhe, Chair

Marilyn L. Fogel

Stephen C. Hart

Jonathan Sanderman

University of California, Merced

2017

TABLE OF CONTENTS

LIST OF FIGURES

LIST OF TABLES

ACKNOWLEDGEMENTS

I gratefully acknowledge the numerous people that made this work possible. I thank Emma McCorkle, Jim Mendez-Lopez, Louis Mielke, and members of the Berhe lab for assistance with fieldwork. Lauren Austin, Timothy Kuhn, Alicia Sherrin, and other National Park Service assisted with fieldwork during the Rim Fire. I am also grateful for assistance with labwork from David Araiza, Christina Bradley, Elizabeth Williams, Bobby Nakamoto, Stephen Hart, and Fernanda Santos.

I would like to thank Fernanda Santos, Stephen Hart, Marilyn Fogel, Jonathan Sanderman, Asmeret Asefaw Berhe, and Carrie Masiello for comments on earlier drafts of this work. Numerous co-authors also assisted with direction of this research, including Timothy Kuhn, Marilyn Fogel, Alex Chow, Dale Johnson, Jonathan Sanderman, Lixia Jin, and William Hockaday.

This work was funded by the UC Merced School of Natural Science, a National Science Foundation award (CAREER EAR - 1352627) and National Park Service (Cooperative agreement no. P14AC00760) grants awarded to A. A. Berhe. Funding for this research was also provided by the Schools of Engineering and Natural Sciences at UC Merced and through the Environmental Systems graduate program.

I would like to thank my committee, Marilyn Fogel, Stephen Hart, and Jonathan Sanderman, for guiding this research and serving as mentors. I would also like to express gratitude to my adviser, Asmeret Asefaw Berhe, without whom this research would not be possible. Asmeret provided boundless guidance and advice throughout my tenure as a graduate student in areas of research, teaching, academia, and life.

CURRICULUM VITAE

REBECCA ABNEY

University of California, Merced

5200 N Lake Rd, Merced, CA 95340

rlever@ucmerced.edu

EDUCATION

University of California, Merced: Ph.D. in Environmental Systems

Adviser: Associate Professor Asmeret Asefaw Berhe 2012-2017

Committee: Marilyn Fogel, Stephen Hart, Jonathan Sanderman

University of St Andrews: B.Sc. Joint Honours

Environmental Biology and Physical Geography 2008-2012

PUBLICATIONS (previously published under name R. Lever)

Abney, R., Berhe, A.A. (*In revision)* Erosional distribution of pyrogenic carbon: implications for persistence of pyrogenic carbon in the soil system. Submission to *Biogeochemistry*.

Oliver, V., Oliveras, I., **Lever, R.,** Kala, J, Teh, Y. (*Accepted).* No long-term effect of land-use activities on soil carbon dynamics in tropical grassland. Submission to *Biogeosciences*.

Berhe, A.A., Kaiser, M., Arnold, C., **Lever, R.,** Jin, L. *(Accepted)* Carbon Dynamics. Submission to *Oxford Bibliographies*.

Berhe, A. A., Arnold, C., Stacy, E., **Lever, R**., McCorkle, E. & Araya, S. N. (2014) Soil erosion controls on biogeochemical cycling of carbon and nitrogen. *Nature Education Knowledge*. 5(8):2.

Johnson, J., **Lever**, **R.,** Storm, J. (2011) *Small Mammal Community Structure in Urban Greenways. USC Upstate Undergraduate Research Journal. (4): 19-22.*

Manuscripts in preparation

Abney, R., Sanderman, J., Johnson, D., Berhe, A.A. *(Expected submission August 2017)* Wildfire and post-fire erosion in mountainous terrain leads to rapid and major

redistribution of soil organic carbon fractions. Frontiers in Earth Science, section Biogeoscience.

Abney, R., Hockaday, W., Fogel, M., Kuhn, T., Austin, L., Sherrin, A., Berhe, A.A. *(Expected mid 2017).* Alterations to soil and eroded sediment carbon after the Rim Fire, Yosemite National Park.

Abney, R., Jin, L., Berhe, A.A. (*Expected 2017*) The role of combustion temperature and landform position in controlling the decomposition of pyrogenic organic matter.

CONFERENCE PRESENTATIONS

Abney, R. and A.A. Berhe. Landform Position and Combustion Temperature as Controls of Decomposition of Pyrogenic Organic Matter. American Geophysical Unional Annual Meeting (Oral presentation – December 2016).

Abney, R., Hockaday, W., Kuhn, T., Austin, L., Sherrin, A., and A.A. Berhe. Erosional Transport of Organic Matter after the Rim Fire, Yosemite National Park. Goldschmidt conference 2016. Yokohama, Japan.

Lever, R., Hockaday, W., Fogel, M., Kuhn, T., Austin, L., Sherrin, A., Berhe, A.A. Alterations to soil and eroded sediment carbon after the Rim Fire, Yosemite National Park. American Geophysical Union Annual Meeting (Oral presentation - December 2015).

Lever, R., Hockaday, W., Kuhn, T., Austin, L., Berhe, A.A. Lateral mobilization of soil and soil organic matter after the Rim Fire, Yosemite National Park. Critical Zone Science, Sustainability, and Services in a Changing World. (Oral presentation - October 2015).

Oliver, V., Kala, J., **Lever**, **R.,** Teh, Y.A. Turnover and storage of soil organic carbon from different land uses on an elevation gradient in the Peruvian Andes. European Geophysical Union Annual Meeting (April 2015).

Lever, R., Kuhn, T., Austin, L., Berhe, A.A. Mobilization of carbon and organic matter after the Rim Fire, Yosemite National Park. American Geophysical Union Annual Meeting (Poster presentation - December 2014).

Lever, R., Sanderman, J., Johnson, D., Berhe, A.A. A chronosequence of soil organic carbon fractions at the Gondola Fire using mid-infrared spectroscopy. Soil Science Society of America Annual Meeting (Poster presentation - November 2014).

Lever, R., Sanderman, J., Johnson, D., Berhe, A.A. A chronosequence of soil organic carbon fractions at the Gondola Fire using mid-infrared spectroscopy. Soil Organic Matter Workshop (Poster presentation - October 2014).

Lever, R., Sanderman, J., Johnson, D., Berhe, A.A. Characterization of soil organic matter fractions in fire-affected hillslopes using mid-infrared spectroscopy. Ecological Society of America General Meeting (Poster presentation - August 2014).

Lever, R., Sanderman, J., Johnson, D., Berhe, A.A. Quantifying organic carbon fluxes in eroding hillslopes through MIR spectroscopy. American Geophysical Union Annual Meeting (Poster presentation - December 2013).

Oliver, V., Kala, J., **Lever**, **R.,** Teh, Y.A. Effects of different land-uses on soil organic carbon pools in the Peruvian tropical forests. American Geophysical Union Annual Meeting (December 2013).

Lever, R., Berhe., A.A. Quantifying pyrogenic carbon fluxes and mean residence time in eroding hillslopes. AGU Chapman Conference on Soil-mediated Drivers of Coupled Biogeochemical and Hydrological Processes (Poster presentation – October 2013).

AWARDS AND HONORS

School of Engineering and Graduate division dissertation fellowship, 2017: **$6000**

ES Travel Award, 2016: **$250**

ES Travel Award, 2015: **$300**

ES Bobcat Fellowship award, 2014: **$7,500**

ES Graduate Program Fellowship Award, 2013: **$10,000**

AGU Chapman Conference on Soil-mediated Drivers of Coupled Biogeochemical and Hydrological Processes Across Scales, 2013: **$1,000**

TEACHING EXPERIENCE

UC Merced Teaching Assistant

Contemporary Biology Laboratory (BIO 001L)	2012; 2013; 2015; 2016
Earth Resources and Society (ESS10)	2013
Soil Science (ESS170L/ES292 30L)	2015; 2016
Contemporary Biology (BIO 001)	2015

UC Merced Grader

Biogeochemistry (ESS105/ES205)	2014

Teaching preparation

UC Merced Assessment as Pedagogy and Planning Project	2015

Guest lectures

Fundamentals of soil science (ESS 170)	2015, 2016
Critical zone science (ESS 192)	2016

PROFESSIONAL AFFLIATIONS

American Geophysical Union
Soil Science Society of America
Ecological Society of America
Earth Science Women's Network
Women in Science, Technology, Engineering, and Math

PROFESSIONAL SERVICE

Peer reviewer for journals:
Forest Ecology and Management
Journal of Soils and Sediments

SERVICE POSITIONS and VOLUNTEER WORK

Presented a workshop and lead a field trip at the Central Region Road Show on using the effects of fire and erosion on soil to teach chemistry basics	2016
Environmental Systems graduate student representative	2014-16
Mentored a high school student volunteering in the Berhe Biogeochemistry lab	2016
Volunteered to put on a workshop on basic soil science for high school students from Mariposa High School	2015
Mentored two Research Experiences for Undergraduate (REU) students	2014

ABSTRACT

Wildfire and erosion are major perturbations to the global carbon cycle in dynamic, fire-affected ecosystems around the world, including temperate forest ecosystems in the Sierra Nevada. As a byproduct of fires, pyrogenic carbon (PyC) is formed due to incomplete combustion of biomass. PyC constitutes an important component of the soil carbon pool and has been noted for its long residence time in soil and its susceptibility to erosion. As part of my dissertation research, I determined the rate of PyC, bulk soil carbon, and other soil constituents erosion after two wildfires: the Gondola Fire that occurred in South Lake Tahoe in 2002, and the Rim Fire that affected parts of Yosemite National Park in 2013. I found significant and preferential erosion of PyC, and vertical mobilization of PyC down into the soil profile after the fires. The preferential erosion of PyC, and overall quality of the soil and eroded sediments were controlled by burn severity, with PyC from higher burn severity sites being more preferentially eroded. To assess the fate of PyC post-fire in dynamic landscapes, I incubated chars formed at different temperatures in soils from eroding and depositional landform positions. Both charring temperature and landform position played significant roles in controlling soil respiration, with the lower temperature chars and the soil from the depositional landform position having much higher respiration than higher temperature chars and the soil from the eroding landform position. The difference in breakdown rates of PyC in soil from different landform positions demonstrates the importance of considering landform position as a control on PyC persistence in soil and that the interaction between charring temperature and landform position plays a significant role in the persistence of PyC. The post-fire erosional transport of PyC may act in a feedback to enhance or decrease overall PyC and bulk carbon stocks in soil. In a modeling exercise, I showed that explicit consideration for erosional loss (from eroding slope positions) and depositional gain (in lower-lying depositional landform positions) of PyC in soil can have its mean residence time in soil. I found that ignoring the role of erosional lateral distribution on PyC dynamics can introduce error in estimated turnover times of up to 150 years. Among the major accomplishments of my dissertation project include the realistic integration of biogeochemical and geomorphological approaches to derive improved representation of mechanisms that regulate soil carbon persistence in dynamic landscapes that routinely experience more than one perturbation. Findings from my dissertation research will have far reaching implications for improving our understanding of fate of terrestrial carbon after it enters streams and other aquatic systems. Furthermore, results of this project will play important role in establishing how the interaction of fire and erosion will play out under anticipated climate change scenarios, and the implications of these interactions on biogeochemical cycling of essential elements in a warmer world with intensified hydrologic cycle.

CHAPTER 1: INTRODUCTION

Globally, the soil system stores more carbon (C) than the atmosphere and the terrestrial biosphere combined and serves as an important sink for atmospheric carbon dioxide (Lal 2003, Lal 2004, Post & Kwon 2000). Soil C storage can contribute to mitigation of anthropogenic climate change, if the C is stabilized in the soil faster than the rate at which it is released back into the atmosphere (Powlson *et al.* 2011). A range of natural and anthropogenic perturbations can stabilize or destabilize this soil C, leading to further storage or release of soil C to the atmosphere, respectively. Fire and erosion are two important perturbations that can have both independent and interactive effects on organic matter (OM) persistence and stabilization in soil (Boot *et al.* 2015, Liang *et al.* 2010, Rumpel *et al.* 2009). Furthermore, fire and erosion are important controls on numerous environmental processes and ecosystem services that human beings depend on, including food production and provision of adequate and good-quality water (Beadle 1940, Worley 1933).

BACKGROUND

Fire

Fire is a common, widespread phenomenon in many ecosystems around the world. In the United States alone, over 150,000 fires were reported in 2016, burning over nine million acres of land (National Interagency Fire Center 2016). Globally, wildfires lead to the release of up to 4.1 Pg C yr^{-1} to the atmosphere in the form of CO_2, with an additional 0.05 to 0.2 Pg C yr^{-1} added to the soil as pyrogenic carbon (Sing *et al.* 2011). Pyrogenic carbon (PyC) is an important byproduct of fire that includes a spectrum of combustion and pyrolysis products, which have a wide range of chemical and physical properties (ranging from slightly charred biomass to ash or soot) largely depending on the conditions of combustion (Masiello 2004, Massman *et al.* 2010). The amount and nature of PyC produced by fires is controlled by the combustion temperature, duration, oxygen availability, soil moisture, and intensity of the fire (Bird *et al.* 2015). Together, these factors, along with available fuel load, control the depth at which heat can penetrate the soil (Certini 2005, Neary *et al.* 1999), which further controls the quality and quantity of SOM left behind (González-Pérez *et al.* 2004). Fire also alters SOM in several ways, including: increase in soil pH and volatization and breakdown of inorganic nutrients (e.g., P, N, S, and K) that are important for primary production (Czimczik *et al.* 2003, Massman *et al.* 2010), decrease in solubility of SOM (Abiven *et al.* 2011), increase in cation exchange capacity and specific surface area (Liang *et al.* 2006), and changes in chemical structures, such as higher aromaticity of sugars and lipids and reduced chain lengths of fatty acids, alcohols, and other alkyl compounds (González-Pérez *et al.* 2004).

The heating of soil, combustion loss of SOM, and input of PyC to can lead to major changes in soil nutrient cycling and other soil properties (Johnson *et al.* 1998, Johnson *et al.* 2007). Input of PyC in the soil can lead to important changes in soil physical and chemical conditions, as PyC tends to be reactive and has decades to centuries longer mean residence times in soil than non-pyrogenic forms of C, making it significant for C sequestration (Hammes *et al.* 2008, Kuzyakov *et al.* 2009). In addition, depending on the intensity of fire, there could be important effects on cycling of other essential elements (Cleveland &

Liptzin 2007, McGroddy *et al.* 2004, Schlesinger 2004). For example, high intensity wildfires can result in loss of more nitrogen (N) compared to C, leading to changes in nutrient availability in soil (Johnson *et al.* 2007). At lower fire temperatures (<150°C), pyrogenic compounds tend to be enriched in N, although this pyrogenic N is more susceptible to oxidative losses than PyC (Knicker 2010). The ability of the soil system to retain both C and N post-fire in part determines ecosystem productivity and services, including C sequestration. Much of the current understanding of the long-term implications of fire and addition of PyC to soil is derived from examining the *Terra Preta* soils of the Amazon, which received historical anthropogenic inputs of charred material and nutrients and are now among the most fertile and productive anthropogenic soils globally (Lehmann *et al.* 2003, Novotny *et al.* 2009). Our understanding of PyC dynamics in systems that are very different than the Brazilian Amazon (such as upland temperate forest ecosystems in the Sierra Nevada) is critical to determine how and why fires, and the associated input of PyC, are likely to affect persistence of C in the global soil system.

Erosion and sediment transport

Erosion is a widespread, global phenomenon that redistributes on the order of 75 Gt of soil and 1-5 Gt soil organic carbon (SOC) annually (Battin *et al.* 2009, Berhe *et al.* 2007, Regnier *et al.* 2013, Stallard 1998). It plays an important role in the development (or lack thereof) of soil (Jenny 1941), since soil thickness at any landform position is a balance between production of soil from bedrock and loss and input of soil through the processes of erosion and deposition, respectively. In upland eroding landform positions, such as crest or backslope positions), erosion leads to a loss of SOM through direct removal of topsoil. However, about 70-90% of this eroded topsoil material is redistributed downhill or downstream and is not exported out of the source watershed (Gregorich *et al.* 1998, Lal 2003, Rumpel *et al.* 2006). In bulk, this eroded material, or sediment, is often reflective of the drivers of the erosion processes mobilizing that material, such as runoff, snowmelt, or wind. Both the source of eroded material, such as upland soil compared with litter, and the type of erosion process, such as rill vs. interrill, act as controls of the quality of material and OM transported (Kattelmann 1997, Schiettecatte *et al.* 2008). Currently, there is some evidence indicating that PyC is preferentially transported via erosion (Rumpel *et al.* 2009, Rumpel *et al.* 2006) and accumulates in depositional positions such as alluvial or colluvial plains (Chaopricha & Marín-Spiotta 2014, Marin-Spiotta *et al.* 2014). Once in these downslope depositional landform positions, the original topsoil becomes buried by successive mass movement events, which can further promote long-term SOM (or PyC) stability (Berhe & Kleber 2013). Also, this eroded and buried SOM can enter into new and reconfigured physical and/or chemical associations with soil minerals that may enhance its stability through SOM protection mechanisms that may include aggregation and chemical bonding, including electrostatic attraction or complexation reactions (Berhe *et al.* 2012, Sharpley 1985).

Globally, the processes of soil erosion and terrestrial sedimentation can lead to a net terrestrial sink of atmospheric carbon dioxide. The magnitude of the erosion induced terrestrial C sink is estimated to be 0.12 – 1.5 Gt C yr^{-1} (Berhe *et al.* 2007, Berhe *et al.*

2008, Harden *et al.* 1999, Stallard 1998, Van Oost *et al.* 2007). Soil erosion can lead to terrestrial sequestration due to at least partial replacement of eroded OM by production of new photosynthate and the stabilization of at least some of the eroded OM in depositional landform positions (Berhe *et al.* 2007). However, there is limited understanding of the role that fire plays in controlling the effect of erosion on soil carbon dynamics and sequestration.

Interactive effects of fire and erosion

Many fire-prone temperate forest ecosystems exist on sloping lands that experience enhanced rates of soil erosion, especially post-fire. In these ecosystems, fire contributes to increased rates of soil erosion due to increased soil hydrophobicity, which causes reduced rates of infiltration in near-surface soil layers (Carroll *et al.* 2007, Larsen *et al.* 2009). These increased rates of post-fire erosion are also attributed to losses of vegetation and leaf litter, which stabilize the soil and slow erosion losses (Johnson *et al.* 2007). The increase in erosion rates is also connected with increased runoff (2-5 times higher after the Rim Fire, in Yosemite National Park and Stanislaus National Forest), which will likely lead to increased sediment transport to streams, rivers, and nearby water bodies (Hill & Region 2013).

The timing of the interaction of these fire and erosion events is particularly important in the Sierra Nevada, where large and intense precipitation events, such as thunderstorms and hailstorms (e.g., thunderstorms and hailstorms) are somewhat regular (50% chance at the Rim Fire to occur within the first year, and 97% chance to occur within the five years post-fire) at the end of the summer dry season, when most fires occur (Hill & Region 2013). When thunderstorms do follow forest fires, these storms can result in large erosion events, including ash flows. These events mobilize a great deal of the charred material and topsoil to downslope depositional environments, like in the Gondola Fire, South Lake Tahoe (Carroll *et al.* 2007). The role of elevation in controlling precipitation type, e.g. rainfall or snow, is also a major control on the overall driving force for erosion (Renard *et al.* 1997).

Even though PyC may be preferentially transported (Rumpel *et al.* 2009, Rumpel *et al.* 2006), it is still unclear what the fate of the transported PyC will be in the depositional environments compared to the hillslope locations from where it originated. Understanding the interaction of these processes is critical for watershed and broader levels of accounting of C and the overall biogeochemical cycling of essential elements in post-fire ecosystems.

Persistence/stabilization and destabilization of SOM and PyC

Both bulk SOM and PyC are stabilized in soil through a combination of various environmental factors that control accessibility of the C to decomposer communities, their extracellular enzymes, oxygen, and water flow (Schmidt *et al.* 2011). Organic matter and PyC can be physically protected from loss through occlusion within soil aggregates, burial, sorption, or microclimatic conditions that are suboptimal for microbial communities (Brodowski *et al.* 2006). Chemical protection of both OM and PyC involves formation of bonds between OM (or PyC) with soil minerals via a number of different chemical processes such as adsorption, which can stabilize PyC over extended time scales (Czimczik & Masiello 2007, Torn *et al.* 1997). These stabilization mechanisms of PyC are

counteracted by a number of different loss processes, including decomposition (Kuzyakov *et al.* 2009), erosion (Rumpel *et al.* 2006), and leaching (Major *et al.* 2010). Erosion and fire very likely act as important fluxes for SOM and PyC in upland forests ecosystems (Johnson *et al.* 2007). The relative magnitude of bulk SOM and PyC losses versus inputs is likely to vary in different ecosystems based on climate, nature of vegetation cover, and nature of soil, among other environmental factors.

RESEARCH OBJECTIVES AND HYPOTHESES

The overall objectives of my dissertation work were to determine:

1. How erosion controls the quality of SOM and concentration of PyC in different types of geomorphic landform positions, slope gradations, and burn severities in fire-adapted ecosystems; and if PyC enrichment in eroded sediment impacts stability of SOM and PyC;
2. How OM and PyC in sediment and source soil change through post-fire recovery; and
3. How rates of oxidative decomposition of PyC in fire-adapted upland temperate forest ecosystems compare with erosion-driven losses.

The overarching hypothesis for this dissertation was:

The stability and transport of PyC and SOM in fire-prone temperate forests is a function of its erosional transport, location within a landscape, and its formation conditions.

This overarching hypothesis was divided into three hypotheses:

a. Soil organic matter is less decomposable when PyC is present, particularly where PyC concentration is high (depositional areas), because post-fire SOM will consist of more decomposition resistant compounds (e.g., aromatic, PyC compounds);
b. Pyrogenic C is preferentially enriched in eroded sediments, and will be found in higher concentrations at depositional landform positions compared to eroding slopes; and
c. Charring temperature of PyC controls its rate of microbial decomposition.

DISSERTATION CHAPTERS

This dissertation is split into the following four chapters:

Chapter 1: *Pyrogenic carbon erosion: implications for persistence of pyrogenic carbon in the soil system*

The first chapter is a review and synthesis of the PyC cycle in soil, with a focus on processes that lead to storage and stabilization of PyC in soil. Rates of PyC decay in field and laboratory studies are compared to assess how erosional distribution of topsoil post-fire affects turnover time of PyC. Additionally, I used a first-order decay model to examine the difference in PyC turnover time and stock in soil of eroding and depositional landform positions. The synthesis quantifies the magnitude of the error introduced into

determinations of PyC turnover rate by not accounting for the variability in erosion as a loss or gain process for PyC in soil.

Chapter 2: *Wildfire and post-fire erosion in mountainous terrain leads to rapid and major redistribution of soil organic carbon fractions*

The second chapter investigates the transport of soil organic C fractions after the Gondola Fire, South Lake Tahoe, California. Soil samples were collected form a burned eroding hillslope and a downslope depositional landform position before the fire, one-year post-fire, and ten-years post-fire. These soil samples were analyzed for distribution of organic C fractions, including PyC, to test the short- and long-term effects of fire and post-fire erosion on transport and storage of PyC and soil C. Additionally, this study investigates the transport of PyC and soil organic C fractions down into the soil profile due to leaching and vertical colloid mobilization.

Chapter 3: *Soil erosion controls pyrogenic carbon dynamics: the effect of fire severity and slope on pyrogenic carbon transport after the Rim Fire, Yosemite National Park*

The third chapter follows patterns of soil and PyC erosion after the Rim Fire, Yosemite National Park, California. Eroded sediments were collected in sediment fences after major precipitation events from immediately following the fire through the first spring, along with representative source soils. These samples were analyzed to investigate chemical differences between the eroded material and source soil. These analyses were also used to assess erosion rates of PyC and to investigate if C, N or PyC were preferentially eroded throughout the initial post-fire recovery.

Chapter 4: *Landform position and combustion temperature control decomposition of pyrogenic organic matter*

The fourth chapter examines the role of landform position and charring temperature on the breakdown of PyC. The PyC was made from charring bark at three different temperatures to simulate differing levels of combustion intensity. Soils were collected from eroding and depositional landform positions, and bark and soil were combined in a factorial design of bark and soil, and soil-only combinations. Microbial respiration from these treatment groups was monitored over a six-month incubation to determine decay rates of PyC. Microbial biomass was measured at four time points during the incubation to determine the role of microbial biomass in the breakdown of PyC. Additionally, concentrations of PyC were measured at the beginning and end of the incubation to confirm PyC decay rates. Respiration was fitted with one- and two-pool exponential models to determine the relative sizes, numbers, and decay constants of soil C pools.

SIGNIFICANCE

The data and knowledge generated from my dissertation research illustrates how fire, geomorphology of the landscape, and erosion control fate of PyC in soil over different timescales, from monthly to decadal, in temperate forest ecosystems. This work provides critical fills critical knowledge gaps on the persistence of PyC in the terrestrial ecosystem and how erosion can act as a control on the redistribution and long-term fate of PyC. Additionally, by assessing the role of burn severity on post-fire erosion of PyC, this work

will provide useful evidence for how fire conditions affect post-fire biogeochemical cycling of essential elements. This is particularly critical as fire regimes in the western US are projected to experience increasingly large and severe wildfires, such as the Gondola and Rim Fires (Westerling *et al.* 2006). Furthermore, the approaches and data from my dissertation research will provide more accurate C accounting for fire-prone landscapes. Improved C accounting is critical for understanding of the short- and long-term processes of C stabilization and may contribute to development of soil C models that more accurately represent the interactive effects of fire and erosion as important perturbations on the global C cycle.

REFERENCES

Abiven S, Hengartner P, Schneider MPW, Singh N, Schmidt MWI (2011) Pyrogenic carbon soluble fraction is larger and more aromatic in aged charcoal than in fresh charcoal. Soil Biology and Biochemistry 43(7): 1615-1617

Battin T, Luyssaert S, Kaplan L, Aufdenkampe A, Richter A, Tranvik L (2009) The boundless carbon cycle. 2(9): 598-600

Beadle N (1940) Soil temperatures during forest fires and their effect on the survival of vegetation. Journal of Ecology 28(1): 180-192

Berhe AA, Harden JW, Torn MS, Harte J (2008) Linking soil organic matter dynamics and erosion-induced terrestrial carbon sequestration at different landform positions. Journal of Geophysical Research-Biogeosciences 113: G4, DOI 10.1029/2008jg000751

Berhe AA, Harden JW, Torn MS, Kleber M, Burton SD, Harte. J (2012) Persistence of soil organic matter in eroding vs. depositional landform positions,. Journal of Geophysical Research-Biogeosciences doi:10.1029/2011JG001790:

Berhe AA, Harte J, Harden JW, Torn MS (2007) The Significance of Erosion-Induced Terrestrial Carbon Sink. BioScience 57(4): 337-346

Berhe AA, Kleber M (2013) Erosion, deposition, and the persistence of soil organic matter: mechanistic considerations and problems with terminology. Earth Surface Processes and Landforms 38(8): 908-912

Bird MI, Wynn JG, Saiz G, Wurster CM, McBeath A (2015) The pyrogenic carbon cycle. Annual Review of Earth and Planetary Sciences 43: 273-298

Boot C, Haddix M, Paustian K, Cotrufo M (2015) Distribution of black carbon in ponderosa pine forest floor and soils following the High Park wildfire. Biogeosciences 12(10): 3029-3039

Brodowski S, John B, Flessa H, Amelung W (2006) Aggregate-occluded black carbon in soil. European Journal of Soil Science 57(4): 539-546

Carroll EM, Miller WW, Johnson DW, Saito L, Qualls RG, Walker RF (2007) Spatial analysis of a large magnitude erosion event following a Sierran Wildfire. Journal of environmental quality 36(4): 1105-1105

Certini G (2005) Effects of fire on properties of forest soils: a review. Oecologia 143: 1-10

Chaopricha NT, Marín-Spiotta E (2014) Soil burial contributes to deep soil organic carbon storage. Soil Biology and Biochemistry 69: 251-264

Cleveland C, Liptzin D (2007) C: N: P stoichiometry in soil: is there a “Redfield ratio” for the microbial biomass? Biogeochemistry 85(3): 235-252

Czimczik C, Preston C, Schmidt M, Schulze E (2003) How surface fire in Siberian Scots pine forests affects soil organic carbon in the forest floor: Stocks, molecular structure, and conversion to black carbon (charcoal). Global Biogeochemical Cycles 17(1): doi:10.1029/2002GB001956

Czimczik CI, Masiello CA (2007) Controls on black carbon storage in soils. Global Biogeochemical Cycles 21(2): GB 3005

González-Pérez J, González-Vila F, Almendros G (2004) The effect of fire on soil organic matter—a review. Environment International 30(6): 855-870

Gregorich E, Greer K, Anderson D, Liang B (1998) Carbon distribution and losses: erosion and deposition effects. Soil Till Res 47(3-4): 291-302

Hammes K, Torn MS, Lapenas AG, Schmidt MWI (2008) Centennial black carbon turnover observed in a Russian steppe soil. Biogeosciences 5(5): 1339-1350

Harden JW, Sharpe JM, Parton WJ, Ojima DS, Fries TL, Huntington TG, Dabney SM (1999) Dynamic replacement and loss of soil carbon on eroding cropland. Global Biogeochemical Cycles 13(4): 885-901

Hill B, Region PS (2013) Burned Area Emergency Response Rim Fire Stanislaus National Forest Hydrology and Watershed Specialist Report September 24, 2013.

Jenny H (1941) Factors of Soil Formation: A System of Quantitative Pedology. McGraw-Hill, New York

Johnson D, Murphy J, Walker R, Glass D, MILLER W (2007) Wildfire effects on forest carbon and nutrient budgets. Ecological Engineering 31(3): 183-192

Johnson D, Susfalk R, Dahlgren R, Klopatek J (1998) Fire is more important than water for nitrogen fluxes in semi-arid forests. Environmental Science and Policy 1(2): 79-86

Kattelmann R (1997) Flooding from rain-on-snow events in the Sierra Nevada. IAHS Publications-Series of Proceedings and Reports-Intern Assoc Hydrological Sciences 239: 59-66

Knicker H (2010) “Black nitrogen”–an important fraction in determining the recalcitrance of charcoal. Organic Geochemistry 41(9): 947-950

Kuzyakov Y, Subbotina I, Chen H (2009) Black carbon decomposition and incorporation into soil microbial biomass estimated by C labeling. Soil Biology and Biochemistry 41(2): 210-219

Lal R (2003) Soil erosion and the global carbon budget. Environment International 29(4): 437-450

Lal R (2004) Soil carbon sequestration impacts on global climate change and food security. Science 304(5677): 1623-1627

Larsen I, Macdonald L, Brown E, Rough D, Welsh M, Pietraszek J, Libohova Z, De Dios Benavides-Solorio J, Schaffrath K (2009) Causes of Post-Fire Runoff and Erosion: Water Repellency, Cover, or Soil Sealing? Soil Science Society of America Journal 73(4): 1393

Lehmann J, Pereira da Silva J, Steiner C, Nehls T, Zech W, Glaser B (2003) Nutrient availability and leaching in an archaeological Anthrosol and a Ferralsol of the Central Amazon basin: fertilizer, manure and charcoal amendments. Plant and soil 249(2): 343–357-343–357

Liang B, Lehmann J, Sohi SP, Thies JE, O'neill B, Trujillo L, Gaunt J, Solomon D, Grossman J, Neves EG (2010) Black carbon affects the cycling of non-black carbon in soil. Organic Geochemistry 41(2): 206-213

Liang B, Lehmann J, Solomon D, Kinyangi J, Grossman J, O'Neill B, Skjemstad JO, Thies J, Luizao FJ, Petersen J, Neves EG (2006) Black carbon increases cation exchange capacity in soils. Soil Science Society of America Journal 70(5): 1719-1730

Major J, Lehmann J, Rondon M, Goodale C (2010) Fate of soil-applied black carbon: downward migration, leaching and soil respiration. Global Change Biology 16(4): 1366-1379

Marin-Spiotta E, Chaopricha NT, Plante AF, Diefendorf AF, Mueller CW, Grandy AS, 1–5. JAM (2014) Long-Term Stabilization of Deep Soil Carbon by Fire and Burial During Early Holocene Climate Change. Nature Geoscience:

Masiello C (2004) New directions in black carbon organic geochemistry. Marine Chemistry 92(1-4): 201-213

Massman WJ, Frank JM, Mooney SJ (2010) Advancing investigation and physical modeling of first-order fire effects on soils. Fire Ecology 6(1): 36-54

McGroddy M, Daufresne T, Hedin L (2004) Scaling of C: N: P stoichiometry in forests worldwide: implications of terrestrial Redfield-type ratios. Ecology 85(9): 2390-2401

National Interagency Fire Center (2016) National Report of Wildland Fires and Acres Burned by State. In: Center NIC (ed). vol 5/11/2017.

Neary D, Klopatek C, DeBano L, Ffolliott P (1999) Fire effects on belowground sustainability: a review and synthesis. Forest Ecology & Management 122: 51-71

Novotny EH, Hayes MH, Madari BE, Bonagamba TJ, Azevedo ERd, Souza AAd, Song G, Nogueira CM, Mangrich AS (2009) Lessons from the Terra Preta de Índios of the Amazon region for the utilisation of charcoal for soil amendment. Journal of the Brazilian Chemical Society 20(6): 1003-1010

Post WM, Kwon KC (2000) Soil carbon sequestration and land-use change: processes and potential. Global Change Biology 6(3): 317-327

Powlson D, Whitmore A, Goulding K (2011) Soil carbon sequestration to mitigate climate change: a critical re-examination to identify the true and the false. European Journal of Soil Science 62(1): 42-55

Regnier P, Friedlingstein P, Ciais P, Mackenzie FT, Gruber N, Janssens IA, Laruelle GG, Lauerwald R, Luyssaert S, Andersson AJ, Arndt S, Arnosti C, Borges AV, Dale AW, Gallego-Sala A, Godderis Y, Goossens N, Hartmann J, Heinze C, Ilyina T, Joos F, LaRowe DE, Leifeld J, Meysman FJR, Munhoven G, Raymond PA, Spahni R, Suntharalingam P, Thullner M (2013) Anthropogenic Perturbation of the Carbon Fluxes From Land to Ocean. Nature Geoscience 6(8): 597-607

Renard KG, Foster GR, Weesies G, McCool D, Yoder D (1997) Predicting soil erosion by water: a guide to conservation planning with the Revised Universal Soil Loss Equation (RUSLE). US Government Printing Office Washington, DC,

Rumpel C, Ba A, Darboux F, Chaplot V, Planchon O (2009) Erosion budget and process selectivity of black carbon at meter scale. Geoderma:

Rumpel C, Chaplot V, Planchon O, Bernadou J, Valentin C, Mariotti A (2006) Preferential erosion of black carbon on steep slopes with slash and burn agriculture. CATENA 65(1): 30-40

Schiettecatte W, Gabriels D, Cornelis W, Hofman G (2008) Enrichment of organic carbon in sediment transport by interrill and rill erosion processes. Soil Science Society of America Journal 72(1): 50-55

Schlesinger W (2004) Better living through biogeochemistry. Ecology 85(9): 2402-2407

Schmidt MWI, Torn MS, Abiven S, Dittmar T, Guggenberger G, Janssens IA, Kleber M, Kogel-Knabner I, Lehmann J, Manning DAC, Nannipieri P, Rasse DP, Weiner S, Trumbore SE (2011) Persistence of soil organic matter as an ecosystem property. Nature 478(7367): 49-56

Sharpley A (1985) The Selection Erosion of Plant Nutrients in Runoff. Soil Science Society of America Journal 49(6): 1527-1534

Sing N, Abiven S, Torn MS, Schmidt MWI (2011) Fire-derived organic carbon turnover in soils on a centennial scale. Biogeosciences discuss 8: 12179-12195

Stallard R (1998) Terrestrial sedimentation and the carbon cycle: Coupling weathering and erosion to carbon burial. Global Biogeochemical Cycles 12(2): 231-257

Torn M, TRUMBORE S, Chadwick O, Vitousek P, Hendricks D (1997) Mineral control of soil organic carbon storage and turnover. Nature 389(6647): 170-173

Van Oost K, Quine T, Govers G, De Gryze S, Six J, Harden J, Ritchie J, McCarty G, Heckrath G, Kosmas C (2007) The impact of agricultural soil erosion on the global carbon cycle. Science 318(5850): 626-629

Westerling AL, Hidalgo HG, Cayan DR, Swetnam TW (2006) Warming and earlier spring increase western US forest wildfire activity. Science 313(5789): 940-943

Worley F (1933) Forest fires in relation to soil fertility. Nature 131: 787-788

CHAPTER 2: PYROGENIC CARBON EROSION: IMPLICATION FOR PERSISTENCE OF PYROGENIC CARBON IN SOIL

ABSTRACT

Fire altered or pyrogenic carbon (PyC) constitutes an important pool of soil organic matter, particularly for its reactivity and long residence times in soil. Over the past several decades, research on the dynamics of PyC in the earth system has focused on quantifying stock and mean residence time of PyC in soil, as well as determining both PyC stabilization mechanisms and loss pathways. Much of the past research has focused on decomposition as the most important loss pathway for PyC from soil, and relatively little attention has been devoted to the role erosional redistribution and export play on persistence of PyC in a soil profile or catchment. Based on the density of PyC and its location on the soil surface after production, a significant proportion of the PyC that enters the soil system is likely laterally transported away from the site of production by wind and water erosion. However, so far, the role of erosional redistribution of PyC in controlling its dynamics in soil has not been fully explored. Here, we present a synthesis of available data and literature to compare the magnitude of erosional PyC flux with other important loss pathways of PyC from soil. Furthermore, we use a simple first-order model of soil PyC dynamics to determine the effect of erosion and deposition on residence time of PyC in eroding landscapes. The current estimates of PyC mean residence time (MRT) range from 250 to 660 years, and we find that ignoring the role of erosion can under- or over-estimate PyC MRT estimates by 150 years, depending on the specific landform positions and timescales considered. Erosion is an important PyC flux that should be considered in assessments of PyC residence time, stock, and cycling in the soil system.

INTRODUCTION

Fires and production of pyrogenic carbon

Fire is a major environmental perturbation and driver of biogeochemical processes across a diversity of landscapes worldwide. In the US alone, wildfires consume over 2.6 million hectares per year in over 74,000 wildfires (National Interagency Fire Center 2015). The amount and properties of organic matter (OM) left behind in soil post-fire are controlled by amount and composition of fuel, and duration and temperature of the fire (i.e., fire severity) (Pyle et al. 2015). Depending on burn severity, or the impact of the fire on the ecosystem, fires also control nutrient availability, water infiltration, soil pH (Certini 2005; Czimczik et al. 2003), and OM stocks and fluxes in soil (González-Pérez et al. 2004; Keeley 2009). Moreover, fires lead to formation of pyrogenic carbon (PyC) from the incomplete combustion of biomass and soil organic matter (SOM) (Masiello 2004; Preston & Schmidt 2006; Schmidt & Noack 2000).

A growing body of literature now demonstrates that PyC is a major component of the global C cycle (Bird et al. 2015; Lehmann et al. 2008; Preston 2009). PyC makes up 2.5-5% of global soil C (Bird et al. 2015; IPCC 2013) and up to 30% of soil C in some soils (Skjemstad et al. 1999; Skjemstad 1996), making it important not just for accounting of global soil C stocks but also for how the soil system plays important role in regulation of global climate (Lehmann et al. 2008). In soil, PyC has an overall longer mean residence time (MRT, centuries to millennia) compared with non-pyrogenically altered OM (decades to centuries) (Hammes et al. 2008; Lehmann et al. 2008). Current estimates of the MRT of PyC in the soil are considerably shorter than previously reported (on the order of millennia), as several studies have demonstrated that some PyC is degraded on shorter (months to years) time scales (Nguyen et al. 2009; Soucémarianadin et al. 2015b; Whitman et al. 2014). Recent observations have indicated that current estimates of PyC residence times may be inaccurate due to failures in accurately quantifying lateral redistribution of PyC in the terrestrial ecosystem and its riverine transfer to the ocean (Jaffé et al. 2013; Masiello & Louchouarn 2013; Rumpel et al. 2006).

Properties of pyrogenic carbon and its effect on burned soil

Fire properties and prevailing environmental conditions in the burned area dictate the effect of fires on soil, and its implications for post-fire soil erosion. During a fire, typically only the top few (2-5) centimeters of soil are directly and significantly impacted by the high temperatures (DeBano 2000). Combustion intensity (maximum temperature and duration of the combustion) at the soil surface plays an important role in determining what aboveground vegetation burns and the properties of the PyC formed during the fire (Pyle et al. 2015), where PyC formed at higher temperatures (above 350 ºC) can be more persistent in soil (DeBano et al. 1977; González-Pérez et al. 2004). Generally, high temperature PyC is smaller, lighter, and hence lower in density and potentially more susceptible to erosional transport than low temperature PyC.

Fire also changes the physical properties of soil with implications for lateral movement of water and PyC. Albalasmeh et al. (2013), for example, showed that low severity fires can have lasting impact on soil aggregate stability, potentially leading to destabilization of topsoil, loss of aggregate protected carbon (C), and increased erodibility of soil post-fires (Al-Hamdan et al. 2012; Johnson et al. 2007; Shakesby & Doerr 2006). Moreover, low to moderate temperature fires can lead to the formation of a hydrophobic layer, or increases in overall soil hydrophobicity, resulting in decreases in infiltration rates (DeBano 2000; Mataix-Solera et al. 2011; Shakesby & Doerr 2006). This decrease in infiltration and altered hydrologic flow paths though the soil matrix can lead to increases in overland flow (Hortonian flow, see Figure 1) and (Shakesby & Doerr 2006), along with loss of soil stabilizing vegetation, drive increased erosion rates and sediment export in fire-affected landscapes (Shakesby et al. 1993).

Uncertainties in the role of pyrogenic carbon in the global carbon cycle

One of the major challenges in quantifying PyC fluxes within the environment is that no single analytical technique can measure the entire PyC spectrum. Many different techniques (e.g., physical separation, nuclear magnetic resonance spectroscopy, mid-infrared spectroscopy, benzene polycarboxylic acid, mid-infrared spectroscopy and partial least squares regression) are currently being used to measure PyC concentration and composition (Cotrufo et al. 2016; De la Rosa et al. 2008; Gustafsson et al. 2001; Hammes et al. 2007; Masiello 2004; Preston & Schmidt 2006; Schmidt & Noack 2000; Wiedemeier et al. 2015; Wiedemeier et al. 2013), with varying degrees of accuracy for quantifying different types of compounds in the PyC spectrum (Hammes et al. 2007; Masiello 2004). Due to the variety of techniques currently used, and a lack of meaningful standardization methods for the different techniques, direct comparison of published results is extremely difficult. Many PyC-like, aromatic materials can be confounded with PyC in some of these techniques, further adding error to these analyses, along with some of them having varying degrees of sensitivity to aromatic condensation (Skjemstad et al. 1999). Hence, the data and arguments presented below are based on the most conservative results and least contradictory conclusions that we could draw from published literature.

Of the many techniques, available to determine concentration and quality of PyC in soil, ^{13}C Nuclear Magnetic Resonance (NMR) spectroscopy and benzene polycarboxylic acids (BPCA) have so far been among the most commonly used. Using these and other approaches, MRTs of PyC are derived by comparing changes in PyC concentrations through fire chronosequences or from long-term incubations. This approach of determining MRT of PyC is sensitive to source of PyC, environmental conditions under consideration, for example laboratory compared with field setting, climate variations, soil type, and water availability (Cheng et al. 2008; Nguyen et al. 2010). In other cases, PyC MRT is determined via radiocarbon dating in older samples to determine mean age of PyC within the soil C pool (Marín-Spiotta et al. 2014). The radiocarbon-based approach is expected to have less variability; but the accuracy of the data is highly dependent on the purity of the source of PyC, which depends on it not being mixed with modern C inputs or fossil fuel derived PyC. Furthermore, some of the variation in residence time estimates is likely caused by the heterogeneity of different materials in the combustion continuum, which may partition the

overall PyC pool into different pools cycling at different rates (Bird et al. 2015; Foereid et al. 2011).

PyC PERSISTENCE IN SOIL

Over the last couple of decades, our understanding of how PyC becomes stabilized in, or is lost from, the soil system has advanced considerably. In the following sections, we discuss historical and modern ideas about PyC persistence within soil, important mechanisms for stabilization and loss of PyC from the soil, and briefly cover methods used to calculate PyC MRT.

Historical perspective

Historically, PyC was thought to be a highly recalcitrant form of soil C that is inherently resistant to microbial decomposition. PyC's presumed 'chemical recalcitrance' was attributed to its chemical structure including large linkages of condensed aromatic structures (Skjemstad et al. 1999), as well as its apparent resistance to forming chemical associations with soil (Masiello 2004; Preston & Schmidt 2006; Schmidt & Noack 2000). This idea of chemical recalcitrance prevailed for decades, even though there was evidence for the breakdown of PyC from the beginning of the twentieth century (Potter 1908). This presumed inherent 'recalcitrance' of PyC was even used to support arguments that PyC storage in soil might be part of the ‘missing C sink’ because it seemed so environmentally stable (Lehmann 2007). At the same time, the ability of PyC to persist in the soil longer than non-PyC OM, has also contributed to the widespread research on the potential of PyC to serve as an agricultural amendment (i.e., biochar). The use of PyC as biochar has been demonstrated to have numerous beneficial effects including: increasing soil C stocks (i.e., improving a soil’s potential to sequester atmospheric CO_2) and improving soil productivity (Lehmann et al. 2008). However, recent works showed PyC can become decomposed or lost from soil rather quickly, over months to years (Nguyen et al. 2010; Zimmermann et al. 2012). There is now a major paradigm shift occurring in our understanding of PyC dynamics in the earth system. Figure 2 shows how published estimates of PyC MRT have changed over the last few decades.

Environmental controls on stability and stabilization mechanisms of PyC

PyC can become stabilized or lost from soil through similar processes that control the fate of bulk or non-PyC. Current estimates of PyC MRT range from weeks to months to millennia (Bird et al. 2015). Lehmann et al. (2008) suggested that PyC MRT in soil could range between 700-9000 years. However, other studies have argued that PyC has considerably shorter MRT in soil. For example, Hammes et al. (2008) found a PyC turnover time of 239 years in a Russian steppe site, and similarly, Boot et al. (2015) found a similar MRT for PyC of 300 years. Overall, laboratory incubation derived estimates of loss of PyC are typically higher (1.5-20% PyC mass loss per year) than field studies (0.08-15% PyC mass loss per year), even though field studies include other forms of loss other than microbial decomposition (e.g., erosion and leaching, Table 1). Much of the variation in field and laboratory studies is due to the range of different processes that control PyC persistence in soil. Below, we present discussion on the major physical and chemical stabilization mechanisms that are important for the persistence of PyC in the soil.

Chemical stabilization mechanisms

Charring of biomass has been associated with increasing pH, specific surface area (SSA), cation exchange capacity (CEC), and hydrophobicity, depending on fire temperature and duration (Certini 2005). In soil, similar increases occur in pH, SSA, and hydrophobicity with charring, however CEC of soil decreases due to OM losses and hydrophobic compounds breakdown at charring temperatures above approximately 250°C (Araya et al. 2016; Araya et al. 2017; Shakesby & Doerr 2006). These changes control the reactivity of PyC and its ability to be stabilized within the soil system (Certini 2005; Doerr & Cerdá 2005). PyC interacts with soil minerals in several ways that can potentially lead to its stabilization in soil, including sorption reactions as both the sorbent and sorbate, hydrophobic interactions with water, and redox reactions, but these reactions depend on the chemical structure of the PyC (Chia et al. 2012; Kupryianchyk et al. 2016).

The hydrophobic nature of PyC can make it more resistant to reacting with constituents in the soil-water solution, and the hydrophobic nature of PyC is controlled by both combustion intensity and fuel characteristics, with moderate combustion intensities having higher hydrophobicity (Kinney et al. 2012). With more hydrophobicity, sorption and electrostatic reactions are less favored, limiting the potential of soil minerals to provide stabilizing interactions with PyC that would increase its persistence in the soil.

Much of the prior research on the breakdown of PyC focused on the role of chemical changes (such as increased aromatization) in OM that can serve to inhibit microbial processing (Alexis et al. 2010; González-Pérez et al. 2004; Knicker et al. 2006; Preston & Schmidt 2006). This aromatization is controlled by charring temperature and duration, with higher temperatures and longer durations having more aromatization (Alexis et al. 2010).

Physical stabilization mechanisms

Aggregation and burial are major physical mechanisms for protection of OM and PyC, as the OM and PyC not only becomes entrapped, but also physically inaccessible for decomposition by microbes and other physical breakdown processes (Buurman & Roscoe 2011; Cusack et al. 2012; Nguyen et al. 2009). Several studies have found that PyC is preferentially stored in the aggregate protected soil C pool (Brodowski et al. 2006; Liang et al. 2008). Although there is evidence that prior to incorporation into aggregates, PyC is at least partially broken down (Mastrolonardo et al. 2015).

The stabilization of PyC can also occur through post-erosion burial of a fraction of the eroded PyC in depositional landform positions, similar to non-pyrogenic C (Berhe et al. 2007; Berhe & Kleber 2013; Doetterl et al. 2016). PyC-rich material eroded from hillslopes can get stabilized in deep soil layers of downhill or downstream depositional landform positions with repeated erosion/deposition events, especially if it is buried at >1 m depths, as was observed in char-rich Paleosols in Nebraska (Chaopricha & Marín-Spiotta 2014; Marín-Spiotta et al. 2014) and the sub-tropics of Brazil (Velasco-Molina et al. 2016). This deep-soil stabilization can also be driven by aeolian-derived deposits burying an existing soil (Chaopricha & Marín-Spiotta 2014; Marín-Spiotta et al. 2014), via anthropogenic burial (e.g., Terra Preta soils of the Amazon; (Glaser 2002; Glaser et al. 2000), or via charring of roots at depth during high intensity fires (Kyuma et al. 1985). The burial of

PyC reduces PyC exposure to microbes, air, and extracellular enzymes, which are major drivers of decomposition.

Loss pathways

Below, we discuss the major effluxes of PyC from soil and the interaction of erosion with these fluxes, including decomposition, chemical breakdown, erosion, leaching and vertical colloid mobilization, consumption in subsequent fires, and medium to long-range atmospheric transport (see Figure 3). Decomposition is a major loss pathway and is currently assumed to be responsible for most PyC loss from soil (Kuzyakov et al. 2009; Whitman et al. 2014). Erosion-driven loss of PyC has received less attention, but erosion plays a major role in the loss of PyC, especially immediately after fires or after application of biochar on soil (Rumpel et al. 2006). Leaching and transport within the soil matrix also play roles in the loss of PyC from soil, especially over decadal and longer timescales. There is evidence for bioturbation of PyC, where earthworms and small mammals can play a significant role in redistributing PyC laterally and vertically on the local scale (Eckmeier et al. 2007). Biomass burning leads to loss of pre-existing PyC, and non-consumed particulate PyC is deposited elsewhere via wind erosion (Bird et al. 2015; Gustafsson et al. 2009). Consumption of PyC in subsequent fires is generally a relatively small loss flux of PyC, as a high intensity repeat fire is not likely to occur within short time span in the same area, whereas the other loss processes begin immediately after a fire event or intentional addition of PyC/biochar to soil (Tinkham et al. 2016).

Decomposition, mineralization, and associated transformations

The decomposition and breakdown of PyC follows the same general mechanisms as non-pyrogenic C. This breakdown includes physical, microbial, and chemical processes (Ascough et al. 2011; Cheng et al. 2006; Major et al. 2010). Complex interactions of environmental factors lead to predictable relationships between PyC decay rate with climate. Notably, Cheng et al. (2008) found that decomposition of non-PyC typically increases with increasing soil temperatures, but with addition of PyC, the amount respired related to total carbon was much less than from soils without PyC additions, which they attribute to the environmental stability of PyC. Jauss et al. (2015) also found higher concentrations of PyC and non-pyrogenic C in sites that have wetter and cooler climate conditions. Generally, studies have reported higher decomposition rates of PyC in warmer climates (see Table 1 for summary).

The effect of nutrient availability on microbial community abundance and composition also influences the rate of PyC decomposition (Baumann et al. 2009). Variation in environmental (or laboratory) conditions controlling PyC decomposition leads to a large range in the measured decomposition rate – with several orders of magnitude of difference in decomposition rates in laboratory experiments alone (see Table 1). This difference is related to the type of PyC precursor material (woody vs. non-woody), incubation temperature, and soil moisture, among other conditions. Laboratory experiments also generally have near optimal conditions for microbial decomposition, whereas field conditions are suboptimal for microbial decomposition due to fluctuations in temperature

and moisture, which drives the much lower decomposition rates reported from these studies.

Microbial processes

Incubation studies using ^{14}C-labeled PyC and CO_2 evolution have provided evidence of microbial utilization and mineralization of PyC (Kuzyakov et al. 2009; Santos et al. 2012; Whitman et al. 2014; Zimmermann et al. 2012). The rate of PyC decomposition reported in laboratory studies ranges from <1% to over 20% of PyC decomposed per year (Hatten & Zabowski 2009; Zimmerman 2010).

While the majority of studies have focused on aerobic decomposition, Knoblauch et al. (2011) showed that PyC decomposition was approximately twice as fast under anaerobic conditions compared with aerobic conditions, potentially due to low oxygen availability. In contrast, Nguyen and Lehmann (2009) found that PyC produced from oak and corn had consistently lower rates of decomposition under saturated conditions compared with unsaturated (but not water limited) or alternating saturated and unsaturated conditions, which was related to oxygen availability and birch effects in the alternating saturated and unsaturated condition (Birch 1958). In eroding landscapes, different landform positions (e.g., depositional or eroding) can have widely varying soil water conditions, including water content and hydraulic conductivity, with significant implications for rate of microbial decomposition of PyC.

Chemical breakdown

Numerous chemical processes are capable of breaking down PyC, including oxidation reactions (Shneour 1966), surface reactions mediated by dominant functional groups of the PyC (Adams et al. 1988; Cheng et al. 2006; Hockaday et al. 2006; Smith & Chughtai 1996), intra-surface breakdown (Zimmerman 2010), and dissolution (Abiven et al. 2011; Czimczik & Masiello 2007). The major oxidation reactions in PyC occur at its surface and involve the loss of CO_2 and H_2O, but these reactions can also include losses of O_2 or CO (Shneour 1966; Smith & Chughtai 1996). The surface or edges of PyC may have charged species that can react with chemical species in the outer zone of the PyC's surface to form oxidized functional groups (Shneour 1966). Over time, chemical reactions can cause the breakdown of inter-surface sites in PyC (Zimmerman 2010). If this breakdown process continues, PyC can take up and retain more water, even from humid air (Adams et al. 1988), which may further increase decomposition. An incubation by Cheng et al. (2006) that compared decomposition of PyC with and without microbial inoculation demonstrated the significant role of abiotic reactions in the breakdown of PyC, although the rates of abiotic breakdown are generally more than half that of microbially driven decomposition (Zimmerman 2010). Such findings suggest that decomposition rates are controlled by environmental and hydrological conditions, which are likely controlled by landform position in dynamic eroding landscapes.

Photooxidation

In addition to reacting with chemical constituents of the soil, PyC is also decomposed via photooxidation, or the breakdown of SOM and PyC under ultraviolet (UV) light with the

presence of oxygen (Goldberg 1985). Photooxidation plays an important role in the breakdown of polycyclic aromatic hydrocarbons (PAHs), which are byproducts of combustion and an important part of the PyC continuum, in addition to the breakdown of litter and bulk soil C (Kamens et al. 1989; Lin & King 2014; Schmidt et al. 2002). When OM is dissolved, photooxidation can play a more important role in its breakdown than microbial processes (Amon & Benner 1996).

Photooxidation is limited by the exposure to light and the properties of the chemical species present (Brandt et al. 2007). However, photooxidation is likely an important process in the breakdown of PyC for several reasons. Firstly, char is mainly produced on the surface of a soil, which experiences a high level of light exposure, particularly after a high intensity fire that consumed much of the aboveground biomass. Secondly, erosion deposits PyC in rivers (Jaffé et al. 2013) and oceans (Masiello & Louchouarn 2013), where the low density of PyC may cause it to float, leaving it more susceptible to photooxidation due to higher levels of UV light at the surface of water bodies.

Erosion

Interest in the role of erosion on soil C dynamics and biogeochemical cycling of essential elements has increased over the last two decades, in particular the potential for erosion to constitute a net sink for atmospheric CO_2, on the order of 0.12 - 1.5 GtC y^{-1} (Battin et al. 2009; Berhe et al. 2007; Doetterl et al. 2016; Lal 2003; Regnier et al. 2013; Stallard 1998). In upland, eroding landform positions (shoulder positions), erosion leads to losses of soil organic matter (SOM) through direct removal of soil mass (Berhe 2012; Berhe et al. 2008; Harden et al. 2008; McCorkle et al. 2016; Nadeu et al. 2012; Stacy et al. 2015). About 70-90% of the eroded topsoil material is redistributed downhill or downstream, and this material is not exported out of the source watersheds but instead is deposited in toeslope and footslope landform positions (Gregorich et al. 1998; Lal 2003; Stallard 1998). Erosion leads to stabilization of at least some of the eroded SOM in depositional landforms through new and reconfigured associations of the eroded SOM with soil minerals (Berhe 2012; Berhe & Kleber 2013; Lal 2003; Lal 2004; Sharpley 1985).

Eroding material is exposed to breakdown mechanisms during the transport phase of erosion, and for non-pyrogenic C, over 20% of the OM transported from eroding landform positions is assumed to be lost via oxidative decomposition during or after transport (Jacinthe & Lal 2001). Erosion is a particularly important flux for PyC in soil when it stays on surface layers (Rumpel et al. 2006) at least on the order of months, if not longer (Boot et al. 2015; Faria et al. 2015), because this leaves PyC vulnerable to weathering forces of wind and water.

Fire increases the susceptibility of soils, particularly surface soils, to erosion by changing soil physical and chemical properties (Bowman et al. 2009). For example, the development of hydrophobicity of soil reduces potential for water infiltration post-fire, increasing topsoil susceptibility to runoff (DeBano 2000). The presence of PyC in litter and surface soil can also increase the rates of erosion, as fire-affected biomass tends to have lower density, compared to uncharred biomass and litter, making it easier to transport by both water and wind erosion processes (Rumpel et al. 2006). In many ecosystems, erosion preferentially

transports carbonaceous topsoil material, compared to mineral constituents of soil, leading to C enrichment in eroded sediments compared to soil in source slopes (Avnimelech & McHenry 1984; Stacy et al. 2015). Similarly, Rumpel et al. (2006) found evidence for selective transport of PyC during interrill erosion due to its lower density and concentration on the soil surface. One study found that interrill sediment erosion was doubled in a burned watershed compared to a neighboring unburned watershed, along with increases in runoff velocity due to increased bare ground coverage (Pierson et al. 2008; Pierson et al. 2013). The relative extent of interrill compared with rill erosion depends upon local landscape and precipitation conditions (Moody et al. 2013).

Leaching and vertical colloid mobilization

PyC is vertically redistributed throughout the soil profile in both dissolved and particulate form, by both water flow and bioturbation, eventually accumulating in subsurface soil horizons (Glaser et al. 2000; Rumpel et al. 2015). In a recent study, Boot et al. (2015) found that 17% of PyC in litter layers was vertically mobilized into deeper layers in the soil profile. The same study also found that the PyC in deeper soil horizons tended to be the oldest, and most processed PyC, compared to PyC in surface of soil (Boot et al. 2015). Similarly, Glaser et al. (2000) reported an accumulation of particulate PyC in deeper horizons (below 30 cm), but reported that within aggregate and mineral-associated fractions of the soil C did not have elevated PyC concentrations at deeper soil horizons.

Relatively few studies have reported a direct measurement of PyC leaching from soil. One of the available studies concluded that less than 1% PyC loss per year can be attributed to leaching of dissolved PyC (Major et al. 2010). However, another study conducted in forested Siberian Arctic river watersheds estimated the PyC leaching rate to be considerably higher, at over 40% per year (Myers-Pigg et al. 2015). The differences in these estimates likely reflect variations in PyC concentration and properties, ecosystem types, climate, fire regimes, and hydrologic conductivity (Leifeld et al. 2007). Even when accounting for the variability within the estimates of loss rates, it remains clear that some PyC in soil is dissolved or transported in particulate form and is transported out of soil into rivers (Wagner et al. 2015). Indirect evidence for this can be found in studies from river systems that estimate that about 10% of dissolved organic matter in rivers globally is likely composed of dissolved PyC that was laterally transported from burned catchments (Hockaday et al. 2006; Jaffé et al. 2013). The vertical transport of PyC is an important control on the amount of surficial PyC available for erosion.

Atmospheric and aeolian transport

The atmospheric component of the global PyC cycle has received considerably more research attention than soil PyC, largely due to the interest in air pollution associated with soot and other aerosol releases to the atmosphere (Campbell et al. 2007; Seiler 1980), and their implications for global climate change and public health (Bond et al. 2013; Highwood & Kinnersley 2006). Fossil fuel combustion and biomass burning produce the majority of atmospheric PyC, which has a relatively short residence time (up to months) in the atmosphere (Chapin et al. 2006; Preston & Schmidt 2006). However, in the lower atmosphere, the residence time is typically less than a week (Parungo et al. 1994).

Dry and wet deposition of PyC from the atmosphere is a global process and transports between 2 and 10 Tg PyC per year globally, to both land and ocean depositional settings over regional and continental scales spanning thousands of km (Bond et al. 2013; Jurado et al. 2008; Parungo et al. 1994). From the soil surface, ash and smaller PyC constituents can be rapidly transported post-fire, depending on local wind and precipitation conditions, such that dry climates are more susceptible to post-fire wind erosion (Pereira et al. 2015; Shakesby 2011). Few studies have focused on wind-driven erosion, atmospheric transport, and terrestrial deposition of PyC post-fire, due to both methodological difficulties and widespread assumptions that it is a very small flux or only a site-specific phenomenon (Shakesby 2011; Wondzell & King 2003).

Consumption in subsequent fires

In ecosystems with short fire return intervals, PyC is lost through subsequent combustion (Santín et al. 2013; Tinkham et al. 2016). Czimczik et al. (2005) proposed that most of the PyC in the surface layer of a Siberian scots pine forest soil (Podzol) had been consumed in a high intensity fire, with no accumulation of PyC within the soil, particularly at depth. A more recent study found that relatively low proportion (median of 15% mass loss) of soil PyC was consumed during fire (Santín et al. 2013). These conflicting results likely reflect the role that fire return interval and combustion intensity play in controlling combustion of PyC.

Significance of erosional redistribution of PyC in the terrestrial ecosystem

Accurate quantification of the rates of PyC loss through biological versus physical processes is necessary for fully understanding its role in the soil C pool for a number of reasons, including its potential role as a C sink (Hammes et al. 2008). Understanding the controls on the fate of PyC in soil is needed for generating more accurate and representative models of dynamics of the soil C pool and how the soil system controls global climate. Current evidence suggests that PyC interacts with the soil minerals and microbial community differently than non-pyrogenic C (Kuzyakov et al. 2009). Thus, improved understanding of PyC interactions in soil and its loss mechanisms are currently needed to elucidate the role of PyC in soil total C stabilization.

Erosion and soil PyC dynamics

The role of erosion in controlling the fate of PyC is likely more important than for non-pyrogenic SOM, as fire can significantly increase the rate of soil erosion, and prior research has demonstrated that PyC is highly erosive (Rumpel et al. 2006; Yao et al. 2014). The increase in rate of soil erosion post-fire results from a combination of environmental changes, including: loss of the protective litter layer, exposure of surface soil to erosive forces (precipitation, wind), increased hydrophobicity of the subsoil (Benavides-Solorio & MacDonald 2001; DeBano 2000; DeBano et al. 1998; MacDonald et al. 2001), and a reduction in water infiltration and water holding capacity of the surface soil (Carroll et al. 2007; DeBano 2000; Doerr & Thomas 2000; Robichaud 1997). Furthermore, how long elevated rates of soil erosion are sustained is at least partially controlled by the extent of vegetation recovery post-fire, but is typically around a year (Baker 1988).

Erosion, in turn, can indirectly affect vegetation and soil water status. Both fire and erosion are controlled by climate to various extents (Imeson & Lavee 1998; Neary et al. 1999; Riebe et al. 2001). Watershed size and topography (Iniguez et al. 2008; Liu et al. 2003), in addition to the amount, intensity, and temporal distribution of precipitation can influence the rate of bulk SOM and PyC loss from or redistribution within an eroding watershed (Cain et al. 1999; Nearing 1998). These relationships have been documented by many erosion prediction models, such as the Universal Soil Loss Equation (Wischmeier & Smith. 1965; Wischmeier & Smith. 1978) and the Water Erosion Prediction Project (WEPP) model (Laflen et al. 1991).

Important inferences can be drawn on factors that control PyC erosion based on available data and by extrapolation of what we know about erosion of non-PyC or bulk C. Below we briefly discuss how specific variables (i.e., the amount and nature of PyC available for transport, climate, geomorphology of the landscape) control how strongly erosion can regulate soil PyC dynamics.

The erodible nature of PyC

The magnitude and composition of PyC that is laterally distributed over the soil surface by erosion, at least in part, depends on the concentration, placement, chemical composition, and physical size of the PyC. These variables are all products of complex interactions among the type and density of vegetation available to be combusted (i.e., fuel load), combustion conditions (e.g., temperature, duration, oxygen availability), and frequency of fire events (Czimczik & Masiello 2007; Hockaday et al. 2006; Knicker 2007; Masiello 2004; Schmidt & Noack 2000).

As of yet, the relative rates of PyC compared with bulk SOM erosion at the plot, hillslope or even watershed scale remain relatively unexplored, so the amount of PyC transported via erosion processes is generally unknown. Transport of PyC is assumed to occur in erosion events immediately after fire when the land surface is covered by a layer of PyC, which can become quickly mobilized through the landscape (Carroll et al. 2007) either via wind- or water-driven erosion. The PyC on the soil surface is likely to be eroded before, and more preferentially, than mineral soil or mineral-associated PyC, except in the cases of landslides and other major mass wasting events. Additionally, the recently formed PyC would not have had enough time to break down and enter into stabilizing physical and chemical interactions with soil minerals prior to preferential transport, as these breakdown process can take years to decades in natural settings (Faria et al. 2015). Over time, the PyC that is not transported by erosion is mobilized downward into the profile via dissolution and leaching processes that render it more susceptible for in-solution transport with flowing water (Güereña et al. 2015), in additional to mobilization down the soil profile via biological processes, such as earthworm bioturbation.

Among the most important physical and chemical properties of PyC that make it susceptible to erosion are its low density compared with soil minerals (Brewer et al. 2014), its hydrophobic properties (Certini 2005; Mataix-Solera & Doerr 2004), and its degree of charring and condensation (Preston & Schmidt 2006). Generally, it is assumed that the low density (<1 Mg/m^3) and hydrophobic properties of PyC allow for flotation and lateral

transport of PyC with flowing water. The slow wetting and filling of the pores of PyC with water, however, is expected to increase its density to be equivalent to that of water, and reducing its potential for floatation and transport with overland flow (personal communication, C. Masiello, Rice University), although this also depends on breakdown of the PyC and incorporation of SOM into the PyC (Zimmermann et al. 2012). The duration, intensity, and frequency of storm events plays a significant role in controlling the wetting of PyC, as the hydrophobic properties of PyC can only delay wetting, not prevent it entirely (Kaiser et al. 2015). Even if the PyC stays on the soil surface, being exposed to wetting- and drying-cycles is likely to render it more susceptible to leaching losses, although some research has indicated that the material left after leaching may be less easily decomposed (Naisse et al. 2015).

Climate and hydrology

The process of soil erosion occurs though detachment of a soil particle which is transported, and deposited away from the source location. During rain-driven erosion, the impact of raindrops breaks down aggregates on the soil surface which leads to transport of soil away from the point of impact, and gravity leads to the downslope mobilization of detached particles across the soil surface (Kinnell 2005). With all other factors held equal, the intensity of precipitation is the leading driver of erosion and runoff (Renard et al. 1997). Large storms are generally thought to drive the major erosion events within a landscape; however, intermediate storms can also mobilize significant amounts of material over the course of a year (Wischmeier 1962). In addition to intense storms, rapid rainfall and rain-on-snow events are important drivers of rapid runoff (Pierson et al. 2001). The loss or reduction of vegetation cover due to fires creates the opportunity for raindrops to reach the soil surface at high velocity, without being slowed down by aboveground vegetation and overlying litter layers. Hence, the same amount or intensity of rainfall can mobilize more PyC, and bulk C, from soil post-fire than it would under unburned conditions if there is loss of vegetation or litter layers. Generally, low intensity precipitation events drive preferential transport of light carbonaceous material (higher enrichment ratios, higher concentration of bulk and pyrogenic C). However, during high intensity or longer duration rainfall events, a mixture of organic/pyrogenic and mineral material is mobilized from the soil surface or even deeper soil horizons (large rainfall events lead to scouring of the surface or river banks or creation of deep rills and gullies), as was observed by Stacy et al. (2015) and McCorkle et al. (2016).

Geomorphology of the landscape

The geomorphology of a landscape can significantly impact the erosion of PyC. In particular, the steepness of a hillslope has a non-linear, direct effect on the amount of sediment transported by soil erosion, where increased gradient increases the mass of transported sediment (Montgomery & Brandon 2002). Slope length and hillslope hydrology (Istanbulluoglu et al. 2008; Munro & Huang 1997; Parsons et al. 2006) also play important roles on PyC transport, as moderate length slopes allow for the greatest transport of material, while shorter slopes are limited in space for runoff to build speed. Longer slopes have increased area for water to meet resistance and for particles to settle out, so the travel distance of particles is a function of their size.

Aspect of a hillslope can impact erosion due to its effects on plant growth, density, OM decomposition, and subsequent implications for fuel availability for fires and soil burn severity (Cerdà et al. 1995). The impacts of aspect on hillslope erosion can be compounded by delays in vegetation recovery, leading to longer-term enhanced erosion rates and continued loss of soil nutrients, and weather-related events, which can cause different erosion rates on different aspects of the same hillslope (Cerdà et al. 1995). Furthermore, the location within a landscape that PyC is formed or deposited can be critical for the long-term fate of the PyC. If PyC is produced on eroding landform positions (convex or linear positions such as summit, shoulder, or back/foot slope positions), then is more likely to be transported laterally by wind or water erosion processes, or gravity driven diffusive mass transport, compared to PyC produced in depositional landform positions (concave or flat positions such as toeslopes, or alluvial and colluvial plains). However, if the PyC is either formed or deposited on depositional landform positions, then it is more likely to persist in the catchment longer and be stabilized in the depositional landform positions by forming physical and/or chemical associations with soil minerals, or if it gets buried by subsequent erosion/deposition events that bring sediment to the depositional position (Berhe 2012; Stallard 1998).

Interactions

The three drivers of PyC erosion also interact with each other to control rates of PyC erosion (Figure 5). For example, different combinations of steepness of a hillslope, size of watershed, and intensity of precipitation may lead to differing rates of erosion (Pierson et al. 2001). Generally, large precipitation events drive the formation of rills or gullies and large mass wasting events, and very steep slopes, which could predispose a landscape to mass wasting events, could further enhance these large movement events. As another example, long-term climate patterns impact the type and amount of vegetation available as fuel for fire, which could further impact the quality and quantity of PyC left behind after fire. The amount and properties of available fuel play an import role in determining the intensity of fire, which controls the resulting PyC properties (Mimmo et al. 2014).

Implications of including erosion as a PyC flux term

While the magnitude of PyC transported by soil erosion is unknown, existing evidence suggests that erosion is a significant driver of PyC redistribution in hillslopes (i.e., loss from soil profiles of eroding landform positions, that may or may not remain in the same catchment as input to the soil profiles of depositional landform positions) (Rumpel et al. 2006). Environmental conditions post-fire and the nature of PyC lead to elevated rates of erosion and enrichment of PyC within the resulting eroded sediments. The large flux of PyC to oceans (Jaffé et al. 2013) is further indication that there is considerable transport of PyC within the terrestrial and to the aquatic system. An approach that considers the geomorphic and biogeochemical changes associated with fires is needed to quantify stock and erosional fluxes of PyC in fire-affected dynamic landscapes and to determine *how* and *why* erosional distribution of PyC could affect our understanding of the dynamics of both bulk SOM and PyC in the terrestrial biosphere.

Calculating loss and MRT of PyC

One of the most common and simplest approaches to estimating PyC mean residence time (MRT) is generally based on calculations of a loss rate from a given reservoir (i.e., soil) using simple one-pool box model approaches. Turnover time (*T*) is assumed to be equivalent to the inverse of the loss rate constant (*k*), with the assumption of steady state. Turnover time is imposed on a first-order kinetic model of PyC dynamics as:

$$T = 1/k \qquad \textit{Equation 1}$$

where,

$$dPyC/dt = I_{PyC} - k*PyC \qquad \textit{Equation 2}$$

where *T* is turnover time (years), *k* is a loss rate constant (as a proportion of the PyC stock, yr^{-1}), *PyC* is stock of PyC in a soil pool (g/m^2), I_{PyC} ($g\ m^{-2}\ yr^{-1}$) is the rate of PyC input to the reservoir. This model assumes a single rate of loss of PyC that is solely comprised of decomposition. Below we argue for the role of erosion as a significant loss factor for PyC and demonstrate the error in MRT calculations when erosion is ignored.

Estimating MRT of PyC in dynamic landscapes

Ignoring the contribution of erosion to soil PyC stocks can lead to errors in both the stock as well as estimated turnover time of PyC in dynamic landscapes. Many fires occur in areas that are prone to erosion, but even if an erosional loss term of PyC is included, the role of erosion as a gain term is rarely accounted for within soil PyC budget models. Not accounting for this gain of PyC can lead to major errors within our budget models of PyC and C within eroding landscapes. We have considered three landform positions or types in the following model: 1) flat, where we assumed erosion plays no role (i.e., landform where no sediment material is being transported to or from that area); 2) an eroding landform position (e.g., shoulder, backslope), where erosion represents a loss term for PyC; and 3) a depositional landform position (e.g., toeslope or plain), where deposition of PyC eroded from upslope positions leads to input of PyC. Following works of Stallard (1998) and Berhe et al. (2008) on erosional redistribution of bulk SOM, here, a model for first order C kinetics was modified to reflect the effect of erosion on PyC dynamics. The first-order loss rate constant (*k*) in the first order model (Equation 2) was replaced with two separate constants for decomposition (k_o) and erosional redistribution (k_e,), where $k = k_o + k_e$ as:

$$\mathrm{dPyC/dt} = I - (k_0 + k_e) * PyC \qquad \textit{Equation 3}$$

where *PyC* = soil PyC stock ($g\ m^{-2}$); *I* = soil pyrogenic carbon inputs ($g\ m^{-2}\ yr^{-1}$); k_o = first-order loss of PyC by oxidation/decomposition (yr^{-1}); and k_e = first-order loss or gain of PyC by erosion (positive or negative k_e, respectively, yr^{-1}). This k_e term describes the different trajectories of PyC at eroding or depositional landform positions and accounts for additions or losses of PyC via erosional processes.

For our model calculations, we used published results from Hammes et al. (2008) where they measured PyC stock in chernozem soils at a steppe preserve in Russia. The soils were sampled twice over about 100 years, first between 1895 and 1903, and then in 1997 and 2004. The authors then used the difference in PyC stock (measured using the BPCA marker

technique) of the soil between the two time periods and radiocarbon measurements of SOM to derive MRT of PyC in soil using a one PyC pool, first-order decay (i.e., linear, donor-controlled) model Hammes et al. (2008). In our calculations, we assumed the soils had initial soil PyC stock of 2.5 kg PyC/m^2 (Hammes et al. 2008) and a relatively low decomposition constant (k_o) for PyC of 0.4%/year (i.e., approximate turnover time of 250 years; (Hammes et al. 2008). Then, we considered erosion or deposition as loss or gain terms, as shown in Equation 3. We calculated the stock of PyC in the flat position by assuming that $k = k_0$ and that $k_e = 0$. For the eroding position k_e represents a loss term for PyC, while for the depositional position it represents a gain to the existing PyC stock. The depositional area has erosional inputs of PyC that maintain a higher PyC stock through the simulation. The eroding area has both erosion and decomposition acting together to remove PyC from the soil, so it has the lowest PyC stock at the end of the 150-year simulation (Figure 6).

This model is an inherently simplified version of PyC dynamics within eroding hillslopes, and thus operates under several assumptions. This model assumes a single input of PyC and initial even distribution and availability of PyC for erosional transport. After the initial time step, the erosional gain of PyC at the depositional landform position is likely no longer a function of the stock of PyC in that landform position, but a function of the PyC in the source eroding landform position. However, depending on specific fire and environmental conditions, this model may still hold as a proximate estimation for the erosion inputs of PyC into a depositional landform position. This model assumes only a single fire event to input PyC, but in many environments, it is likely that there would be more than a single input of PyC over the duration of 150 years. We found that, for the specific conditions we considered, not accounting for erosional redistribution of PyC lead to around 200 g m^{-2} of PyC stock difference between the maximum erosion gain and minimum erosion loss scenarios over a 150-year simulation. Note that the model presented here is simplistic by design, as it is aiming to demonstrate the role of soil erosion under three landform positions. In any given hillslope, the actual role of erosional redistribution depends on the nature of the landscape, rate of PyC input, and the environmental variables that control rate of PyC loss through decomposition, leaching, and/or erosion. For example, future models could be designed for specific environments to include additional fluxes of PyC that have yet to be well quantified, such as bioturbation, leaching, and subsequent fires, and likely control its stock and residence time in the soil.

The model presented above can also be used to determine the effect of erosion on mean residence times or persistence of PyC in soil. The more that erosion contributes to the k term as a loss of PyC, the larger the overall k term and the faster the turnover of PyC in a soil, since a portion of the PyC stock would be moved laterally to downslope positions. Conversely, for depositional landform positions, the k_e adds to the soil profile's PyC stock, and because k_e would be negative in this case, it lowers the effective k term in Equation 1, leading to longer turnover times for PyC in soil profiles of depositional landform positions.

On the local scale, explicitly considering erosion as a loss or gain term (depending on the landform positions considered) for PyC in dynamic landscapes leads to considerable differences in MRT at different geomorphic landform positions. Across even a single hillslope, soil properties and controls on decomposition vary considerably. We calculated

turnover times for eroding and depositional landform positions, by assuming a decomposition rate (k_0 from equation 3 of 0.04%/year and an erosion rate of 0.01%/year (1000-year turnover time from erosion processes alone). The erosion rate (k_e) was positive for the eroding landform position (indicating erosional loss of PyC from eroding landform positions, and making net loss of PyC faster) and negative for the depositional landform position (indicates an addition of PyC, and decreasing the net loss of PyC). This erosion rate was further divided into different fractions, such that 0% indicates no erosion, or no erosion accounted for, and 100% indicates 100% of the 0.01% erosion rate accounted for within the model. We found that if 100% of this theoretical erosion rate is accounted for, then the difference in calculated turnover time is approximately 150 years (Figure 7). If 50% of the erosional loss of PyC from a soil is accounted for, then the difference between the maximum turnover time with erosion as a gain and the minimum turnover time with erosion as a loss is approximately 70 years. If the erosion rate were higher (i.e., the theoretical 100% erosion was a higher background erosion rate), then this difference in turnover time would be even greater. This difference in erosion indicates that over the scale of a landscape, local topographical differences that determine whether PyC is eroded or deposited over time can play a major role in the fate of that PyC.

This model only applies to PyC that remains on the surface soils, which is the fraction that is likely to experience erosion. The fraction of soil PyC that is found in deep soil layers or gets buried overtime is not likely to experience significant lateral redistribution with erosion, and hence is not included in this discussion. Also, the importance of the role of erosion as a gain or a loss term is also dependent on the relative role of erosion in each landscape (Figure 7), as different landscape geomorphologies can lead to drastically different erosional rates and processes (Section *3.1.3*). Furthermore, the intensity, type, and timing of post-fire precipitation play an important role in erosion of PyC (Hammes et al. 2008).

Explicitly considering erosion in modeling global PyC dynamics in soil

The role of erosion in redistributing PyC can also impact global models of PyC cycling and storage. To investigate how an erosion event can affect our estimates of soil PyC dynamics, we ran a simple box model with current estimates of PyC pools and flux rates (Figure 3). This box model includes pools (or sinks) of PyC and fluxes that are known to impact PyC with the assumption that no shifts in flux rates are occurring (i.e., fire is occurring at a constant rate, erosion operates at a constant rate). In reality, these rates are constantly varying, but this model is useful to probe whether current measurements of loss processes of PyC are generally on the correct order of magnitude, assuming steady state and that first-order loss applies.

The major global pools of PyC incorporated into this model are soil, buried soil from erosional processes, groundwater, oceans, and marine sediments, and the major fluxes (input and output processes) of PyC are fire (burning of biomass, input of PyC to soil), decomposition (loss of PyC from soil), percolation and leaching to groundwater (loss of PyC from soil, gain to groundwater), erosional transport (loss of PyC from original soil pool), decomposition of eroded material (loss of PyC from erosional PyC pool), export to oceans by rivers (constant rate), and sedimentation of oceanic PyC (loss from ocean and

gain to marine sediment). These loss processes and stocks were incorporated into a simple box model using Microsoft Excel (Version 15.12.3, see Figure 3) to assess steady state assumptions of global PyC stocks and fluxes (see Table 2 for model assumptions and parameter inputs).

This model was initialized with stocks of PyC in the soil, ocean, and marine sediment. Since there are no reliable measurements for representative rates of PyC eroded and buried or leached into groundwater, these stocks were assumed to initially be 0. However, there is evidence for buried PyC being able to persist within an environment for longer periods in Paleosols (Marín-Spiotta et al. 2014).

Fluxes (inputs and outputs of PyC into stocks) were entered into the model as either a constant flux rate (e.g., river to ocean flux – 7.4×10^{12} g/year; Jaffé et al. (2013)), or as a stock dependent flux (e.g., decomposition - 5% of soil PyC stock per year). Because no terrestrial to aquatic flux rate has been reported to date, this flux was not included in the model and was assumed to equal the ocean export flux of PyC. Each flux process was scaled to a year time scale, and the model was integrated to run for 100 years. A sensitivity analysis conducted by varying the initial stocks and fluxes found that soil PyC stocks were sensitive to initial stocks, but not the magnitude of fluxes.

The results of this model indicate that the current literature is not fully accounting for PyC throughout the global ecosystem, as the stocks and fluxes used in this model did not reach steady state by the end of the simulation. The final soil PyC stock was 5.78×10^{14} g, which was considerably lower than the initial 'steady state' hypothesis (maintaining an initial steady state concentration of 1.05×10^{15} g). This indicates that the current available flux measurements and controls on soil PyC storage are not fully describing the dynamics of PyC in soil. However, the buried soil PyC pool, when totaled with the soil PyC pool, exceeds the initial total soil PyC pool. This indicates that erosion may is serving as a sink or stabilization mechanism of PyC, as it is comprising a significant portion of the long-term soil PyC pool.

Additionally, by assuming steady state and a low decomposition rate (5%), erosion must not be playing a significant role in the net loss of total soil PyC (on this theoretical global scale), even if there is local-scale loss of PyC. These results suggest that erosion is playing a role in redistributing PyC and burying it for longer-term storage within the soil system. However, this model is a major simplification of the global PyC cycle that does not include quantitative inputs such as type of erosion, climate data, topography, and the preexisting soil PyC pool, which would usually comprise a global scale model. What can conclusively be drawn from this model is the role of erosion of PyC should not be ignored as a factor controlling its long-term fate within the soil.

The connection of soil PyC to rivers and oceans is a critical missing output component of this model, and is outside the scope of this synthesis. This terrestrial to aquatic transfer of PyC is also a topic that currently has very little data or consensus about the mechanism of PyC transport and subsequent dynamics in the aquatic systems. This transfer likely includes both erosion and leaching driven processes, but these are not yet well understood, and riverine breakdown and storage of PyC may serve as critical missing sinks and fluxes in the PyC cycle. However, it is plausible to expect that, if this output (land-river transfer)

was included in a model like the one we present here, then the soil PyC may potentially be at steady state, since this additional loss of PyC to rivers would decrease the overall soil PyC stock.

Furthermore, the box model presented here does not necessarily represent natural variation in timing and magnitude of fire and future climates that may alter the global PyC cycle, particularly as large erosion and fire events are strongly controlled by local weather conditions (Westerling et al. 2006). The loss of PyC from the soil is likely more episodic and variable in nature than this model accounts for, and therefore this loss may be different than predicted by constant rate functions used in this model. Also, this model does not account for the decomposition or loss of PyC from groundwater or from deep-sea sediments, which result in them acting as considerable sinks for PyC within this model.

In addition to limitations of the knowledge surrounding the loss of PyC in different sinks, it is likely that the many laboratory-based incubation studies are over-estimating the rate of PyC decomposition due to the disturbance of the soil, along with optimal decomposition conditions in the laboratory. Many of these estimates are over 10% PyC loss per year (Foereid et al. 2011; Nguyen et al. 2010), which is inconsistent with calculated PyC MRT measurements that range from several hundred years to several millennia (Hammes et al. 2008; Lehmann et al. 2008). It is also possible that erosional deposition and burial of PyC is a more significant process for the long-term stabilization of PyC than previously considered. If erosion is playing a significant role in the stabilization of PyC and if decomposition rates of PyC are consistently over-estimated, this could have major implications for global models of PyC cycling and storage. PyC could be serving a major role in the unaccounted for C in our global C budgets (Lehmann 2007) and could potentially represent a previously unaccounted C sink within the soil system (Santin et al. 2015).

Remaining uncertainties in PyC erosion and recommendations for future research

The variation in the estimates of loss of PyC reflects both the spectrum of methodologies used to measure PyC and the lack of inclusion of erosion and other processes as loss mechanisms. The dynamics of PyC within the soil system depends on prevalent environmental conditions, such as temperature, precipitation, land use, slope, aspect, and vegetation. Available data on the magnitude of loss of PyC from the soil by different processes is currently incomplete, and has a lot of uncertainty, making model parameterization very difficult (see Table 1 for published magnitudes of fluxes and stocks of PyC). In particular, the rates of erosion and burial of PyC and the mechanisms and magnitude of the transport of PyC from land to water need further investigation. Making comparisons between stocks of PyC from different techniques that is also difficult, as each technique measures a different portion of the PyC combustion continuum, and the assumptions underlying the different techniques vary considerably. As far as we can tell, there is no way to convert data derived using the many different approaches into a standard unit, making integration of previous research into global and watershed scale models a challenge.

In the simple box model presented here, in the absence of new input, the soil's PyC stocks were declining considerably lower than the current PyC soil stock measurements would suggest. It is likely that the inferred or measured rates of PyC loss in soils are overestimating the effectiveness of microbial decomposition, especially for the studies generated from short-term laboratory experiments conducted under ideal climate and environmental conditions. In longer-term laboratory incubations and models, rates of PyC decomposition are considerably lower (Foereid et al. 2011; Kuzyakov et al. 2009). Furthermore, uncertainties also remain as to the role of erosional transport in physical breakdown and decomposition of PyC during erosional transport. In the model presented here, the rate of decomposition during erosional transport was assumed the same as non-pyrogenic carbon. If this assumption proves invalid and PyC decomposition during erosion is considerably lower, this would have important implications for the long-term stabilization of PyC. Finally, even though erosion of PyC from slopes represents a loss process, it serves the opposite role in depositional landform positions. If we assume that erosional redistribution, and subsequent burial of eroded PyC in depositional soil profiles can effectively reduce its decomposition rate, then the process of soil erosion can potentially be a stabilization mechanism for PyC in some eroding landscapes (Berhe et al. 2007; Berhe & Kleber 2013).

CONCLUSION

Interactions of environmental perturbations such as fire and erosion can play significant roles in regulating PyC and SOM persistence in dynamic landscapes. The synthesis of published results and models presented here illustrates how not accounting for integrated biogeochemical and geomorphological processes can lead to significant errors in our current understanding of PyC dynamics in the terrestrial ecosystem. Specifically, not accounting for post-fire erosion can lead to significant differences in projected stocks and turnover times of PyC within the soil. These differences in stock and turnover time vary based on landform position, rates and drivers of erosion, among other factors.

Understanding the long-term fate of terrestrial OM and PyC is critical for generating accurate models and to better manage these ecosystems to maximize soil C storage. Considering imminent climate change, understanding the controls on the PyC cycle may become ever more critical for managing soil C cycle. This is particularly relevant as the relative roles of fire and erosion as controlling forces for the soil PyC cycle may act in different ways under altered climatic regimes. PyC is an important component of the global C cycle that is being assessed for its potential to account for the missing C sink and biochar addition to soil is being discussed as one of many approaches that can be used to mitigate climate change (Santin et al. 2015). It is critically important to gain better understanding of the major loss processes for PyC from the soil, including decomposition, erosion, leaching, and further fires. However, currently, the uncertainties in comparing loss rates from different ecosystems and measurement techniques make global budget modeling difficult. Future research should focus on mechanisms and magnitude of PyC loss from the soil system, as well as development of approaches to enable comparisons and conversions between different measurement techniques for PyC.

ACKNOWLEDGEMENTS

The authors gratefully acknowledge Caroline Masiello, Fernanda Santos, Stephen Hart, Marilyn Fogel, and Jonathan Sanderman for their helpful and detailed comments on earlier versions of this manuscript. Funding for this work was provided from the National Science Foundation (CAREER EAR - 1352627) award to A. A. Berhe.

REFERENCES

Abiven S, Hengartner P, Schneider MPW, Singh N, Schmidt MWI (2011) Pyrogenic carbon soluble fraction is larger and more aromatic in aged charcoal than in fresh charcoal. Soil Biology and Biochemistry 43(7): 1615-1617

Adams LB, Hall CR, Holmes RJ, Newton RA (1988) An examination of how exposure to humid air can result in changes in the adsorption properties of activated carbons. Carbon 26(4): 451-459

Al-Hamdan OZ, Pierson FB, Nearing MA, Williams CJ, Stone JJ, Kormos PR, Boll J, Weltz MA (2012) Concentrated flow erodibility for physically based erosion models: temporal variability in disturbed and undisturbed rangelands. Water Resources Research 48(7): W07504

Albalasmeh AA, Berli M, Shafer DS, Ghezzehei TA (2013) Degradation of moist soil aggregates by rapid temperature rise under low intensity fire. Plant and Soil 362(1-2): 335-344

Alexis M, Rumpel C, Knicker H, Leifeld J, Rasse D, Péchot N, Bardoux G, Mariotti A (2010) Thermal alteration of organic matter during a shrubland fire: a field study. Organic Geochemistry 41(7): 690-697

Amon R, Benner R (1996) Photochemical and microbial consumption of dissolved organic carbon and dissolved oxygen in the Amazon River system. Geochimica et Cosmochimica Acta 60(10): 1783-1792

Araya S, Meding S, Berhe A (2016) Thermal alteration of soil physico-chemical properties: a systematic study to infer response of Sierra Nevada climosequence soils to forest fires. Soil 2(3): 351-366

Araya SN, Fogel ML, Berhe AA (2017) Thermal alteration of soil organic matter properties: a systematic study to infer response of Sierra Nevada climosequence soils to forest fires. Soil 3: 31-44

Ascough P, Bird M, Francis S, Thornton B, Midwood A, Scott A, Apperley D (2011) Variability in oxidative degradation of charcoal: influence of production conditions and environmental exposure. Geochimica et Cosmochimica Acta 75(9): 2361-2378

Avnimelech Y, McHenry J (1984) Enrichment of transported sediments with organic carbon, nutrients, and clay. Soil Science Society of America Journal 48(2): 259-266

Baker VR (1988) Flood erosion. Flood Geomorphology. John Wiley & Sons New York. :

Battin T, Luyssaert S, Kaplan L, Aufdenkampe A, Richter A, Tranvik L (2009) The boundless carbon cycle. 2(9): 598-600

Baumann K, Marschner P, Smernik RJ, Baldock JA (2009) Residue chemistry and microbial community structure during decomposition of eucalypt, wheat and vetch residues. Soil Biology and Biochemistry 41(9): 1966-1975

Benavides-Solorio J, MacDonald LH (2001) Post-fire runoff and erosion from simulated rainfall on small plots, Colorado Front Range. Hydrological Processes 15(15): 2931-2952

Berhe AA (2012) Decomposition of organic substrates at eroding vs. depositional landform positions. Plant and Soil 350: 261-280

Berhe AA, Harden JW, Torn MS, Harte J (2008) Linking soil organic matter dynamics and erosion-induced terrestrial carbon sequestration at different landform positions. Journal of Geophysical Research-Biogeosciences 113: G4, DOI 10.1029/2008jg000751

Berhe AA, Harte J, Harden JW, Torn MS (2007) The Significance of Erosion-Induced Terrestrial Carbon Sink. BioScience 57(4): 337-346

Berhe AA, Kleber M (2013) Erosion, deposition, and the persistence of soil organic matter: mechanistic considerations and problems with terminology. Earth Surface Processes and Landforms 38(8): 908-912

Birch H (1958) The effect of soil drying on humus decomposition and nitrogen availability. Plant and Soil 10(1): 9-31

Bird MI, Wynn JG, Saiz G, Wurster CM, McBeath A (2015) The pyrogenic carbon cycle. Annual Review of Earth and Planetary Sciences 43: 273-298

Bond TC, Doherty SJ, Fahey D, Forster P, Berntsen T, DeAngelo B, Flanner M, Ghan S, Kärcher B, Koch D (2013) Bounding the role of black carbon in the climate system: A scientific assessment. Journal of Geophysical Research: Atmospheres 118(11): 5380-5552

Boot C, Haddix M, Paustian K, Cotrufo M (2015) Distribution of black carbon in ponderosa pine forest floor and soils following the High Park wildfire. Biogeosciences 12(10): 3029-3039

Bowman DMJS, Balch JK, Artaxo P, Bond WJ, Carlson JM, Cochrane MA, D'Antonio CM, DeFries RS, Doyle JC, Harrison SP, Johnston FH, Keeley JE, Krawchuk MA, Kull CA, Marston JB, Moritz MA, Prentice IC, Roos CI, Scott AC, Swetnam TW, van der Werf GR, Pyne SJ (2009) Fire in the Earth System. Science 324(5926): 481-484

Brandt LA, King JY, Milchunas DG (2007) Effects of ultraviolet radiation on litter decomposition depend on precipitation and litter chemistry in a shortgrass steppe ecosystem. Global Change Biology 13(10): 2193-2205

Brewer CE, Chuang VJ, Masiello CA, Gonnermann H, Gao X, Dugan B, Driver LE, Panzacchi P, Zygourakis K, Davies CA (2014) New approaches to measuring biochar density and porosity. Biomass and Bioenergy 66: 176-185

Brodowski S, John B, Flessa H, Amelung W (2006) Aggregate-occluded black carbon in soil. European Journal of Soil Science 57(4): 539-546

Buurman P, Roscoe R (2011) Different chemical composition of free light, occluded light and extractable SOM fractions in soils of Cerrado and tilled and untilled fields, Minas Gerais, Brazil: a pyrolysis-GC/MS study. European Journal of Soil Science 62(2): 253-266

Cain M, Subler S, Evans J, Fortin M (1999) Sampling spatial and temporal variation in soil nitrogen availability. Oecologia 118(4): 397-404

Campbell J, Donato D, Azuma D, Law B (2007) Pyrogenic carbon emission from a large wildfire in Oregon, United States. Journal of Geophysical Research: Biogeosciences 112(G4):

Carroll EM, Miller WW, Johnson DW, Saito L, Qualls RG, Walker RF (2007) Spatial analysis of a large magnitude erosion event following a Sierran Wildfire. Journal of environmental quality 36(4): 1105-1105

Cerdà A, Imeson A, Calvo A (1995) Fire and aspect induced differences on the erodibility and hydrology of soils at La Costera, Valencia, southeast Spain. Catena 24(4): 289-304

Certini G (2005) Effects of fire on properties of forest soils: a review. Oecologia 143: 1-10

Chaopricha NT, Marín-Spiotta E (2014) Soil burial contributes to deep soil organic carbon storage. Soil Biology and Biochemistry 69: 251-264

Chapin F, Woodwell G, Randerson J, Rastetter E, Lovett G, Baldocchi D, Clark D, Harmon M, Schimel D, Valentini R, Wirth C, Aber J, Cole J, Goulden M, Harden J, Heimann M, Howarth R, Matson P, McGuire A, Melillo J, Mooney H, Neff J, Houghton R, Pace M, Ryan M, Running S, Sala O, Schlesinger W, Schulze ED (2006) Reconciling Carbon-cycle Concepts, Terminology, and Methods. Ecosystems 9: 1041-1050

Cheng CH, Lehmann J, Thies JE, Burton SD (2008) Stability of black carbon in soils across a climatic gradient. Journal of Geophysical Research-Biogeosciences 113(G2): -

Cheng CH, Lehmann J, Thies JE, Burton SD, Engelhard MH (2006) Oxidation of black carbon by biotic and abiotic processes. Organic Geochemistry 37(11): 1477–1488-1477–1488

Chia C, Munroe P, Joseph S, Lin Y, Lehmann J, Muller D, Xin H, Neves E (2012) Analytical electron microscopy of black carbon and microaggregated mineral matter in Amazonian dark Earth. Journal of microscopy 245(2): 129-139

Cope M, Chaloner W (1980) Fossil charcoal as evidence of past atmospheric composition. Nature 283(5748): 647-649

Cotrufo MF, Boot C, Abiven S, Foster EJ, Haddix M, Reisser M, Wurster CM, Bird MI, Schmidt MW (2016) Quantification of pyrogenic carbon in the environment: An integration of analytical approaches. Organic Geochemistry 100: 42-50

Cusack DF, Chadwick OA, Hockaday WC, Vitousek PM (2012) Mineralogical controls on soil black carbon preservation. Global Biogeochemical Cycles 26(2): GB2019

Czimczik C, Preston C, Schmidt M, Schulze E (2003) How surface fire in Siberian Scots pine forests affects soil organic carbon in the forest floor: Stocks, molecular structure, and conversion to black carbon (charcoal). Global Biogeochemical Cycles 17(1): doi:10.1029/2002GB001956

Czimczik C, Schmidt M, Schulze ED (2005) Effects of increasing fire frequency on black carbon and organic matter in Podzols of Siberian Scots pine forests. European Journal of Soil Science 56(3): 417-428

Czimczik CI, Masiello CA (2007) Controls on black carbon storage in soils. Global Biogeochemical Cycles 21(2): GB 3005

De la Rosa JM, González-Pérez JA, González-Vázquez R, Knicker H, López-Capel E, Manning DAC, González-Vila FJ (2008) Use of pyrolysis/GC–MS combined with thermal analysis to monitor C and N changes in soil organic matter from a Mediterranean fire affected forest. Catena 74(3): 296-303

DeBano LF (2000) The role of fire and soil heating on water repellency in wildland environments a review. Journal of Hydrology: 195-206

DeBano LF, Dunn PH, Conrad CE (1977) Fire's effect on physical and chemical properties of Chaparral soils. In: General Technical Report WO-3 USDA.

DeBano LF, Neary DG, Ffolliott PF (1998) Fire's effects on ecosystems. John Wiley and Sons, New York, NY

Dittmar T, De Rezende CE, Manecki M, Niggemann J, Ovalle ARC, Stubbins A, Bernardes MC (2012) Continuous flux of dissolved black carbon from a vanished tropical forest biome. Nature Geoscience 5(9): 618-622

Doerr S, Cerdá A (2005) Fire effects on soil system functioning: new insights and future challenges. International Journal of Wildland Fire 14(4): 339-342

Doerr SH, Thomas AD (2000) The role of soil moisture in controlling water repellency: new evidence from forest soils in Portugal. Journal of Hydrology 231: 134-147

Doetterl S, Berhe AA, Nadeu E, Wang Z, Sommer M, Fiener P (2016) Erosion, deposition and soil carbon: A review of process-level controls, experimental tools and models to address C cycling in dynamic landscapes. Earth Science Reviews 154: 102-122

Eckmeier E, Gerlach R, Skjemstad J, Ehrmann O, Schmidt M (2007) Minor changes in soil organic carbon and charcoal concentrations detected in a temperate deciduous forest a year after an experimental slash-and-burn. Biogeosciences 4(3): 377-383

Faria S, De la Rosa J, Knicker H, González-Pérez J, Keizer J (2015) Molecular characterization of wildfire impacts on organic matter in eroded sediments and topsoil in Mediterranean eucalypt stands. Catena 135: 29-37

Foereid B, Lehmann J, Major J (2011) Modeling black carbon degradation and movement in soil. Plant and soil 345(1-2): 223-236

Glaser B (2002) Past anthropogenic influence on the present soil properties of anthropogenic dark earths (Terra Preta) in Amazonia (Brazil). In: Glaser B & Woods WI (eds) Amazonian Dark Earths: Explorations in Space and Time. Springer-Verlag Berlin Heidelberg. p 517-530

Glaser B, Balashov E, Haumaier L, Guggenberger G, Zech W (2000) Black carbon in density fractions of anthropogenic soils of the Brazilian Amazon region. Organic Geochemistry 31(7-8): 669-678

Goldberg ED (1985) Black carbon in the environment: properties and distribution. J. Wiley, New York

González-Pérez J, González-Vila F, Almendros G (2004) The effect of fire on soil organic matter—a review. Environment International 30(6): 855-870

Gregorich E, Greer K, Anderson D, Liang B (1998) Carbon distribution and losses: erosion and deposition effects. Soil Till Res 47(3-4): 291-302

Güereña DT, Lehmann J, Walter T, Enders A, Neufeldt H, Odiwour H, Biwott H, Recha J, Shepherd K, Barrios E (2015) Terrestrial pyrogenic carbon export to fluvial ecosystems: Lessons learned from the White Nile watershed of East Africa. Global Biogeochemical Cycles 29(11): 1911-1928

Gustafsson Ö, Bucheli TD, Kukulska Z, Andersson M, Largeau C, Rouzaud JN, Reddy CM, Eglinton TI (2001) Evaluation of a protocol for the quantification of black carbon in sediments. Global Biogeochemical Cycles 15(4): 881-890

Gustafsson ö, Krusa M, Zencak Z, Sheesley R, Granat L, Engström E, Praveen P, Rao P, Leck C, Rodhe H (2009) Brown clouds over South Asia: Biomass or Fossil Fuel Combustion? Science 323:

Hammes K, Schmidt MWI, Smernik RJ, Currie LA, Ball WP, Nguyen TH, Louchouarn P, Houel S, Gustafsson O, Elmquist M, Cornelissen G, Skjemstad JO, Masiello CA, Song J, Peng Paa, Mitra S, Dunn JC, Hatcher PG, Hockaday WC, Smith DM, Hartkopf-Froeder C, Boehmer A, Lueer B, Huebert BJ, Amelung W, Brodowski S, Huang L, Zhang W, Gschwend PM, Flores-Cervantes DX, largeau C, Rouzaud J-N, Rumpel C, Guggenberger G, Kaiser K, Rodionov A, Gonzalez-Vila FJ, Gonzalez-Perez JA, de la Rosa JM, Manning DAC, Lopez-Capel E, Ding L (2007) Comparison of quantification methods to measure fire-derived (black/elemental) carbon in soils and sediments using reference materials from soil, water, sediment and the atmosphere. Global Biogeochemical Cycles 21(3): GB3016

Hammes K, Torn MS, Lapenas AG, Schmidt MWI (2008) Centennial black carbon turnover observed in a Russian steppe soil. Biogeosciences 5(5): 1339-1350

Harden JW, Berhe AA, Torn M, Harte J, Liu S, Stallard RF (2008) Soil Erosion: Data Say C Sink. Science 320(5873): 178-179

Hatten JA, Zabowski D (2009) Changes in soil organic matter pools and carbon mineralization as influenced by fire severity. Soil Science Society of America Journal 73(1): 262-273

Highwood EJ, Kinnersley RP (2006) When smoke gets in our eyes: The multiple impacts of atmospheric black carbon on climate, air quality and health. Environment International 32(4): 560-566

Hockaday WC, Grannas AM, Kim S, Hatcher PG (2006) Direct molecular evidence for the degradation and mobility of black carbon in soils from ultrahigh-resolution mass spectral analysis of dissolved organic matter from a fire-impacted forest soil. Organic Geochemistry 37(4): 501-510

Imeson A, Lavee H (1998) Soil erosion and climate change: the transect approach and the influence of scale. Geomorphology 23(2-4): 219-227

Iniguez J, Swetnam T, Yool S (2008) Topography affected landscape fire history patterns in southern Arizona, USA. Forest Ecology and Management:

IPCC (2013) Climate Change 2013: The Physical Science Basis, Working Group I Contribution to the Fifth Assessment Report of the Intergovernmental Panel on Climate Change. Summary for Policymakers. In: Stocker TF, Qin D, Plattner G-K, Tignor M, Allen SK, Boschung J, Nauels A, Xia Y, Bex V & Midgley PM (eds). Cambridge, United Kingdon and New York, NY, USA. p 1-30

Istanbulluoglu E, Yetemen O, Vivoni ER, Gutiérrez-Jurado HA, Bras RL (2008) Eco-geomorphic implications of hillslope aspect: Inferences from analysis of landscape morphology in central New Mexico. Geophysical Research Letters 35(14): L14403

Jacinthe P, Lal R (2001) A mass balance approach to assess carbon dioxide evolution during erosional events. Land Degradation & Development 12(4): 329-339

Jaffé R, Ding Y, Niggemann J, Vähätalo AV, Stubbins A (2013) Global Charcoal Mobilization from Soils via Dissolution and Riverine Transport to the Oceans. Science:

Jaffé R, Ding Y, Niggemann J, Vähätalo AV, Stubbins A, Spencer RGM, Campbell J, Dittmar T (2013) Global charcoal mobilization from soils via dissolution and riverine transport to the oceans. Science 340: 345-347

Jauss V, Johnson M, Krull E, Daub M, Lehmann J (2015) Pyrogenic carbon controls across a soil catena in the Pacific Northwest. Catena 124: 53-59

Johnson D, Murphy J, Walker R, Glass D, MILLER W (2007) Wildfire effects on forest carbon and nutrient budgets. Ecological Engineering 31(3): 183-192

Jurado E, Dachs J, Duarte CM, Simó R (2008) Atmospheric deposition of organic and black carbon to the global oceans. Atmospheric Environment 42(34): 7931-7939

Kaiser M, Kleber M, Berhe AA (2015) How air-drying and rewetting modify soil organic matter characteristics: An assessment to improve data interpretation and inference. Soil Biology and Biochemistry 80: 324-340

Kamens RM, Karam H, Guo J, Perry JM, Stockburger L (1989) The behavior of oxygenated polycyclic aromatic hydrocarbons on atmospheric soot particles. Environmental science & technology 23(7): 801-806

Keeley JE (2009) Fire intensity, fire severity and burn severity: a brief review and suggested usage. International Journal of Wildland Fire 18(1): 116-126

Kinnell P (2005) Raindrop-impact-induced erosion processes and prediction: a review. Hydrological processes 19(14): 2815-2844

Kinney TJ, Masiello CA, Dugan B, Hockaday WC, Dean MR, Zygourakis K, Barnes RT (2012) Hydrologic properties of biochars produced at different temperatures. Biomass and Bioenergy 41: 34-43

Knicker H (2007) How does fire affect the nature and stability of soil organic nitrogen and carbon? A review. Biogeochemistry 85(1): 91-118

Knicker H, Almendros G, González-Vila FJ, González-Pérez JA, Polvillo O (2006) Characteristic alterations of quantity and quality of soil organic matter caused by forest fires in continental Mediterranean ecosystems: a solid-state 13C NMR study. European Journal of Soil Science 57(4): 558-569

Knoblauch C, Maarifat A-A, Pfeiffer E-M, Haefele SM (2011) Degradability of black carbon and its impact on trace gas fluxes and carbon turnover in paddy soils. Soil Biology and Biochemistry 43(9): 1768-1778

Kupryianchyk D, Hale S, Zimmerman AR, Harvey O, Rutherford D, Abiven S, Knicker H, Schmidt H-P, Rumpel C, Cornelissen G (2016) Sorption of hydrophobic organic compounds to a diverse suite of carbonaceous materials with emphasis on biochar. Chemosphere 144: 879-887

Kuzyakov Y, Subbotina I, Chen H, Bogomolova I, Xu X (2009) Black carbon decomposition and incorporation into soil microbial biomass estimated by C-14 labeling. Soil Biology and Biochemistry 41(2): 210-219

Kyuma K, Tulaphitak T, Pairintra C (1985) Changes in soil fertility and tilth under shifting cultivation. Soil Science and Plant Nutrition 31(2): 227-238

Laflen JM, Lane LJ, Foster GR, Usda ARS (1991) WEPP: a new generation of erosion prediction technology. Journal of Soil And Water Conservation 46(1): 34-38

Lal R (2003) Soil erosion and the global carbon budget. Environment International 29(4): 437-450

Lal R (2004) Soil carbon sequestration impacts on global climate change and food security. Science 304(5677): 1623-1627

Lehmann J (2007) Bio-energy in the black. Frontiers in Ecology and the Environment 5(7): 381–387-381–387

Lehmann J, Skjemstad J, Sohi S, Carter J, Barson M, Falloon P, Coleman K, Woodbury P, Krull E (2008) Australian climate–carbon cycle feedback reduced by soil black carbon. Nature Geoscience 1(12): 832-835

Leifeld J, Fenner S, Müller M (2007) Mobility of black carbon in drained peatland soils. Biogeosciences Discussions 4(2): 871-891

Liang B, Lehmann J, Solomon D, Sohi S, Thies JE, Skjemstad JO, Luizao FJ, Engelhard MH, Neves EG, Wirick S (2008) Stability of biomass-derived black carbon in soils. Geochimica et Cosmochimica Acta 72(24): 6069-6078

Lin Y, King JY (2014) Effects of UV exposure and litter position on decomposition in a California grassland. Ecosystems 17(1): 158-168

Liu S, Bliss N, Sundquist E, Huntington T (2003) Modeling carbon dynamics in vegetation and soil under the impact of soil erosion and deposition. Global Biogeochemical Cycles 17(2): 1074

MacDonald LH, Sampson RW, Anderson DM (2001) Runoff and Road Erosion at the Plot and Road Segment Scales, St John, US Virgin Islands Earth Surf Process. Landforms 26: 251-272

Major J, Lehmann J, Rondon M, Goodale C (2010) Fate of soil-applied black carbon: downward migration, leaching and soil respiration. Global Change Biology 16(4): 1366-1379

Marín-Spiotta E, Chaopricha NT, Plante AF, Diefendorf AF, Muller CW, Grandy S, Mason JA (2014) Long-term stabilization of deep soil carbon by fire and burial during early Holocene climate change. Nature Geoscience doi: 10.1038/NGEO2169:

Masiello C (2004) New directions in black carbon organic geochemistry. Marine Chemistry 92(1-4): 201-213

Masiello CA (1998) Black carbon in deep-sea sediments. Science 280(5371): 1911-1913

Masiello CA, Louchouarn P (2013) Fire in the Ocean. Science 340(6130): 287-288

Mastrolonardo G, Rumpel C, Forte C, Doerr SH, Certini G (2015) Abundance and composition of free and aggregate-occluded carbohydrates and lignin in two forest soils as affected by wildfires of different severity. Geoderma 245: 40-51

Mataix-Solera J, Cerda A, Arcenegui V, Jordan A, Zavala LM (2011) Fire effects on soil aggregation: a review. Earth-Science Reviews 109(1-2): 44-60

Mataix-Solera J, Doerr S (2004) Hydrophobicity and aggregate stability in calcareous topsoils from fire-affected pine forests in southeastern Spain. Geoderma 118(1): 77-88

McCorkle EP, Berhe AA, Hunsaker CT, Johnson DW, MacFarlane KJ, Fogel ML, Hart SC (2016) Tracing the source of soil organic matter eroded from temperate forest catchments using carbon and nitrogen isotopes. Chemical Geology 445: 172-184

Mimmo T, Panzacchi P, Baratieri M, Davies C, Tonon G (2014) Effect of pyrolysis temperature on miscanthus (Miscanthus× giganteus) biochar physical, chemical and functional properties. Biomass and Bioenergy 62: 149-157

Montgomery DR, Brandon MT (2002) Topographic controls on erosion rates in tectonically active mountain ranges. Earth and Planetary Science Letters 201(3): 481-489

Moody JA, Shakesby R, Robichaud P, Cannon S, Martin DA (2013) Current research issues related to post-wildfire runoff and erosion processes. Earth-Science Reviews 122: 10-37

Munro DS, Huang L (1997) Rainfall, evaporation and runoff responses to hillslope aspect in the Shenchong Basin. Catena 29(2): 131-144

Myers-Pigg AN, Louchouarn P, Amon RM, Prokushkin A, Pierce K, Rubtsov A (2015) Labile pyrogenic dissolved organic carbon in major Siberian Arctic rivers: Implications for wildfire-stream metabolic linkages. Geophysical Research Letters 42(2): 377-385

Nadeu E, Berhe AA, De Vente J, Boix-Fayos C (2012) Erosion, deposition and replacement of soil organic carbon in Mediterranean catchments: a geomorphological, isotopic and land use change approach. Biogeosciences 9: 1099-1111, Doi:1010.5194/bg-1099-1099-2012

Naisse C, Girardin C, Lefevre R, Pozzi A, Maas R, Stark A, Rumpel C (2015) Effect of physical weathering on the carbon sequestration potential of biochars and hydrochars in soil. GCB Bioenergy 7(3): 488-496

National Interagency Fire Center (2015) National Report of Wildland Fires and Acres Burned by State. In: Center NIC (ed). vol 6/5/2015.

Nearing M (1998) Why soil erosion models over-predict small soil losses and under-predict large soil losses. Catena 32(1): 15-22

Neary DG, Klopatek CC, DeBano LF, Ffolliott PF (1999) Fire effects on belowground sustainability: a review and synthesis. Forest ecology and management 122(1): 51-71

Nguyen BT, Lehmann J (2009) Black carbon decomposition under varying water regimes. Organic Geochemistry 40(8): 846-853

Nguyen BT, Lehmann J, Hockaday WC, Joseph S, Masiello CA (2010) Temperature sensitivity of black carbon decomposition and oxidation. Environmental science & technology 44(9): 3324-3331

Nguyen BT, Lehmann J, Kinyangi J, Smernik R, Riha SJ, Engelhard MH (2009) Long-term black carbon dynamics in cultivated soil. Biogeochemistry 92(1-2): 163-176

Parsons AJ, Brazier RE, Wainwright J, Powell DM (2006) Scale relationships in hillslope runoff and erosion. Earth Surface Processes and Landforms 31(11): 1384-1393

Parungo F, Nagamoto C, Zhou M-Y, Hansen AD, Harris J (1994) Aeolian transport of aerosol black carbon from China to the ocean. Atmospheric Environment 28(20): 3251-3260

Pereira P, Cerdà A, Úbeda X, Mataix-Solera J, Arcenegui V, Zavala L (2015) Modelling the impacts of wildfire on ash thickness in a short-term period. Land Degradation & Development 26(2): 180-192

Pierson FB, Robichaud PR, Moffet CA, Spaeth KE, Hardegree SP, Clark PE, Williams CJ (2008) Fire effects on rangeland hydrology and erosion in a steep sagebrush-dominated landscape. Hydrological Processes 22(16): 2916-2929

Pierson FB, Slaughter CW, Cram ZK (2001) Long-Term Stream Discharge and Suspended-Sediment Database, Reynolds Creek Experimental Watershed, Idaho, United States. Water Resources Research 37(11): 2857-2861

Pierson FB, Williams CJ, Hardegree SP, Clark PE, Kormos PR, Al-Hamdan OZ (2013) Hydrologic and erosion responses of sagebrush steppe following juniper encroachment, wildfire, and tree cutting. Rangeland Ecology & Management 66(3): 274-289

Potter M (1908) Bacteria as agents in the oxidation of amorphous carbon. Proceedings of the Royal Society of London. Series B, Containing Papers of a Biological Character 80(539): 239-259

Preston C, Schmidt M (2006) Black (pyrogenic) carbon in boreal forests: a synthesis of current knowledge and uncertainties. Biogeosciences Discussions 3(1): 211-271

Preston CM (2009) Biogeochemistry: Fire and it's black legacy. Nature Geoscience 2(10): 674

Pyle LA, Hockaday WC, Boutton T, Zygourakis K, Kinney TJ, Masiello CA (2015) Chemical and isotopic thresholds in charring: implications for the interpretation of charcoal mass and isotopic data. Environmental science & technology 49(24): 14057-14064

Regnier P, Friedlingstein P, Ciais P, Mackenzie FT, Gruber N, Janssens IA, Laruelle GG, Lauerwald R, Luyssaert S, Andersson AJ, Arndt S, Arnosti C, Borges AV, Dale AW, Gallego-Sala A, Godderis Y, Goossens N, Hartmann J, Heinze C, Ilyina T, Joos F, LaRowe DE, Leifeld J, Meysman FJR, Munhoven G, Raymond PA, Spahni R, Suntharalingam P, Thullner M (2013) Anthropogenic perturbation of the carbon fluxes from land to ocean. Nature Geoscience 6(8): 597-607

Renard KG, Foster GR, Weesies G, McCool D, Yoder D (1997) Predicting soil erosion by water: a guide to conservation planning with the Revised Universal Soil Loss Equation (RUSLE). US Government Printing Office Washington, DC,

Riebe C, Kirchner J, Granger D, Finkel R (2001) Minimal climatic control on erosion rates in the Sierra Nevada, California. Geology 29(3): 447-450

Robichaud PR (1997) Spatially-varied erosion potential from harvested hillslopes after prescribed fire in the interior Northwest. In. University of Idaho, Moscow. p 219

Rumpel C, Chaplot V, Planchon O, Bernadou J, Valentin C, Mariotti A (2006) Preferential erosion of black carbon on steep slopes with slash and burn agriculture. CATENA 65(1): 30-40

Rumpel C, Leifeld J, Santin C, Doerr S (2015) Movement of biochar in the environment. Biochar for Environmental Management: Science, Technology and Implementation (second edition). New York: Routledge: 283-298

Santín C, Doerr S, Preston C, Bryant R (2013) Consumption of residual pyrogenic carbon by wildfire. International Journal of Wildland Fire 22(8): 1072-1077

Santin C, Doerr SH, Preston CM, Gonzalez-Rodriguez G (2015) Pyrogenic organic matter production from wildfires: a missing sink in the global carbon cycle. Global Change Biology 21(4): 1621-1633

Santos F, Torn MS, Bird JA (2012) Biological degradation of pyrogenic organic matter in temperate forest soils. Soil Biology and Biochemistry:

Schmidt MW, Skjemstad JO, Jäger C (2002) Carbon isotope geochemistry and nanomorphology of soil black carbon: Black chernozemic soils in central Europe originate from ancient biomass burning. Global Biogeochemical Cycles 16(4): 1123

Schmidt MWI, Noack AG (2000) Black carbon in soils and sediments: Analysis, distribution, implications, and current challenges. Global Biogeochemical Cycles 14(3): 777-793

Schmidt MWI, Torn MS, Abiven S, Dittmar T, Guggenberger G, Janssens IA, Kleber M, Kogel-Knabner I, Lehmann J, Manning DAC, Nannipieri P, Rasse DP, Weiner S, Trumbore SE (2011) Persistence of soil organic matter as an ecosystem property. Nature 478(7367): 49-56

Seiler W (1980) Estimates of gross and net fluxes of carbon between the biosphere and the atmosphere from biomass burning. Climatic Change 2(3): 207-247

Shakesby R, Coelho C, Ferreira A, Terry J, Walsh R (1993) Wildfire impacts on soil-erosion and hydrology in wet Mediterranean forest, Portugal. International Journal of Wildland Fire 3(2): 95-110

Shakesby R, Doerr S (2006) Wildfire as a hydrological and geomorphological agent. Earth-Science Reviews 74(3): 269-307

Shakesby RA (2011) Post-wildfire soil erosion in the Mediterranean: Review and future research directions. Earth Science Reviews 105(3): 71-100

Sharpley A (1985) The Selection Erosion of Plant Nutrients in Runoff. Soil Science Society of America Journal 49(6): 1527-1534

Shneour EA (1966) Oxidation of graphitic carbon in certain soils. Science 151(3713): 991-992

Skjemstad J, Taylor J, Smernik R (1999) Estimation of charcoal (char) in soils. Communications in Soil Science & Plant Analysis 30(15-16): 2283-2298

Skjemstad JO (1996) The chemistry and nature of protected carbon in soil. Australian Journal of Soil Research 34(2): 251-271

Smith D, Chughtai A (1996) Reaction kinetics of ozone at low concentrations with n-hexane soot. Journal of Geophysical Research: Atmospheres 101(D14): 19607-19620

Soucémarianadin LN, Quideau SA, MacKenzie MD, Munson AD, Boiffin J, Bernard GM, Wasylishen RE (2015a) Total and pyrogenic carbon stocks in black spruce forest floors from eastern Canada. Organic Geochemistry 82: 1-11

Soucémarianadin LN, Quideau SA, Wasylishen RE, Munson AD (2015b) Early-season fires in boreal black spruce forests produce pyrogenic carbon with low intrinsic recalcitrance. Ecology 96(6): 1575-1585

Spokas K, Novak J, Masiello C, Johnson M, Colosky E, Ippolito J, Trigo C (2014) Physical disintegration of biochar: an overlooked process. Environmental Science & Technology Letters 1: 326-332

Stacy E, Hart SC, Hunsaker CT, Johnson DW, Berhe AA (2015) Soil carbon and nitrogen erosion in forested catchments: implications for erosion-induced terrestrial carbon sequestration. Biogeosciences Discuss. 12(3): 2491-2532

Stallard RF (1998) Terrestrial sedimentation and the carbon cycle: Coupling weathering and erosion to carbon burial. Global Biogeochemical Cycles 12(2): 231-257

Tinkham WT, Smith AM, Higuera PE, Hatten JA, Brewer NW, Doerr SH (2016) Replacing time with space: using laboratory fires to explore the effects of repeated burning on black carbon degradation. International Journal of Wildland Fire 25(2): 242-248

Velasco-Molina M, Berns AE, Macías F, Knicker H (2016) Biochemically altered charcoal residues as an important source of soil organic matter in subsoils of fire-affected subtropical regions. Geoderma 262: 62-70

Wagner S, Cawley KM, Rosario-Ortiz FL, Jaffé R (2015) In-stream sources and links between particulate and dissolved black carbon following a wildfire. Biogeochemistry 124(1-3): 145-161

Westerling AL, Hidalgo HG, Cayan DR, Swetnam TW (2006) Warming and earlier spring increase western US forest wildfire activity. Science 313(5789): 940-943

Whitman TL, Zhu Z, Lehmann J (2014) Carbon mineralizability determines interactive effects on mineralization of pyrogenic organic matter and soil organic carbon. Environmental Science & Technology, 141031101135005. doi:10.1021/es503331y:

Wiedemeier DB, Abiven S, Hockaday WC, Keiluweit M, Kleber M, Masiello CA, McBeath AV, Nico PS, Pyle LA, Schneider MP (2015) Aromaticity and degree of aromatic condensation of char. Organic Geochemistry 78: 135-143

Wiedemeier DB, Hilf MD, Smittenberg RH, Haberle SG, Schmidt MW (2013) Improved assessment of pyrogenic carbon quantity and quality in environmental samples by high-performance liquid chromatography. Journal of Chromatography A 1304: 246-250

Wischmeier W (1962) Storms and soil conservation. Journal of soil and water conservation 17(2): 55-59

Wischmeier WH, Smith. DD Predicting rainfall-erosion losses from cropland east of the Rocky Mountains - Guide for selection of practices for soil and water conservation. . In: Agr. Handbk. No. 282. USDA, Washington, D.C. 1965.

Wischmeier WH, Smith. DD Predicting rainfall erosion losses. In: Agr. Handbk. No. 537. U.S. Dept. Agr. Washington, D.C. 1978.

Wondzell SM, King JG (2003) Postfire erosional processes in the Pacific Northwest and Rocky Mountain regions. Forest Ecology and Management 178(1): 75-87

Yao J, Hockaday WC, Murray DB, White JD (2014) Changes in fire-derived soil black carbon storage in a subhumid woodland. Journal of Geophysical Research: Biogeosciences 119(9): 1807-1819

Zimmerman A (2010) Abiotic and microbial oxidation of laboratory-produced black carbon (biochar). Environmental Science & Technology 44(4): 1295-1301

Zimmermann M, Bird MI, Wurster C, Saiz G, Goodrick I, Barta J, Capek P, Santruckova H, Smernik R (2012) Rapid degradation of pyrogenic carbon. Global Change Biology 18(11): 3306-3316

Ziolkowski L, Druffel E (2010) Aged black carbon identified in marine dissolved organic carbon. Geophysical Research Letters 37(16): L16601

FIGURES

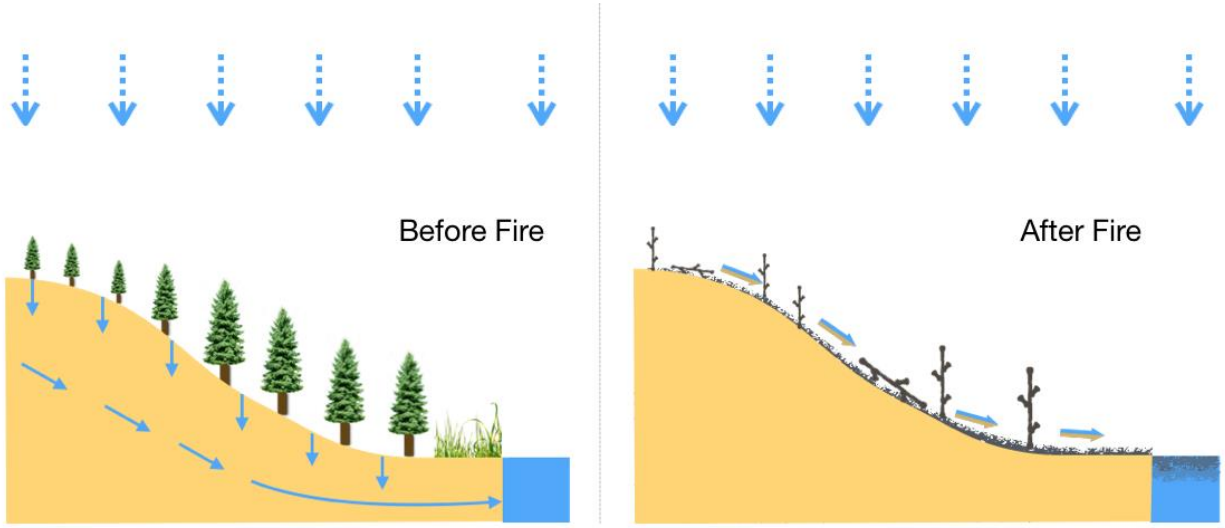

Figure 2-1 Even on the hillslope scale, fires alter dominant hydrologic flow regimes in soil, reducing infiltration and subsurface flow of water, and increasing surface runoff (Santin et al. 2015).

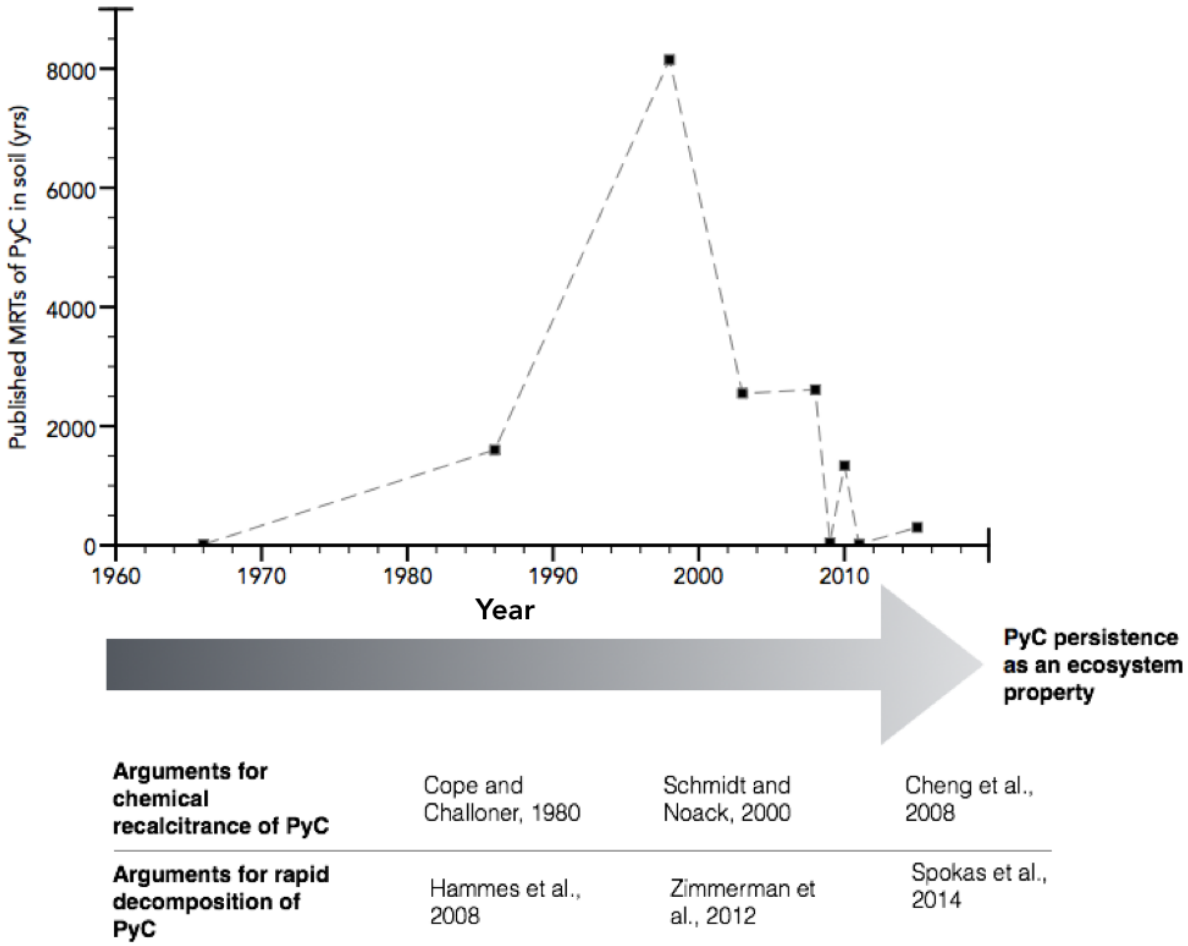

Figure 2-2. This timeline of estimated MRTs of PyC and key papers illustrates the changing paradigm on controls of PyC persistence in the soil system. Some earlier studies argued that PyC persists in soil for over thousands of years mainly due to its perceived inherent recalcitrance. Initial estimates were much higher, but around 2008 (marked by a star), a gradual shift in viewpoints (large arrow) happened as evidence for rapid decomposition and mobilization became apparent. Papers that provide support for the more rapid decomposition of PyC are listed above the large arrow, and papers arguing for the inherent chemical recalcitrance of PyC are listed below the large arrow. The estimate for char age from Cope and Chaloner (1980) was not included in the average of 300 million years, because it was not an estimate of turnover time, but it does reflect the view that PyC would reside in soil for very extended periods of time. Also, note that the x-axis is not numeric. Some of the most recent research suggests that the rate of PyC decomposition is tightly controlled by environmental conditions and its persistence in soil is a property of the ecosystem (Schmidt et al. 2011).

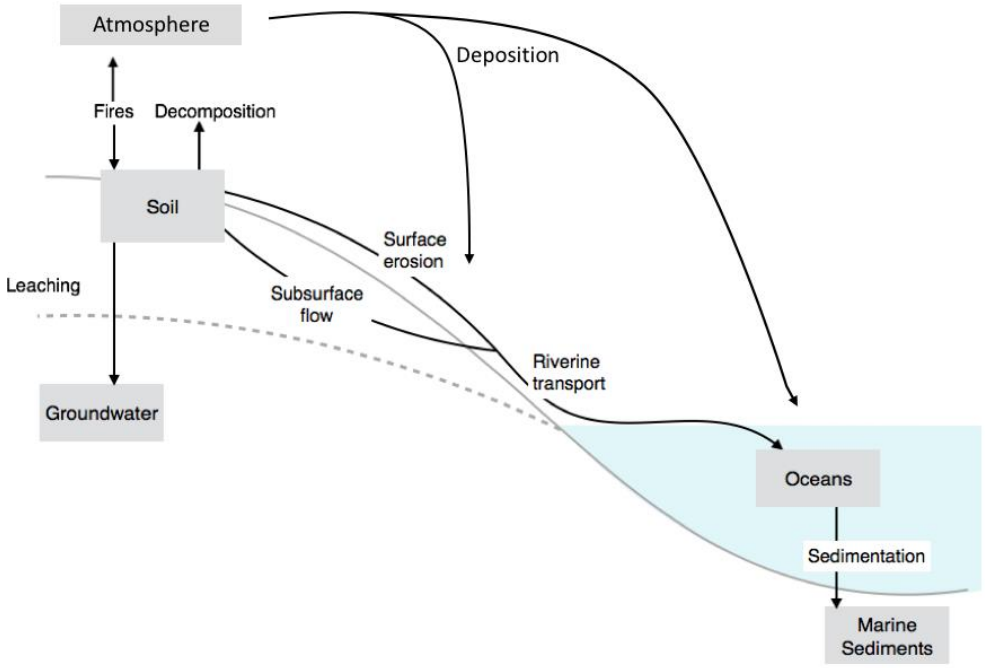

Figure 2-3 Major fluxes of PyC in the earth system. Grey boxes represent stocks of PyC and arrows indicate fluxes of PyC between stocks.

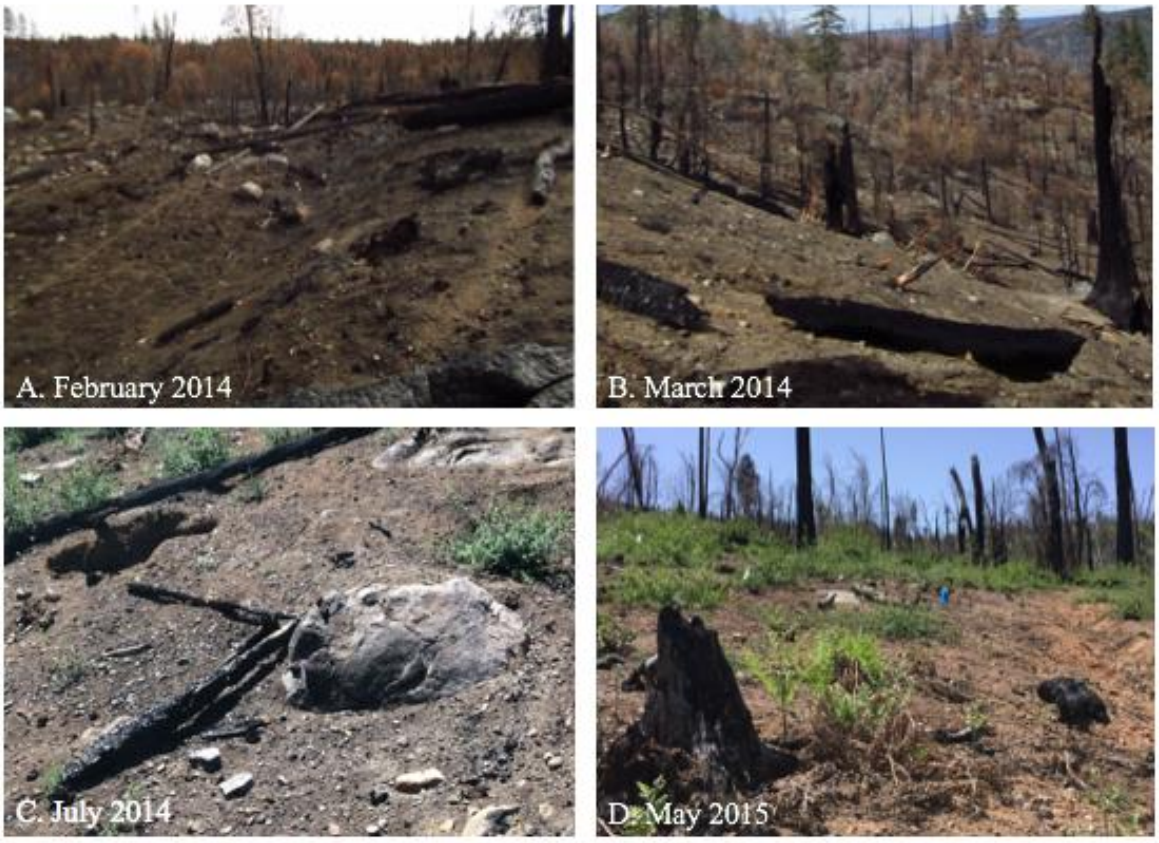

Figure 2-4. Erosion in upland temperate forests is dependent upon precipitation and topography. This progression of photographs from the Rim Fire (2013, in Yosemite National Park and Stanislaus National Forest in California, USA) illustrates the significant loss of PyC post-fire in a high-severity burn area and post-fire vegetation regrowth (all photos, R. Abney). The Rim Fire began in August of 2013 and was contained in November of 2014, with the aid of snowfall. The picture in panel A (from February 2014, three months' post-fire) illustrates the significant PyC layer remaining after the first snowmelt. The picture in panel B from March 2014 is the remaining PyC after the first major rainfall post-fire. The soil color is considerably lighter, which is evidence of loss (erosion) of highly charred material (PyC). The pictures in panels C and D have considerably less PyC covering the soil surface and illustrate the beginnings of vegetation regrowth.

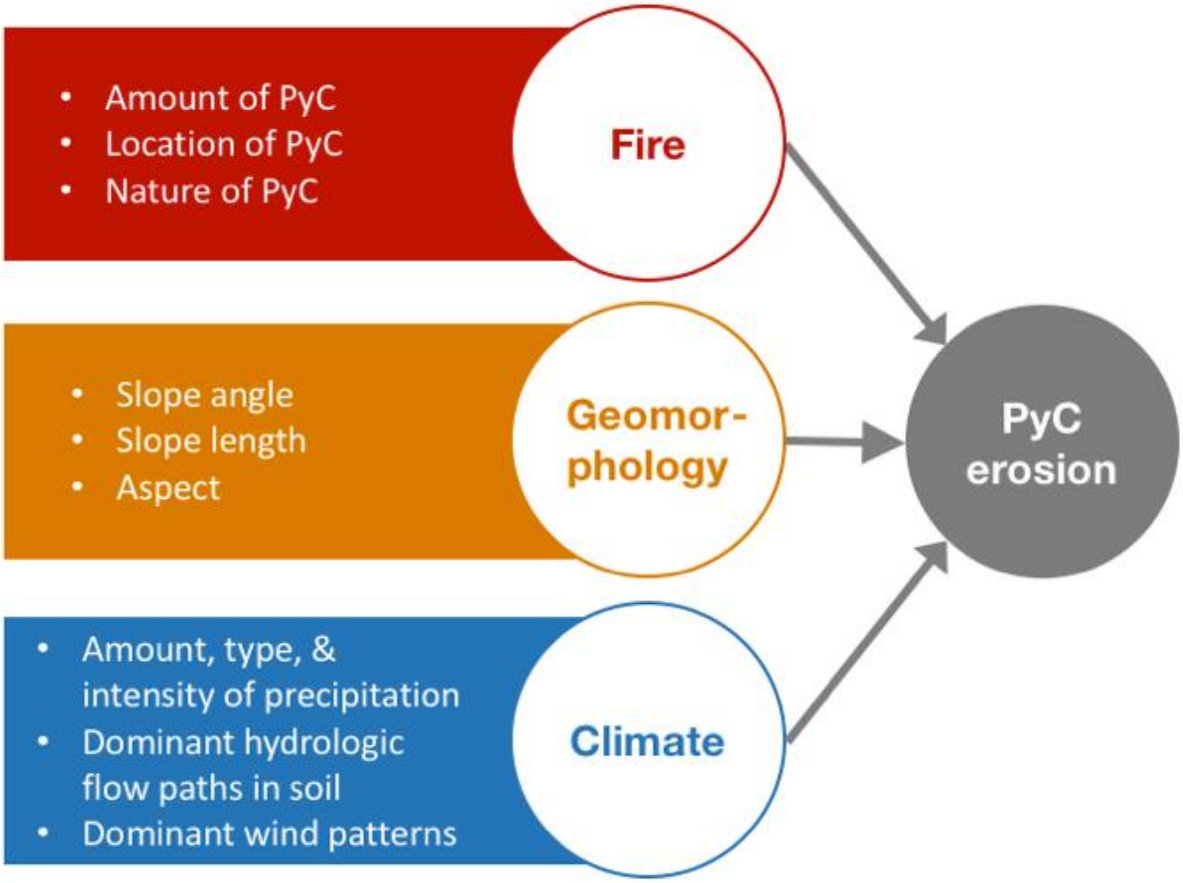

Figure 2-5. Three main factors interact to control the erosion of PyC in any environment: landscape, climate and hydrology, and the amount and nature of PyC produced from fire. These three factors interact with each other in both space and time to impact the fate of PyC.

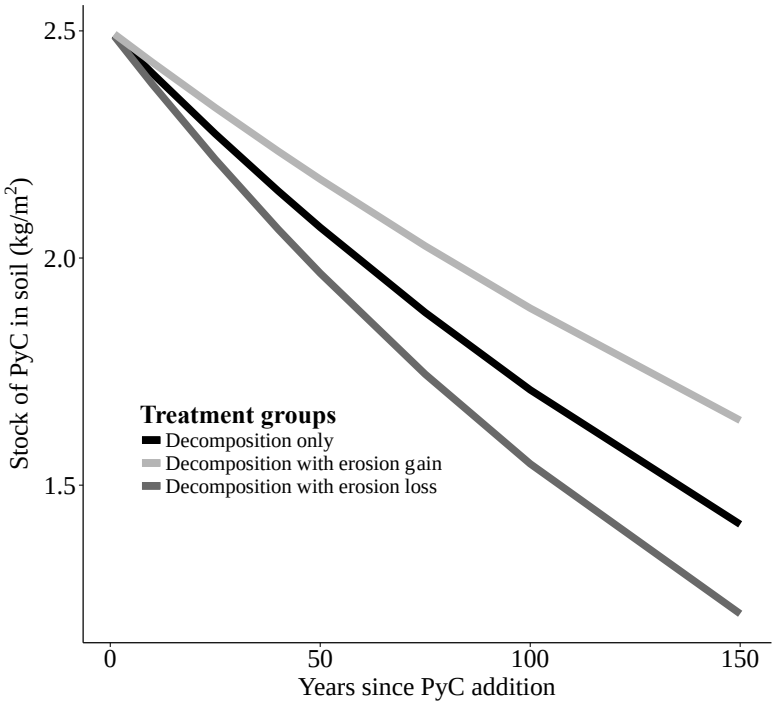

Figure 2-6. The difference in PyC stock when erosion is considered as a loss (e.g. via transport out of a soil) vs. a gain (e.g. in depositional landform positions) in a model of PyC loss over 150 years can lead to around a 200 g difference in PyC stock per m^2 after 100 years. The assumed initial stock of PyC was 2.5 kg/m^2 (Hammes et al. 2008), and the base decomposition rate was derived from a 263-year turnover time (k_0 = 0.0038, from Equation 1). The rate of erosion was assumed to be 0.001 (K_e, from Equation 1), which equates to a 1000-year turnover time. This model also assumes a single input of PyC into the soil. In reality, multiple fires would have occurred during the 150-year run of this model, suggesting that soil PyC stocks would not decline at this rate.

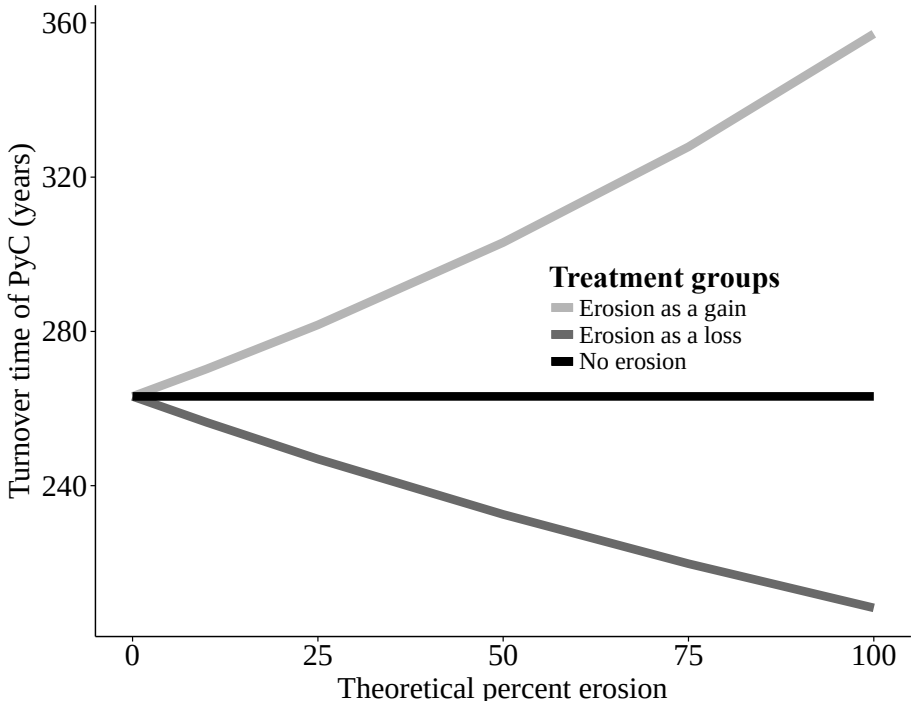

Figure 2-7. The error associated with discounting erosion as either an input (deposition of material) or loss (erosion of material) term can lead to an approximately 150-year difference error in turnover time. The theoretical percent erosion is the percent of an erosion rate (K_e, from Equation 1) that is accounted for within this model from an assumed rate of erosion of 0.001 (1000-year turnover time of PyC via erosion, a slow erosion rate). This erosion rate is added (deposition of material) or subtracted (erosion of material) from a base decomposition rate (k_0, from Equation 1) of 0.004, corresponding to a 250-year turnover time (Hammes et al. 2008). A theoretical percent erosion of 0% corresponds to no erosion contribution of input or output of PyC from a soil; whereas a theoretical percent erosion of 100% would lead to either an input (gain) of PyC into the soil or loss of PyC from the soil that would increase or decrease the turnover time of PyC by approximately 70 years respectively.

TABLES

Table 2-1 Decomposition rates measured in laboratory and field studies, as converted to percent mass loss of PyC per year. The range of reported loss rates for incubation experiments (1.5-20%) is considerably higher than field experiments (0.08-15%). For the box model, the decomposition was assumed to be 5% loss per year, which was selected as a conservative estimate within the range of decomposition rates reported within the current literature.

%PyC mass loss in a year	Type of experiment	Source of PyC	Method to measure PyC	Citation
Laboratory experiments				
2	Incubation, at tropical conditions	Mulga (*Acacia aneura*)	^{13}C direct polarization NMR spectroscopy, hydrogen pyrolysis	Zimmermann et al. (2012)
10-20	Incubation, temperature change from 4°C to 60°C	Laboratory generated corn (*Zea mays L.*) char at 350°C	^{13}C direct polarization NMR spectroscopy	Nguyen et al. (2010)
4-20		Corn char at 600°C		
2.3-15		Oak (*Quercus spp.*) char at 350°C		
1.5-14		Oak char at 600°C		
0.02-4.89	Three simulations of PyC loss via decomposition ranging from 2 to 2000 years	N/A	N/A	Foereid et al. (2011)
0.38	Laboratory incubation – O horizon	Laboratory generated char from ponderosa pine (*Pinus ponderosa*)	Chemo-thermal oxidation at 375°C	Hatten and Zabowski (2009)
0.24	A1 horizon			
0.08	A2 horizon			

0.7	Laboratory incubation: average over 8.5 years	Ryegrass (*Lolium spp.*)	^{14}C labeled biochar	_ENREF_88 Kuzyakov et al. (2009)
0.25	Average PyC loss between years 5 and 8			
	Field experiments			
1	Field chronosequence: first 30 years after production	Field burning of maize (*Zea mays L.*)	^{13}C CPMAS NMR spectroscopy, FTIR	Nguyen and Lehmann (2009)
3.2	Field chronosequence: first 5 years after production		Manual identification	
1.1	Field experiment in native savannah	Mango trees (*Mangifera indica L.*)	Mixing model from $\delta^{13}C$ of PyC and field soil	Major et al. (2010)
0.25	Field experiment	Natural PyC in chernozem	BPCA	Hammes et al. (2008)

Table 2-2 Stocks and fluxes of PyC used our simple box model to assess steady state hypotheses. The initial conditions for the stocks and fluxes were found from a variety of sources within the available literature on PyC. Where stock information was not available, initial starting values were assumed to be 0 (marked N/A), even though this is likely not the case in reality. For example, Paleosols provide evidence that buried soil can store PyC for long periods of time (Chaopricha & Marín-Spiotta 2014). Flux data in terms of input and loss of PyC from the various stocks were used as rates of loss from each of the stocks or movements between the pools within the box model. These rates of loss or transfer of PyC were applied as a fraction of the pool lost per year.

Model parameter	Amount	Citation
Initial global stocks of PyC		
Soil PyC	$1.05x10^{15}$ g PyC	Nguyen and Lehmann (2009), Soucémarianadin et al. (2015a)
Ocean	$9.87x10^{18}$ g PyC	Ziolkowski and Druffel (2010)
Buried soil	0 g PyC	N/A
Groundwater	0 g PyC	N/A
PyC in marine sediments initial stock	$1.79x10^{22}$ g PyC	Masiello (1998)
Loss of PyC from soil		
Percolation and leaching to groundwater	1% per year	Abiven et al. (2011), Major et al. (2010)
Erosion of PyC	0.38% per year	N/A* corresponds to turnover time from Hammes et al. (2008)
Decomposition of PyC in soil	5% per year	Foereid et al. (2011), Hatten and Zabowski (2009), Nguyen et al. (2010), Spokas et al. (2014), Zimmermann et al. (2012), conservative for field setting
Decomposition during transport or after burial	20.2% per year	Jacinthe and Lal (2001), from non-pyrogenic carbon loss in transported soil
Groundwater flow through rivers to ocean	1%	Major et al. (2010)
PyC exported to oceans by rivers	$7.4x10^{12}$ g PyC per year	Dittmar et al. (2012), Jaffé et al. (2013)
PyC sedimentation in ocean	0.02% leaves by sedimentation per year	Masiello (1998)
Input of PyC to soil		
Fire inputs of PyC	$1x10^{14}$g PyC per year	Jauss et al. (2015), Preston and Schmidt (2006)

CHAPTER 3: PYROGENIC CARBON EROSION AFTER THE RIM FIRE, YOSEMITE NATIONAL PARK: ROLE OF FIRE SEVERITY AND TOPOGRAPHY ON DETERMINING FATE OF PYC

ABSTRACT

Pyrogenic carbon (PyC), an important component of the global soil carbon (C) cycle, may constitute up to 35% of all soil C and have longer soil residence times compared with non-pyrogenic components of the soil C pool. The physical and chemical nature of PyC, including its low density and concentration in surface soils, leads to its preferential erosion in fire-prone dynamic landscapes. To investigate geomorphic and fire-related controls on PyC erosion, sediment fences were established in three combinations of slope (high slope of 13.9-37.3%; moderate slope 0-6.7%) and burn severity (moderate and severe) plots in the area affected by the Rim Fire in 2013, Yosemite National Park, California, USA. After each major precipitation event, immediately following the Rim Fire, we determined transport rates of total bulk sediment trapped in sediment fences, fine and coarse sediment fraction transport, and carbon (C) and nitrogen (N) transport. In addition, we measured stable isotope ($\delta^{13}C$ and $\delta^{15}N$) compositions and ^{13}C-nuclear magnetic resonance (NMR) spectra of soils from eroding hillslopes and eroded sediments. The highest rates of total and fine (<2 mm) sediment transport in high severity burned areas was correlated with the initial discharge peaks from an adjacent stream, while the moderate burn severity sites had considerably more of the >2 mm fraction transported than the high burn severity sites. The $\delta^{13}C$ and $\delta^{15}N$ values and ^{13}C-NMR analyses indicated that the sediment eroded from the moderate severity burn areas included fresh organic matter that was not as significantly affected by the fire, whereas sediments from high severity burn areas were enriched in pyrogenic matter. Our results suggest that burn severity, not geomorphology of the landscape, plays a primary role in controlling soil or PyC transport dynamics post-fire. The preferential erosion of PyC post-fire has major implications for the long-term fate of PyC within the soil system, and may be an important in determining whether PyC is transported to aquatic systems.

INTRODUCTION

Fire and erosion can have multiple independent and interactive effects on soil health, plant productivity, and biogeochemical cycling of essential elements. Little is known about how the interactions of complex topography and changes in soil properties due to fire (i.e., loss of vegetative plant and litter cover and increased hydrophobicity in topsoil) can affect post-fire soil carbon (C) and overall terrestrial organic matter (OM) dynamics, however the terrestrial biosphere is dominated by sloping landscapes (Staub & Rosenzweig 1992) and around 450 Mha of the globe is impacted by fire annually (Randerson et al. 2012). These interactions can determine the redistribution of nutrients and OM post-fire, which are important controls on the available nutrients for post-fire regrowth (Johnson et al. 2007). These erosional geomorphic processes play crucial roles in controlling soil chemical and physical properties, biogeochemical processes within the soil system, and flux of elements from terrestrial to aquatic systems (Berhe 2012; Berhe et al. 2012a; Harden et al. 1999; Stallard 1998).

Erosion and SOM dynamics

Erosion globally redistributes 75 Gt of soil and 1-5 Gt soil organic carbon (SOC) annually (Battin et al. 2009; Berhe et al. 2007; Regnier et al. 2013; Stallard 1998). Erosional redistribution of topsoil affects numerous processes in the source catchments and moves soil and essential elements from terrestrial to aquatic ecosystems. About 70-90% of that eroded material is redistributed downhill or downstream but is not exported out of the source watershed (Gregorich et al. 1998; Lal 2003; Rumpel et al. 2006a). In upslope eroding landform positions, erosion leads to a loss of SOM from soil profiles through direct removal of soil mass. In contrast, in depositional landform positions, erosion leads to input and stabilization of at least some of the eroded soil organic matter (SOM) through processes including: (1) enhanced rates of plant productivity in depositional landform positions; (2) new and reconfigured associations of the eroded SOM with soil minerals, and (3) burial from subsequently eroded material (Berhe et al. 2012b; Sharpley 1985). When considered at the watershed scale, and accounting for the replacement of eroded OM by production of new photosynthate in eroding slopes and the stabilization of some eroded OM in depositional settings, soil erosion and deposition act together to induce a net terrestrial sink of 0.12 – 1.5 Gt C yr^{-1}, (Berhe et al. 2008; Berhe et al. 2007; Harden et al. 1999; Stallard 1998; Van Oost et al. 2007).

Fire and SOM dynamics

One of the major by-products of fire is the formation of pyrogenic carbon (PyC), which results from the incomplete combustion of biomass and includes a range of products such as ash, charcoal, and charred biomass (Bird et al. 2015; Masiello 2004). In the soil system, PyC is persistent with reported mean residence times ranging from centuries to millennia (Hammes et al. 2007; Hammes et al. 2008; Lehmann 2007; Lehmann et al. 2008). Additionally, PyC has a high surface area, which allows it to have higher reactivity compared with non-pyrogenic C, and has been shown to serve as a sorbent for SOM (Chia et al. 2012; Cornelissen et al. 2005; Mukherjee et al. 2011). Condensation of volatile organic compounds during moderate to low combustion temperatures also render soil more

hydrophobic compared to unburned soil (DeBano 2000; Doerr et al. 2004; Mataix-Solera et al. 2011; Shakesby & Doerr 2006). The properties of PyC and charred soil depend heavily on the combustion temperature, with higher temperatures leading to the loss of many soil nutrients and higher pH, among other soil property shifts (Araya et al. 2016; Araya et al. 2017).

Significance and effects of PyC erosion

There are numerous complex interactions between fire and erosion, and the extent of these interactions depends on fire intensity, post-fire management, climate (Certini 2005), and rate of vegetation recovery (Baker 1988). Erosion, in turn, can indirectly affect vegetation and soil moisture content. Both fire and erosion are controlled by climate to various extents (Imeson & Lavee 1998; Neary et al. 1999; Riebe et al. 2001). The size of watershed and topography (Iniguez et al. 2008; Liu et al. 2003), and amount, intensity, and temporal distribution of precipitation can influence the rate of bulk SOM and PyC loss from or redistribution within an eroding watershed (Cain et al. 1999; Nearing 1998). Many erosion prediction models such as the Universal Soil Loss Equation (Wischmeier & Smith. 1965; Wischmeier & Smith. 1978) have confirmed the importance of slope and topographic characteristics for soil erosion.

Numerous properties of PyC make it highly susceptible to erosion (Abney & Berhe In Review; Rumpel et al. 2006a). The majority of PyC is produced and deposited on the soil surface, which is the first material to erode from a hillslope. During low- to moderate-temperature combustion, hydrophobic layers can form beneath the soil surface, leading to decreases in the infiltration rate of water (DeBano 2000; DeBano et al. 1998; Doerr & Thomas 2000; Robichaud 1996). The hydrophobic properties and low density of PyC also increase the likelihood for it to be transported by flowing water by, for example, saturated overland or Hortonian flows (Shakesby & Doerr 2006). These properties can interact to make PyC susceptible to preferential erosion over non-pyrogenic material (Abney & Berhe In Review).

A handful of previous studies (Rumpel et al. 2009; Rumpel et al. 2006b) have provided direct evidence for the preferential erosion of PyC post-fire, and some research has provided some evidence for the non-erosive nature of PyC (Nguyen et al. 2009). However, as of yet, the relative rates of PyC vs. bulk SOM erosion at the scales of plots, hillslopes or watersheds remain relatively unexplored. Our investigation seeks to determine how and if the preferential erosion of PyC is a function of both the properties of the PyC, as a function of burn severity, or PyC formation conditions, as well as the timing and magnitude of erosion events at the hillslope scale.

Research Objectives

This project aims to understand how the interaction of burn severity and slope control erosional transport of organic matter (total SOM and PyC) in upland temperate forest ecosystems. Specifically, we determine: (a) how slope and fire severity interact to control transport of different soil constituents (i.e., fine and coarse sediments, soil C, N, and PyC

concentration in sediments); and (b) how fire intensity controls nature of bulk C and PyC mobilized by erosion.

METHODS

Study site

This study was conducted in the Sierra Nevada mountain range of California, in the area affected by the Rim Fire in 2013. The Rim Fire burned over 1000 km^2 land from August to November of 2013, in an area that covered parts of Yosemite National Park and Stanislaus National Forest. The specific study watershed used in this study is Poopenaut West, which is located within Yosemite National Park, in a sub-watershed of the Tuolumne River basin. The watershed has a mean annual precipitation of 915 mm. For the one-year study period, the Tuolumne River basin was at 58% of average precipitation (CDEC 2016), and the watershed was under transitive snow cover from the time of burn containment to initial sampling.

Sites were selected along a single hillslope in the watershed within the perimeter of the Rim Fire, near the Hetch Hetchy entrance to Yosemite National Park, with elevations ranging from 1475 to 1740 m above sea level (Figure 1). Holocene era granitic glacial deposits underlie the study area (Huber et al. 1989), and the soils are dominated by coarse-loamy, isotic, frigid Typic Dystroxerepts; coarse-loamy, isotic, frigid Humic Dystroxerepts; coarse-loamy, isotic, mesic Typic Dystroxerepts (United States Department of Agriculture 2007). The study area is a mixed conifer forest, with *Pinus jeffreyii, Pinus ponderosa, Ceanothus sp.,* and *Manzanita sp.*

Vegetation and soil burn severity were assessed using the Burned Area Reflectance Classification (BARC), which assesses the infrared reflectance of a landscape in comparison to references (Hudak et al. 2014), and this burn classification was ground truthed to create a soil burn severity map (Parsons et al. 2010). Burn severity and topographical maps (Figure 1) were used to select sites that varied on burn severity and slope. We set up sampling areas in three classification groups: (a) **HH**: High severity burn, high slope (26-41º); (b) **HM**: High severity burn, moderate slope (5-23º); and **MH**: Moderate severity burn, high slope (21-27º). The major difference we observed among the three classification groups was the remaining vegetation. The high severity burn areas were completely stripped of vegetation cover, mainly leaving behind burned tree trunks and exposed soil surfaces overlain by a patchy, and occasionally several cm thick, char cover. In the medium severity burned areas, a considerable number of trees survived the fire, leaving 65% canopy cover compared with <30% canopy cover in high severity burn sites and hence, the groundcover constituted a mixture of charred and fresh litter that presumably fell after the fire.

Field sampling methods

Sediment fences were established by staking down a tarp with rebar parallel to the hillslope and the upslope source area was delineated with trenches. Source areas for sediment fences were 100 m^2, with dimensions of 20 m long and 5 m wide. Seven sediment fences were established within each classification group (n=3) for a total of 21 fences (Figure 2). The sediments within these fences were sampled after every precipitation event post-fire

beginning after spring snowmelt, with a total of four precipitation events during the spring of 2014 and 84 sediment samples (see Figure 3). Precipitation events were monitored via a tipping bucket rain gauge in the Poopenaut West stream that flows below the sediment fences (Figure 1). Sediment was allowed to dry for several days within the fence and was collected by sweeping the entire fenced area with a broom until it was cleared. Once collected, the sediment was weighed, and dry sediment mass was determined by gravimetrically correcting for water content by drying subsamples of the sediments in the oven for 24 hours at 105ºC.

Soils were collected during the spring of 2014 from the area directly upslope from the marked source material for the sediment fence areas that represent putative source soils for the material eroded into the sediment fences. Soils were collected from three randomly selected sites to capture the variability of the soil and within a meter of the source area perimeter and at least a meter apart from each other. Soils were collected at each sediment fence from each treatment group, for a total of 63 soil samples. Soils were collected using a closed bucket metal auger with a 5-cm diameter with plastic sleeve, and capped after removal from the ground. Soils were kept on ice until returning to the laboratory, where they were stored at 4 ºC until further analysis. Soils were separated into depths of 0-5 cm and 5-10 cm in the laboratory.

Laboratory analyses

Additionally, *Pinus ponderosa* litter and duff was collected from unburned forest near the Rim Fire affected area immediately after the fire (November 2013). This litter was collected to assess the changes in litter chemistry with increasing charring temperature. The litter was charred under no oxygen, pyrolysis conditions in a furnace at two temperatures (250ºC, 550ºC), with a 50ºC control, for an hour to determine how fire temperature controls the nature of the organic matter that is typically found on the soil surface post-fire.

Field-moist sediment and source soil samples were passed through a 2 mm sieve (defined as coarse and fine fractions). The <2 mm fraction was analyzed for pH in both deionized water and 0.01M $CaCl_2$ 1:2 soil (sediment):solution mass ratio (Hendershot et al. 2008; Schofield & Taylor 1955). We determined particle size distribution via the hydrometer method (Bouyoucos 1962) and bulk density of the source area soils using the core method (Blake & Hartge 1986). Soils and sediments were tested for the presence of carbonates using 1M HCl, and no carbonates were found in any sample.

A representative subsample of the sieved <2 mm fraction of the soil and sediment samples was air-dried and ground using a SPEX Mill (SPEX Sample Prep, Metuchen, NJ, USA). Carbon and nitrogen concentrations, as well the $\delta^{13}C$, and $\delta^{15}N$ values of these samples, were determined on a Costech ECS 4010 CHNSO Analyzer interfaced with a Conflo IV interface to a Delta V Plus Isotope Ratio Mass Spectrometer at UC Merced's Stable Isotope Laboratory. Approximately 7 mg of air-dried sample was weighed into 4x6 mm tin capsules. The samples were measured relative to an acetanilide standard and a laboratory soil internal standard. These internal standards were compared with international standards: atmospheric N for the $\delta^{15}N$ standard and to Vienna Pee Dee Belemnite for the

δ^{13}C. Standards were measured in triplicate with precision of ±1.84% C, 0.29 % N, 0.77‰ δ^{13}C, and 0.09‰ δ^{15}N. Samples were measured in triplicate with precision of ±0.80% C, 0.02% N, 0.07‰ δ^{13}C, and 0.02‰ δ^{15}N. Sample error was likely smaller than the standard error due to the considerably larger number of standard replicates that were run. Concentrations of C and N were corrected to air-dry weights by oven-drying previously air-dried, ground samples at 105ºC for 24 hours, and multiplying the C or N concentration by the ratio of weight of air-dried sample by the weight of oven-dried sample.

For the NMR analyses, a subset of 16 soils and sediments was selected to incorporate the different treatment groups and sampling time points. This subset of samples was demineralized with a 10% HF/HCl solution, followed by rinsing five times with MilliQ DI water to increase the C concentration in the samples as well as to remove minerals and paramagnetic interference from iron and manganese in soil, and thereby improve the signal to noise ratio of the NMR analysis (Gélinas et al. 2001). These demineralized samples, along with the laboratory-charred litter, were analyzed on a 300 MHz Bruker Avance III NMR (nuclear magnetic resonance) spectrometer using MAS (magic angle spinning) and a 4 mm probe spun at 12 kHz. Between 50-150 mg of sample was packed into a 4 mm zirconia rotor, which had a frequency of 75 MHz to collect cross polarization spectra. Between 1,600 and 64,000 scans were taken, with a ≥2.5 second relaxation delay. Phase and baseline corrections, along with integrations, were completed in Bruker TopSpin software (Version 3.0).

Spectra were integrated into 7 regions: 0-45 ppm (Alkyl), 45-60 ppm (N Alkyl/Methoxyl), 60-95 ppm (O-Alkyl), 95-110 ppm (Di-O-Alkyl), 110-145 ppm (Aromatic), 145-165 ppm (Phenolic), and 165-215 ppm (Amide/Carboxyl). The percentages from the integrated spectra, constrained by their C and N concentrations, were used to run the 6-component molecular mixing model (MMM) to infer biomolecular SOM constituents (Baldock et al. 2004a; Nelson & Baldock 2005).

Statistical analyses

All sediment, bulk C, N, and isotope data were analyzed for differences across treatment group using mixed linear effects models. We used classification group and sampling time as fixed effects both with and without interactions. The specific plot number (e.g. HH1) was entered into the models as a random effect to account for the repeated measurements on each sediment fence. P-values were obtained using ANOVA and Tukey honest significant difference test to compare models with empty models that had no fixed effects and were considered significant at $p<0.05$. No transformations were applied to the data prior to statistical analysis. Data were organized and archived in Microsoft Excel, and all statistical analyses and plots were generated in R (www.r-project.org).

Enrichment ratios (ER) were calculated by dividing concentrations of C, N, and PyC in eroded sediments with those in the top source soils from 0-5 cm for each of the sediment fences. However, it is likely that it is only the top cm of soil that is eroded, so this calculation may serve to overestimate enrichment ratios. An enrichment ratio greater than one indicates that the sediment has higher concentration of PyC (or C, N) than the source

soil, and that the PyC (C, N) is being preferentially transported away from its source location compared to other soil constituents.

RESULTS

Source soils and mobilized sediment

Source soils from the Rim Fire area had neutral to basic pH values that ranged from 6.5 to 7.8, and they were significantly dependent on slope classification group and month (χ^2 (5)=24.538, p=0.000171, Table 1). Source soils had C concentrations ranging from 3-4%, with the high burn severity sites having non-significantly higher C concentration (p=0.06) than the moderate burn severity sites. The C concentration did not vary significantly with depth (p=0.12). The high burn severity classification sites also had almost double the concentration of N compared with the moderate burn severity plots, but this was statistically non-significant (p=0.06). However, the N concentration declined significantly with depth (p=0.04).

The mobilized sediment from high and moderate severity classification areas had slightly lower pH values to the source soils, ranging from 5.4 to 7.4. There were no major trends in the pH throughout the sampling period, however the March sampling point was significantly (p=0.007) lower than the rest of the sampling times. There were no significant differences in the pH between the classification groups (p=0.95, 0.99, 0.92).

There were no significant differences in sand transport between the classification groups (p=0.21, p=0.77, p=0.05). However, the sand fraction varied significantly by month (χ^2 (5)=24.272, p=0.000192), with May having significantly lower sand transport compared with April (p=0.001) and March (p=0.001). May had significantly higher silt transport than any of the other sampling times (p=0.001, p=0.001, p=0.001). There were no significant trends in the clay fraction with either sampling time or classification group (χ^2 (5)=2.8871, p=0.7174).

The most sediment was transported during the time periods of greatest precipitation (Table 2), with February and March having significantly higher (p=0.007, p=0.001, p=0.001, p=0.001) sediment transport across all classification groups (high severity, high slope; high severity, moderate slope; and moderate severity, high slope) than April or May. The moderate severity plots produced significantly less (p=0.03) sediment than the high severity moderate slope classification group, and non-significantly less (p=0.73) than the higher burn severity high slope classification group.

Erosion of the fine sediment fraction was significantly higher (p=0.001, p=0.001) in February and March than in April or May (p=0.001, p=0.001). The moderate burn severity classification group had significantly less fine fraction transport compared with the high burn severity moderate slope classification group (p=0.01) and non-significantly less than the high burn severity high slope classification group (p=0.58). The coarse fraction was comprised of pine needles, pinecones, deciduous leaves, twigs, bark, charcoal, and small rocks. The coarse fraction had significantly lower (p=0.001, p=0.025, p=0.001) transport in the month of May, and the moderate burn severity sites had significantly higher

(p=0.018, p=0.001) sediment transport than either of the high burn severity classification groups. The moderate burn severity sites still had live and dying trees undergoing needle drop and aerial litter deposition, which served as a major contributor to the coarse sediment fraction.

Carbon and nitrogen mobilization

In the sediment, carbon and nitrogen concentrations changed significantly throughout the sampling period, with April having significantly less C than February (p=0.001) and March having significantly more than February (p=0.001, Figure 5), and they were significantly predicted by sampling time and classification group (χ^2 (5)=24.538, p=0.00009). Average carbon concentration ranged from 3-10%, and the average nitrogen concentration ranged from 0.1-0.5%. There were no significant differences in C concentrations between the treatment groups (p=0.14, p=0.89, p=0.34), however the high severity burn high slope had almost double the concentrations of N compared with the moderate burn severity classification group, which was statistically significant (p=0.02). The atomic C:N ratio for the high severity plots ranged from 18 to 40, and ranged from 19 to 48 in the moderate burn severity plots, and there were no significant trends with classification group or sampling time (χ^2 (5)=7.6238, p=0.1782). The C:N in the moderate burn severity burn plots was non-significantly higher (p=0.09) than in the high burn severity, high slope plots, and was none significantly (p=0.15) higher than the high burn severity, moderate slope plots.

A comparison of source soil and eroded sediment revealed that the moderate severity classification group had sediment that was enriched (enrichment ratio > 1) in both C and N compared to the source soil (Figure 6). The sediments from the two high severity classification groups were enriched in C and N compared to their source soils only during the month of March. During the rest of the time points, these higher severity sites were depleted (enrichment ratio < 1) in C and N compared to source soils.

Stable isotope analyses

The δ^{13}C from the sediment and soil samples collected from the Rim Fire (Figure 7) ranged from -27 to -25‰ and there were no significant (p=0.33, p=0.14, p=0.88, Figure 7) isotopic changes over the between the burn and slope classification groups. There also was one significant differences in δ^{13}C values between the sampling months, in that February was slightly, but significantly higher than April (p=0.03). The δ^{13}C of sediments from the medium severity burn were more variable than those from the high severity burn areas. The δ^{15}N values ranged from -2 to 4‰, and February and March were significantly higher than April (p=0.001, p=0.001), and May was significantly lower than February or March (p=0.002, p=0.001). However, there were significant differences of about 1‰ in the δ^{15}N values between each of the burn severities, where the HM group was significantly higher than the HH group (p=0.001) and MH was significantly lower than HM and HH (p=0.0000, p=0.0000).

NMR and MMM analyses

The NMR analyses of the sediments and soils indicated that the increasing charring temperatures of litter led to significant changes in the chemical composition of the litter

(Figure 8, Table 4), with the lower temperature char spectrum showing a higher proportion of sugars and other aliphatic compounds compared with the high temperature char, which had a more prominent aromatic peak at 128 ppm. The field collected char from the moderate severity burn area most closely resembles the laboratory *Pinus* litter charred at 250 ºC (Figure 8).

The high burn severity soils had higher proportions of alkyl functional groups (16-20%) compared with high burn severity sediments (8-15%), which had 42-50% aromatics compared with the soil range of 32-36% aromatic functional groups (Table 4). The moderate severity burn soils had 30-44% aromatics with 13-24% alkyl functional groups, which the moderate severity burn sediments had a higher proportion of alkyl C, ranging from 13 to 21%, and a lower proportion of aromatics, ranging from 25-34%.

The MMM indicated that with increasing charring temperature, the *Pinus* litter lost carbohydrates going from 27% carbohydrates for fresh litter, compared to 1% after charring at 550ºC. Other important changes in litter chemistry with increased charring temperature included loss of lipids, carbonyl groups, and lignin (Table 5). The increased proportion of aromatic functional groups in the charred *Pinus* litter translated to 79.9% of char for the 550ºC temperature. We also observed an increase in the proportion of proteins up to 250ºC, followed by a decline in protein concentration in 550ºC char. The high burn severity sediments had twice as much char-C compared with the moderate severity burn sediments, with lower proportions of carbohydrates and lipids (Table 5). The moderate severity burn sediments had higher proportions of carbohydrates and lower proportions of carbonyl groups and proteins.

Spectra from sediments in the high severity burn areas (HH and HM) showed consistently higher proportions of aromatic functional groups (i.e., charred remains) compared with their source soils (Figure 9). In contrast, spectra for sediments from the medium severity burn area (MH) were considerably different than HH and HM. Sediments from this treatment group had spectra that contain higher concentrations of presumably fresh, uncharred OM as indicated by the large peak in the O-alkyl region, which represents simple carbohydrates and proteins.

PyC enrichment ratios

Sediments eroded from the two high burn severity classification groups (HH and HM) were consistently enriched in PyC, while sediments from the moderate severity burn sediments were consistently depleted in PyC (Figure 6). The enrichment ratio of PyC in the high burn severity sediments declined throughout the sampling period, although not enough spectra were collected to perform statistical analyses on these data.

DISCUSSION

The interaction of fire intensity and slope in controlling sediment transport

Erosion-driven transport and redistribution of OM and PyC post-fire was controlled by both burn severity and slope after the Rim Fire. The major driver of total sediment transport was precipitation intensity, which aligns with the USLE (Wischmeier & Smith. 1965; Wischmeier & Smith. 1978) and other field research (Renard et al. 1997). Slope alone did

not play a significant role in controlling the sediment erosion in this hillslope as suggested by the USLE. In moderate burn severity sites, as more coarse litter material was left unconsumed by the fire, more litter remained available to be eroded. Conversely, the high burn severity sites had considerably more erosion of the fine fraction, likely resulting from a loss of soil physical stabilization mechanisms, such as aggregation (Albalasmeh et al. 2013; Shakesby & Doerr 2006), and loss of surface protection from cover by vegetation and litter, as evidenced by the greater proportion of the >2mm fraction in the moderate burn severity sites.

While slope and burn severity can each control the transport of material, in this study burn severity played a bigger role, which is likely reflective of the unprotected nature of the soils in the high burn severity plots. These exposed soils would have experienced the full force of raindrop impact due to lack of vegetative or litter cover, which can further break down aggregates and enhance erodibility of topsoil (Kinnell 2005) and associated bulk SOM and PyC. If the moderate burn severity sites had not had a thick litter cover, considerably more sediment transport may have occurred.

The role of burn severity in controlling soil and sediment OM quality

Burn severity played a role in controlling the amount of both coarse and fine sediment transported after the Rim Fire. Sediment eroded from the moderate severity burn areas was enriched in C and N concentrations compared to their source soils and contained more fresh, organic-rich material than the high severity plots (Figure 6). Greater OM in eroded material from moderate severity burn sites, was likely a result of the post-burn needle drop, which was, at least partially, incorporated into the OM of the soil and eroded material.

The high burn severity sites had lower OM and more highly charred material, which is reflected in the relatively enriched ^{15}N value in the high burn severity sediments. This enrichment of ^{15}N with higher burn severity is characteristic of biomass exposed to higher charring intensities, which has been widely reported to impact the $\delta^{15}N$ value of soils (Grogan et al. 2000; Huber et al. 2013; Pyle et al. 2015; Saito et al. 2007) by consuming the relatively fresh OM, that is depleted in ^{15}N, on the surface of soil, by selectively consuming ^{14}N during combustion or pyrolysis (Pyle et al. 2015), or by the loss of NH_4^+ compared with NO_3^- (Schmidt & Stewart 1997). The similarity in the $\delta^{13}C$ value of sediments is expected in soils with the same or similar vegetation, as previous research has indicated that $\delta^{13}C$ typically does not shift with increasing charring temperature (Pyle et al. 2015).

In high severity burn sites, the enrichment ratios of C and N were closer to one, and more closely resembled the soil mineral material. The high severity burn sites had no remaining live trees to drop needles; thus, mineral material and large woody char fragments dominated the coarse fraction. However, the sediments from these plots were enriched in PyC, whereas the sediments from the moderate burn severity plots were depleted in PyC. This observation suggests that formation temperature of PyC can control its rate of erosion, which is critical for understanding the fate of PyC within an ecosystem (Mimmo et al. 2014). Other research has demonstrated that temperature exhibits a significant control on the properties of PyC, including hydrophobicity, specific surface area, C and N

concentration, hydrophobicity, and density, among other properties (Doerr et al. 2004; Massman et al. 2010). These properties likely led to the enhanced erosion of PyC in the high burn severity sites, and depressed erosion of PyC in the moderate burn severity sites.

The moderate and high burn severity sediments differed in terms of functional group distribution. The high severity burn sites had aromatic functional groups making up 10-20% more of the organic matter than the moderate severity burn sites (Table 3). This is consistent with previous findings, which have indicated that with moderate burning, aromatic functional groups may account for between 20-30% of the total functional groups, and that aromatic functional groups may make up 40-60% of high severity burn sites (Knicker et al. 2006; Mastrolonardo et al. 2015; Miesel et al. 2015; Nave et al. 2011).

In terms of sediment quality, burn severity played a major role in chemical differences between the treatment groups, which was reflected in the distribution of OM functional groups. Higher proportions of carbohydrates and lipids in the moderate severity plots could have resulted from the input of fresh OM from needle drop, or from not being consumed during the fire.

In the charred litter, a similar pattern in increasing and then decreasing protein contents with increasing charring temperature was also found by Miesel et al. (2015), who charred forest floor and top soil material. The high burn severity sites also had a higher proportion of protein. This be due to elevated microbial functioning post-burn with the input of PyC, and the release of N from previously living biomass (Schmidt & Stewart 1997) increasing inputs of soil protein. Alternatively, this may be an artifact of the molecular mixing model, which was developed for idealized SOM mixtures (Baldock et al. 2004b). This biomolecular model may also be over-estimating the proportion of char in these samples, as our control lab made char at 50°C contained 8% char, which was not consistent with what would be expected for litter samples.

Implications of OM and PyC enrichment in eroded sediments

The erosional transport and deposition of PyC can lead to significant changes to its environmental persistence (Abney & Berhe In Review). For example, if PyC were to be eroded from the slopes post-fire and become stabilized within downslope depositional landform positions, it would likely have greater environmental persistence, particularly if the sediment becomes buried (Chaopricha & Marín-Spiotta 2014; Marin-Spiotta et al. 2014). Alternatively, PyC may have a shorter residence time, if it becomes exposed to breakdown processes during transport, or is transported to a location that has higher decomposition potential than its formation location (Bird et al. 2015). Nevertheless, the enrichment of PyC or C in eroding sediment can significantly impact the nutrient budgets of a landscape (Stacy et al. 2015). This preferential erosion can enhance the spatial variability in nutrient distribution throughout a landscape, and enhance the difference in nutrient concentration between upslope eroding landform positions and depositional positions. Additionally, erosional enhancements of PyC concentrations in depositional landform positions can serve to increase soil CEC and available nutrients, in addition to sorbing nutrients to enhance nutrient retention (Araya et al. 2016; Johnson et al. 2007). By not accounting for variability in the rates of PyC erosion, considerable error is added to

field-based estimates of the residence time and fate of PyC *in situ*, on the order of centuries (Abney & Berhe In Review), depending on the rate of erosion.

These results suggest that erosive transport of PyC also depends on the formation temperature of the PyC. The relationship between combustion intensity and erosive properties of PyC, whereby increased combustion temperature increases the erodibility of PyC, can control the post-fire redistribution and fate of PyC over larger scales. Additionally, this relationship suggests that under low and moderate burn severities, the burned area may need less management to retain the PyC, which higher burn severity sites may require more intensive management strategies. Additionally, the soils in this study site were weakly developed Entisols on relatively steep slopes, more developed soils with higher organic matter input may have more surface roughness that could slow erosion forces, along with enhanced stabilization or breakdown of PyC *in situ*.

The role of geomorphology in controlling the long-term fate of PyC

Eroding and depositional landform positions can exhibit distinct hydrologic and environmental properties. These differences can significantly affect decomposition rates for PyC and OM across the landscape (Berhe 2012; Berhe et al. 2008). The impact of the landform position on the persistence of C or PyC also depends on whether that material is burned in depositional landform positions, decomposed *in situ*, or eroded farther down a watershed. The C storage potential of depositional landform positions can be over 1.6 to 6.2 times that of eroding landform positions (Doetterl et al. 2012). However, because PyC typically has a longer environmental residence time (Boot et al. 2015; Hammes et al. 2008; Lehmann et al. 2008) than non-pyrogenic SOM, this burial-enhanced extended residence time of PyC may be an even more critical factor for controlling its overall environmental residence time.

Over 50,000 ha of the Rim Fire was classified as high burn severity, and over 30,000 ha was classified as moderate burn severity (Potter 2014). By combining an approximate sediment load of 20 g/m^2/year with the areas impacted by differing burn severities and the mean PyC fraction from moderate and high burn severity treatment groups, erosion can account for the redistribution of over 3,000 and 5,000 metric tons of PyC from the moderate burn severity areas and high burn severity areas, respectively. Therefore, by not incorporating considerations of gemorphology and how it dictated landscape level distribution of PyC into the current understanding of PyC and C cycling, considerable error is being introduced into our local and global-scale models of both C and PyC budgets.

Limitations and Future Directions

The persistence of PyC in soil strongly depends on whether the PyC decomposes *in situ* or is eroded and subsequently deposited in a site with different decomposition or stabilization potential. The role of landform position on controlling decomposition of SOM has been well described (Berhe 2012; Doetterl et al. 2012), but this control needs to be assessed for PyC. This study did not address the role of decomposition of PyC during erosional transport, which is a significant process in the breakdown of non-pyrogenic C (Jacinthe & Lal 2001), or from the soil as a result of leaching (Santos et al. 2016). The deposition of

PyC throughout different landform positions in a landscape can control its long-term stability or breakdown.

A major limitation of this study is the lack of a moderate burn severity, moderate slope classification group. Without this group, it is impossible to statistically assess interactions between burn severity and slope, though doubtless they exist. This research demonstrates that PyC from high burn severity areas is preferentially erosive, however the role of slope is unclear as it acts to control loss of PyC from soil. Future research should consider the interactions between landscape factors and burn severity, along with depositional environments and how these environmental factors can control the long-term, landscape-scale persistence of PyC. Understanding the magnitude and controls of PyC fluxes is crucial to understanding the persistence of PyC in the soil.

CONCLUSIONS

Sediment transport during the first year (2014) following the Rim Fire was greatest in the first two post-fire study months (February and March), across all combinations of slope and burn severity studied. This higher transport corresponded to higher intensity and total precipitation in these two months compared with the latter two sampling months (April and May). The eroded material from moderate severity burn areas more closely resembled the source soil than the eroded material from the high severity burn areas, and much of this difference was likely due to chemical changes that occurred during combustion. The sediment from moderate severity burn plots had more fresh organic matter than the high intensity burn plots, which were depleted in both C and N. However, in the high severity burn plots, the sediment was enriched in PyC and was less similar to its source soil. This enrichment of PyC in only the high burn severity areas suggests that burn severity plays an important role in controlling the quality of OM eroded post-fire based on functional group distribution. This preferential erodibility of PyC from these high burn severity sites also indicates that burn severity may play a critical role in determining management strategies for mitigating against post-fire erosion and loss of PyC from soil. Overall, these results illustrate that both the amount and quality of OM and PyC that is eroded post-fire is primarily controlled by fire severity and secondarily by geomorphology of the landscape. However, the influence of burn severity, slope, and landform position on the transport of PyC within soil needs further investigation, as these likely interact to control the long-term fate of PyC.

ACKNOWLEDGEMENTS

We would like to acknowledge lab and field work support from Jim Mendez-Lopez and Louis Mielke from the Research Experience for Undergraduates at UC Merced. Lauren Austin, Alicia Sherrin, and technician staff the NPS assisted with collecting samples in the field. We also acknowledge members of the Fogel Stable Isotope laboratory at UC Merced, especially Christina Bradley and David Araiza, for their assistance conducting elemental and stable isotope analyses of sediments and soils. We thank Stephen C. Hart and Jonathan Sanderman for helpful comments on earlier versions of this manuscript. This work was funded by the National Science Foundation (CAREER, EAR 1352627) and the National Park Service (Cooperative agreement no. P14AC00760) grants to AAB. The authors have declared that no competing interests exist.

REFERENCES

Abney R, Berhe AA (In Review) Erosional redistribution of pyrogenic carbon: implications for persistence of PyC in the soil system.

Albalasmeh AA, Berli M, Shafer DS, Ghezzehei TA (2013) Degradation of moist soil aggregates by rapid temperature rise under low intensity fire. Plant and Soil 362(1-2): 335-344

Araya S, Meding S, Berhe A (2016) Thermal alteration of soil physico-chemical properties: a systematic study to infer response of Sierra Nevada climosequence soils to forest fires. Soil 2(3): 351-366

Araya SN, Fogel ML, Berhe AA (2017) Thermal alteration of soil organic matter properties: a systematic study to infer response of Sierra Nevada climosequence soils to forest fires. Soil 3: 31-44

Baker VR (1988) Flood erosion. Flood Geomorphology. John Wiley & Sons New York. :

Baldock JA, Masiello CA, Gelinas Y, Hedges JI (2004) Cycling and composition of organic matter in terrestrial and marine ecosystems. Marine Chemistry 92(1-4): 39-64

Battin T, Luyssaert S, Kaplan L, Aufdenkampe A, Richter A, Tranvik L (2009) The boundless carbon cycle. 2(9): 598-600

Berhe AA (2012) Decomposition of organic substrates at eroding vs. depositional landform positions. Plant and Soil 350: 261-280

Berhe AA, Harden J, Torn M, Kleber M, Burton S, Harte J (2012a) Persistence of Soil Organic Matter in Eroding vs. Depositional Landform Positions. Journal Of Geophysical Research-Biogeosciences 117, G02019, doi:10.1029/2011JG001790:

Berhe AA, Harden JW, Torn MS, Harte J (2008) Linking soil organic matter dynamics and erosion-induced terrestrial carbon sequestration at different landform positions. Journal of Geophysical Research-Biogeosciences 113: G4, DOI 10.1029/2008jg000751

Berhe AA, Harden JW, Torn MS, Kleber M, Burton SD, Harte. J (2012b) Persistence of soil organic matter in eroding vs. depositional landform positions,. Journal of Geophysical Research-Biogeosciences doi:10.1029/2011JG001790:

Berhe AA, Harte J, Harden JW, Torn MS (2007) The Significance of Erosion-Induced Terrestrial Carbon Sink. BioScience 57(4): 337-346

Bird MI, Wynn JG, Saiz G, Wurster CM, McBeath A (2015) The pyrogenic carbon cycle. Annual Review of Earth and Planetary Sciences 43: 273-298

Blake GR, Hartge KH (1986) Bulk Density. In: Klute A (ed) Methods of Soil Analysis: Part 1 Physical and Mineralogical Methods. American Society of Agronomy and Soil Science Society of America, Madison, WI. p 425-442

Boot C, Haddix M, Paustian K, Cotrufo M (2015) Distribution of black carbon in ponderosa pine forest floor and soils following the High Park wildfire. Biogeosciences 12(10): 3029-3039

Cain M, Subler S, Evans J, Fortin M (1999) Sampling spatial and temporal variation in soil nitrogen availability. Oecologia 118(4): 397-404

CDEC (2016) California Data Exchange Center. In.

Certini G (2005) Effects of fire on properties of forest soils: a review. Oecologia 143: 1-10

Chaopricha NT, Marín-Spiotta E (2014) Soil burial contributes to deep soil organic carbon storage. Soil Biology and Biochemistry 69: 251-264

Chia C, Munroe P, Joseph S, Lin Y, Lehmann J, Muller D, Xin H, Neves E (2012) Analytical electron microscopy of black carbon and microaggregated mineral matter in Amazonian dark Earth. Journal of microscopy 245(2): 129-139

Cornelissen G, Gustafsson Ö, Bucheli T, Jonker M, Koelmans A, van Noort P (2005) Extensive sorption of organic compounds to black carbon, coal, and kerogen in sediments and soils: Mechanisms and consequences for distribution, bioaccumulation, and biodegradation. Environmental Science & Technology 39(18): 6881-6895

DeBano L (2000) The role of fire and soil heating on water repellency in wildland environments: a review. Journal of Hydrology 231: 195-206

DeBano LF, Neary DG, Ffolliott PF (1998) Fire's effects on ecosystems. John Wiley and Sons, New York, NY

Doerr SH, Blake WH, Shakesby RA, Stagnitti F, Vuurens SH, Humphreys GS, Wallbrink P (2004) Heating effects on water repellency in Australian eucalypt forest soils and their value in estimating wildfire soil temperatures. International Journal of Wildland Fire 13(2): 157-163

Doerr SH, Thomas AD (2000) The role of soil moisture in controlling water repellency: new evidence from forest soils in Portugal. Journal of Hydrology 231: 134-147

Doetterl S, Six J, Van Wesemael B, Van Oost K (2012) Carbon cycling in eroding landscapes: geomorphic controls on soil organic C pool composition and C stabilization. Global Change Biology 18(7): 2218-2232

Gélinas Y, Baldock JA, Hedges JI (2001) Demineralization of marine and freshwater sediments for CP/MAS 13 C NMR analysis. Organic Geochemistry 32(5): 677-693

Gregorich E, Greer K, Anderson D, Liang B (1998) Carbon distribution and losses: erosion and deposition effects. Soil Till Res 47(3-4): 291-302

Grogan P, Burns T, Chapin Iii F (2000) Fire effects on ecosystem nitrogen cycling in a Californian bishop pine forest. Oecologia 122(4): 537-544

Hammes K, Schmidt MWI, Smernik RJ, Currie LA, Ball WP, Nguyen TH, Louchouarn P, Houel S, Gustafsson O, Elmquist M, Cornelissen G, Skjemstad JO, Masiello CA, Song J, Peng Paa, Mitra S, Dunn JC, Hatcher PG, Hockaday WC, Smith DM, Hartkopf-Froeder C, Boehmer A, Lueer B, Huebert BJ, Amelung W, Brodowski S, Huang L, Zhang W, Gschwend PM, Flores-Cervantes DX, largeau C, Rouzaud J-N, Rumpel C, Guggenberger G, Kaiser K, Rodionov A, Gonzalez-Vila FJ, Gonzalez-Perez JA, de la Rosa JM, Manning DAC, Lopez-Capel E, Ding L (2007) Comparison of quantification methods to measure fire-derived (black/elemental) carbon in soils and sediments using reference materials from soil, water, sediment and the atmosphere. Global Biogeochemical Cycles 21(3): GB3016

Hammes K, Torn MS, Lapenas AG, Schmidt MWI (2008) Centennial black carbon turnover observed in a Russian steppe soil. Biogeosciences 5(5): 1339-1350

Harden JW, Sharpe JM, Parton WJ, Ojima DS, Fries TL, Huntington TG, Dabney SM (1999) Dynamic replacement and loss of soil carbon on eroding cropland. Global Biogeochemical Cycles 13(4): 885-901

Hendershot WH, Lalande H, Duquette M (2008) Soil Reaction and Exchangeable Acidity. In: Carter MR & Gregorich EG (eds) Soil Sampling and Methods of Analysis. CRC Press, Boca Raton, FL.

Huber E, Bell TL, Adams MA (2013) Combustion influences on natural abundance nitrogen isotope ratio in soil and plants following a wildfire in a sub-alpine ecosystem. Oecologia 173(3): 1063-1074

Huber NK, Bateman PC, Wahrhaftig C (1989) Geologic map of Yosemite National Park and vicinity, California. In: Miscellaneous Investigations Series I-1874. US Geological Survey

Hudak AT, Robichaud P, Evans JS, Clark J, Lannom K, Morgan P, Stone C (2014) Field validation of Burned Area Reflectance Classification (BARC) products for post fire assessment. USDA Forest Service/UNL Faculty Publication Paper 220. In.

Imeson A, Lavee H (1998) Soil erosion and climate change: the transect approach and the influence of scale. Geomorphology 23(2-4): 219-227

Iniguez JM, Swetnam TW, Yool SR (2008) Topography affected landscape fire history patterns in southern Arizona, USA. Forest Ecology and Management 256(3): 295–303

Jacinthe P, Lal R (2001) A mass balance approach to assess carbon dioxide evolution during erosional events. Land Degradation & Development 12(4): 329-339

Johnson D, Murphy J, Walker R, Glass D, MILLER W (2007) Wildfire effects on forest carbon and nutrient budgets. Ecological Engineering 31(3): 183-192

Kinnell P (2005) Raindrop‐impact‐induced erosion processes and prediction: a review. Hydrological processes 19(14): 2815-2844

Knicker H, Almendros G, González‐Vila FJ, González‐Pérez JA, Polvillo O (2006) Characteristic alterations of quantity and quality of soil organic matter caused by forest fires in continental Mediterranean ecosystems: a solid‐state 13C NMR study. European Journal of Soil Science 57(4): 558-569

Lal R (2003) Soil erosion and the global carbon budget. Environment International 29(4): 437-450

Lehmann J (2007) Bio-energy in the black. Frontiers in Ecology and the Environment 5(7): 381–387

Lehmann J, Skjemstad J, Sohi S, Carter J, Barson M, Falloon P, Coleman K, Woodbury P, Krull E (2008) Australian climate–carbon cycle feedback reduced by soil black carbon. Nature Geoscience 1(12): 832-835

Liu S, Bliss N, Sundquist E, Huntington T (2003) Modeling carbon dynamics in vegetation and soil under the impact of soil erosion and deposition. Global Biogeochemical Cycles 17(2): 1074

Marin-Spiotta E, Chaopricha NT, Plante AF, Diefendorf AF, Mueller CW, Grandy AS, 1–5. JAM (2014) Long-Term Stabilization of Deep Soil Carbon by Fire and Burial During Early Holocene Climate Change. Nature Geoscience 7(6): 428

Masiello C (2004) New directions in black carbon organic geochemistry. Marine Chemistry 92(1-4): 201-213

Massman WJ, Frank JM, Mooney SJ (2010) Advancing investigation and physical modeling of first-order fire effects on soils. Fire Ecology 6(1): 36-54

Mastrolonardo G, Rumpel C, Forte C, Doerr SH, Certini G (2015) Abundance and composition of free and aggregate-occluded carbohydrates and lignin in two forest soils as affected by wildfires of different severity. Geoderma 245: 40-51

Mataix-Solera J, Cerda A, Arcenegui V, Jordan A, Zavala LM (2011) Fire effects on soil aggregation: a review. Earth-Science Reviews 109(1-2): 44-60

Miesel JR, Hockaday WC, Kolka RK, Townsend PA (2015) Soil organic matter composition and quality across fire severity gradients in coniferous and deciduous forests of the southern boreal region. Journal of Geophysical Research: Biogeosciences 120(6): 1124-1141

Mimmo T, Panzacchi P, Baratieri M, Davies C, Tonon G (2014) Effect of pyrolysis temperature on miscanthus (Miscanthus× giganteus) biochar physical, chemical and functional properties. Biomass and Bioenergy 62: 149-157

Mukherjee A, Zimmerman A, Harris W (2011) Surface chemistry variations among a series of laboratory-produced biochars. Geoderma 163(3): 247-255

Nave LE, Vance ED, Swanston CW, Curtis PS (2011) Fire effects on temperate forest soil C and N storage. Ecological Applications 21(4): 1189-1201

Nearing M (1998) Why soil erosion models over-predict small soil losses and under-predict large soil losses. Catena 32(1): 15-22

Neary D, Klopatek C, DeBano L, Ffolliott P (1999) Fire effects on belowground sustainability: a review and synthesis. Forest Ecology & Management 122: 51-71

Nelson PN, Baldock JA (2005) Estimating the molecular composition of a diverse range of natural organic materials from solid-state C-13 NMR and elemental analyses. Biogeochemistry 72(1): 1-34

Nguyen BT, Lehmann J, Kinyangi J, Smernik R, Riha SJ, Engelhard MH (2009) Long-term black carbon dynamics in cultivated soil. Biogeochemistry 92(1-2): 163-176

Parsons A, Robichaud PR, Lewis SA, Napper C, Clark JT (2010) Field guide for mapping post-fire soil burn severity. In. United States Department of Agriculture, Forest Service, Rocky Mountain Research Station, Fort Collins, CO. p 49

Potter C (2014) Geographic analysis of burn severity for the 2013 California Rim Fire. Natural Resources 5(11): 597-606

Pyle LA, Hockaday WC, Boutton T, Zygourakis K, Kinney TJ, Masiello CA (2015) Chemical and isotopic thresholds in charring: implications for the interpretation of charcoal mass and isotopic data. Environmental science & technology 49(24): 14057-14064

Randerson JT, Chen Y, van der Werf GR, Rogers BM, Morton DC (2012) Global burned area and biomass burning emissions from small fires. Journal of Geophysical Research: Biogeosciences 117: G04012

Regnier P, Friedlingstein P, Ciais P, Mackenzie FT, Gruber N, Janssens IA, Laruelle GG, Lauerwald R, Luyssaert S, Andersson AJ, Arndt S, Arnosti C, Borges AV, Dale AW, Gallego-Sala A, Godderis Y, Goossens N, Hartmann J, Heinze C, Ilyina T, Joos F, LaRowe

DE, Leifeld J, Meysman FJR, Munhoven G, Raymond PA, Spahni R, Suntharalingam P, Thullner M (2013) Anthropogenic Perturbation of the Carbon Fluxes From Land to Ocean. Nature Geoscience 6(8): 597-607

Renard KG, Foster GR, Weesies G, McCool D, Yoder D (1997) Predicting soil erosion by water: a guide to conservation planning with the Revised Universal Soil Loss Equation (RUSLE). US Government Printing Office Washington, DC,

Riebe CS, Kirchner JW, Granger DE, Finkel RC (2001) Minimal climatic control on erosion rates in the Sierra Nevada, California. Geology 29(5): 447-450

Robichaud PR (1996) Spatially-varied erosion potential from harvested hillslopes after prescribed fire in the Interior Northwest. In. University of Idaho. p 219

Rumpel C, Ba A, Darboux F, Chaplot V, Planchon O (2009) Erosion budget and process selectivity of black carbon at meter scale. Geoderma 154(1): 131-137

Rumpel C, Chaplot V, Planchon O, Bernadou J, Valentin C, Mariotti A (2006a) Preferential erosion of black carbon on steep slopes with slash and burn agriculture. CATENA 65(1): 30-40

Rumpel C, Rabia N, Derenne S, Quenea K, Eusterhues K, Kögel-Knabner I, Mariotti A (2006b) Alteration of soil organic matter following treatment with hydrofluoric acid (HF). Organic Geochemistry 37(11): 1437-1451

Saito L, Miller WW, Johnson DW, Qualls R, Provencher L, Carroll E, Szameitat P (2007) Fire Effects on Stable Isotopes in a Sierran Forested Watershed. Journal of Environmental Quality 36(1): 91-100

Santos F, Russell D, Berhe AA (2016) Thermal alteration of water extractable organic matter in climosequence soils from the Sierra Nevada, California. Journal of Geophysical Research: Biogeosciences 121(11): 2877-2885

Schmidt S, Stewart G (1997) Waterlogging and fire impacts on nitrogen availability and utilization in a subtropical wet heathland (wallum). Plant, Cell & Environment 20(10): 1231-1241

Schofield R, Taylor AW (1955) The measurement of soil pH. Soil Science Society of America Journal 19(2): 164-167

Shakesby R, Doerr S (2006) Wildfire as a hydrological and geomorphological agent. Earth-Science Reviews 74(3): 269-307

Sharpley A (1985) The Selection Erosion of Plant Nutrients in Runoff. Soil Science Society of America Journal 49(6): 1527-1534

Stacy E, Hart SC, Hunsaker CT, Johnson DW, Berhe AA (2015) Soil carbon and nitrogen erosion in forested catchments: implications for erosion-induced terrestrial carbon sequestration. Biogeosciences Discuss. 12(3): 2491-2532

Stallard R (1998) Terrestrial sedimentation and the carbon cycle: Coupling weathering and erosion to carbon burial. Global Biogeochemical Cycles 12(2): 231-257

Staub B, Rosenzweig C (1992) Global Zobler soil type, soil texture, surface slope, and other properties. Digital raster data on a 1-degree geographic (lat/long) 180X360 grid. In: Global ecosystems database version 2.0. Seven independent spatial layers. 561,782 bytes in 16 files. NOAA National Geophysical Data Center, Boulder CO.

United States Department of Agriculture NRCS (2007) Soil survey of Yosemite National Park, California. In.

Van Oost K, Quine T, Govers G, De Gryze S, Six J, Harden J, Ritchie J, McCarty G, Heckrath G, Kosmas C (2007) The impact of agricultural soil erosion on the global carbon cycle. Science 318(5850): 626-629

Wischmeier WH, Smith. DD Predicting rainfall-erosion losses from cropland east of the Rocky Mountains - Guide for selection of practices for soil and water conservation. . In: Agr. Handbk. No. 282. USDA, Washington, D.C. 1965.

Wischmeier WH, Smith. DD Predicting rainfall erosion losses. In: Agr. Handbk. No. 537. U.S. Dept. Agr. Washington, D.C. 1978.

FIGURES

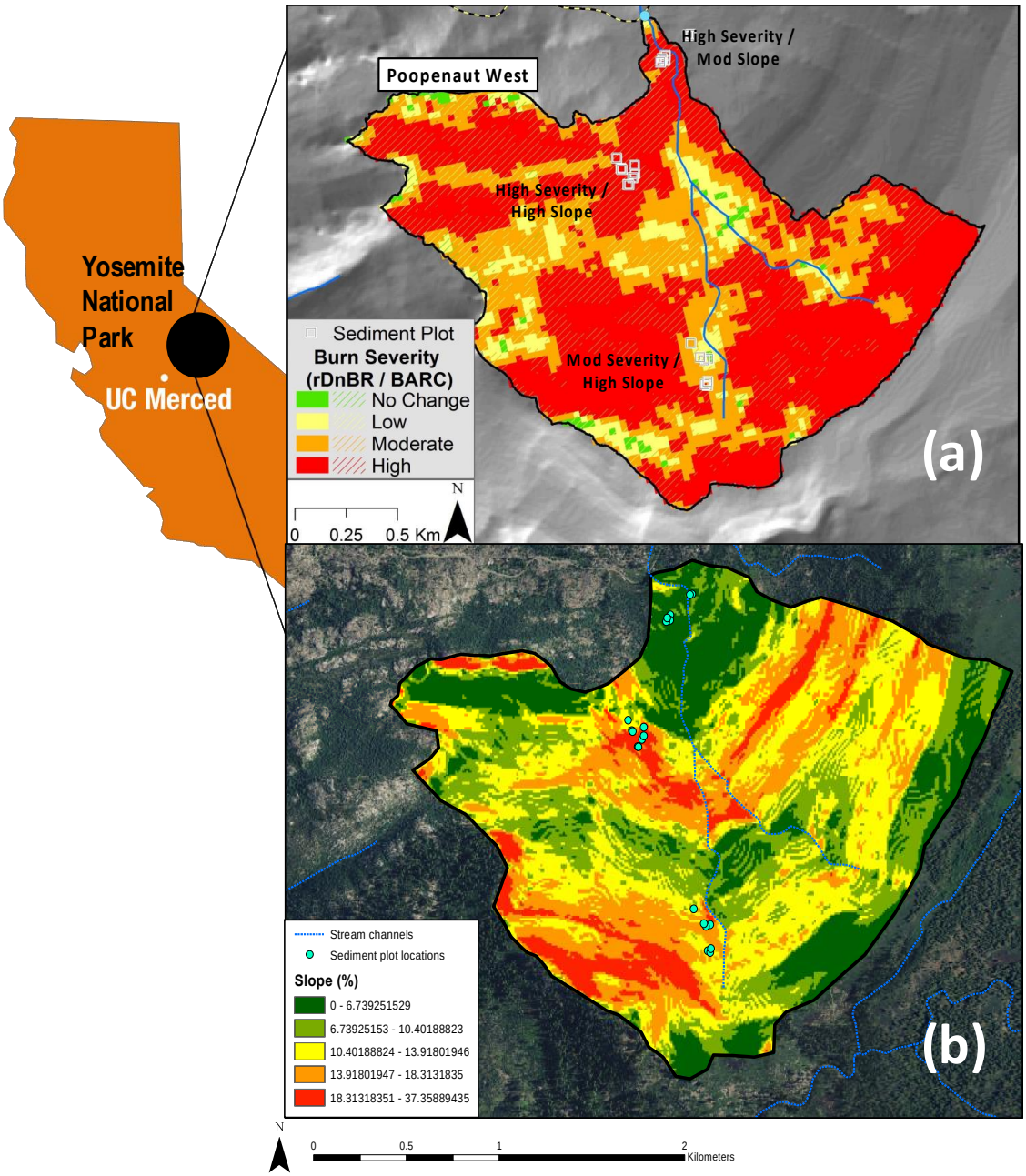

Figure 3-1. Soil burn severity and slope in the Poopenaut watershed within Yosemite National Park. The 21 sediment plots are denoted by grey squares, and were chosen based on combination of fire severity (a) and slope (b). The Poopenaut watershed is near the Hetch Hetchy entrance to Yosemite National Park.

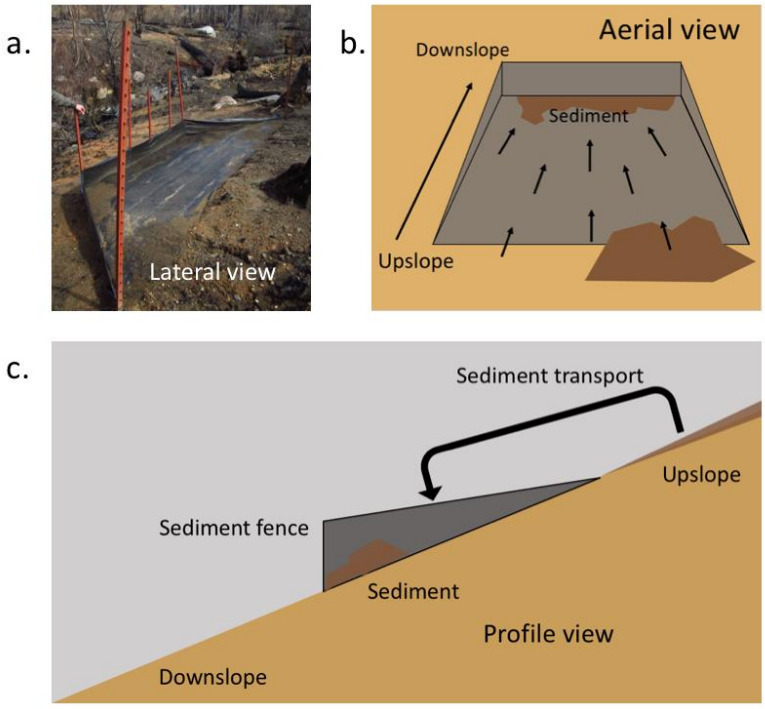

Figure 3-2. Sediment fences were established alongside a single hillslope in the Poopenaut West watershed. Photo (a) is from February 2014 within the high burn severity moderate slope sampling area (R. Abney). During precipitation events, upslope sediment was washed into the sediment fences (b-c). Sediment fences were swept after every major precipitation event in the watershed.

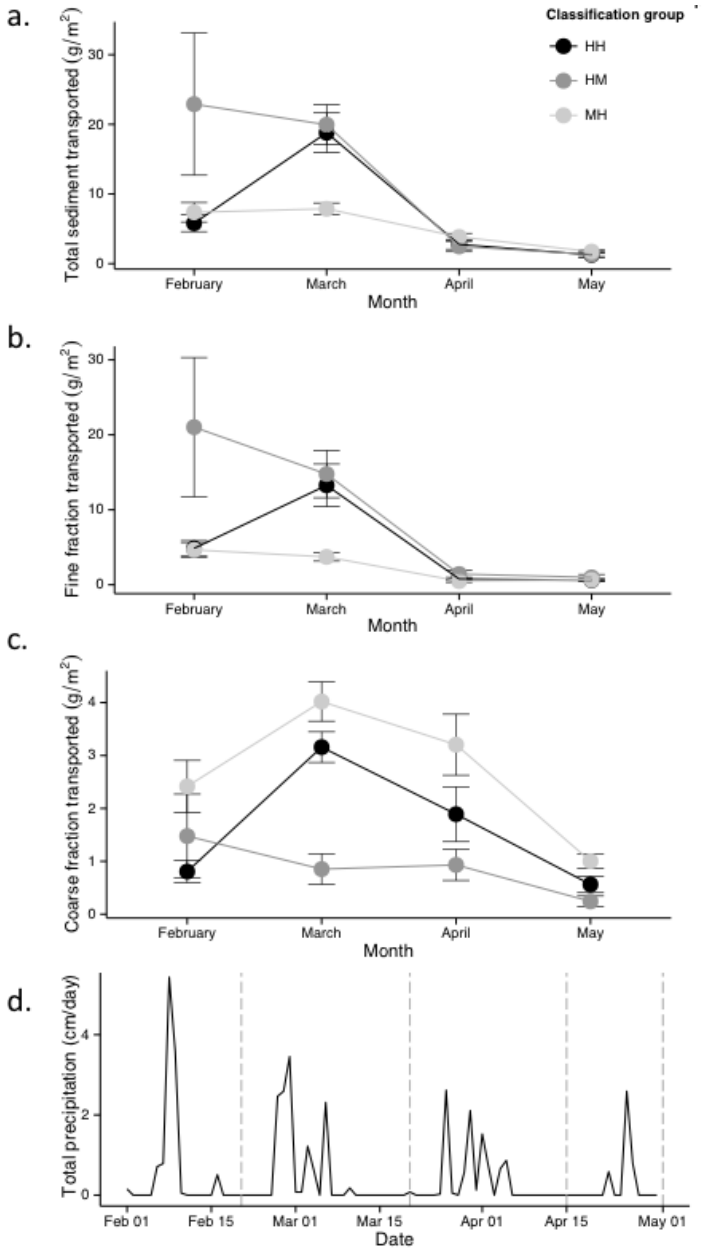

Figure 3-3. The total sediment (a) transported during each sampling event was weighed and dried from each of the three classification groups (HH – high burn severity, high slope; HM – high burn severity, moderate slope; and MH – moderate burn severity, high slope). The sediment was sieved into fine (<2 mm, b) and coarse (>2 mm, c) fractions. Precipitation was summed per day, and sediment sampling occurred after major precipitation events (d, dashed grey lines indicate dates of the four sampling points). The sampling points represent sediment transported from precipitation events prior to the sampling point.

Figure 3-4. Photo of Poopenaut West watershed inside the perimeter of the Rim Fire from February 201. The dashed line delineates the boundary between high (a) and moderate (b) severity burn areas (Photo Credit: R. Abney).

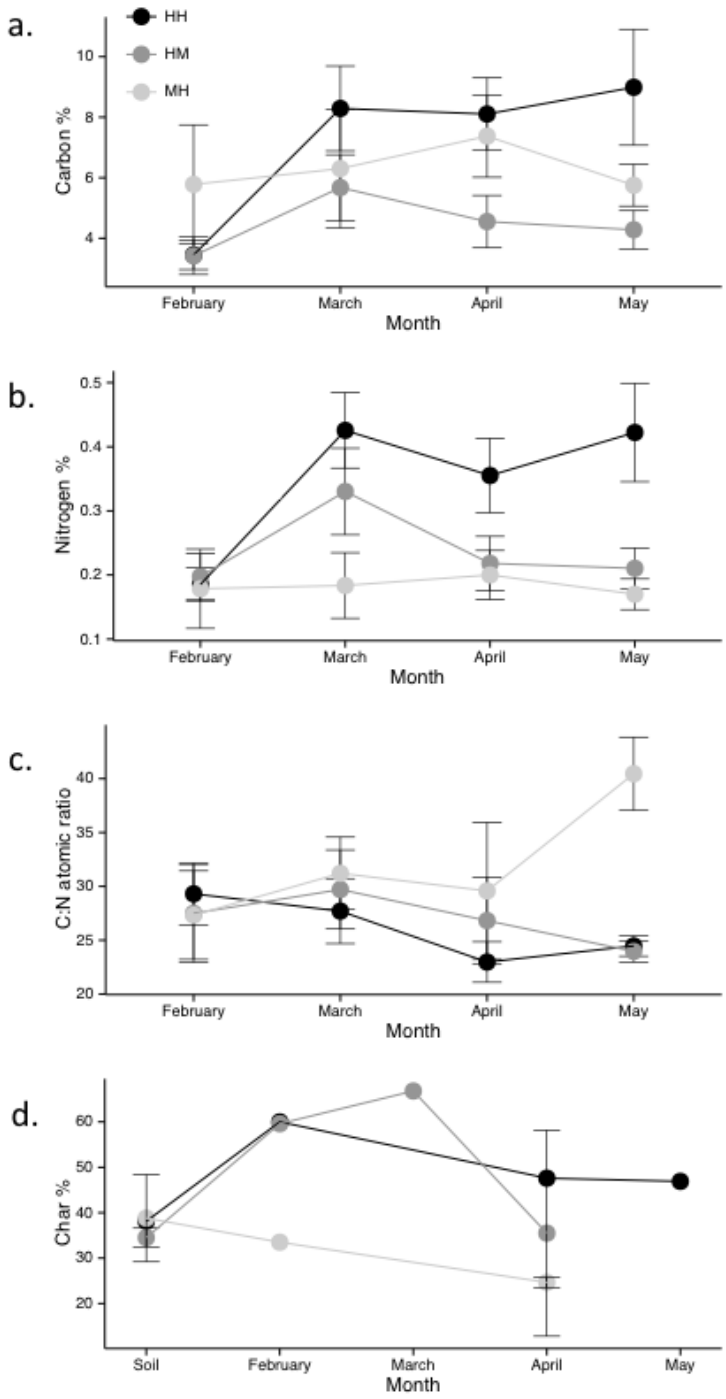

Figure 3-5. The fine (<2 mm) sediment fraction was analyzed for bulk C (a) and N (b), and the atomic C:N ratio (c) was calculated. Sediments were analyzed for char-C (d) using ^{13}C CPMAS NMR and the molecular mixing model. Error bars represent standard error (n=7), except for char-C, due to limitations in the number of samples able to be analyzed via NMR. The sites were divided into three classification groups: high severity burn, high slope

(HH); high severity burn, moderate slope (HM); and moderate severity burn, high slope (MH).

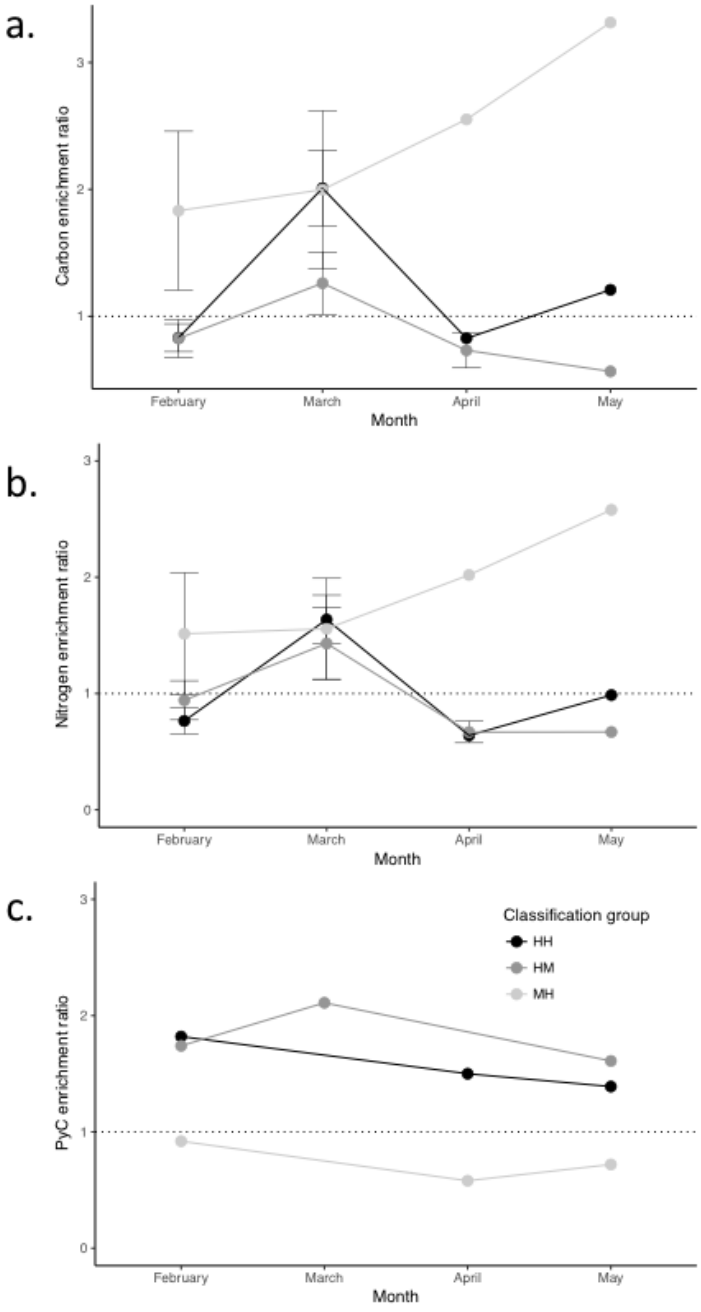

Figure 3-6. Enrichment ratios for carbon (a), nitrogen (b), and pyrogenic carbon (c) transported sediment from the fine fraction (<2mm). The line at 1 indicates the enrichment

line, where >1 is enriched and <1 is depleted in that component. The sites were divided into three classification groups: high severity burn, high slope (HH); high severity burn, moderate slope (HM); and moderate severity burn, high slope (MH).

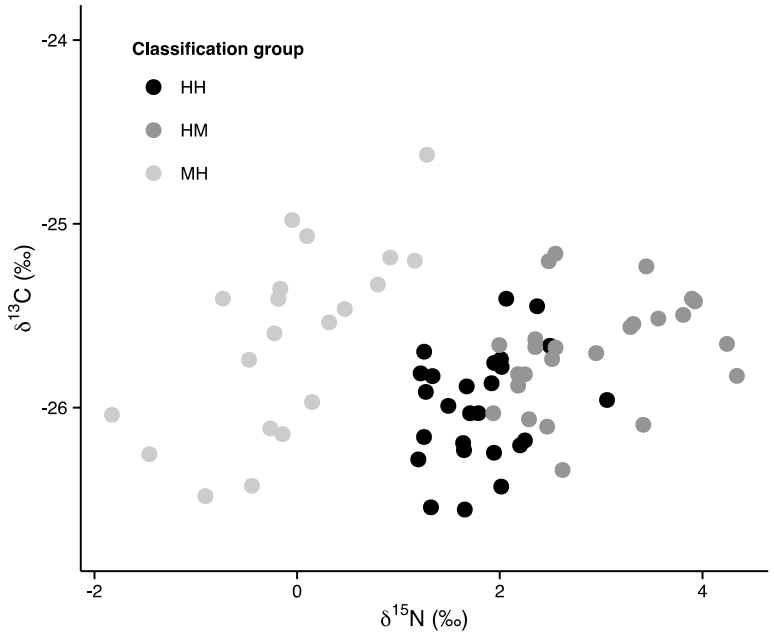

Figure 3-7. The sediment fine fraction was analyzed for stable C and N isotopes from the different classification groups. The high burn severity classification groups (HH and HM) differ from the moderate burn severity (MH) group by enrichment in the $\delta^{15}N$ isotope ratio. There were only small, less than one per mil, differences between the groups across the $\delta^{13}C$ isotope ratio.

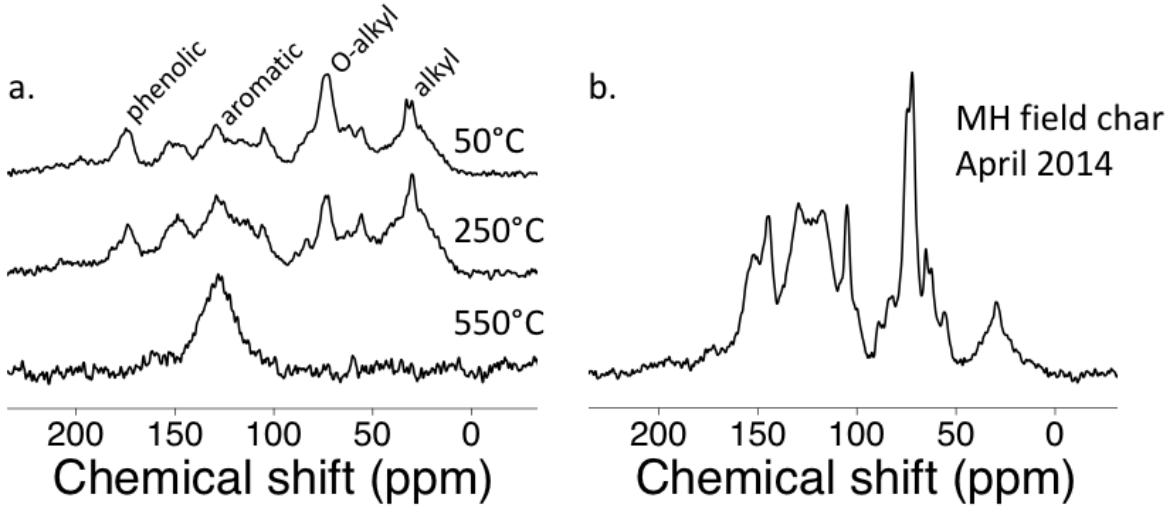

Figure 3-8. ^{13}C CPMAS NMR Comparison of laboratory-produced (a) char and Rim Fire char (b). As the laboratory produced char (a) was exposed to increased temperatures, the alkyl, O-alkyl, and phenolic functional groups were lost and the aromatic region was enhanced. The field char from a moderate burn severity sediment (MH, panel b) site contains higher proportions of aromatic functional groups than the 250°C char, but retained the alkyl and phenolic peaks.

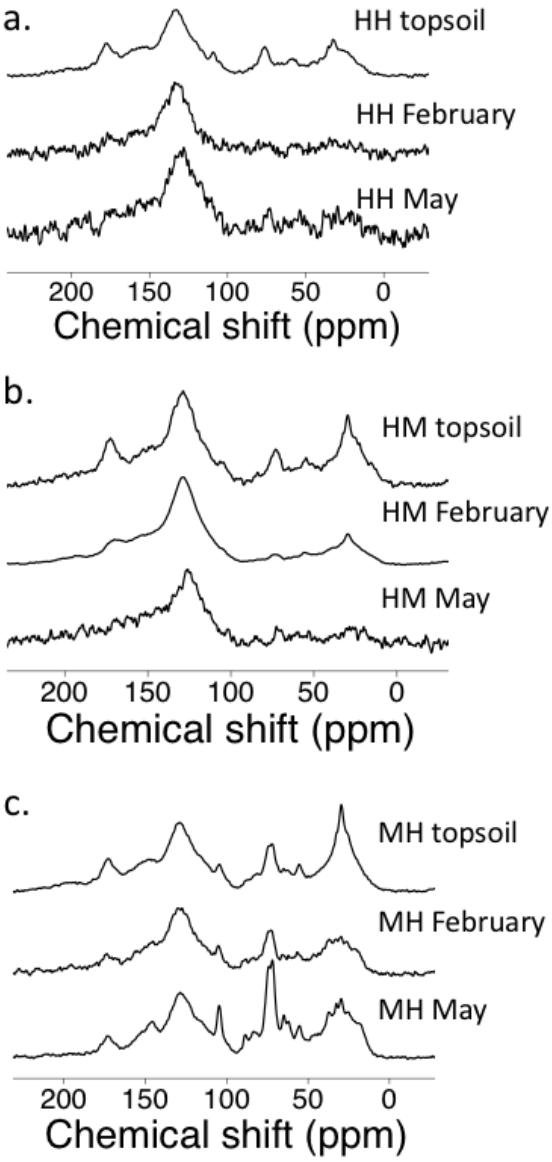

Figure 3-9. ^{13}C CP-MAS NMR (cross polarization magic angle spinning nuclear magnetic resonance) spectra of soil organic matter in soil and sediment eroded from the different burn severity and slope classifications. Top soil samples (0-5 cm) are the top lines of the spectra, followed by the first and last sampling points of the 2014 water year. HH (a) indicates high burn severity, high slope. HM (b) indicates high burn severity, moderate slope, and MH (b) indicates moderate burn severity, high slope.

TABLES

Table 3-1. Soil physical and chemical characteristics. Parentheses indicate standard error with n=3 analytical replicates.

	HH		HM		MH	
Depth	0-5cm	5-10cm	0-5cm	5-10cm	0-5cm	5-10cm
%C	4.48 (1.36)	3.33 (0.59)	4.15 (0.36)	3.77 (0.37)	3.11 (0.80)	1.52 (0.23)
%N	0.27 (0.11)	0.13 (0.03)	0.21 (0.02)	0.15 (0.00)	0.11 (0.02)	0.04 (0.00)
$\delta^{13}C$	-25.38 (0.37)	-24.60 (0.19)	-24.90 (0.19)	-24.65 (0.21)	-25.15 (0.71)	-24.80 (0.21)
$\delta^{15}N$	2.10 (0.31)	3.27 (0.37)	3.44 (0.74)	3.83 (0.34)	1.76 (0.26)	2.45 (0.21)
Bulk density (0-10 cm)	0.92 (0.02)	N/A	0.95 (0.05)	N/A	0.88 (0.03)	N/A
pH in H_2O	6.89 (0.06)	6.87 (0.06)	6.98 (0.14)	6.97 (0.13)	7.09 (0.13)	6.93 (0.11)
pH in $CaCl_2$	6.68 (0.24)	5.75 (0.26)	6.61 (0.19)	5.45 (0.13)	6.98 (0.09)	6.14 (0.08)
Sand %	79.29 (0.66)	80.54 (0.42)	79.44 (1.42)	77.66 (1.06)	80.62 (0.92)	80.19 (0.59)
Silt %	13.49 (0.38)	11.61 (0.32)	14.93 (0.44)	15.60 (0.80)	12.37 (1.07)	12.63 (0.20)
Clay %	7.20 (0.61)	7.84 (0.37)	5.62 (1.13)	6.72 (0.57)	7.00 (1.00)	7.16 (0.74)

Table 3-2. Precipitation totals and peaks from the nearby Poopenaut valley for the spring 2014 season were measured using a tipping bucket rain gauge.

Sampling time	Precipitation total between sampling times (in)	Peak precipitation (cm precipitation/10 min)
February	8.46	0.32
March	3.20	0.27
April	3.68	0.30
May	1.56	0.15

Table 3-3. Sediment chemical and physical characteristics by treatment groups: high burn severity, high slope (HH); high burn severity, moderate slope (HM); and moderate burn severity, high slope (MH). Sediments were analyzed for pH in both water and calcium chloride solutions in 1:2 soil to solution ratios. Parentheses indicate standard error by sediment fence, with n=7, and those without standard error did not collect enough sediment to conduct replicate analyses.

	HH				HM				MH			
Collect-ion date	Feb	Mar	Apr	May	Feb	Mar	Apr	May	Feb	Mar	Apr	May
%C	3.45 (0.48)	8.28 (1.40)	8.10 (1.19)	8.98 (1.91)	3.42 (0.62)	5.67 (1.08)	4.55 (0.86)	4.27 (0.63)	5.77 (1.97)	6.29 (2.14)	7.37 (1.36)	5.75 (0.68)
%N	0.18 (0.02)	0.42 (0.05)	0.35 (0.05)	0.42 (0.07)	0.19 (0.03)	0.33 (0.06)	0.21 (0.04)	0.21 (0.03)	0.17 (0.06)	0.18 (0.05)	0.20 (0.03)	0.16 (0.02)
pH in H_2O	7.47 (0.11)	6.43 (0.52)	7.18 (0.13)	7.14 (0.07)	7.58 (0.06)	5.76 (0.46)	7.38 (0.12)	7.36 (0.11)	7.37 (0.07)	7.03 (0.28)	6.60 (0.21)	7.12 (0.11)
pH in $CaCl_2$	6.79 (0.10)	6.09 (0.52)	6.88 (0.08)	6.75 (0.11)	6.96 (0.10)	5.41 (0.50)	6.83 (0.14)	6.88 (0.14)	6.53 (0.13)	6.51 (0.21)	6.40 (0.12)	6.44 (0.11)
Sand %	83.89 (0.84)	74.21 (2.44)	81.97 (2.09)	75.11 (4.53)	78.80 (3.42)	72.23 (5.46)	79.17 (5.07)	86.07	83.86 (1.40)	84.00 (1.37)	87.12 (2.34)	N/A
Clay %	5.92 (0.62)	6.74 (0.99)	6.73 (2.09)	7.73 (1.21)	5.93 (1.25)	5.44 (1.56)	6.67 (0.50)	6.00	7.49 (1.19)	8.05 (0.46)	4.46 (3.42)	N/A
Silt %	10.20 (0.68)	19.05 (1.86)	11.31 (1.02)	17.17 (3.33)	15.27 (2.80)	22.33 (4.40)	14.15 (5.28)	7.93	8.65 (1.30)	7.96 (1.07)	8.43 (1.08)	N/A

Table 3-4. Chemical functional group integrated regions from ^{13}C NMR analysis. The classification group indicates the combination of slope and burn severity (HH = high burn severity, high slope, HM = high burn severity, moderate slope, MH = moderate burn severity, high slope) or the temperature of the *Pinus* litter char.

Sample type	Classification group	Sampling time	Alkyl C	N-Alkyl & Methoxyl C	O-Alkyl C	Di-O-Alkyl C	Aromatic C	Phenolic C	Amide & Carboxyl C	Ketone & Aldehyde C
			Carbon molar percentage							
Pinus litter	50 ºC	November 2013	20.9	7.7	24.7	7.8	18.6	7.5	9.1	3.6
	250 ºC char	November 2013	22.8	7.7	15.5	6.9	24.8	10.4	8.8	3.1
	550 ºC char	November 2013	3.4	1.5	1.2	9.5	61.6	12.9	6.6	3.3
Field char	MH	April 2014	9.6	4.1	24.3	10.3	33.8	12.3	3.7	1.9
Sediment	HH	February 2014	8.5	2.8	6	8.1	50	12.8	9	2.8
	HH	April 2014	11.7	2.9	10.1	5.6	43.6	13.6	9.4	3.1
	HH	May 2014	15.4	3.9	7	4.8	42.6	14.1	9.1	3.1
	HM	February 2014	13	3.6	4.4	4.6	48.5	13.4	9.5	3
	HM	March 2014	8.3	1.4	1.9	4.3	53.9	15.1	11.7	3.4
	HM	April 2014	10.4	3.3	7	5.2	43.5	14.6	11.4	4.5
	HM	April 2014	13.2	3.7	6.6	5.6	48	12.1	8.1	2.7
	HM	May 2014	11.2	3.2	7.1	7.8	47	13.8	7.4	2.6
	MH	February 2014	17.7	5.6	13.9	7	34.8	9.9	7.9	3.1
	MH	April 2014	32	5.2	15.7	5.7	25	8	6.5	1.9
	MH	April 2014	22.3	6.1	21.8	7.2	28.1	8.1	4.9	1.5
Soil	HH 0-5 cm	Spring 2014	16.5	4.6	9	6	36.7	12.5	11.5	3.1
	HH 5-10 cm	Spring 2014	20	5.9	12.4	7	32.5	10.5	9.1	2.7

HM 0-5 cm	Spring 2014	19.4	5.1	8.6	4.9	35.6	11.4	11.2	3.8
HM 0-5cm	Spring 2014	23.1	5.3	10.2	5	32.2	10	11.4	2.9
MH 0-5 cm	Spring 2014	24	5.2	12.9	5.4	30.5	9.8	8.9	3.2
MH 0-5 cm	Spring 2014	13.4	3.3	4.7	5.4	44.8	14.5	10.1	3.9

Table 3-5. Molecular mixing model results for each of the sediments and chars analyzed via NMR. The classification group indicates the combination of slope and burn severity (HH = high burn severity, high slope, HM = high burn severity, moderate slope, MH = moderate burn severity, high slope) or the temperature of the *Pinus* litter char.

Sample type	Classification group	Sampling time	Carbohydrate	Protein	Lignin	Lipid	Carbonyl	Char (PyC)
			Carbon molar percentage					
Pinus litter	50ºC	November 2013	27.0	9.5	27.4	14.3	13.1	8.8
	250ºC char	November 2013	13.5	11.1	33.5	16.2	10.4	15.3
	550ºC char	November 2013	1.0	8.9	0.7	0.2	9.4	79.9
Sediment	HH	February 2014	6.2	14.1	6.9	2.7	10.0	60.0
	HH	April 2014	9.6	9.5	13.3	7.0	13.1	47.6
	HH	May 2014	4.0	14.1	15.7	9.4	9.8	46.9
	HM	March 2014	0.0	17.0	0.0	1.6	14.6	66.8
	HM	April 2014	5.7	12.4	6.4	9.0	8.3	58.2
	HM	April 2014	18.2	13.1	13.6	12.0	30.3	12.8
	HM	February 2014	2.3	18.8	4.5	6.3	8.5	59.6
	MH	April 2014	15.8	8.3	16.8	31.5	4.2	23.5
	MH	February 2014	13.9	6.8	20.2	14.1	11.4	33.5
	MH	April 2014	25.7	6.3	20.1	20.0	2.0	25.8
Soil	HH 0-5 cm	Spring 2014	7.8	19.7	14.3	7.9	12.1	38.1
	HH 5-10 cm	Spring 2014	11.8	14.1	20.5	13.8	9.1	30.8
	HM 0-5 cm	Spring 2014	6.4	16.1	13.9	12.7	14.4	36.6
	HM 0-5cm	Spring 2014	8.5	14.6	13.4	17.6	13.5	32.4

MH 0-5 cm	Spring 2014	11.8	9.7	17.3	20.4	11.6	29.2
MH 0-5 cm	Spring 2014	0.7	11.0	16.9	8.0	15.0	48.4

CHAPTER 4: POST-WILDFIRE EROSION IN MOUNTAINOUS TERRAIN LEADS TO RAPID AND MAJOR REDISTRIBUTION OF SOIL ORGANIC CARBON

ABSTRACT

Catchments impacted by wildfire typically experience elevated rates of post-fire erosion and formation and deposition of pyrogenic carbon (PyC). To better understand the role of erosion in post-fire soil carbon dynamics, we determined distribution of soil organic carbon in different chemical fractions before and after the Gondola fire in South Lake Tahoe, CA. We analyzed soil samples from eroding and depositional landform positions in control and burned plots pre- and post-wildfire (in 2002, 2003, and 10-years post-fire in 2013). Elemental concentrations, stable isotope compositions, and mid-infrared (MIR) absorption spectra were conducted on all of the samples. A subset of samples was analyzed by ^{13}C cross polarization magic angle spinning nuclear magnetic resonance spectroscopy (CPMAS NMR). We combined the MIR and CPMAS NMR data in the Soil Carbon Research Program (SCaRP) partial least squares regression model to predict distribution of soil carbon into three different fractions: particulate, humic, and resistant organic matter fractions representing relatively fresh larger pieces of organic matter (OM), fine, decomposed OM, and pyrogenic C, respectively. The post-fire eroding samples showed no major difference in soil organic carbon (SOC) fractions one year post-fire, but the depositional samples had increased concentrations of all SOC fractions, and particularly the fraction that resembles PyC, the resistant organic carbon fraction, one year post-fire (2002). The increase in all SOC fractions in the post-fire depositional landform position one year post-fire indicates significant lateral mobilization of the eroded PyC. In addition, our NMR analyses revealed a post-fire increase in both the aryl and O-aryl carbon compounds, indicating increases in soil PyC concentrations post-fire. After 10 years, the C concentration from all three fractions declined in the depositional landform position to levels below pre-fire concentrations. This decline may have been due to further erosion or elevated rates of decomposition. Thus, we found that both fire and erosion play significant roles in controlling the distribution of PyC throughout a landscape and its long-term fate in soil system.

INTRODUCTION

The soil system plays major role in the global terrestrial carbon (C) cycle, as it stores more C than the terrestrial biosphere and atmosphere combined (Lal 2003, Post & Kwon 2000, Scharlemann *et al.* 2014) in pools that cycle at a slower rate than the C in the atmosphere or biosphere (Lal 2004). The ability of the soil system to store and cycle carbon, however, is modified by a range of physical perturbations that the soil system experiences, including fire and erosion (Abney & Berhe In Prep).

Fire can have multiple direct and indirect effects on the biogeochemical cycling of C in the terrestrial ecosystem. For example, the release of nutrients from burned biomass can lead to a spike in initial productivity and subsequent regrowth in plant life post-fire (Johnson *et al.* 2007, Johnson *et al.* 2004). The loss of vegetation that would otherwise stabilize soil in eroding landform positions, along with increased soil hydrophobicity after moderate severity fires leaves soil more directly exposed to weathering and susceptible to erosive forces (DeBano 2000, Larsen *et al.* 2009, Shakesby *et al.* 2000). Fires can also raise soil pH, alter cation exchange capacity, and change the soil organic matter (SOM) composition (Araya *et al.* 2017, Certini 2005, DeBano 1990, Giovannini *et al.* 1988, Liang *et al.* 2006).

Fire leads to the formation and deposition of pyrogenic carbon (PyC) on topsoil. Broadly, PyC is C that has been chemically altered by fire, and includes a spectrum of materials ranging from charred biomass to soot and ash (Bird *et al.* 2015, Masiello 2004). Generally, PyC is considered to have a longer mean residence time than non-pyrogenic soil C, typically on the centennial time scale (Bird *et al.* 2015, Hammes *et al.* 2008). However, in the past two decades, there has been growing evidence for PyC decomposing on shorter time scales, on the order of days to years (Cheng *et al.* 2006, Nguyen *et al.* 2009, Soucémarianadin *et al.* 2015). Furthermore, Bird et al. (2015) suggested a multi-pool model of PyC decomposition, where physical or chemical components of PyC are considerably more susceptible to decomposition than others. Ultimately, the breakdown of PyC and its loss from the soil system appear to be controlled by environmental conditions, particularly temperature and moisture, in addition to soil-specific conditions, such as landform position, aggregation, and depth, among others (Bird *et al.* 2015, Boot *et al.* 2015). Current estimates of PyC mean residence time in soil range from 250 to 300 years (Hammes *et al.* 2008), but the lack of data or predictive capability for the time scales and magnitude of PyC erosion post-fire potentially adds considerable uncertainty to these estimates (Bird *et al.* 2015).

Soil erosion laterally transports 1-5 Gt C per year (Battin *et al.* 2009, Stallard 1998). The amount of material mobilized in a particular watershed is dependent on the intensity and duration of rainfall, groundcover, vegetation, slope gradient, and recent fire history (Pierson *et al.* 2009, Renard *et al.* 1997). Between 70 and 90% of the soil and associated carbon mobilized from eroding landscapes is deposited within the source or adjacent watersheds (Gregorich *et al.* 1998, Stallard 1998). Local deposition of eroded material, along with dynamic replacement of eroded C by production of new photosynthate and stabilization of at least some of the eroded C in the depositional settings, leads to an erosion induced terrestrial sink for atmospheric CO_2 (Berhe *et al.* 2007, Harden *et al.* 1999).

Fire and erosion interact to modify a range of soil physical and chemical properties post-fire. The loss of vegetation after high severity fires is one of the main drivers of post-fire erosion, as vegetation plays a major role in stabilizing eroding soils (Larsen *et al.* 2009, Pierson *et al.* 2009, Shakesby *et al.* 1993). In extreme cases, this loss of vegetation can lead to debris and ash flows when intense rainfall events occur on recently burned hillslopes (Carroll *et al.* 2007). In addition

to the loss of stabilizing vegetation, fire can produce a hydrophobic layer below the surface of the soil which can change the hydrologic flow along a hillslope (DeBano 1990, Shakesby *et al.* 2000), reducing rate of water infiltration to soil and enhancing rates of runoff, which is a major driver of erosion (DeBano 1990, Pierson *et al.* 2013, Shakesby *et al.* 2000).

Post-fire erosion of topsoil rich in PyC can plan an important role in controlling the accumulation and residence times of PyC in the soil system. So far, relatively few studies have focused specifically on the erosion of PyC. From the available data, it is becoming increasingly clear that PyC is highly susceptible to erosive forces, more so than non-pyrogenic C (Rumpel *et al.* 2006, Yao *et al.* 2014). After high severity wildfires, PyC has been documented to have enrichment ratios, or concentration in eroded sediment divided by concentration in source soils, of $1.4 - 2.1$ at the plot scale (Abney *et al.* In prep), and 2.3 across the watershed scale (Rumpel *et al.* 2006). The observed high enrichment ratios of PyC are partly due to its relatively lower density compared with other SOM constituents, along with its concentration in the upper soil horizons and hydrophobicity (Brewer *et al.* 2014, DeBano 2000, Rumpel *et al.* 2015, Rumpel *et al.* 2006). There is some evidence that erosion of PyC is controlled by different processes than non-pyrogenic C. Yao *et al.* (2014) found that erosion of PyC decreases with increasing soil erosion, while non-pyrogenic C erosion increases with bulk soil erosion, potentially due to the periodic inputs of PyC compared with the continual inputs of non-pyrogenic C to soil. Erosional loss of PyC from slope positions and depositional input of PyC into lower-lying depositional landform positions post-fire can significantly decrease or increase its mean residence time in soil by up to 100 years (Abney & Berhe In Prep), and the burial of PyC in depositional positions can increase the mean residence time to the millennial scale (Bird *et al.* 2015, Marin-Spiotta *et al.* 2014).

Vertical mobilization of PyC and other SOM within a soil profile occurs mainly due to leaching, bioturbation, and illuviation (Eckmeier *et al.* 2007, Rumpel *et al.* 2015). Leaching is primarily responsible for vertical transport of dissolved constituents, while bioturbation and illuviation, or the downwards transport of particles via water flow, can move particulate PyC and OM down the soil profile. In post-fire environments, the rate of vertical mobilization of PyC depends on the size and solubility of the PyC, the nature of the porous media, including soil texture, bulk density, and porosity, and the rate of water flow through soil, which is driven by rainfall amount and intensity (Bird *et al.* 2015). Literature reported values for vertical mobilization of freshly applied PyC are typically on the order of mm per year (Major *et al.* 2010, Rumpel *et al.* 2015), although this may differ after natural wildfires and with aged char. The degradation of PyC, and release into the dissolved phase, creates a slow, centennial-scale loss of PyC from the soil. As PyC is exposed to environmental conditions, it degrades and becomes more soluble and can be mobilized at rates more than 40-55 times that from fresh char (Abiven *et al.* 2011).

The main objective of this study is to understand how PyC is mobilized laterally and vertically within soil profiles post-fire and to understand how mobilization of PyC impacts its long-term persistence in soil. To accomplish these objectives, we used a combination of spectroscopic techniques to determine how post-fire erosion changes distribution of C and soil organic carbon (SOC) fractions at the site of the Gondola Fire, South Lake Tahoe, California. Specifically, we determine: (a) how stocks of PyC and other SOC fractions in eroding and depositional landform positions change after fire; (b) how much PyC and SOC fractions are laterally redistributed by erosion over short (1^{-yr}) and longer (10^{-yr}) timescales; and (c) how much PyC and C in other fractions is vertically mobilized down the soil profile post-fire?

METHODS

Site description

The Gondola Fire burned over 270 ha on July 3, 2002, on the south shore of Lake Tahoe (38º57' N; 119º55' W, Figure 1), near Stateline, NV (Saito *et al.* 2007). The Gondola fire was characterized as a moderate severity burn, with partial consumption of the O horizon, and significant heat transfer down to 1 cm of mineral soil, where temperatures reached up to 200ºC (Carroll *et al.* 2007). Two weeks after the fire, on July 18, an intense precipitation event that deposited 15.2 mm of precipitation as rain and hail mobilized 380 Mg (metric tons) of material downslope, which was deposited in a downslope riparian area that borders the Edgewood Creek (Figure 2). The depositional area was about 0.8 ha in size and was densely vegetated with slopes of 0 to 5 % (Carroll *et al.* 2007, Saito *et al.* 2007).

The study area is characterized by Mediterranean climate with cold and snowy winters and warm to hot summers. The site receives most of its 87 cm of mean annual precipitation as snow and has a mean annual temperature of 6.7°C. The study area is underlain by granitic parent material and is a part of the Cagwin-Rock Outcrop. Soils of the study area are classified as coarse, loamy sand, mixed Typic Cryopsamments (Carroll *et al.* 2007, Johnson *et al.* 2007). The dominant vegetation in the area includes white fir (*Abies concolor),* Jeffery pine (*Pinus jeffreyi*), and Sugar pine (*Pinus lambertianna*) in the overstory; and Sierra chinquapin (*Castanopsis sempervirens*), currant (*Ribes spp.)*, snowbrush (*Ceanothus velutinis*), and bitter brush (*Purshia tridentata*) in the understory (Saito *et al.* 2007).

Sampling design

This site had 16 previously established hillslope sampling plots (Figure 1), in which seven were burned during the fire, seven were unburned, and two were partially burned (Carroll *et al.* 2007). Directly below the burned hillslope, within the identified deposition area of eroded material from the hillslope plots, 17 sites were selected within the depositional area (Carroll *et al.* 2007). These plots were sampled before the Gondola Fire, in late spring in 2002. The same plots were resampled one-year post-fire, during the summer of 2003, and then 10-years post-fire in the summer of 2013, with the addition of 13 new sites in the depositional area to capture the variability of this area. In the eroding hillslope plots, soil samples were collected from five random locations within each plot by depths of 0-10 cm, 10-30 cm, 30-60 cm, and 60-100 cm, which approximately corresponds to genetic horizons A11, A12, AC, and C (Johnson *et al.* 2007). In the depositional sites, soil was collected from the depth of 0-15 cm. The five replicates from the hillslope soils were composited and homogenized, and all samples were passed through a 2-mm sieve prior to further laboratory analysis.

Basic soil, elemental, and isotopic analyses

Air-dried, sieved soils were analyzed for pH in a 1:2 ratio of soil to both water and 0.01M $CaCl_2$ solutions with a Fisher Scientific Basic Probe (AB15 meter, Waltham, MA). Gravimetric water content was measured via drying approximately 10 g subsets of field-moist soil in an oven at 105°C for 48 hours. Bulk density was determined by the core method, where a 5x10 cm core was hammered into the soil, and dried at 105°C for 48 hours.

Prior to C and N elemental and isotopic analysis, air-dried soils were ground for 3 min in a ball mill (8000M Spex Mill, SPEX Sample Prep, Metuchen, NJ) to a homogenous fine powder.

Samples were tested for carbonates by reacting them with 1M HCl. No effervescence was observed, so we concluded that these samples had no carbonates and hence the total organic carbon concentration in the soils is equal to total carbon concentration. For C, N, and stable isotopic analyses for $\delta^{13}C$ and $\delta^{15}N$, we weighed between 15 and 40 mg of ground soil into tin capsules. These samples were combusted in a Costech ECS 4010 CHNSO Environmental Analyzer (Valencia, CA) connected via a Conflo IV interface (Thermo Finnegan, San Jose, CA) to a Delta V Plus Isotope Ratio mass spectrometer (ThermoFisher Scientific, Waltham MA). All C and N concentration values are reported as oven-dry sample weight. The stable isotope values are reported using the δ notation, in units of per mil (‰). Samples were measured against peach leaf and acetanilide, with standard errors of ± 0.23 $\delta^{15}N$ and ± 0.09 $\delta^{13}C$ variation for peach leaf and ± 0.15 $\delta^{15}N$ and ± 0.07 $\delta^{13}C$ variation for acetanilide. Duplicate samples had standard errors of ± 0.20 $\delta^{15}N$ and ± 0.05 $\delta^{13}C$. The higher variation in standards compared with samples is likely due to them spanning numerous sample runs and due to variations in the size of the standards across different sample runs. Our results were calibrated relative to international standards (e.g., NBS-22, N-1, and N-2) and are referenced relative to atmospheric N_2 and Vienna Pee Dee Belemnite (VPDB).

Spectroscopy

Bulk chemical characterization and determination of PyC concentrations in the samples were carried out by combining ^{13}CPMAS - Nuclear Magnetic Resonance (NMR) and Mid-Infrared (MIR) Spectroscopy. The data derived from ^{13}C NMR and MIR along with partial least squares regression analysis (MIR/PLSR) was then used to determine the proportion of PyC in the soil samples. This NMR and MIR/PLSR technique reliably estimates the concentration of PyC across a range of soil types and concentrations of bulk C and PyC (Baldock *et al.* 2012, Janik *et al.* 2007, Skjemstad *et al.* 2004), and is also the most cost and time-effective technique for quantifying the amount of PyC in soil to date.

Mid-Infrared spectroscopy (MIR) analysis was conducted on all ground soils on a Thermo Nicolet 6700 spectrometer (ThermoFisher Scientific, Waltham, MA) using a Pike AutoDiff diffuse reflectance attachment (Pike Technologies, Madison, WI), as described in Sanderman *et al.* (2011). A KBr beam-splitter scanned the samples 60 times and produced absorbance spectra from wavenumbers 7800-400 cm^{-1}. Spectra were background corrected against silicon carbide and then baseline corrected. Peak region assignments were adapted from Araya *et al.* (2017).

A subset of samples was analyzed via ^{13}C-CPMAS NMR spectroscopy on a Bruker Avance system (200MHz). The Kennard-Stone algorithm was utilized to pick 20 samples for NMR analysis that incorporated the most variability in the MIR dataset (Kennard & Stone 1969). This algorithm and principal components analysis demonstrated that most variability was in the deposition samples, and first axis accounted for 86% of the variance in the MIR data. The NMR analyses were conducted on only depositional landform position soils, as the eroding soils did not produce usable spectra, but principal component analysis of the MIR spectra demonstrated that most of the variability in the soil chemical properties was in the depositional soil samples. Samples for NMR analysis were packed into a 7 mm rotor, along with a glycine reference to calculate carbon observability, and analyzed at the magic angle with a 1 ms contact time (Baldock *et al.* 2012, Sanderman *et al.* 2011).

Of the 20 samples selected for NMR, nine of them produced poor quality spectra and were demineralized with HF prior to re-analysis to increase C content of samples, decrease noise in the

spectra, and remove interference from paramagnetic species in soil (Smernik & Oades 2002). This method can alter SOM composition, but has been widely used to make spectra collection possible (Berhe *et al.* 2012, Schmidt *et al.* 1997). To demineralize the samples, they were washed nine times with 45 mL of 2% HF over the course of a week, and then three times with DI water (Sanderman *et al.* 2011). To determine C observability, glycine was used as a reference (Smernik *et al.* 2000), and from the NMR analysis, 18 usable spectra were produced, with C observability over 25%. Spectra were corrected to a glycine standard for observability. For these NMR analyses, 10-20,000 scans were collected per sample, and the collected spectra were integrated into eight regions: 0-45 ppm (Alkyl), 45-60 ppm (N-Alkyl/Methoxyl), 60-95 ppm (O-Alkyl), 95-110 ppm (Di-O-Alkyl), 110-145 ppm (Aryl), 145-165 ppm (O-Aryl), 165-190 ppm (Amide/Carboxyl), and 190-215 ppm (Ketone).

Post-analysis, MIR and NMR data were combined to predict organic C fractions within the soil samples in a partial least squares regression combining MIR and NMR data (Baldock *et al.* 2013, Baldock *et al.* 2013). This model has proven to be a reliable and time-effective method for predicting soil fractions and has been calibrated across numerous soil and land-use types (Baldock *et al.* 2013b, Baldock *et al.* 2012). The SCaRP model independently predicts three organic carbon fractions, based on 312 soils collected across agricultural sites in Australia (Baldock *et al.* 2013, Baldock *et al.* 2013): resistant organic carbon (ROC, particles <50 μm that are chemically similar to charcoal), particulate organic carbon (POC, particles 50-2000 μm), and humic organic carbon (HOC, particles <50 μm). Due to the independent predictions of the three fractions, the sum of %C in each fraction will not necessarily add up to 100.

Additionally, due to poor fit of the SCaRP model to the ROC fraction in the depositional soils, a separate NMR/MIR PLSR was created from the NMR and MIR data collected on these samples using the partitioning of OC into PyC and non-PyC components as described by Baldock *et al.* (2013). This separate model captures the high variability of the depositional samples, which likely was due to the high concentrations of ash and the mixture of materials deposited in that setting (Carroll *et al.* 2007).

Data analysis

All data analysis and figure generation was conducted in RStudio (version 1.0.316, rstudio.com). Separate linear mixed effects models were built to (1) assess the transport of organic carbon fractions and bulk carbon through the soil profile with time, and (2) to assess surficial transport of these fractions across the surface of the landscape (0-10 cm for eroding hillslope and 0-15 cm for depositional soil). The depth model (1) predicted SOC fraction using time, depth, and burning as fixed factors and plot number as a random factor. The surface transport model (2) predicted SOC fraction used time, landform position, and burning as fixed factors and plot as a random factor. Models were tested for significance ($p<0.05$) by comparing null intercept-only models to models with fixed and random effects using the likelihood test. Differences between treatments were assessed using a Tukey Honest Significant Difference test and were also assumed significant at $p<0.05$. For all other statistical comparisons without time as a factor, two-way ANOVAs were used with depth and burn or control as predictors. Means are presented with standard error with n=8 for eroding hillslope samples and n=30 for depositional samples.

RESULTS

Bulk soil properties and elemental concentrations

Soils from the eroding landform positions were generally acidic pre-fire. However, at depths below 30 cm in 10-year post-fire sampling period the soil pH values were in the neutral range (Table 1). The pH of the eroding soils, in both the burn and control plots, increased after the fires by up to 1.25 units. Bulk density showed less than 0.2 g/cm^3 change post-fire with the values increasing in the burned plots and decreasing in control plots. Soils at the depositional landform position had a pH range and bulk density values that were similar to the topsoil from the eroding position.

Soils from the eroding positions had <2% C, in which C concentrations showed a consistent, but statistically not significant (p=0.83), decreasing trend with depth in both the burn and control plots in the control and burn plots (Figure 3). The soils generally had very low N concentrations (<0.1%). There was a marked increase in concentration of both C and N in topsoil (0-10 cm) immediately post-fire, but the values reverted to pre-fire levels at the 10-year post-fire sampling period (Figure 3). In contrast to the eroding soils, the total C concentrations in depositional soils ranged from 2-10%. The depositional soils did not significantly (p=0.38) differ in N concentration than those from the eroding positions, when accounting for the effects of depth and time. The mean total N during the 2013 sampling period was 0.05% and the mean total C was 1.87% (Table 2).

SOC in fractions and PyC

The concentrations of total C and SOC fractions in the depositional landform position increased significantly between the pre-fire and one-year post-fire sampling time points (p=0.00, Figures 4 and 5). However, there was a significant decrease in the concentration of all three SOC fractions at the 10-year post-fire sampling point (p=0.00) to below the pre-fire concentrations.

Linear mixed effects models indicated that the C concentration in the organic carbon fractions from the eroding soils (Figure 5) significantly depended on sampling time, depths, and burn condition (Tables 3 and 4). Concentrations of SOC fractions did not decline significantly with depth (ROC p=0.82, POC p=0.94, HOC p=0.60), but the top horizon had higher concentrations of each of the SOC fractions than the deeper horizons. The eroding soil regressions also indicated that the 2013 sampling time had significantly higher concentrations (p=0.02) of each of the SOC fractions than was non-significantly (ROC p=0.66, POC p=0.36, HOC p=0.18), more concentrated in burn plots compared with control plots, and was significantly (p=0.02) more concentrated in 2013 compared with the earlier sampling points.

The statistical model of the SOC fractions in the surface soil indicated that there was no statistically significant difference between the pre-burn and one year post-fire sampling times, but that the 10-year post-fire sampling had significantly lower SOC concentrations (p=0.00), largely driven by the large decline in SOC fractions in the depositional landform positions. There were no significant differences in the burn and control plots on the eroding hillslope (ROC p=0.92, POC p=0.79, HOC p=0.834). Across the three SOC fractions and accounting for sampling time and burn, the eroding plots had significantly lower concentrations of the SOC fractions than the depositional landform positions (HOC p=0.00, POC p=0.00), except for the ROC fraction (p=0.05). However, the eroding landform position had significantly higher concentration of SOC fractions at the final sampling point than the depositional landform position.

In the eroding plots only model, the burned plots had non-significantly higher ROC concentrations than the unburned plots, and the 10-years post-fire sampling point had significantly higher concentrations of ROC compared with pre-burn (p=0.00) and one-year post-burn (p=0.02) concentrations. Both the burned and unburned plots had significantly higher HOC concentrations in the 10-years post-fire sampling point compared with the pre- and post-fire sampling point (p=0.00 and p=0.00). The unburned plots had slightly, but non-significantly (p=0.64), lower concentrations of HOC than the burned plots.

In each of the sites, the three SOC fractions were summed and the proportion of ROC to total C was calculated (Figure 6, Tables 3 and 4). There was no significant trend with ROC fraction with depth (p=0.11) or between burn and control plot (p=0.44), but ROC made up a significantly higher proportion of hillslope SOC compared with the depositional landform position (p=0.00). The ROC fraction was also significantly lower in the 10-years post-fire time point compared with either of the first two time points(p=0.00).

Isotopic and Spectroscopic composition of SOM

For the eroding plots, δ^{13}C was significantly enriched (p=0.02) in the control plot compared with the burned plot (Figure 7). The δ^{13}C of bulk SOM declined with depth but the relationship was not statistically significant (p=0.72). With increasing depth into the soil profiles of the eroding plots, the δ^{15}N values were significantly more enriched in the control plots compared with the burned plots (p=0.02).

Both the control and 10-year post-fire plots showed an increase in peak heights in the –OH function group (3700 cm^{-1}) with depth and a decrease in the –CH (2940 cm^{-1}). The ester and phenol regions (1159 and 995 cm^{-1}) also showed a decrease in peak heights with depth into the soil profile in both the pre- and post-fire spectra based on DRIFT spectra designations of Parikh *et al.* (2014). The most important differences in the MIR spectra in the soils from the burned and control plots, for regions of interest to SOM composition, (Figure 8) were observed in the spectral regions representing asymmetric and symmetric C-H stretching vibrations in aliphatic compounds (2924 and 2850 cm^{-1}, respectively); C=C stretching vibrations of aromatic compounds (1650 cm^{-1}); N-H bending vibrations and C=N stretching vibrations in amides (1575 cm^{-1}); C-H bending (1390, 1405, and 1470 cm^{-1}) in aliphatic; C-O stretching and asymmetric stretching vibrations in carboxylic and phenolic groups (1270 cm^{-1}); and C-O symmetric vibrations in polysaccharides (1080 and 1110 cm^{-1}). The peak heights in the aromatic and polysaccharide regions both increased in the top soil (0-10 cm), due to higher C concentrations there. We also observed increased peak highest in the aromatic region at 10-30 and 60-100 depths, and in the polysaccharide regions below 60cm depths. All soil depths had increased peak heights in the amide region.

Comparing the pre-fire (2002) and post-fire (2003) spectra of soil from the depositional position (Table 5, Figure 9) shows increased contribution of aryl and O-aryl groups (110-165 ppm), alkyl (0-45ppm), and ketones (190-215 ppm); and reduced contribution of O- and N-substituted alkyls (45-110 ppm) and amide and carboxylic groups (165-190 ppm). The largest shift in distribution of C in the different organic functional groups was observed in the aryl region that saw an increase by 1.9% post-fire.

DISCUSSION

Following the Gondola fire, erosion redistributed soil C and PyC laterally down the hillslope. Overall, we found an increase in all SOC fractions in the depositional landform position 1-year

post-fire. By conservatively assuming the concentration of C and ROC in the transported sediment was equivalent to the concentration in post-fire control eroding plots, the initial mass movement of 380 Mg of material (Carroll *et al.* 2007) equates to the transport of 7.6 Mg C and 2.4 Mg ROC. When accounting for the 3.8 ha of source area, this is transport equates to 2.0 Mg C and 0.6 Mg PyC per ha. This transport contributed to the increase in the depositional soil C content from 6.3 to 8.9% C, but this transport alone did not contribute all the increase in soil C. It is likely that erosion events from the remainder of the post-fire year preferentially transported SOC and PyC to this depositional landform position (Rumpel *et al.* 2006, Stacy *et al.* 2015). However, by 10-years post-fire, the SOC fractions in the depositional landform position sites declined to below pre-fire levels. This decline suggests either burial by subsequently eroded material or the rapid decomposition of SOC in that landform position. In the long-term, there were no significant changes in the carbon concentration of the top soil of the eroding plots, even after the major erosion event post-fire.

Transport and loss of different SOC fractions due to post-fire erosion

The slightly increased contribution of the ROC fraction in eroding hillslope plots that persisted even 10 years after the Gondola fire confirms the input of pyrogenic carbon from the fire (Figures 4, 5, 9). From our findings, the PyC continued to be lost from the eroding plots, presumably via ongoing erosion processes. Our data also shows that PyC is a dynamic pool of SOC, as seen by the significant drop in the ROC fraction in the topsoil of the depositional landform position (Figure 5). These findings are consistent with our previous work, where we showed that erosion can play major role in lateral redistribution of PyC post-fire, with implications for persistence of PyC in dynamic landscapes (Abney & Berhe In Prep).

All the SOC fractions in the depositional landform position increased in the one-year post-fire sampling point and decreased to below pre-fire concentrations at the ten-year sampling point. This large initial increase is likely due to the mass-movement erosion event that deposited fire-altered material downhill after the fire. The subsequent loss of C in all the SOC fractions in the long-term suggests that this SOC material may not be stabilized if it remains on the surface of the depositional landform position. The depositional, riparian area characterized by higher concentrations of both C and N, as well as wetter soil water conditions, which could support higher decomposition rates. In comparison, the well-drained coarse soils in the eroding landform positions were relatively C- and N-poor, but contained a higher proportion of the ROC as a fraction of total C (Figure 6). This is consistent with previous decomposition and other SOC studies that showed that rate of SOC loss through decomposition could be faster on the surface of organic matter rich and poorly drained depositional landform positions (Berhe 2012, Berhe 2013). In addition to decomposition, SOC loss from the surface soil in the depositional landform position may become stabilized in the depositional landform positions if it is buried by subsequently eroded material (Berhe 2007, Doetterl *et al.* 2016).

The cycling and persistence of ROC, or PyC, post-fire is controlled by numerous factors, including erosion and decomposition conditions (Bird *et al.* 2015). The ROC fraction in eroding positions increased slightly over time starting at pre-fire levels than increasing at 1 and 10 years after the Gondola Fire. This increase is likely due to the redistribution of material or further inputs of charred material. The Sierra Nevada is a highly fire-prone region (Westerling *et al.* 2006), and it might be that numerous fires in the Sierras after the Gondola Fire deposited ash and smoke in the vicinity (Peterson *et al.* 2015). The lack of significant difference in the ROC and other SOC

fractions in the eroding burn and control plots also suggests input of ROC from sources other than the Gondola Fire itself, or that much of the ROC formed on the eroding hillslope was lost in the initial erosion event (Carroll *et al.* 2007) or via rapid decomposition (Kuzyakov *et al.* 2009, Nguyen *et al.* 2009).

In the depositional landform position, potentially further erosion events may have resulted in the loss of SOC fractions on the longer-term scale, although this was likely a small loss, due to the lower slope in this landform position. The initial eroded material contained a considerable concentration of ash (Carroll *et al.* 2007), which is highly susceptible to both wind and water erosion (Pereira *et al.* 2015). The mobilization of 1.5 Mg C/ha and 0.7 Mg ROC/ha in the initial erosion event was significant, however, the one-year post-fire concentration of ROC in the depositional landform position is double that of the hillslope plots, suggesting that after the initial erosion event, more pyrogenic material was eroded and deposited there.

Topsoil material in depositional landform positions can become buried by subsequently eroded material, such that it is possible that the eroded SOC fractions that were initially eroded were buried by subsequent deposition of eroded material without higher levels of ROC-SOC (Berhe *et al.* 2007). These later erosion events generally transport more mineral material that the earlier erosion events, since pyrogenic material is typically preferentially transported in early erosion events (Rumpel *et al.* 2009, Rumpel *et al.* 2006, Yao *et al.* 2014). If the relatively SOC-rich material that was originally deposited in the depositional landform position is buried with subsequent erosion, PyC and associated other soil C is likely to be physically stabilized in the soil profile of the depositional position.

The lower $\delta^{13}C$ and $\delta^{15}N$ values in the surface soil of burned eroding sites at the 10-year post-fire sampling time point (Figure 5) suggests that there may have been preferential combustion of organic matter with higher $\delta^{13}C$ and $\delta^{15}N$ values. This is opposite to previously published work that demonstrated that soil $\delta^{15}N$ values increase with increasing charring temperature and time (Pyle *et al.* 2015, Saito *et al.* 2007). It is possible that this difference is related to input of new, isotopically light material post-fire, or if isotopically heavier material was preferentially consumed during the fire, leaving behind isotopically light material, such as lignin (Benner *et al.* 1987).

At the 10-years post-fire sampling point, the depositional landform position had a relatively similar isotopic composition to the eroding surface soil, $\delta^{15}N$ values of 2.4‰ and 3.84‰ and $\delta^{13}C$ values of -26.2‰ and -25.73‰ for the burned eroding hillslope and depositional landform positions, respectively (Table 2 and Figure 5). This similarity is further evidence for the transport of surface soil and OM from the eroding positions and depositional within the depositional landform position. This long-term erosion may have led to the burial of earlier deposited material, that has much higher SOC concentration one-year post-fire, such that what was sampled as top soil in the depositional landform position 10-years post-fire was mineral material that was more recently transported from the upslope eroding landform position.

It is likely that at least a fraction of the SOC fractions in the depositional landform position post-fire were lost via elevated decomposition (Berhe 2012, Doetterl *et al.* 2012). The input of SOC and nutrients into the depositional landform position from the original mass flow event, along with the accumulation of water from precipitation and the nearby creek, could create ideal conditions for decomposition at this location compared with the eroding plots (Cheng *et al.* 2006, Johnson *et al.* 2007). The depositional landform position presents a range of conditions that can favor rapid loss of PyC that remains on the surface.

Downwards mobilization of SOC and SOM

Leaching can also mobilize SOC downward in a soil profile, as evidenced by the small, but not significant, increase in HOC and ROC fractions at depth in the eroding landform positions at the final time point (Figure 5), along with a decrease in δ^{13}C and δ^{15}N values throughout the burned eroding plots in the final sampling point (Figure 7). The soils in the eroding positions of the Gondola fire site are coarse textured and porous, creating optimum conditions for vertical mobilization of bulk C and PyC in dissolved and/or particulate form. The small shift in isotopic compositions of SOM suggest that the preexisting organic material and nutrients were lost during post-fire recovery. The organic matter that is left behind may be more complex biomolecules, such as lignin that are more difficult to breakdown. Additionally, there may have been a nutrient or substrate limitation on microbial processing that led to relatively heavier OM components, such as cellulose, being consumed in these systems, leaving behind isotopically lighter material that is susceptible to leaching. Even so, the leaching process is generally slow, as Major *et al.* (2010) found that in a year only 1% of their applied PyC was mobilized downward in the profile, and this change was not apparent at the one-year post-fire sampling point. The leaching of PyC also depends on the size (dissolved vs. particulate form) and vegetation type. Slow leaching of ROC downward may be altered by the quality of ROC material left after the initial mass movement event and the post-fire vegetation recovery (Güereña *et al.* 2015, Kindler *et al.* 2011, Major *et al.* 2010). Leaching may be occurring in the depositional landform position, but we did not sample at depth into this landform position, as no pre-fire comparison samples exist for the deep soils in the depositional landform position.

Implications of post-fire erosion for long-term persistence of SOC and PyC

Lateral redistribution of topsoil by soil erosion after wildfires has important implications for the dynamics of both bulk SOC and specific fractions. In the Gondola fire site, large amounts of C in all the SOC fractions were mobilized by a large erosive event immediately post-fire. However, we also found that significant amount of C from all the SOC fractions was lost from the surface depositional zone in the long term. It is clear from this 10 year, three sampling period study that C in all the SOC fractions in the eroding plots was considerably altered in the 10-years post-fire.

This change in C in the different SOC fractions suggests a contribution of likely elevated biological production post-fire for increases in the HOC and POC fractions. The increase in the ROC fraction that we observed could be due to either erosion of ROC from upslope or from deposition of ROC in the form of ash or soot from nearby wildfires, such as the Rim Fire (Peterson *et al.* 2015). Vertical mobilization of C in the different SOC fractions can lead to enhanced protection of both bulk C and PyC due to the decline in availability of oxygen and/or lower microbe biomass or active in deeper soil layers (Marin-Spiotta *et al.* 2014).

In contrast to the eroding landform positions, the depositional landform position lost significant proportions of C from all the SOC fractions over the 10 years likely due to combination of factors that includes ongoing transport of top soil material from the eroding hillslope that is deposited in the riparian area, leaching of C down the soil profile, burial of surficial soil from continually eroding upslope material, and decomposition *in situ*. The long-term stability of SOC in depositional landform positions critically depends on the local decomposition conditions (Berhe 2012) and erosion potential, as burial of SOC in depositional landform has also been demonstrated to be a stabilization mechanism for SOC and PyC (Berhe & Kleber 2013, Berhe *et al.* 2007, Chaopricha & Marín-Spiotta 2014).

Findings of our study have highlighted that lateral and vertical redistribution of C post-fire can have implications for soil carbon dynamics. So far, the comparative roles of lateral and vertical transport of PyC, such as erosion, leaching, and bioturbation, across differing landscapes remains largely unknown (Güereña *et al.* 2015, Rumpel *et al.* 2015). Depending on the prevailing environmental conditions at any particular site, wind- and water-driven erosion, leaching, and deposition from other fires (Bird *et al.* 2015) can play major roles in controlling stock, fluxes, stability and stabilization mechanisms of bulk C and PyC post-fire.

Limitations and future directions

One inherent limitation of this work is the use of the SCaRP model to predict SOC fractions. Since this model was developed using agricultural soils, there is some error associated with the SOC fraction predictions based on the difference in forest soils compared with arable soils. However, this model has been tested on thousands of soil types and has been demonstrated a reasonable predictor across different land uses and vegetation types in Australia (Sanderman *et al.* 2011).

A second major limitation of this work is the depth of sampling in the depositional landform positon. Without being able to predict the SOC fractions at depth in this landform position makes it impossible to determine whether the long-term loss of the SOC rich material that was deposited was due to burial by subsequently deposited material or via some other process. Additionally, the sampling of depositional and eroding hillslope surface soils at different depths can confuse some of the statistical models, becaise these were collected based on previous sampling strategies. Future research on the erosion of PyC should focus on the role of burial and vertical transport of PyC into the soil profile. Additionally, future research should focus on the episodic nature of erosion events that may bias reported loss rates of PyC erosion during post-fire recovery and hinder understanding of its fate in soils in dynamic landscapes.

CONCLUSIONS

After the Gondola fire, erosion changed the carbon sequestration trajectory of the system as over 1.5 Mg ROC/ha and 0.7 Mg C/ha of C in all SOC fractions was distributed away from the surface of the eroding landform positions, and deposited in the downhill riparian area. At the ten-year sampling point, the depositional landform position had considerably lower concentrations of all SOC fractions, and retained proportionally lower concentrations of ROC than the eroding hillslope. This suggests that either the highly charred and SOC-rich material was buried in the depositional landform position, or was more rapidly decomposed than in the eroding hillslope landform position.

The relatively low $\delta^{13}C$ and $\delta^{15}N$ values in the burned soils suggests persistence of SOM with isotopically lower values, such as those from lignin, while other material with higher isotopic values is consumed either during combustion or via post-fire microbial processing. Better understanding of the long-term fate of C in dynamic landscapes post-fire is critical for constraining of terrestrial carbon budgets in a changing world.

ACKNOWLEDGEMENTS

We thank Emma McCorkle for her help in the field and lab, and Erin Carroll for help with archived data on the study site. We thank Bruce Hawke and Janine McGowan for performing FTIR and NMR spectroscopic analyses of soil samples at CSIRO in Adelaide, Australia, and David Araiza, Christina Bradley, Elizabeth Williams, and Bobby Nakamoto of the Fogel Stable Isotope lab at

UC Merced for their assistance with the elemental and isotopic analyses. We also thank Stephen Hart for comments on earlier versions of this manuscript. Funding for this work was provided from Hellman Family Foundation Grant and a National Science Foundation award (CAREER EAR - 1352627) to A. A. Berhe and from UC Merced School of Natural Science to M. L. Fogel.

FIGURES

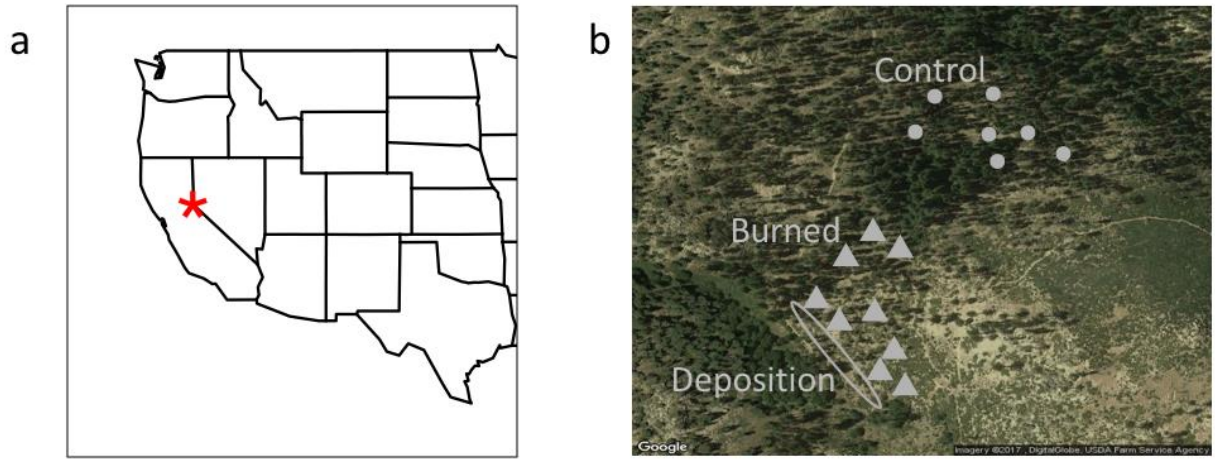

Figure 4-1. The Gondola Fire occurred outside Stateline, Nevada, in the Van Sickle Bi-State Park (a). Burned plots are indicated by triangles and unburned, control plots are indicated by circles (b). Moderate vegetative recovery has occurred since the fire in the burned area.

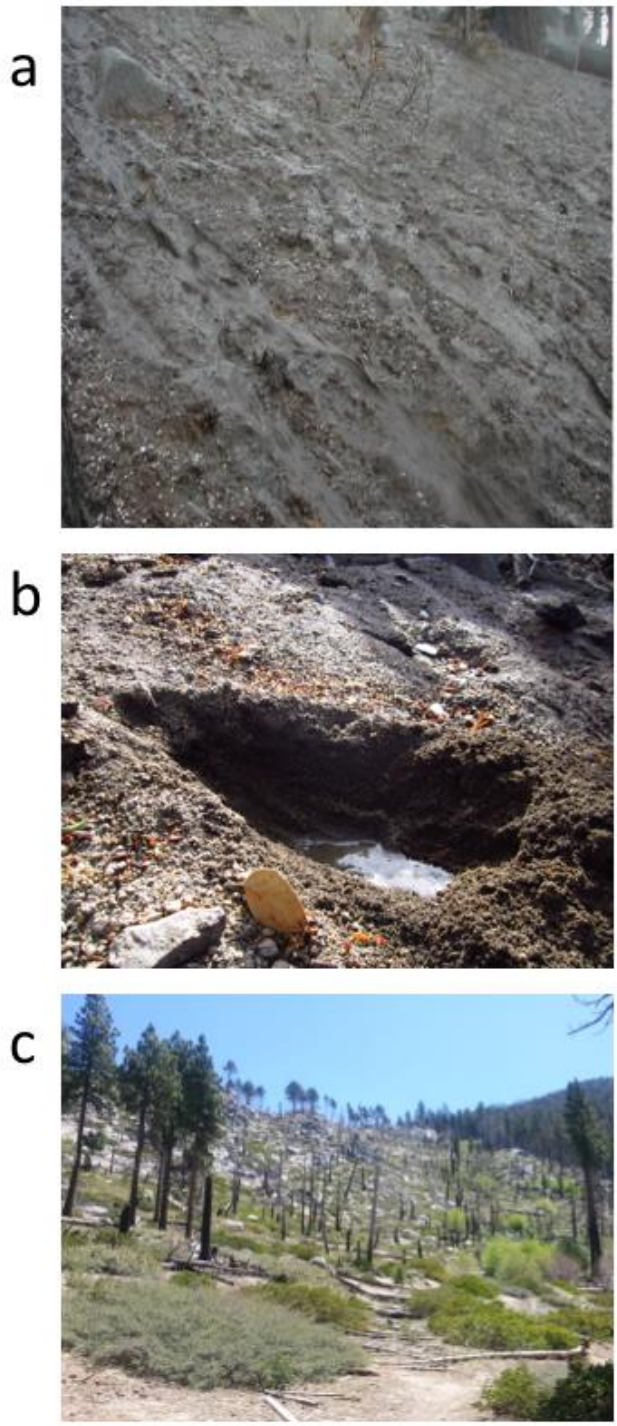

Figure 4-2. major ash flow occurred after the fire in 2002 (panel a, photo by J. Howard). The hydrophobic layer (panel b, photo R. Abney) created during the fire persists through the recent sampling (photo from November 2012, R. Abney). No canopy is left in portions of this moderate severity fire (panel c, May 2013, R. Abney).

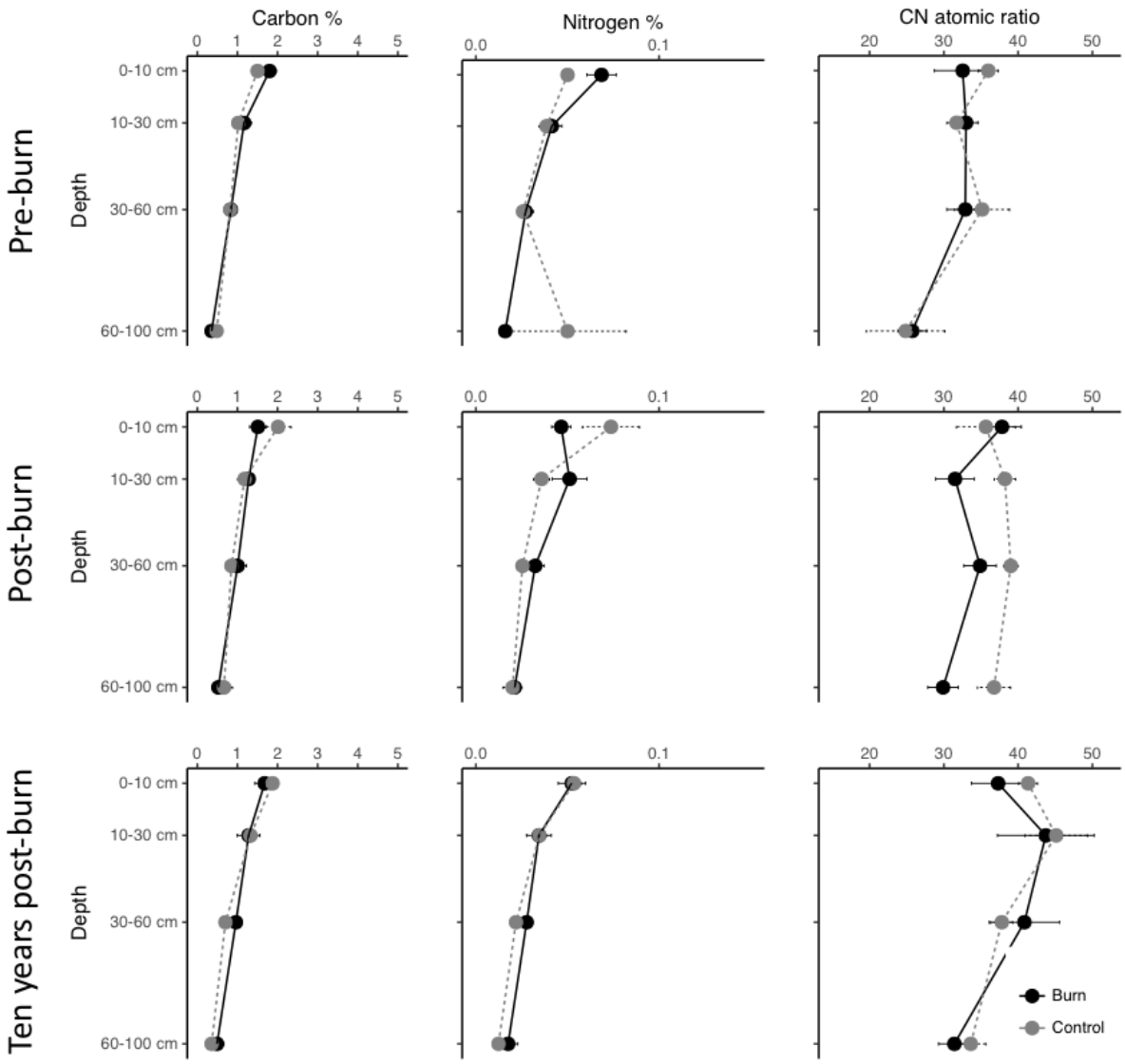

Figure 4-3. Carbon (C), nitrogen (N), and the atomic C:N ratio in the eroding position before burn, one year post-fire, and 10-years post-fire. Error bars represent standard error.

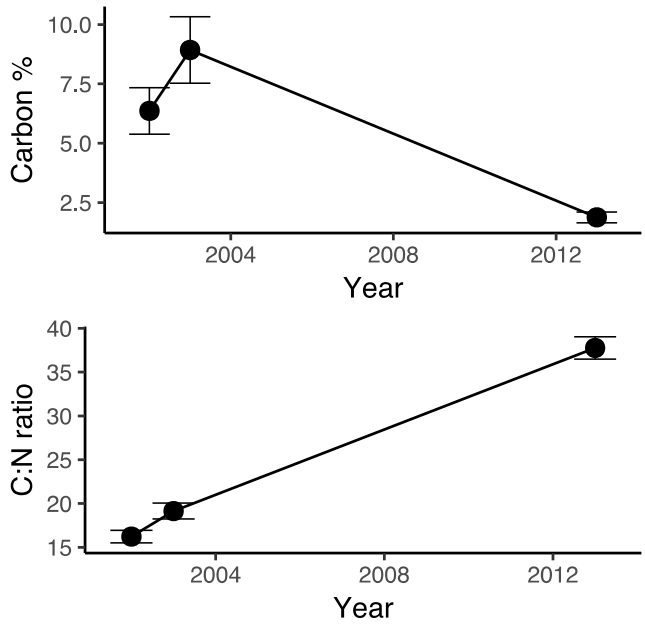

Figure 4-4. Total C and C:N ratio for the depositional landform position. Error bars represent standard error with n=30.

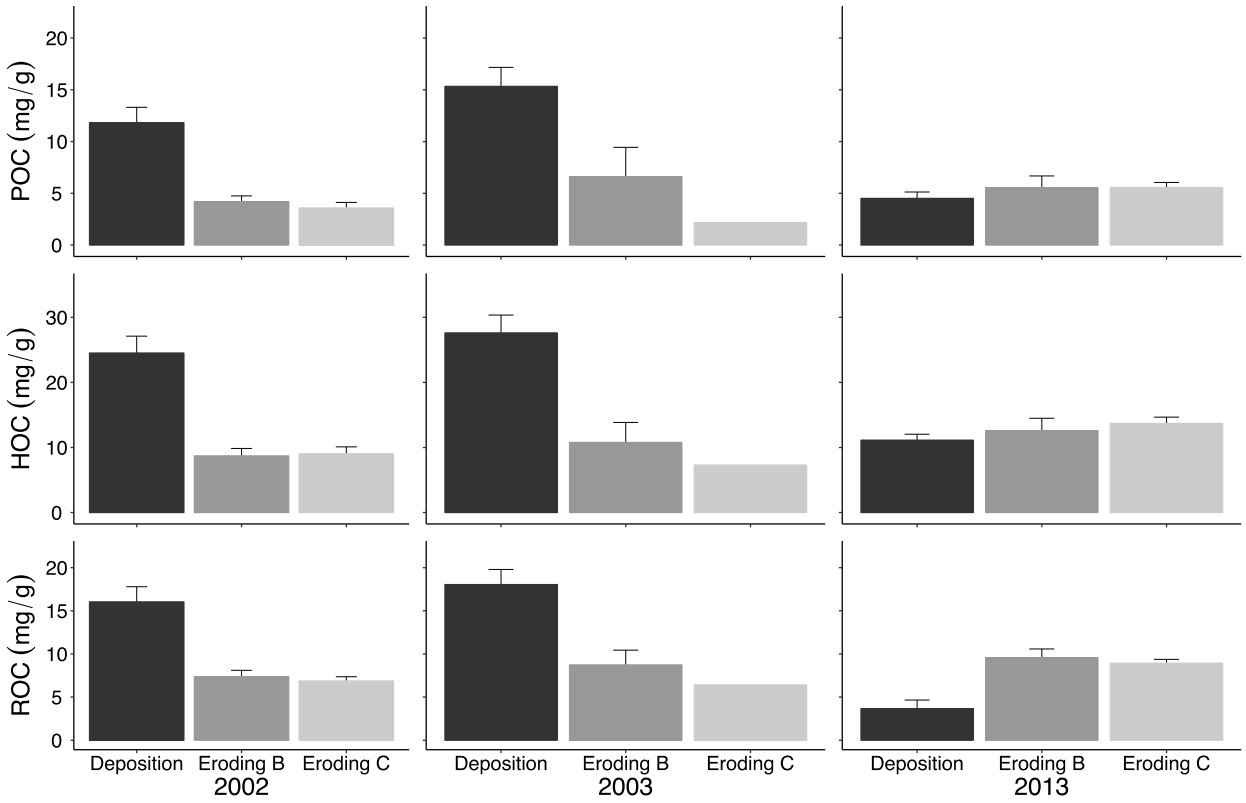

Figure 4-5. Soil organic carbon fractions (POC, HOC, and ROC) from pre-fire (2002), one-year post-fire (2003), and ten-years post-fire (2013) surface soils. Eroding surface soils were collected from 0-10 cm and depositional soils were collected from 0-15 cm. Error bars represent standard error with n=16 for eroding sites and n=30 for depositional sites. Eroding B refers to the burned eroding plots, and Eroding C refers to the control (unburned) eroding plots.

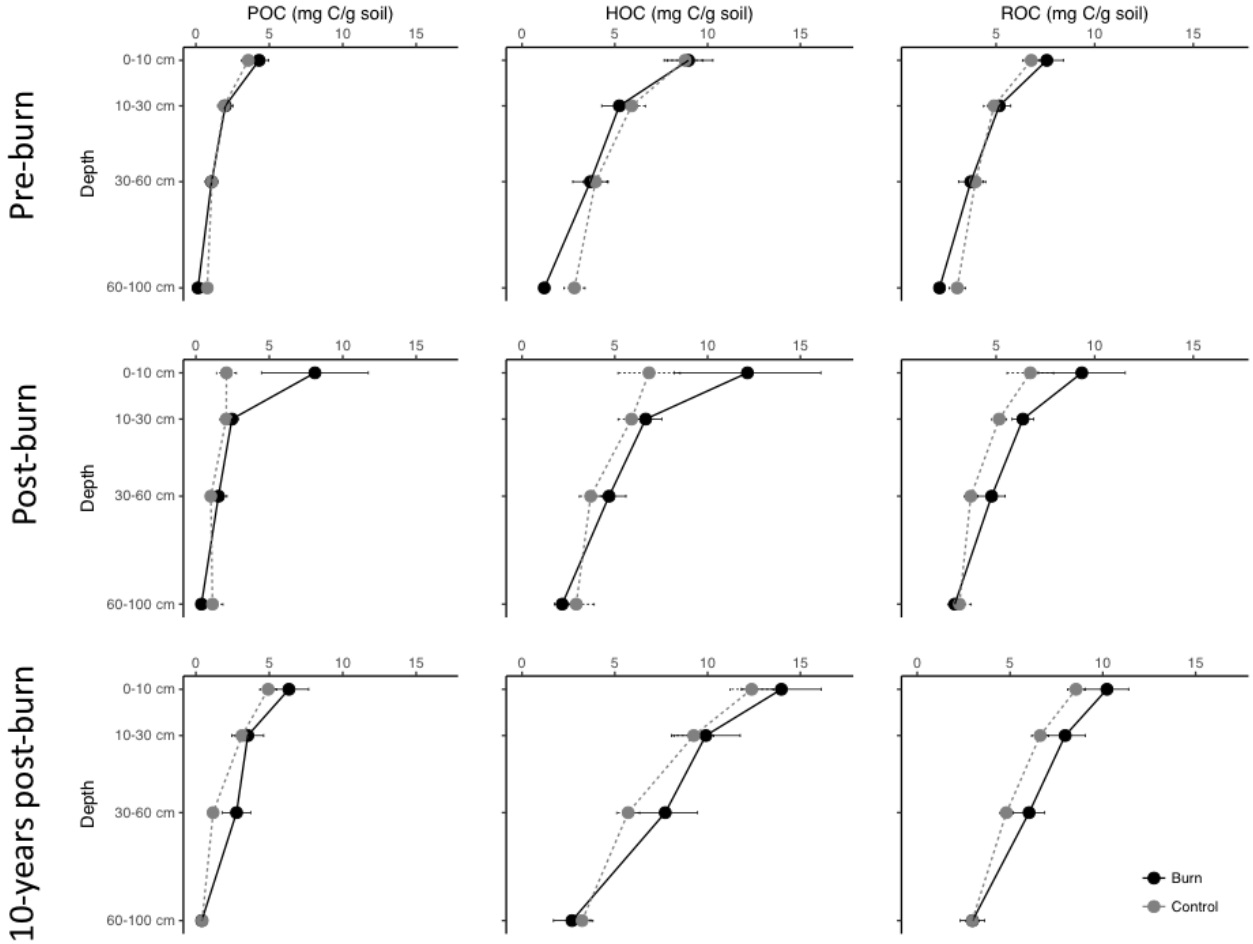

Figure 4-6. Organic carbon fractions for the eroding hillslope position from pre-fire, one-year post-fire, and 10-years post-fire in burn and eroding plots. Error bars represent standard error with n=8.

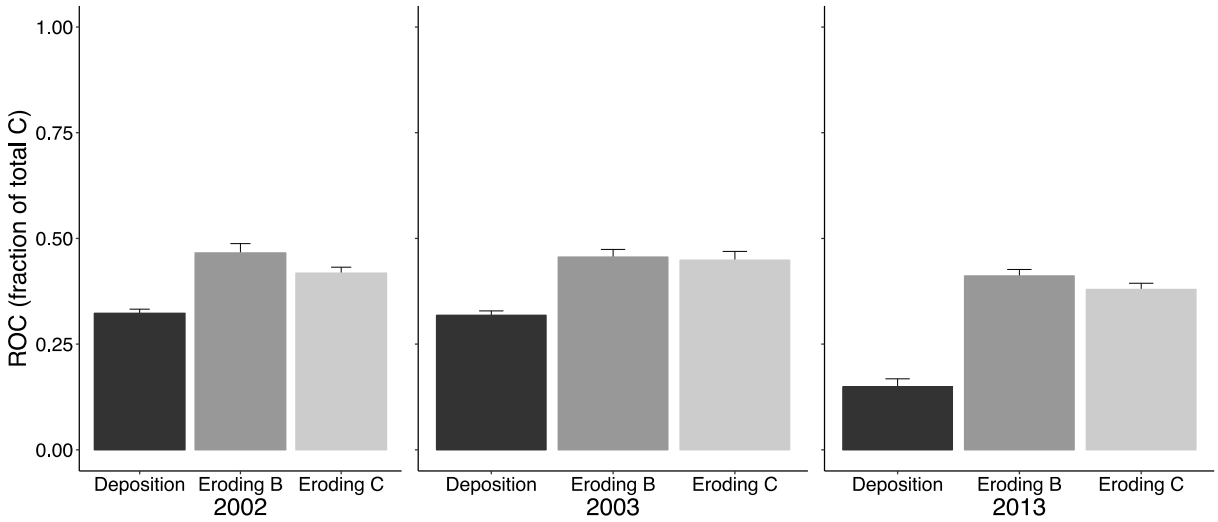

Figure 4-7. Resistant organic carbon as a fraction of total soil carbon. Eroding B refers to the burned eroding plots, and Eroding C refers to the control (unburned) eroding plots. Means are presented here for each sampling year with error bars representing standard error.

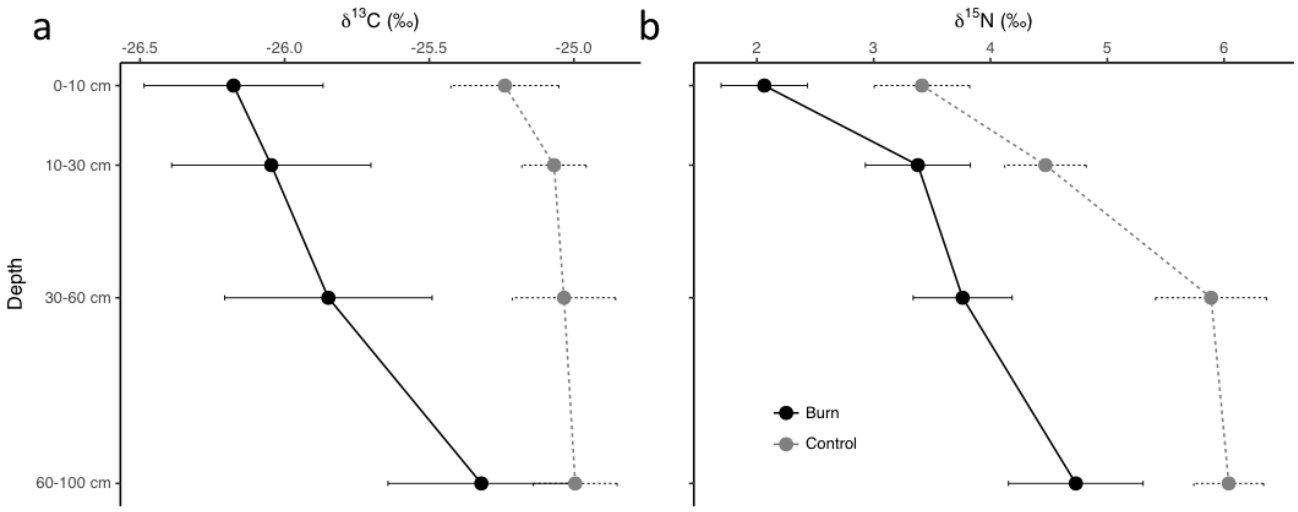

Figure 4-8. Stable carbon (a) and nitrogen (b) isotopes for the eroding landform position. Error bars represent standard error.

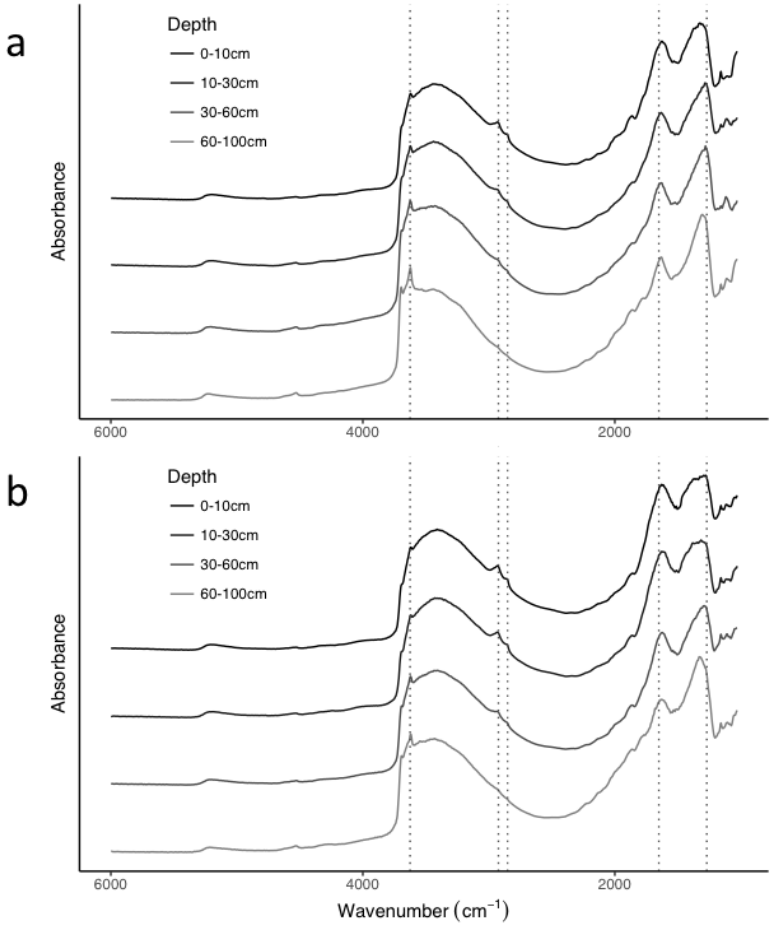

Figure 4-9. MIR spectra of soil from control (a) and burned (b) plots from the eroding position in the 10-year post-fire sampling time point. Shifts in peak intensities occurred at wavenumbers 1270 cm^{-1} (carboxylic and phenolic groups), 1650 cm^{-1} (aromatic compounds), 2924 cm^{-1} (asymmetric C-H stretching), 2850 cm^{-1} (symmetric C-H stretching), and 3625 cm^{-1} (O-H bonding).

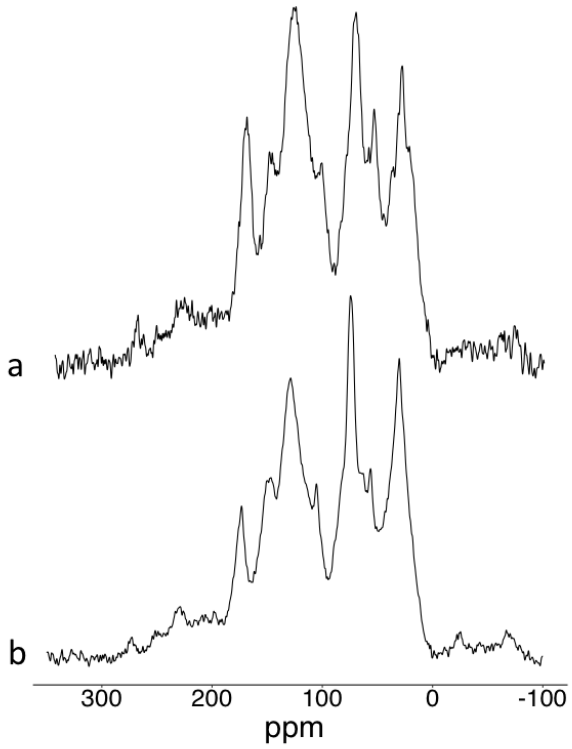

Figure 4-10. ^{13}C CPMAS NMR spectra of soil from pre-fire (a) and 10-year post-fire (b) samples from the depositional landform position. The spectra were divided into the following regions: 0-45 ppm (Alkyl), 45-60 ppm (N-Alkyl/Methoxyl), 60-95 ppm (O-Alkyl), 95-110 ppm (Di-O-Alkyl), 110-145 ppm (Aryl), 145-165 ppm (O-Aryl), 165-190 ppm (Amide/Carboxyl), and 190-215 ppm (Ketone).

TABLES

Table 4-1. Soil pH and bulk density for the eroding landform position, and summary elemental and stable isotope analyses for the depositional landform position. Standard error presented in parentheses (n=7 control, and n=8 burned).

		Pre-fire			Post-fire		Ten-years post-fire		
Location	Depth	pH in H_2O	pH in $CaCl_2$	Bulk Density (g/cm^3)	pH in H_2O	pH in $CaCl_2$	pH in H_2O	pH in $CaCl_2$	Bulk Density (g/cm^3)
Eroding (burned)	0-10 cm	5.82 (0.11)	5.09 (0.11)	1.24 (0.07)	6.69 (0.11)	5.98 (0.20)	6.54 (0.13)	5.57 (0.11)	1.41 (0.05)
	10-30 cm	5.77 (0.10)	4.98 (0.08)	-	6.37 (0.23)	5.74 (0.29)	6.64 (0.10)	5.68 (0.13)	-
	30-60 cm	6.08 (0.24)	5.30 (0.28)	-	6.35 (0.19)	5.65 (0.22)	6.77 (0.11)	5.72 (0.12)	-
	60-100 cm	6.12 (0.17)	5.39 (0.15)	-	6.40 (0.09)	5.61 (0.11)	7.37 (n/a)	6.15 (n/a)	-
Eroding (control)	0-10 cm	5.99 (0.18)	5.33 (0.20)	1.24 (0.05)	6.09 (0.06)	5.46 (0.05)	6.79 (0.14)	5.91 (0.18)	1.13 (0.04)
	10-30 cm	5.85 (0.22)	5.03 (0.23)	-	5.87 (0.06)	5.21 (0.06)	6.77 (0.17)	5.57 (0.17)	-
	30-60 cm	5.37 (0.14)	4.88 (0.17)	-	5.59 (0.11)	4.98 (0.03)	6.40 (0.21)	5.23 (0.27)	-
	60-100 cm	5.86 (0.11)	5.10 (0.16)	-	5.97 (0.09)	5.17 (0.08)	6.65 (0.12)	5.72 (0.24)	-

Table 4-2. Soil pH and bulk density for the depositional landform position, and summary elemental and stable isotope analyses for the depositional landform position soil collected in 2013. Standard error presented in parentheses (n=30).

Deposit-ion	Depth	pH in H_2O	pH in $CaCl_2$	Bulk Density (g/cm^3)	$\delta^{15}N$	$\delta^{13}C$	C:N atomic ratio	Nitrogen (%)	Carbon (%)
	0-15 cm	6.85 (0.12)	5.80 (0.14)	1.22 (0.12)	3.84 (0.18)	-25.73 (0.47)	37.76 (1.27)	0.05 (0.00)	1.87 (0.22)

Table 4-3. Eroding hillslope and surface soil model parameter estimates.

	Eroding hillslope model				Surface soil model			
	Parameter	Estimate	Std. error	t value	Parameter	Estimate	Std. error	t value
ROC	Intercept	-210.75	49.17	-4.28	Intercept	1634.39	295.22	5.53
	Time	0.10	0.02	4.46	Time	-0.80	0.14	-5.49
	Depth: 10-30 cm	-2.16	0.33	-6.52	Eroding hillslope	-3.74	1.95	-1.91
	Depth: 30-60 cm	-3.73	0.33	-11.26	Control (unburned)	-0.25	2.82	-0.09
	Depth: 60-100 cm	-4.94	0.36	-13.55				
	Control (unburned)	-0.92	0.69	-1.32				
POC	Intercept	-96.99	67.76	-1.43	Intercept	1101.91	272.39	4.04
	Time	0.05	0.03	1.51	Time	-0.54	0.13	-4.00
	Depth: 10-30 cm	-2.44	0.46	-5.30	Eroding hillslope	-4.96	1.80	-2.75
	Depth: 30-60 cm	-3.57	0.46	-7.74	Control (unburned)	-0.66	2.60	-0.25
	Depth: 60-100 cm	-4.21	0.50	-8.31				
	Control (unburned)	-0.59	0.65	-0.90				
HOC	Intercept	-441.09	87.56	-5.03	Intercept	1723.54	428.06	4.02
	Time	0.22	0.04	5.17	Time	-0.84	0.21	-3.97
	Depth: 10-30 cm	-3.59	0.59	-6.08	Eroding hillslope	-10.07	2.83	-3.55
	Depth: 30-60 cm	-5.90	0.59	-10.00	Control (unburned)	0.85	4.10	0.20
	Depth: 60-100 cm	-7.72	0.64	-11.89				
	Control (unburned)	-0.59	1.21	-0.48				
ROC fraction	Intercept	7.39	1.90	3.88	Intercept	24.20	2.59	9.31

Time	-0.00	0.00	-3.68	Time	-0.01	0.00	-9.21
Depth: 10-30 cm	0.04	0.01	3.14	Eroding hillslope	0.11	0.01	6.65
Depth: 30-60 cm	0.08	0.01	6.40	Control (unburned)	-0.02	0.02	-0.93
Depth: 60-100 cm	0.16	0.01	11.27				
Control (unburned)	-0.03	0.02	-1.58				

2

Table 4-4. Eroding hillslope and surface soil model comparisons with null model with maximum likelihood method.

Hillslope model					
SOC Fraction	χ^2	df	p	AIC	BIC
ROC	149.33	5	0.00	629.8	654.4
null model				769.2	778.4
POC	73.18	5	0.00	722.7	747.3
null model				785.9	795.1
HOC	130.48	5	0.00	812.8	837.4
null model				933.3	942.5
ROC fraction	110.87	6	0.00	-408.9	-381.2
null model				-310.0	-300.8
Surface soil model					
ROC	34.30	3	0.00	1011.3	1029.0
null model				1039.6	1048.5
POC	28.36	3	0.00	988.7	1006.4
null model				1011.1	1020.0
HOC	32.50	3	0.00	1115.4	1133.0
null model				1141.9	1150.7
ROC fraction	91.67	4	0.00	-310.6	-290.0
null model				-226.9	-218.1

Table 4-5. NMR functional group assignments of the depositional samples from before (2002) and after (2003) the Gondola Fire. Samples were chosen using the Kennard-Stone algorithm to accurately include the variance within the dataset. *indicates samples that were treated with HF prior to NMR analysis due to extremely poor signal acquisition.

Sampling time	Alkyl (0-45 ppm)	N-Alkyl/ Methoxyl (45-60 ppm)	O-Alkyl (60-95 ppm)	Di-O-Alkyl (95-110 ppm)	Aryl (110-145 ppm)	O-Aryl (145-165 ppm)	Amide/ Carboxyl (165-190 ppm)	Ketone (190-215 ppm)
Pre-fire	12.9	5.7	17.4	6.0	31.5	11.2	12.0	3.2
Pre-fire	14.0	7.2	26.8	7.4	18.9	8.7	13.2	3.7
Pre-fire*	16.5	6.3	22.1	6.3	26.1	8.9	11.7	2.2
Pre-fire*	17.0	5.4	14.0	5.1	37.9	9.9	7.8	2.7
Pre-fire*	15.9	6.5	22.2	6.2	22.5	9.6	13.8	3.3
Pre-fire*	16.2	7.4	25.2	7.3	20.2	8.7	11.9	3.0
Pre-fire	14.8	6.6	24.9	6.7	20.6	8.5	14.5	3.4
Pre-fire*	18.9	7.5	25.6	6.9	18.7	7.0	12.9	2.5
Pre-fire*	13.5	6.3	16.1	5.3	32.8	12.1	10.6	3.3
Pre-fire*	14.1	6.4	21.0	7.7	23.5	11.6	11.6	4.1
Mean	15.4	6.5	21.5	6.5	25.3	9.6	12.0	3.1
Post-fire	15.6	5.8	20.5	6.1	29.9	10.6	8.4	3.1
Post-fire	18.3	7.1	25.6	6.4	17.2	7.2	15.2	3.0
Post-fire	18.7	6.5	18.1	5.6	29.4	9.3	9.3	3.1
Post-fire	15.7	6.6	20.8	6.5	25.4	9.8	11.9	3.4
Post-fire	15.5	6.4	20.5	5.7	26.7	9.3	12.9	3.0
Post-fire*	13.3	5.7	14.8	5.5	34.8	12.5	10.2	3.3
Post-fire	15.8	6.9	25.6	7.2	17.5	8.2	14.8	3.8
Post-fire*	14.0	4.6	13.5	5.7	37.1	13.1	8.7	3.3
Mean	15.9	6.2	19.9	6.1	27.2	10.0	11.4	3.3

REFERENCES

Abiven S, Hengartner P, Schneider MPW, Singh N, Schmidt MWI (2011) Pyrogenic carbon soluble fraction is larger and more aromatic in aged charcoal than in fresh charcoal. Soil Biology and Biochemistry 43(7): 1615-1617

Abney R, Berhe AA (In Prep) The role of soil erosion in lateral distribution of pyrogenic carbon. Biogeochemistry:

Abney R, Kuhn T, Chow A, Hockaday W, Fogel M, Berhe A (In prep) Soil erosion controls pyrogenic carbon dynamics: the effect of fire severity and slope on pyrogenic carbon transport after the Rim Fire, Yosemite National Park

Araya SN, Fogel ML, Berhe AA (2017) Thermal alteration of soil organic matter properties: a systematic study to infer response of Sierra Nevada climosequence soils to forest fires. Soil 3: 31-44

Baldock J, Hawke B, Sanderman J, Macdonald L (2013a) Predicting contents of carbon and its component fractions in Australian soils from diffuse reflectance mid-infrared spectra. Soil Research 51(8): 577-595

Baldock J, Hawke B, Sanderman J, Macdonald L, Schmidt E, Szarvas S, Puccini A, McGowan J (2012) Soil Carbon Research Program: Project 2, Developing a cost effectie soil carbon analytical capability In. The Commonwealth Scientific and Industrial Research Organisation (CSIRO) - Land and Water Division Adelaide, Australia.

Baldock JA, Sanderman J, Macdonald LM, Puccini A, Hawke B, Szarvas S, McGowan J (2013b) Quantifying the allocation of soil organic carbon to biologically significant fractions. Soil Research 51(8): 561-576

Battin T, Luyssaert S, Kaplan L, Aufdenkampe A, Richter A, Tranvik L (2009) The boundless carbon cycle. 2(9): 598-600

Benner R, Fogel ML, Sprague EK, Hodson RE (1987) Depletion of 13 C in lignin and its implications for stable carbon isotope studies. Nature 329(6141): 708-710

Berhe AA (2007) Storage, replacement, stabilization, and destabilization of soil organic carbon in eroding and depositional settings.

Berhe AA (2012) Decomposition of organic substrates at eroding vs. depositional landform positions. Plant and Soil 350: 261-280

Berhe AA (2013) Effect of litterbags on rate of organic substrate decomposition along soil depth and geomorphic gradients. Journal of Soils and Sediments 13(4): 629-640

Berhe AA, Harden J, Torn M, Kleber M, Burton S, Harte J (2012) Persistence of Soil Organic Matter in Eroding vs. Depositional Landform Positions. Journal Of Geophysical Research-Biogeosciences 117, G02019, doi:10.1029/2011JG001790:

Berhe AA, Harte J, Harden JW, Torn MS (2007a) The Significance of Erosion-Induced Terrestrial Carbon Sink. BioScience 57(4): 337-346

Berhe AA, Harte J, Harden JW, Torn MS (2007b) The Significance of the erosion-induced terrestrial carbon sink. BioScience 57: 337-346

Berhe AA, Kleber M (2013) Erosion, deposition, and the persistence of soil organic matter: mechanistic considerations and problems with terminology. Earth Surface Processes and Landforms 38(8): 908-912

Bird MI, Wynn JG, Saiz G, Wurster CM, McBeath A (2015) The pyrogenic carbon cycle. Annual Review of Earth and Planetary Sciences 43: 273-298

Boot C, Haddix M, Paustian K, Cotrufo M (2015) Distribution of black carbon in ponderosa pine forest floor and soils following the High Park wildfire. Biogeosciences 12(10): 3029-3039

Brewer CE, Chuang VJ, Masiello CA, Gonnermann H, Gao X, Dugan B, Driver LE, Panzacchi P, Zygourakis K, Davies CA (2014) New approaches to measuring biochar density and porosity. Biomass and Bioenergy 66: 176-185

Carroll EM, Miller WW, Johnson DW, Saito L, Qualls RG, Walker RF (2007) Spatial analysis of a large magnitude erosion event following a Sierran Wildfire. Journal of environmental quality 36(4): 1105-1105

Certini G (2005) Effects of fire on properties of forest soils: a review. Oecologia 143: 1-10

Chaopricha NT, Marín-Spiotta E (2014) Soil burial contributes to deep soil organic carbon storage. Soil Biology and Biochemistry 69: 251-264

Cheng C, Lehmann J, Thies J, Burton S, Engelhard M (2006) Oxidation of black carbon by biotic and abiotic processes. Organic Geochemistry 37(11): 1477-1488

DeBano L (1990) The effect of fire on soil properties. Paper presented at the symposium on management and productivity of western-montane forest soils:

DeBano L (2000) The role of fire and soil heating on water repellency in wildland environments: a review. Journal of Hydrology 231: 195-206

Doetterl S, Berhe AA, Nadeu E, Wang Z, Sommer M, Fiener P (2016) Erosion, deposition and soil carbon: A review of process-level controls, experimental tools and models to address C cycling in dynamic landscapes. Earth Science Reviews 154: 102-122

Doetterl S, Six J, Van Wesemael B, Van Oost K (2012) Carbon cycling in eroding landscapes: geomorphic controls on soil organic C pool composition and C stabilization. Global Change Biology 18(7): 2218-2232

Eckmeier E, Gerlach R, Skjemstad J, Ehrmann O, Schmidt M (2007) Minor changes in soil organic carbon and charcoal concentrations detected in a temperate deciduous forest a year after an experimental slash-and-burn. Biogeosciences 4(3): 377-383

Giovannini G, Lucchesi S, Giachetti M (1988) Effect of heating on some physical and chemical parameters related to soil aggregation and erodibility. Soil Science 146: 255-262

Gregorich E, Greer K, Anderson D, Liang B (1998) Carbon distribution and losses: erosion and deposition effects. Soil Till Res 47(3-4): 291-302

Güereña DT, Lehmann J, Walter T, Enders A, Neufeldt H, Odiwour H, Biwott H, Recha J, Shepherd K, Barrios E (2015) Terrestrial pyrogenic carbon export to fluvial ecosystems: Lessons learned from the White Nile watershed of East Africa. Global Biogeochemical Cycles 29(11): 1911-1928

Hammes K, Torn MS, Lapenas AG, Schmidt MWI (2008) Centennial black carbon turnover observed in a Russian steppe soil. Biogeosciences 5(5): 1339-1350

Harden JW, Sharpe JM, Parton WJ, Ojima DS, Fries TL, Huntington TG, Dabney SM (1999) Dynamic replacement and loss of soil carbon on eroding cropland. Global Biogeochemical Cycles 13(4): 885-901

Janik LJ, Skjemstad JO, Shepherd KD, Spouncer LR (2007) The prediction of soil carbon fractions using mid-infrared-partial least square analysis. Australian Journal of Soil Research 45(2): 73-81

Johnson D, Murphy J, Walker R, Glass D, MILLER W (2007) Wildfire effects on forest carbon and nutrient budgets. Ecological Engineering 31(3): 183-192

Johnson D, Susfalk R, Caldwell T, Murphy J, Miller W, Walker R (2004) Fire effects on carbon and nitrogen budgets in forests. Water, Air, & Soil Pollution: Focus 4(2): 263-275

Kennard RW, Stone LA (1969) Computer aided design of experiments. Technometrics 11(1): 137-148

Kindler R, Siemens J, Kaiser K, Walmsley DC, Bernhofer C, Buchmann N, Cellier P, Eugster W, Gleixner G, GRÛNWALD T (2011) Dissolved carbon leaching from soil is a crucial component of the net ecosystem carbon balance. Global Change Biology 17(2): 1167-1185

Kuzyakov Y, Subbotina I, Chen H (2009) Black carbon decomposition and incorporation into soil microbial biomass estimated by C labeling. Soil Biology and Biochemistry 41(2): 210-219

Lal R (2003) Global potential of soil carbon sequestration to mitigate the greenhouse effect. Critical Reviews in Plant Sciences 22(2): 151-184

Lal R (2004) Soil carbon sequestration impacts on global climate change and food security. Science 304(5677): 1623-1627

Larsen I, Macdonald L, Brown E, Rough D, Welsh M, Pietraszek J, Libohova Z, De Dios Benavides-Solorio J, Schaffrath K (2009) Causes of Post-Fire Runoff and Erosion: Water Repellency, Cover, or Soil Sealing? Soil Science Society of America Journal 73(4): 1393

Liang B, Lehmann J, Solomon D, Kinyangi J, Grossman J, O'Neill B, Skjemstad JO, Thies J, Luizao FJ, Petersen J, Neves EG (2006) Black carbon increases cation exchange capacity in soils. Soil Science Society of America Journal 70(5): 1719-1730

Major J, Lehmann J, Rondon M, Goodale C (2010a) Fate of soil-applied black carbon: downward migration, leaching and soil respiration. Global Change Biology 16(4): 1366-1379

Major J, Lehmann J, Rondon M, Goodale C (2010b) Fate of soil‐applied black carbon: downward migration, leaching and soil respiration. Global Change Biology 16(4): 1366-1379

Marin-Spiotta E, Chaopricha NT, Plante AF, Diefendorf AF, Mueller CW, Grandy AS, 1–5. JAM (2014) Long-Term Stabilization of Deep Soil Carbon by Fire and Burial During Early Holocene Climate Change. Nature Geoscience 7(6): 428

Masiello C (2004) New directions in black carbon organic geochemistry. Marine Chemistry 92(1-4): 201-213

Nguyen BT, Lehmann J, Kinyangi J, Smernik R, Riha SJ, Engelhard MH (2009) Long-term black carbon dynamics in cultivated soil. Biogeochemistry 92(1-2): 163-176

Parikh SJ, Goyne KW, Andrew J Margenot, Mukome FND, Calderon FJ (2014) Soil Chemical Insights Provided Through Vibrational Spectroscopy. Advances in Agronomy 126:

Pereira P, Cerdà A, Úbeda X, Mataix‐Solera J, Arcenegui V, Zavala L (2015) Modelling the impacts of wildfire on ash thickness in a short‐term period. Land Degradation & Development 26(2): 180-192

Peterson DA, Hyer EJ, Campbell JR, Fromm MD, Hair JW, Butler CF, Fenn MA (2015) The 2013 Rim Fire: Implications for predicting extreme fire spread, pyroconvection, and smoke emissions. Bulletin of the American Meteorological Society 96(2): 229-247

Pierson FB, Moffet CA, Williams CJ, Hardegree SP, Clark PE (2009) Prescribed‐fire effects on rill and interrill runoff and erosion in a mountainous sagebrush landscape. Earth Surface Processes and Landforms 34(2): 193-203

Pierson FB, Williams CJ, Hardegree SP, Clark PE, Kormos PR, Al-Hamdan OZ (2013) Hydrologic and erosion responses of sagebrush steppe following juniper encroachment, wildfire, and tree cutting. Rangeland Ecology & Management 66(3): 274-289

Post WM, Kwon KC (2000) Soil carbon sequestration and land-use change: processes and potential. Global Change Biology 6(3): 317-327

Pyle LA, Hockaday WC, Boutton T, Zygourakis K, Kinney TJ, Masiello CA (2015) Chemical and isotopic thresholds in charring: implications for the interpretation of charcoal mass and isotopic data. Environmental science & technology 49(24): 14057-14064

Renard KG, Foster GR, Weesies G, McCool D, Yoder D (1997) Predicting soil erosion by water: a guide to conservation planning with the Revised Universal Soil Loss Equation (RUSLE). US Government Printing Office Washington, DC,

Rumpel C, Ba A, Darboux F, Chaplot V, Planchon O (2009) Erosion budget and process selectivity of black carbon at meter scale. Geoderma 154(1): 131-137

Rumpel C, Chaplot V, Planchon O, Bernadou J, Valentin C, Mariotti A (2006) Preferential erosion of black carbon on steep slopes with slash and burn agriculture. CATENA 65(1): 30-40

Rumpel C, Leifeld J, Santin C, Doerr S (2015) Movement of biochar in the environment. Biochar for Environmental Management: Science, Technology and Implementation (second edition). New York: Routledge: 283-298

Saito L, Miller WW, Johnson DW, Qualls R, Provencher L, Carroll E, Szameitat P (2007) Fire Effects on Stable Isotopes in a Sierran Forested Watershed. Journal of Environmental Quality 36(1): 91-100

Sanderman J, Baldock J, Hawke B, Macdonald L, Massis-Puccini A, Szarvas S (2011) National soil carbon research programme: Field and laboratory methodologies. Urrbrae, S. Aust.: CSIRO:

Scharlemann JP, Tanner EV, Hiederer R, Kapos V (2014) Global soil carbon: understanding and managing the largest terrestrial carbon pool. Carbon Management 5(1): 81-91

Schmidt MWI, Knicker H, Hatcher PG, Kogel-Knabner I (1997) Improvement of 13C and 15N CPMAS NMR spectra of bulk soils, particle size fractions and organic material by treatment with 10% hydrofluoric acid. European Journal of Soil Science 48: 319-328

Shakesby R, Coelho C, Ferreira A, Terry J, Walsh R (1993) Wildfire impacts on soil-erosion and hydrology in wet Mediterranean forest, Portugal. International Journal of Wildland Fire 3(2): 95-110

Shakesby R, Doerr S, Walsh R (2000) The erosional impact of soil hydrophobicity: current problems and future research directions. Journal of Hydrology 231: 178-191

Skjemstad JO, Spouncer LR, Cowie B, Swift RS (2004) Calibration of the Rothamsted organic carbon turnover model (RothC ver. 26.3) using measurable soil organic carbon pools. Australian Journal of Soil Research 42: 79-88

Smernik R, Oades J (2002) Paramagnetic effects on solid state carbon-13 nuclear magnetic resonance spectra of soil organic matter. Journal of Environmental Quality 31(2): 414-420

Smernik RJ, Skjemstad J, Oades JM (2000) Virtual fractionation of charcoal from soil organic matter using solid state 13C NMR spectral editing. Soil Research 38(3): 665-683

Soucémarianadin LN, Quideau SA, Wasylishen RE, Munson AD (2015) Early‐season fires in boreal black spruce forests produce pyrogenic carbon with low intrinsic recalcitrance. Ecology 96(6): 1575-1585

Stacy E, Hart SC, Hunsaker CT, Johnson DW, Berhe AA (2015) Soil carbon and nitrogen erosion in forested catchments: implications for erosion-induced terrestrial carbon sequestration. Biogeosciences Discuss. 12(3): 2491-2532

Stallard R (1998) Terrestrial sedimentation and the carbon cycle: Coupling weathering and erosion to carbon burial. Global Biogeochemical Cycles 12(2): 231-257

Westerling AL, Hidalgo HG, Cayan DR, Swetnam TW (2006) Warming and earlier spring increase western US forest wildfire activity. Science 313(5789): 940-943

Yao J, Hockaday WC, Murray DB, White JD (2014) Changes in fire‐derived soil black carbon storage in a subhumid woodland. Journal of Geophysical Research: Biogeosciences 119(9): 1807-1819

CHAPTER 5: LANDFORM POSITION AND COMBUSTION TEMPERATURE CONTROL DECOMPOSITION RATE OF PYROGENIC ORGANIC MATTER

ABSTRACT

Pyrogenic carbon (PyC) is the material left behind after incomplete combustion of biomass, including a spectrum of materials ranging from ash to lightly charred biomass. We investigated the roles of combustion temperature and landform position on decomposition rate of PyC. Bark from *Pinus jeffreyi* was charred at three temperatures (200ºC, 350ºC, and 500ºC) for an hour to create PyC. We then incubated the charred bark with soil collected from eroding and depositional landform positions along the same hillslope. We measured the rate of CO_2 production from the soil and soil plus bark PyC mixtures over a period of six months, and determined the rate of char decomposition by difference. Microbial biomass, elemental C and nitrogen, along with their stable isotopes, was measured four times throughout the incubation. Fraction of PyC in soil C was determined at the beginning and end of the incubation. We found that the best fit for the data collected on rate of decomposition of the soil and char mixtures was a two-pool exponential model. The bark charred at higher temperatures decomposed at rates two times slower than that charred at 200ºC. We also found rates of microbial respiration in soil from the depositional landform position was over three times higher than the rates of decay from char decomposing in soils from the eroding landform position. This elevated respiration was driven by elevated microbial biomass in the depositional soils. PyC concentrations decreased only in soil and char mixtures with lower temperature chars and in the depositional soils, which indicates that low temperature PyC decayed at a faster rate, compared to other OM, in the depositional soils with optimal soil conditions for decomposition. The nature of soil from the different landform positions imposed major control PyC decomposition. This study confirms that lateral distribution of char by post-fire erosion plays a significant role in controlling the long-term fate of PyC in soil.

INTRODUCTION

Pyrogenic carbon (PyC) is an important component of the global carbon cycle that makes up to 30% of the soil organic matter pool in some soils (Skjemstad et al. 1999), and 2-5% of overall soil carbon (Bird et al. 2015). Pyrogenic carbon is the byproduct of incomplete combustion of biomass and soil, and includes a range of constituents including ash, soot, charcoal, and lightly charred biomass (Bird et al. 2015; Masiello 2004). The properties of PyC depend on its precursor material and the charring intensity, in particular the combination of burn temperature and duration (Pyle et al. 2015). Generally, grasses and other light materials are more likely to be entirely consumed by fire, and they form PyC that has a lower density and more environmentally mobile (Alexis et al. 2010; Pereira et al. 2015). In contrast, PyC formed from woody materials at higher charring temperatures is typically more environmentally persistent, and tends to be constructed of highly condensed aromatic rings (Wiedemeier et al. 2015). These structural differences resulting from differing levels charring intensity can lead to significantly different environmental interactions and persistence (Bird et al. 2015). Additionally, with increases in charring temperature, both biomass and soil can have increased pH, cation exchange capacity, and C concentration (Araya et al. 2016; Araya et al. 2017; Massman et al. 2010) that affect long term fate of PyC in the soil system.

In soil, PyC has decades to millennia longer soil residence times than non-pyrogenic components (Hammes et al. 2008). The long residence time of PyC in soil has attracted considerable research attention for its role in soil carbon (C) sequestration (Lehmann 2007). However, there are still major gaps in our understanding and quantification of variables controlling rate of PyC loss from soil. Multiple questions remain unanswered about where in the landscape most of PyC produced from fire (or intentionally applied as biochar) decomposes, rate of lateral transport of different types of PyC with wind or water erosion, and how environmental conditions affect rate of PyC decomposition in the terrestrial ecosystem.

Lateral transport of PyC with soil erosion can have major implications for its long-term fate in soil, depending on the landform position that it is deposited. recent research has indicated that PyC is preferentially eroded over non-pyrogenic C (Rumpel et al. 2006; Rumpel et al. 2015; Yao et al. 2014). Based on current understanding of the role of erosion and soil properties on bulk soil OM decomposition, PyC will likely decompose at different rates in different landform positions, with PyC in eroding hillslopes likely decomposing at slower rates of compared with PyC in depositional landform positions (Berhe 2012; Berhe et al. 2012). Higher rates of OM decay in depositional landform positions is a result of combination of factors, including higher rate of input of nutrients and OM from upslope eroding landform positions, as well as higher water contents than upslope positions, which facilitates physical breakdown and higher microbial decomposition of both bulk and PyC that remains on the soil surface of lower-lying, potentially more poorly drained depositional landform positions (Famiglietti et al. 1998; Papiernik et al. 2009). We expect that burial of PyC by subsequently eroded material, is likely to lead to slower rate of decay of PyC, compared to PyC that decomposes on the surface of depositional position soils. Burial of OM and PyC can limit availability of oxygen and thus rates of decomposition, leading to stabilization of buried PyC for thousands of years (Chaopricha & Marín-Spiotta 2014; Marin-Spiotta et al. 2014). In this study, we investigate how the landform position that PyC is located within a landscape can control its long-term fate in soil.

Several recent studies have reported decomposition rates for PyC (Kuzyakov et al. 2009b; Nguyen & Lehmann 2009; Nguyen et al. 2010; Whitman et al. 2014). Rates of reported microbial

breakdown of PyC range from <0.1 to 20% per year, much of which depends on the soil conditions, such as water content, nutrient availability, temperature, soil type, depth, and time scale considered (Foereid et al. 2011; Hammes et al. 2008; Kuzyakov et al. 2009b; Nguyen & Lehmann 2009; Nguyen et al. 2010; Zimmermann et al. 2012). So far, no studies have investigated how erosional movement of PyC from across the landscape leads to differential rates of PyC breakdown and further vertical or horizontal transport across hillslopes, in the subsurface, or from terrestrial to aquatic systems. This is in spite of recent works that have shown that erosional transport of PyC is a major flux in the PyC cycle as PyC is deposited at or near the soil surface after fires or during intentional application of biochar. Hence, the low density and high concentration of PyC on the soil surface combine to render it susceptible to preferential lateral transport by soil erosion (Abney et al. In prep).

Breakdown of PyC at or near the soil surface occurs through both abiotic and biotic pathways. Abiotic pathways include both chemical and physical processes (Cheng et al. 2006). Physical breakdown occurs through processes such as fragmentation and mobilization by biota, churning by water, and soil shrink-swell (Spokas et al. 2014). Chemically, PyC is broken down by dissolution and interactions with the soil matrix. PyC can lose functional groups and nutrients via dissolution in soil water (Abiven et al. 2011; Adams et al. 1988; Cheng et al. 2006). It can serve as both a sorbent and sorbate in soil solution, acting to both store and release nutrients to the soil, where the release of nutrients from PyC leads to its breakdown, but by sorbing onto soil minerals or encapsulation inside aggregates, PyC can become stabilized (Chia et al. 2012; Kupryianchyk et al. 2016). Breakdown of PyC by microbial processes leads to the release of CO_2 and CH_4, depending on oxygen availability in the soil environment that PyC decomposes. In some soils, a priming effect has been demonstrated with PyC additions, where a pulse of nutrients gives microbes enough energy to begin breaking down PyC within soil. This priming effect can lead to higher net rates of PyC breakdown, depending on the soil type and environmental conditions (Whitman et al. 2014).

Several studies have utilized two- and three-pool models to simulate the breakdown of PyC as a slow cycling-pool, compared to other pools of presumably slower cycling OM in soil. The CENTURY model, for example, has a separate pool for ‘slow-cycling’ soil C, which could represent a component of the soil C pool like PyC (Parton et al. 1987). However, considerable research has demonstrated that PyC is not an inherently recalcitrant pool within the soil, and can breakdown on much shorter time scales (Kuzyakov et al. 2009b; Zimmermann et al. 2012), relative to the slow pool in Century and similar models. Even so, there is considerable evidence that the dynamics of PyC in soil is different than non-pyrogenic C, and that the fate of PyC largely depends on environmental conditions (Liang et al. 2010).

This study utilizes PyC produced from tree bark (combusted at 200, 350, and 550ºC), and soils from eroding and depositional landform positions to further our understanding of how fire temperature and landform position interact to determine fate of PyC in fire-affected dynamic landscapes. Typical PyC source materials previously used for such experiments included hardwood (Hatten et al. 2005; Major et al. 2010; Sarkhot et al. 2012; Zimmerman 2010), grasses (Kuzyakov et al. 2009; Zimmerman et al. 2011), and agricultural byproducts (Nguyen et al. 2010; Novak et al. 2009). Few studies, however, have investigated the decomposition of charred bark, which is an important source of PyC in fire-affected forest ecosystems. Next to leaf and needle litter, bark is among the plant components that experiences some of the highest combustion intensity during fires, even during lower intensity fires that might not burn wood. Additionally,

charred bark may act as a long-term input of PyC into soil, as surviving trees can take several years to slough off charred bark (Sutherland 2001). This study seeks to understand the interactive roles of charring temperature of bark and landform position on its breakdown rates within soil. Specifically, we answer three critical questions:

1. Does charred bark PyC decompose at different rates in soil from eroding vs. depositional landform positions?
2. How does the decomposition rate of PyC in eroding vs. depositional landform positions change over time?
3. How does charring temperature control the fate of PyC in eroding vs. depositional landform position soils?

Improved understanding of the decomposition processes of charred bark (as opposed to wood) is critical for our understanding of the effects of fires on input of PyC to soil, particularly for low intensity fires.

METHODS

Soil collection

For this study, topsoil (0-10 cm) was collected from an unburned area outside the Gondola Fire perimeter in South Lake Tahoe, NV (38°57'N, 119°55'W). The soils in the study area are derived from granitic parent material and are classified as typic Cryopsamments (Carroll et al. 2007). Soils were collected in two different landform positions, an eroding hillslope (40-50% slope) and a depositional (<5% slope) landform position, located about 50 m away, at the base of the same hillslope. We selected sites that had not experienced wildfire for over 100 years to capture the impact of new input of PyC into the soil. After collection, soils were immediately put on ice and kept at 4ºC until analysis.

Bark char collection and preparation

Bark was collected from *Pinus jeffreyi* outside the Gondola Fire area, with a steel hammer to remove the bark from mature live trees. *Pinus jeffrei* typically has thick and plated bark, and the collected samples ranged from 1.5 to 2.5 inches in thickness. This bark was air-dried, and then crushed into smaller fragments, which were sieved to <2mm and >1mm in size to maintain a relatively uniform sized PyC material. Approximately 125 cm^3 of the bark fragments were placed in closed ceramic crucibles in a muffle furnace and charred at three maximum temperatures (200ºC, 350ºC, 500ºC) for an hour following the method of Araya et al. (2017). Oxygen in the furnace was limited by covering the crucibles with ceramic lids and by the air space in the furnace. The ratio of volume of bark to air in the furnace was approximately 1:20. For the 350ºC and 500ºC chars, bark was placed in the muffle furnace once it reached 200ºC and then heated to maximum temperature at 3ºC per minute to avoid overly long ramping times, and since dehydration reactions dominate below 200ºC (Pyle et al. 2015; Wiedemeier et al. 2014). After charring, samples were allowed to cool, and evenness of charring was assessed by color comparison within a crucible. Three bark charring temperatures (200ºC, 350ºC, 500ºC) were selected to capture the shift in properties of SOM and litter with increased charring intensity, including increases in specific surface area, pH, charring of organic matter, and decreases in N functional groups that occur with increasing temperature of charring (Araya et al. 2016; Araya et al. 2017; Massman et al. 2010).

Additionally, these temperatures represent the range of low to high severity fires, each of which have occurred in the area (Beaty & Taylor 2008).

Soil preparation

Soils were passed through a 2 mm sieve and were homogenized. Field moist soils were analyzed for pH in 1:2 (w/w) solutions with H_2O and 0.01M $CaCl_2$ with a ThermoFisher Accumet probe (Waltham, MA, USA). Subsamples of each of each soil were oven dried at 105ºC for 48 hours and then were analyzed for particle size distribution via the hydrometer method (Bouyoucos 1962).

For the incubation experiment, after homogenizing, field-moist soils were brought to field capacity. Soils were placed in funnels with Whatman #2 filter paper and saturated to the point of ponding at the surface, and drained for 24 hours. After 24 hours, the samples were rehomogenized and stored at 4ºC for one week, until the start of the incubation. A subsample of the field capacity soils was dried in an oven at 105ºC to determine the gravimetric water content of the samples at field capacity.

Experimental set up

The incubation was conducted in pint-sized mason jars, where the lid was fitted with a rubber septa to allow for gas sampling. Previously homogenized soils and chars were mixed in a factorial design of three charring temperatures and soil from two landform positions, eroding and depositional. We included soils from the two landform positions with no char addition as controls. At the beginning of the incubation, each treatment group had sixteen replicates, but at four time points throughout the incubation, four samples were destructively sampled for further analysis.

Soil was added to the mason jars to the equivalent of 50 (±0.1) g soil dry mass and char was added at 10% of soil mass equivalent (5 ± 0.01) g dry char. After mixing the soil and char, we incubated the samples in the dark at room temperature, which averaged throughout the incubation was 22ºC. The mason jars were loosely covered, but not sealed, in a dark incubation chamber to allow for aeration. A beaker of MilliQ ultrapure water was kept in the dark incubation chamber with the mason jars, to help maintain water content. The initial water contents in the soils used for the incubation experiment were maintained by gently spraying MilliQ ultrapure water into the jars once per week to maintain the initial weight of the soil and char mixtures. The mixtures typically lost 3-4 mL of water per week, but this water loss ranged from 1 to 9 mL. Water was only added after any gas measurements to avoid causing a birch effect that might impact CO_2 measurements (Birch 1958).

Chemical analyses

Gas sampling was conducted on days 1, 3, 7, 14, 28, 60, 90, 120, 180 of this incubation. On sampling days 1, 28, 90, 180, four samples from each treatment group were destructively sampled for bulk C, N, stable isotopes of C and N, and for microbial biomass via chloroform fumigation incubation. On sampling days 1 and 180, four samples from each treatment group were subsampled after gas sampling and analyzed for PyC concentration via the Kurth-Mackenzie-Deluca method (Kurth et al. 2006).

Gas Chromatography

To collect gas, all mason jars were sealed for 24 hours, allowing CO_2 to build up, and then 15 mL of gas was pulled from each jar and stored in evacuated Exetainers for no longer than 8 weeks until analysis via gas chromatography. Two additional mason jars were incubated with no soil or char to measure the background CO_2 signal. These were sampled during each sampling point of the soil and char mixture samples, and this value was subtracted from each gas analysis to yield flux above the background air CO_2 concentration. Gas samples were analyzed on a Shimadzu 2014 gas chromatograph (Kyoto, Japan) fitted with a thermal conductivity detector for CO_2 concentration.

Bulk C and N concentrations, and stable isotope analyses

During destructive sampling points, incubated soil and char samples were subsampled for bulk C and N concentrations and stable C and N isotopes analysis. Prior to analysis, the samples were homogenized, air-dried, and ground to a fine power on a SPEX SamplePrep 8000M mill (Metuchen, NJ). Approximately 5 mg of sample was weighed into tin cups, and analyzed on a Costech ECS CHNSO 4010 (Valencia, CA) analyzer fitted with an isotope ratio Delta V Plus mass spectrometer (Waltham, MA). Samples were compared with standards of peach leaf (±0.10‰ $\delta^{15}N$ and ±0.02‰ $\delta^{13}C$) and acetanilide (± 0.06‰ $\delta^{15}N$ and ± 0.01‰ $\delta^{13}C$). These standards were compared to international standards of atmospheric N for $\delta^{15}N$ and Vienna Pee Dee Belemnite for $\delta^{13}C$. Soil samples analysis varied ± 0.10‰ for $\delta^{15}N$ and ± 0.02‰ for $\delta^{13}C$. The bulk C and N concentration results were corrected for difference in air-dry to oven dry concentrations by subsampling the air-dried, ground sample and drying for 24 hours at 105ºC. This correction was less than 4% of the C and N concentrations.

Chemical composition of soil and PyC

Prior to incubation, representative samples from the two soils and the three chars were finely ground and dried at 60ºC for 24 hours. The samples were analyzed prior to incubation using a diffuse reflectance infrared Fourier transform spectroscopy (DRIFT) technique under vacuum on a Bruker IFS 66v/S FT-IR (Billerica, MA, USA). Spectra were collected from the integration of 64 scans over the MIR range of 4000-400 cm^{-1}, and were background corrected with a KBr spectrum. Spectra were baseline corrected using OPUS software (version 6.5). Samples were not diluted, to capture the variability in the samples and to minimize sample preparation (Janik et al. 1998). Spectral peaks were assigned using the work of Araya et al. (2017), with the following peaks: aryl peaks at 765 and 825 cm^{-1}, ester and phenol peaks at 995 cm^{-1}, carboxyl peak at 1600 cm^{-1}, keytone and carbonyl peak at 1740 cm^{-1}, methyl peak at 2940 cm^{-1}, and hydroxyl peaks at 3625 and 3700 cm^{-1}.

Microbial Biomass

Soil and char mixtures were subsampled for chloroform fumigation incubation at days 1, 28, 90, and 180 after the gas sampling was completed using a method similar to Horwath and Paul (1994). Around 20 g of the soil and char mixture was weighed into small glass beakers, and the remainder of the mixture was kept in the mason jar in the dark until the chloroform fumigation was completed. The glass beakers with subsamples were placed in a glass desiccator lined with paper towels saturated with MilliQ ultrapure water. An Erlenmeyer flask with 75 mL of ethanol-free chloroform and approximately 20 boiling chips was placed in the center of the desiccator. The desiccator was evacuated and until the chloroform boiled. This was repeated three times, allowing air to enter the

desiccator between each boil, and after the third boiling, the desiccator was sealed under vacuum and kept in the dark. This boiling procedure was repeated the following two days, and after the third boiling, the beaker with chloroform and boiling chips was removed, and the desiccator was evacuated eight times for three minutes, allowing for air to enter the desiccator between each evacuation. The chloroform fumigated samples were placed in mason jars in the dark, with the control samples, and all were sealed to allow gas to build up. After 24 hours, gas samples were collected from control and fumigated samples and stored in evacuated Exetainers until analysis via GC (as described above). Fumigated and control respiration data were comparing using Equation 1 below to calculate microbial biomass (Horwath et al. 1996). This approach can account for the shorter incubation time of one day in the study.

$$MBC = \left(1.73 \cdot R_f\right) - \left(0.56 \cdot R_{uf}\right) \qquad \textit{Equation 1}$$

where, *MBC* = microbial biomass carbon (μg microbial biomass C/g soil), R_f = Fumigated respiration (μg CO_2-C/g soil), and R_{uf} = Unfumigated respiration (μg CO_2-C/g soil).

PyC analysis

The Kurth Mackenzie Deluca (KMD) method was utilized to estimate charcoal concentration in incubation soil char mixtures from the first time point and the last time point of the incubation, in addition to chars alone. In brief, 0.5 to 1 g of soil and charcoal incubation mixtures were measured out (lower weights for higher C concentration samples) into 125 mL Erlenmeyer flasks. Then, 10 mL of 1M nitric acid and 20 mL of hydrogen peroxide was added to each flask. The flasks were swirled and allowed to rest for 30 minutes on hot plates. The flasks were slowly brought to 100ºC over an hour, and the flasks were kept at 100ºC for 16 hours. After 16 hours, the flasks were cooled for 30 minutes at room temperature, and then the samples were filtered using a Whatman #2 filter and washed 5 times with MilliQ DI water. Post-filtering, the filter and sample were placed in the oven at 60ºC for 24 hours, and after drying, samples were removed from the filters, ground, and homogenized. These samples were then analyzed for C and N as described above. Two of the samples were analyzed in triplicate to assess the replicability of this method, which had a standard error ± 0.4%. PyC concentration was calculated as below, from Buma et al. (2014):

$$PyC = \frac{C_{pd} - M_{pd}}{M_0} \qquad \textit{Equation 2}$$

where *PyC* = percent of soil mass that is PyC (%); C_{pd} = soil carbon post-digestion (%); M_{pd} = mass of soil sample post-digestion (g); M_0 = original (pre-digestion mass) of soil sample (g). This calculation accounts for the loss of mass during the digestion.

Imaging

Char pieces were imaged with environmental scanning electron microscopy (ESEM) before and after the incubation to investigate the changes in structure of char with increasing temperature and to assess the incorporation of native SOM into the char post-incubation. The post-incubation pieces were removed from the soil and char mixtures by gently removing them with tweezers. The char pieces were placed on an aluminum stop covered with double sided tape. Microscope images were taken with a FEI Quanta 200 ESEM (Hillsboro, OR) under vacuum conditions and were processed with EDAX Genesis software.

Data analyses

Data are presented as means and standard error with n=4, except where otherwise noted. Differences in means were tested with a two-way ANOVA and Tukey HSD post-hoc test with treatment group as a factor at the significance level of $p<0.05$. Multiple linear regression techniques were utilized to assess the role of microbial biomass, soil type, charring temperature on soil respiration and on PyC concentrations in soil throughout the incubation.

Concentrations of CO_2 from the soil and char mixtures were corrected to both g C in the soil and char mixtures and to the respiration per g soil. Cumulative respiration fluxes were calculated by summing the continuous respiration fluxes over the time of incubation. We fit one- and two- pool decay models to our cumulative respiration data as equations 3 and 4 below:

One pool: $C_t = C_0(_{1-}e^{-kt})$ *Equation 3*

Two pools: $C_t = C_0(1-e^{-k0*t}) + C_1(1-e^{-k1*t})$ *Equation 4*

In these exponential functions, C_t is the cumulative µg C in the incubated soil at day t, C_0 is the initial carbon pool (µg C) available for mineralization. C_1 represents the slower pool. The terms k_0 and k_1 are the decay constants (day^{-1}) for the fast and slow cycling pools, respectively. To fit the models, a non-linear regression approach was used to predict each carbon pool and decay constant. The Akaike Information Criterion (AIC) was used to comparatively test the fit of the one- and two-pool models. All figure generation and data analysis was conducted in RStudio (Version 1.0.136).

RESULTS

Soil and char initial properties

Charring lead to important changes in the physical and chemical properties of the bark. Charring increased the bark pH from 3.5 to 7.7 from the 200ºC to 500ºC, and the C concentration increased from 55% to 85% from the 200ºC to 500ºC chars (Table 1). The $\delta^{15}N$ of the char was less negative with higher temperatures, from –13‰ at 200ºC to –9‰ at 500ºC. However, the $\delta^{13}C$ of the bark remained around -25‰ throughout increased charring temperature.

The two soils had relatively similar pH, both around 6.4, but the depositional soil held more than double the amount of water at field capacity (20% compared with 8%) than the eroding soil. The depositional soil also had significantly higher C and N concentrations ($p< 0.001$, $p<0.001$) than the eroding soil. The depositional soil also had around double both the silt and clay concentrations than the eroding soil (Table 2).

Effect of PyC input on soil CO_2 efflux

In the soil treatments groups, the depositional soil alone had a significantly ($p<0.05$) higher rate of respiration than the eroding soils. In the first two weeks of the incubation, the cumulative CO_2 loss in the depositional soil was higher than the eroding soils by 1349 mg CO_2-C/kg C and 36 mg CO_2-C/kg soil, equivalent to a difference of 58 and 65 % CO_2 flux, respectively. The cumulative respiration from the eroding soil increased by more than two-fold from the initial two-week period (over 950 mg CO_2-C/kg C and 19 mg CO_2-C/kg soil) to the end of the six-month incubation (over 2100 mg CO_2-C/kg C and 42 mg CO_2-C/kg soil). By the end of the six-month incubation period, the cumulative CO_2 flux in the depositional soil was higher than that from the eroding soil by 218 and 269 % for the values reported as mg CO_2-C/kg C and mg CO_2-C/kg soil, respectively (Table 3, Figure 1). In the eroding soil, the initial two-weeks of cumulative respiration accounted for 45

% of the total cumulative respiration over the six-month incubation, while the initial cumulative respiration of the depositional soil only account for 52% of the total cumulative respiration (Table 3).

Soil with 200°C char addition had significantly higher absolute CO_2 flux ($p<0.001$) compared to the soil only treatment group in both the eroding and depositional soils (Figure 1). In the depositional soil and char mixures, the absolute rates of CO_2 flux from the 350°C and 500°C char addition treatments were higher than the bulk soil alone ($p<0.001$), but the differences were not significantly significant in the 500°C char treatment group ($p=0.54$). The rate of CO_2 flux per unit C in the soil only and 200°C char addition treatment groups was higher than the soils with 350°C and 500°C char addition ($p<0.001$). Both eroding and depositional soils had significantly lower rate of CO_2 efflux ($p<0.001$) in the 350°C and 500°C addition treatment groups, compared to their respective soil-only treatments.

Addition of PyC, for chars produced at all three temperatures, reduced the rate of CO_2 flux per total C during the first two weeks of the incubation. But the magnitude of the response of the CO_2 efflux to PyC addition strongly depended on landform position from where the soils were derived from and temperature at which the bark PyC was charred. In the short term, the rate of CO_2 flux per g C was significantly higher in the depositional soil and depositional soil + char treatments, compared to the eroding soil and eroding soil + char treatments ($p<0.001$). Considering the total amount of C that was in the incubation vessels (from soil or soil + PyC), the short-term response of CO_2 efflux to PyC addition decreased with increasing charring temperature (Table 3). Cumulative CO_2 flux at the end of the six-month incubation showed that the depositional soil treatment groups, with and without char addition, respired significantly more than the eroding soil treatment groups ($p<0.001$).

After fitting the CO_2 flux data (mg CO_2-C/kg C) with a first order decay curve, all models were best fit by a two-pool decay function (Table 4). The two-pool models explained more of the variance of the data (73-96 % adjusted r^2 compared with 57-84 % adjusted r^2 for the singe pool models, and lower AIC scores), and the models were significant predictors of the respiration ($p=0.00$). In these two-pool models, there was a large fast-cycling pool (C_0), and a much smaller slow-cycling pool (C_1) that had a decay constant two orders of magnitude smaller, which declined with increasing char temperature.

Microbial biomass

The depositional soil treatment groups had significantly higher ($p=0.00$) microbial biomass than the treatment groups with eroding soil (Figure 2). Microbial biomass carbon in the eroding soil treatment groups increased ($p<0.001$) over the duration of the incubation experiment. In the eroding soils, the mixtures with 350°C and 500°C char treatments had significantly higher microbial biomass ($p=0.01$, <0.001; 4.1 and 6.3 mg/kg soil, respectively) than the soil alone or soil with 200°C char. In the depositional soils, the soil only treatment had significantly higher ($p<0.001$) microbial biomass than the treatments with 200°C and 350°C char additions, but not in the 500°C char treatment group. The depositional soil treatment groups showed a marked decrease in microbial biomass carbon during the incubation all but the 500°C char treatment group, which did not significantly decline ($p=0.34$).

SEM images

The unburned bark was relatively amorphous in structure. In the SEM images of char from before incubation, we observed increased structural differentiation in the char with increased combustion temperature (Figure 3). The 500°C char has smaller pores (~20-30 µm across), and the 350°C and 200°C chars have larger pores (~30-40 µm across). Also, the pores in the 500°C char have micropores within them, while the pores in the 350°C char are smooth. After the six-month incubation, there were observable OM particles within the large pores of the char (Figure 4), particularly in the 350°C and 500°C chars. The micropores observed in the 500°C char before incubation were no longer visible.

FTIR spectroscopy

The eroding and depositional soils did not differ majorly in the distribution of OM compounds (Figure 5), but differed from the chars in having greater peak heights in the O-H, aliphatic regions. The chars had higher peaks in the aryl regions, specifically asymmetric stretching in the C=C (1600 cm^{-1}) and C=O (1740 cm^{-1}) peaks, with increases in peak height with increasing charring temperature. However, the chars decreased in –CH (2940 cm^{-1}) peak height, with increasing charring temperature, and have no stretching in the O-H peak areas (3627 and 3700 cm^{-1}), suggesting the loss of aliphatic and oxygenated functional groups and increase in the proportion of aromatic functional groups at higher charring temperatures.

Pyrogenic carbon

In the eroding soil and char mixtures, the concentration of PyC did not change significantly ($p=0.08$) between the beginning and end time points (after KMD analysis, Figure 6), but the soil and char mixtures with 350°C and 500°C char had significantly higher PyC concentrations compared to the 200°C and soil only treatments. The PyC concentration in depositional soil, and 200°C and 350°C char mixtures declined during the six months of the incubation from 1.1 to 0.7% and from 8.2 to 9.7%, respectively, but the change in 350°C was not statistically significant ($p=0.07$). In eroding soil and char mixtures, the concentration of PyC increased between the beginning and end of the incubation, but the difference was not statistically significant ($p=0.09$).

DISCUSSION

Over the course of the laboratory incubation experiment, the overall rates of CO_2 flux from soil were higher in the depositional soil and soil and char treatment groups. The increase in charring temperature of the bark lead to a loss of aliphatic and oxygenated functional groups (Figure 5), along with increased percent of PyC (Figure 6), and smaller, more structured macropores (Figure 3), each of which likely contributed to making PyC more difficult to breakdown by microbially facilitated oxidative decomposition in the short term (Mimmo et al. 2014). This is further illustrated in the elevated rates of respiration in the soil and 200°C treatment groups over the higher temperature chars, and the loss of PyC from those treatment groups (Figure 1).

Throughout the incubation, the depositional soil was around 2-2.5 times that of the eroding soil treatment groups. Overall, the respiration from the 200°C char additions was 2.7-4.7 times over the respiration of the 350°C and 500°C char addition treatment groups after two-weeks. After six months, the cumulative respiration in the 200°C char treatment group decreased to 2.2-4.3 times the respiration of the 350°C and 500°C char addition treatment groups. This elevated respiration in the 200°C char treatment groups indicates that this char is more susceptible to breakdown on

both shorter and long-term scales. The lower respiration in high temperature chars on the per g C calculations suggests that these chars may be acting as a stable C pool, as there is more C proportionally remaining in the soil. Charring temperature is generally accepted to be a control on the long-term persistence of PyC in soil (Bird et al. 2015; Masiello 2004), and similarly, an incubation using charred *Miscanthus* found that 360°C was a threshold temperature for significantly increased PyC turnover time (Mimmo et al. 2014).

The difference in fit between the single- and double-pool respiration decay models between the soil only treatment groups and the soil and char treatment groups suggests that the char addition to soil may be acting as an addition of a slow-cycling C pool to these soils. This slow pool is susceptible to breakdown, but interestingly the size of the C pools available for mineralization in both the single and double pool models decreases with increasing char temperature. This decrease may indicate that some of the added PyC is respiring at such a slow rate that it is not observed in this model.

CO_2 flux from surface soils at eroding vs. depositional landform positions

The significant differences we noted in rates of CO_2 flux from the eroding soil and soil + char treatment groups, compared to the depositional soil and soil + char treatment groups clearly illustrate that soil properties at the different landform position impose controls on rate of both bulk and PyC decomposition. The higher rates of OM decomposition in depositional landform positions, compared to eroding ones has previously been attributed to differences in OM and nutrient availability, hydrologic flow regimes, microbial communities, and soil physico-chemical properties in soil profiles at different landform position within even a single hillslope (Berhe 2012; Doetterl et al. 2012). Soils from the surface of the depositional landform position in our study system in a forest ecosystem in the Sierra Nevada were respiring at rates over four times slower compared with soils compared with the grassland ecosystems studied by Berhe et al. (2008). In this incubation, this difference in respiration was supported by the elevated microbial biomass community in the depositional soil treatment groups, in combination with higher C and N concentrations and water content in the soil from this landform position. So, in this area, wildfire and the production of PyC may act as a significant C sink, where once PyC is produced, it may remain in the soil for longer periods than other warmer and more productive ecosystems.

In the treatment groups with soil from the eroding landform position, the initial respiration was proportionally double that of the soils in the depositional landform positions. This suggests that these soils had early loss of easily mineralizable C compared with the depositional soils, and that these soils may have less of a long-term mineralizable C pool. However, in the depositional soils, the long-term higher respiration and slight decline in PyC concentrations is due to more favorable decompositions conditions there, such as higher water content, greater C and N concentration, and higher microbial biomass (Nguyen & Lehmann 2009). The slight increase in concentration of the PyC in the eroding soil suggests preferential consumption of the non-pyrogenic C, leaving behind the PyC added as bark (Nguyen & Lehmann 2009; Schmidt et al. 2011). However, the decrease in PyC concentration in the depositional soil (Figure 6) from the lower temperature chars suggests that these lower temperature chars are susceptible to more rapid loss based on environmental conditions, particularly water content and available C and N for mineralization.

The role of charring temperature in controlling respiration

Most soil and char mixtures during the incubation had lower rate of CO_2 flux per g C compared to soil alone on a per g soil basis, owing to the high C concentration of the high temperature char additions (Figure 1). The higher respiration in the 200°C char addition treatment groups is partly a reflection of the chemical composition of the char produced at 200ºC that was comprised of less aromatic, more O- or N-substituted aliphatic groups (Figure 5), which is a characteristic shift with charring (Araya et al. 2017; Mimmo et al. 2014). In contrast, the bark char produced at higher temperatures had higher proportion of PyC (Figure 6). However, even while the breakdown of lower-temperature char was double the rate of breakdown of higher-temperature char (Table 4), this breakdown is orders of magnitude slower compared with the larger, fast-cycling soil C pools (Kuzyakov et al. 2009b). Our findings agree with previous studies that showed that the progressive changes that occur in biomass with charring can render it less susceptible to breakdown (Bruun et al. 2011; Massman et al. 2010) under different environmental conditions. In particular, our results demonstrate that a shift occurs in the stability of PyC in moderate (200ºC and 350ºC) compared with high (500ºC) intensity combustion conditions. This shift may be critical for understanding the role that wildfire intensity plays in controlling soil C stocks and PyC persistence through post-fire recovery, whereby high intensity fires produce PyC that is significantly more environmentally persistent.

Decomposition of PyC

The one and two pool decay models illustrated that the PyC added to the soils acted as a different C pool with separate decay constants, due to the soil-only treatments fitting significantly better than the two-pool models. This two-pool model also fit better to PyC decay data from previous work by Kuzyakov et al. (2009), who characterized the breakdown of PyC in soil by a small fast-cycling pool and a larger slow-cycling pool of C. Building on their work, Bird et al. (2015) used a three-pool model for PyC breakdown, with fast, intermediate, and slow pools, however this approach is difficult to constrain based upon different pool sizes, and different PyC properties, such as temperature of formation. Our two-pool model explains over 70% of the variability in CO_2 fluxes in the soil and char treatment groups, while the fit for the soil-only models is better with a single pool. Hence it suggests that charred bark PyC represents a distinct pool of C added to the soils at both the eroding and depositional landform positions (Kuzyakov et al. 2009). However, the calculated slow pool decay rates are more than double that of Kuzyakov et al. (2014), which may suggest that these calculated pools are not fully representative of the breakdown of PyC alone. This difference in decay rates could also represent differences in soil properties or substrate availability.

The dynamics of the added bark PyC are moderated by the charring temperatures that likely dictates the differential turnover times the added PyC (Bird et al. 2015; Bruun et al. 2011). In addition to affecting rate of microbial breakdown, charring temperature can also influence nutrient transfer from char to soil to support microbial decomposition or can result in a priming effect based on the initial nutrient pulse (Whitman et al. 2014). A priming effect is potentially reflected in the higher rates of respiration in the 200°C char treatment groups compared with the 350°C and 500°C char addition treatment groups. Additionally, the soil in which the PyC is decomposing controls its long-term fate, as the rates of decay of these soils have decay rates that are an order of magnitude faster than those found by Santos et al. (2012) using 450°C charred wood over a six-month incubation in a Sierra Nevada Alfisol, compared with the Sierra Nevada Entisol in this incubation.

Implications for the long-term fate of PyC

In fire-prone environments, the transport and deposition of material post-burn is a significant driver of soil C and nutrient cycling (Johnson et al. 2007), with the potential for major redistribution of C and PyC post-fire (Abney et al. In prep; Carroll et al. 2007). This redistribution can lead to the deposition of PyC in either further eroding or depositional landform positions, each of which can play a significant role in controlling the long-term persistence of C and PyC in soil (Doetterl et al. 2012). Together, these can act to decrease the persistence of PyC in the soil, in the case of low-burn severity PyC in depositional landform positions, or increase its persistence in the case of higher-burn severity PyC stabilized in eroding landform positions.

The interaction of burn severity and landform position as controls on soil C and PyC is confounded by the complex and dynamic nature of post-fire landscapes. High- and moderate-severity burns generally lead to higher post-burn erosion rates (Pierson et al. 2008), and even mass-transport events (Carroll et al. 2007). High-severity burns also produce PyC that is susceptible to preferential erosion (Abney et al. In prep), which can lead to the stabilization of this more persistent char in depositional landform positions. Thus, burn severity controls both the potential environmental persistence of the PyC itself, but also the conditions governing its eventual decomposition based on erosional transport to different landform positions.

Limitations and future directions

This incubation experiment only considered decomposition rates of surface soil. We expect that the decay rates of both the bulk soil and soil + PyC would decrease with depth into the soil profile (Berhe 2012), potentially leading to net stabilization of SOM and/or PyC in the depositional soil profile if the C- and PyC-rich topsoil is buried by eroded material. Previous studies have shown that burial of PyC by thick layer of sediment can preserve PyC rich soil C for over 12,000 years (Chaopricha & Marín-Spiotta 2014; Marin-Spiotta et al. 2014). However, the results from this investigation suggest that PyC deposited on the surface soil of depositional landform positions can breakdown much more rapidly than from eroding landform positions.

Additionally, laboratory soil incubations typically overestimate decay rates, as found in the field, due to more idealized conditions for decomposition and by isolating loss processes (Abney & Berhe In Prep). Furthermore, short-term incubations may overestimate decomposition rates of SOM and PyC by focusing on the early breakdown stages and priming that tend to be more rapid than later stages (Hamer 2004; Kuzyakov 2011; Whitman et al. 2014). It is possible that the addition of PyC, particularly in the 200°C PyC, is acting as a priming mechanism for the enhanced respiration in these soil and char mixtures. Future studies on the persistence of PyC should focus on the relative role of PyC charring temperature as a control on the respiration and stability of total C in the soil. It is likely that different soil C pools interact in ways that impact the stability of the overall soil C pool.

CONCLUSIONS

Overall, C and PyC from the same soil can have different environmental persistence, depending on charring temperature of the PyC and on the landform position where it is decomposing. In soil from the depositional landform position, the CO_2 flux was over three times that of those from the eroding landform positions. Soils amended with PyC formed at 200°C had significantly lower concentrations of PyC over the six-month incubation, while those amended with PyC formed at 350°C and 500°C did not significantly decline in PyC concentration. We found a two-pool decay

model provided the best explanation of the respiration of the soil and char treatment groups. The slow-cycling pool in the two-pool model, which we attribute the breakdown of PyC and soil C separately, suggested that PyC serves as a small, but slow-cycling pool in the soil C cycle. Higher temperature char decay rates were up to two times slower than those for the 200°C char. Altogether, we found that the breakdown of PyC is controlled by both charring temperature and landform position, due to the range in decomposition rates found in the same soil. Additionally, charring temperature can control both the properties of PyC that make it erosive, which in turn controls where PyC is redistributed throughout a landscape via erosion. Therefore, post-fire erosion acts as an important control on the long-term persistence of PyC in soil.

ACKNOWLEDGEMENTS

The authors gratefully acknowledge laboratory assistance from Bobby Nakamoto from the UC Merced Stable Isotope lab, Fernanda Santos, and Steve Hart for their assistance with elemental and isotope analyses, the KMD method, and gas chromatography analysis, respectively. The authors also acknowledge Jonathan Sanderman and Marilyn Fogel for comments on earlier versions of this manuscript. Funding for this work was provided from the National Science Foundation (CAREER EAR -1352627) award to A. A. Berhe.

REFERENCES

Abiven S, Hengartner P, Schneider MPW, Singh N, Schmidt MWI (2011) Pyrogenic carbon soluble fraction is larger and more aromatic in aged charcoal than in fresh charcoal. Soil Biology and Biochemistry 43(7): 1615-1617

Abney R, Berhe AA (In Prep) The role of soil erosion in lateral distribution of pyrogenic carbon. Biogeochemistry

Abney R, Kuhn T, Chow A, Hockaday W, Fogel M, Berhe A (In prep) Soil erosion controls pyrogenic carbon dynamics: the effect of fire severity and slope on pyrogenic carbon transport after the Rim Fire, Yosemite National Park

Adams LB, Hall CR, Holmes RJ, Newton RA (1988) An examination of how exposure to humid air can result in changes in the adsorption properties of activated carbons. Carbon 26(4): 451-459

Alexis M, Rumpel C, Knicker H, Leifeld J, Rasse D, Péchot N, Bardoux G, Mariotti A (2010) Thermal alteration of organic matter during a shrubland fire: a field study. Organic Geochemistry 41(7): 690-697

Araya S, Meding S, Berhe A (2016) Thermal alteration of soil physico-chemical properties: a systematic study to infer response of Sierra Nevada climosequence soils to forest fires. Soil 2(3): 351-366

Araya SN, Fogel ML, Berhe AA (2017) Thermal alteration of soil organic matter properties: a systematic study to infer response of Sierra Nevada climosequence soils to forest fires. Soil 3: 31-44

Beaty RM, Taylor AH (2008) Fire history and the structure and dynamics of a mixed conifer forest landscape in the northern Sierra Nevada, Lake Tahoe Basin, California, USA. Forest Ecology and Management 255(3): 707-719

Berhe AA (2012) Decomposition of organic substrates at eroding vs. depositional landform positions. Plant and Soil 350: 261-280

Berhe AA, Harden J, Torn M, Kleber M, Burton S, Harte J (2012) Persistence of Soil Organic Matter in Eroding vs. Depositional Landform Positions. Journal Of Geophysical Research-Biogeosciences 117, G02019, doi:10.1029/2011JG001790:

Berhe AA, Harden JW, Torn MS, Harte J (2008) Linking soil organic matter dynamics and erosion-induced terrestrial carbon sequestration at different landform positions. Journal of Geophysical Research-Biogeosciences 113: G4, DOI 10.1029/2008jg000751

Birch H (1958) The effect of soil drying on humus decomposition and nitrogen availability. Plant and Soil 10(1): 9-31

Bird MI, Wynn JG, Saiz G, Wurster CM, McBeath A (2015) The pyrogenic carbon cycle. Annual Review of Earth and Planetary Sciences 43: 273-298

Bouyoucos GJ (1962) Hydrometer method improved for making particle size analyses of soils. Agronomy Journal 54(5): 464-465

Bruun EW, Hauggaard-Nielsen H, Ibrahim N, Egsgaard H, Ambus P, Jensen PA, Dam-Johansen K (2011) Influence of fast pyrolysis temperature on biochar labile fraction and short-term carbon loss in a loamy soil. Biomass and Bioenergy 35(3): 1182-1189

Buma B, Poore RE, Wessman CA (2014) Disturbances, their interactions, and cumulative effects on carbon and charcoal stocks in a forested ecosystem. Ecosystems 17(6): 947-959

Carroll EM, Miller WW, Johnson DW, Saito L, Qualls RG, Walker RF (2007) Spatial analysis of a large magnitude erosion event following a Sierran Wildfire. Journal of environmental quality 36(4): 1105-1105

Chaopricha NT, Marín-Spiotta E (2014) Soil burial contributes to deep soil organic carbon storage. Soil Biology and Biochemistry 69: 251-264

Cheng C, Lehmann J, Thies J, Burton S, Engelhard M (2006) Oxidation of black carbon by biotic and abiotic processes. Organic Geochemistry 37(11): 1477-1488

Chia C, Munroe P, Joseph S, Lin Y, Lehmann J, Muller D, Xin H, Neves E (2012) Analytical electron microscopy of black carbon and microaggregated mineral matter in Amazonian dark Earth. Journal of microscopy 245(2): 129-139

Doetterl S, Six J, Van Wesemael B, Van Oost K (2012) Carbon cycling in eroding landscapes: geomorphic controls on soil organic C pool composition and C stabilization. Global Change Biology 18(7): 2218-2232

Famiglietti J, Rudnicki J, Rodell M (1998) Variability in surface moisture content along a hillslope transect: Rattlesnake Hill, Texas. Journal of Hydrology 210(1): 259-281

Foereid B, Lehmann J, Major J (2011) Modeling black carbon degradation and movement in soil. Plant and soil 345(1-2): 223-236

Hamer U (2004) Interactive priming of black carbon and glucose mineralisation. Organic Geochemistry 35(7): 823-830

Hammes K, Torn MS, Lapenas AG, Schmidt MWI (2008) Centennial black carbon turnover observed in a Russian steppe soil. Biogeosciences 5(5): 1339-1350

Hatten J, Zabowski D, Scherer G, Dolan E (2005) A comparison of soil properties after contemporary wildfire and fire suppression. Forest Ecology and Management 220(1): 227-241

Horwath W, Paul E (1994) Microbial biomass. In ‘Methods of soil analysis. Part 2. Microbiological and biochemical properties’.(Ed. RW Weaver) pp. 753–773. Soil Science Society of America: Madison, WI:

Horwath WR, Paul EA, Harris D, Norton J, Jagger L, Horton KA (1996) Defining a realistic control for the chloroform fumigation-incubation method using microscopic counting and 14C-substrates. Canadian Journal of Soil Science 76(4): 459-467

Janik LJ, Merry RH, Skjemstad JO (1998) Can mid infrared diffuse reflectance analysis replace soil extractions? Australian Journal of Experimental Agriculture 38(7): 681-696

Johnson D, Murphy J, Walker R, Glass D, MILLER W (2007) Wildfire effects on forest carbon and nutrient budgets. Ecological Engineering 31(3): 183-192

Kupryianchyk D, Hale S, Zimmerman AR, Harvey O, Rutherford D, Abiven S, Knicker H, Schmidt H-P, Rumpel C, Cornelissen G (2016) Sorption of hydrophobic organic compounds to a diverse suite of carbonaceous materials with emphasis on biochar. Chemosphere 144: 879-887

Kurth VJ, MacKenzie MD, DeLuca TH (2006) Estimating charcoal content in forest mineral soils. Geoderma 137(1): 135-139

Kuzyakov Y (2011) How to link soil C pools with CO2 fluxes? Biogeosciences 8(6): 1523

Kuzyakov Y, Bogomolova I, Glaser B (2014) Biochar stability in soil: decomposition during eight years and transformation as assessed by compound-specific 14 C analysis. Soil Biology and Biochemistry 70: 229-236

Kuzyakov Y, Subbotina I, Chen H, Bogomolova I, Xu X (2009) Black carbon decomposition and incorporation into soil microbial biomass estimated by C-14 labeling. Soil Biology and Biochemistry 41(2): 210-219

Lehmann J (2007) Bio-energy in the black. Frontiers in Ecology and the Environment 5(7): 381–387

Liang B, Lehmann J, Sohi SP, Thies JE, O'neill B, Trujillo L, Gaunt J, Solomon D, Grossman J, Neves EG (2010) Black carbon affects the cycling of non-black carbon in soil. Organic Geochemistry 41(2): 206-213

Major J, Lehmann J, Rondon M, Goodale C (2010) Fate of soil‐applied black carbon: downward migration, leaching and soil respiration. Global Change Biology 16(4): 1366-1379

Marin-Spiotta E, Chaopricha NT, Plante AF, Diefendorf AF, Mueller CW, Grandy AS, 1–5. JAM (2014) Long-Term Stabilization of Deep Soil Carbon by Fire and Burial During Early Holocene Climate Change. Nature Geoscience 7(6): 428

Masiello C (2004) New directions in black carbon organic geochemistry. Marine Chemistry 92(1-4): 201-213

Massman WJ, Frank JM, Mooney SJ (2010) Advancing investigation and physical modeling of first-order fire effects on soils. Fire Ecology 6(1): 36-54

Mimmo T, Panzacchi P, Baratieri M, Davies C, Tonon G (2014) Effect of pyrolysis temperature on miscanthus (Miscanthus× giganteus) biochar physical, chemical and functional properties. Biomass and Bioenergy 62: 149-157

Nguyen BT, Lehmann J (2009) Black carbon decomposition under varying water regimes. Organic Geochemistry 40(8): 846-853

Nguyen BT, Lehmann J, Hockaday WC, Joseph S, Masiello CA (2010) Temperature sensitivity of black carbon decomposition and oxidation. Environmental science & technology 44(9): 3324-3331

Novak JM, Busscher WJ, Laird DL, Ahmedna M, Watts DW, Niandou MA (2009) Impact of biochar amendment on fertility of a southeastern coastal plain soil. Soil science 174(2): 105-112

Papiernik S, Schumacher T, Lobb D, Lindstrom M, Lieser M, Eynard A, Schumacher J (2009) Soil properties and productivity as affected by topsoil movement within an eroded landform. Soil and tillage research 102(1): 67-77

Parton WJ, Schimel DS, Cole C, Ojima D (1987) Analysis of factors controlling soil organic matter levels in Great Plains grasslands. Soil Science Society of America Journal 51(5): 1173-1179

Pereira P, Cerdà A, Úbeda X, Mataix‐Solera J, Arcenegui V, Zavala L (2015) Modelling the impacts of wildfire on ash thickness in a short‐term period. Land Degradation & Development 26(2): 180-192

Pierson FB, Robichaud PR, Moffet CA, Spaeth KE, Hardegree SP, Clark PE, Williams CJ (2008) Fire effects on rangeland hydrology and erosion in a steep sagebrush‐dominated landscape. Hydrological Processes 22(16): 2916-2929

Pyle LA, Hockaday WC, Boutton T, Zygourakis K, Kinney TJ, Masiello CA (2015) Chemical and isotopic thresholds in charring: implications for the interpretation of charcoal mass and isotopic data. Environmental science & technology 49(24): 14057-14064

Rumpel C, Chaplot V, Planchon O, Bernadou J, Valentin C, Mariotti A (2006) Preferential erosion of black carbon on steep slopes with slash and burn agriculture. CATENA 65(1): 30-40

Rumpel C, Leifeld J, Santin C, Doerr S (2015) Movement of biochar in the environment. Biochar for Environmental Management: Science, Technology and Implementation (second edition). New York: Routledge: 283-298

Santos F, Torn MS, Bird JA (2012) Biological degradation of pyrogenic organic matter in temperate forest soils. Soil Biology and Biochemistry 51: 115-124

Sarkhot DV, Berhe AA, Ghezzehei TA (2012) Impact of Biochar Enriched with Dairy Manure Effluent on Carbon and Nitrogen Dynamics. Journal of Environment Quality doi:10.2134/jeq2011.0123:

Schmidt MWI, Torn MS, Abiven S, Dittmar T, Guggenberger G, Janssens IA, Kleber M, Kogel-Knabner I, Lehmann J, Manning DAC, Nannipieri P, Rasse DP, Weiner S, Trumbore SE (2011) Persistence of soil organic matter as an ecosystem property. Nature 478(7367): 49-56

Skjemstad J, Taylor J, Smernik R (1999) Estimation of charcoal (char) in soils. Communications in Soil Science & Plant Analysis 30(15-16): 2283-2298

Spokas K, Novak J, Masiello C, Johnson M, Colosky E, Ippolito J, Trigo C (2014) Physical disintegration of biochar: an overlooked process. Environmental Science & Technology Letters 1: 326-332

Sutherland E (2001) Terminology and biology of fire scares in selected central hardwoods. Tree-ring research 57(2): 141-147

Whitman TL, Zhu Z, Lehmann J (2014) Carbon mineralizability determines interactive effects on mineralization of pyrogenic organic matter and soil organic carbon. Environmental Science & Technology, 48(23): 13727-13734

Wiedemeier DB, Abiven S, Hockaday WC, Keiluweit M, Kleber M, Masiello CA, McBeath AV, Nico PS, Pyle LA, Schneider MP (2014) Aromaticity and degree of aromatic condensation of char. Organic Geochemistry 78: 135-143

Wiedemeier DB, Abiven S, Hockaday WC, Keiluweit M, Kleber M, Masiello CA, McBeath AV, Nico PS, Pyle LA, Schneider MP (2015) Aromaticity and degree of aromatic condensation of char. Organic Geochemistry 78: 135-143

Yao J, Hockaday WC, Murray DB, White JD (2014) Changes in fire‐derived soil black carbon storage in a subhumid woodland. Journal of Geophysical Research: Biogeosciences 119(9): 1807-1819

Zimmerman A (2010) Abiotic and microbial oxidation of laboratory-produced black carbon (biochar). Environmental Science & Technology 44(4): 1295-1301

Zimmerman AR, Gao B, Ahn M-Y (2011) Positive and negative carbon mineralization priming effects among a variety of biochar-amended soils. Soil Biology and Biochemistry 43(6): 1169-1179

Zimmermann M, Bird MI, Wurster C, Saiz G, Goodrick I, Barta J, Capek P, Santruckova H, Smernik R (2012) Rapid degradation of pyrogenic carbon. Global Change Biology 18(11): 3306-3316

FIGURES

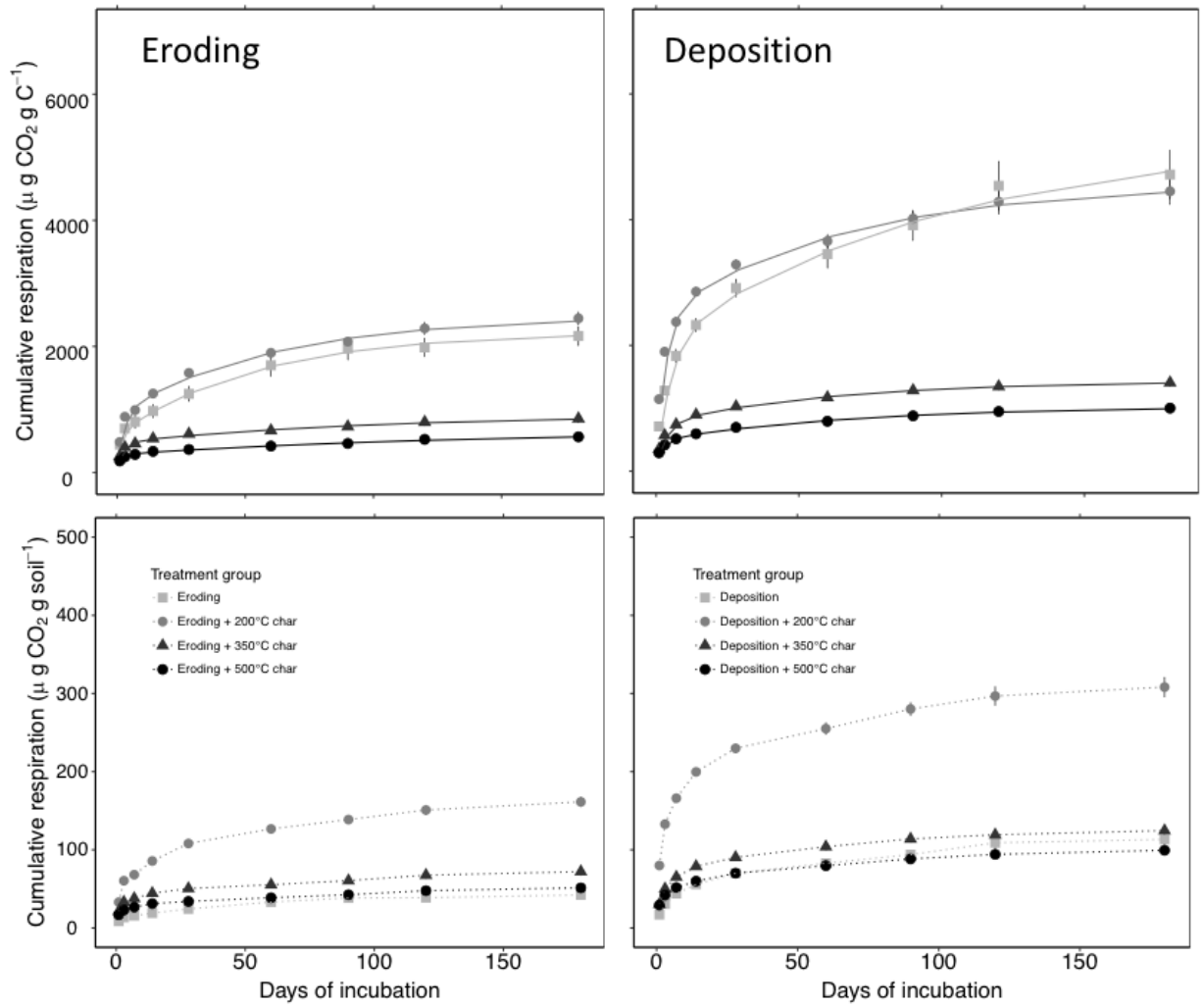

Figure 5-1. Cumulative respiration throughout the six-month incubation by treatment group was calculated by g soil and char in the mixture (top row) and by g C in the mixture (bottom row). Error bars represent standard error with n=16 for days 0-14, n=12 for days 13-60, n=8 for days 61-120, and n=4 for days 121-180. Fitted cumulative respiration curves for the per g C calculations are plotted through the data points.

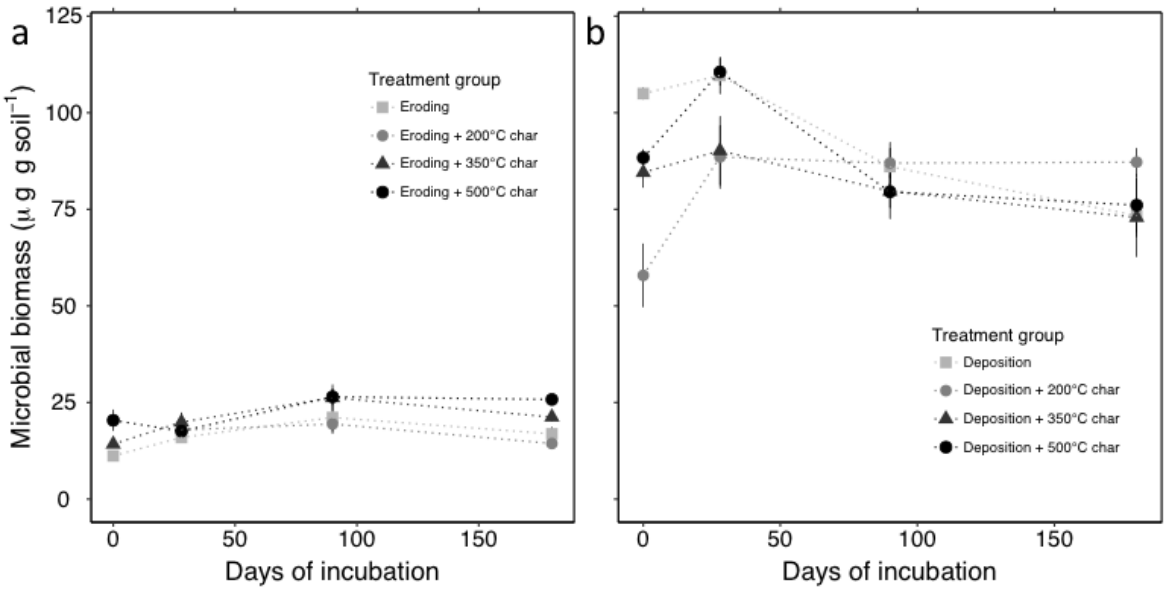

Figure 5-2. Microbial biomass in the eroding (a) and depositional (b) soil and char treatment groups. Microbial biomass was determined using chloroform fumigation incubation (Horwath & Paul 1994) biomass was calculated using an approach from Horwath et al. (1996). Error bars represent standard error with n=4.

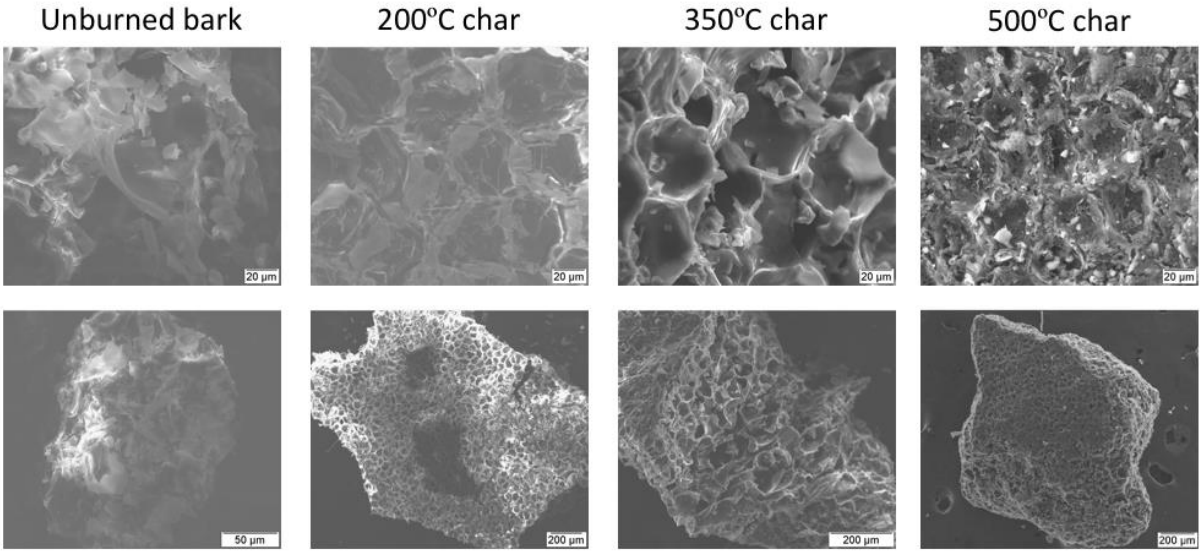

Figure 5-3. SEM images of unburned bark and chars formed at 200ºC, 350ºC, and 500ºC. The top row of SEM images was taken at 750x magnification, and the bottom row was taken at 150x magnification, except for the unburned bark, which was taken at 527x magnification.

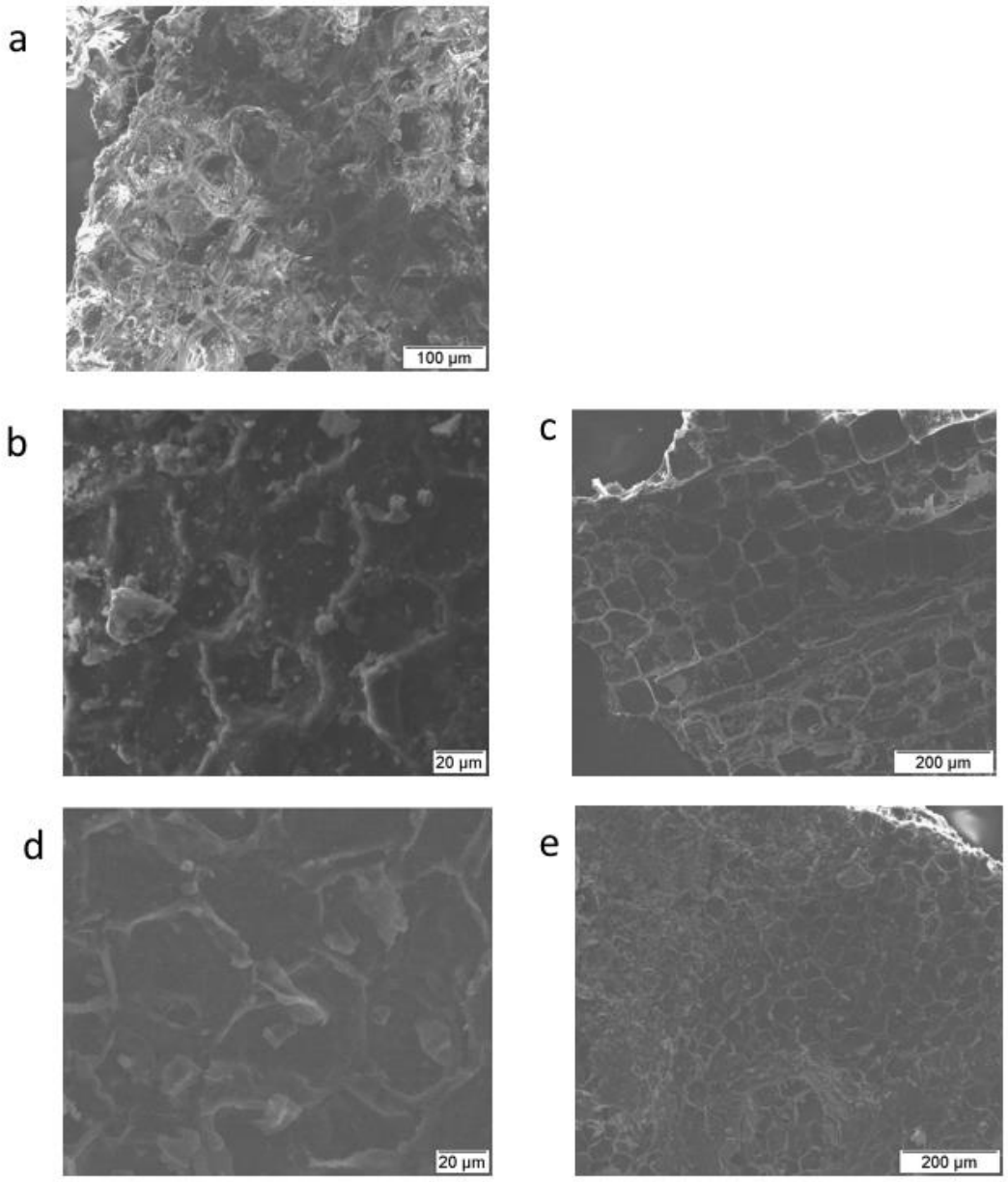

Figure 5-4. SEM images of post-incubation char from 200C char (a) 350C char (b, c) and 500C char (d, e). Images b and e were taken at 750x magnification, and images c and e were taken at 150x magnification. Image a was taken at 248x magnification.

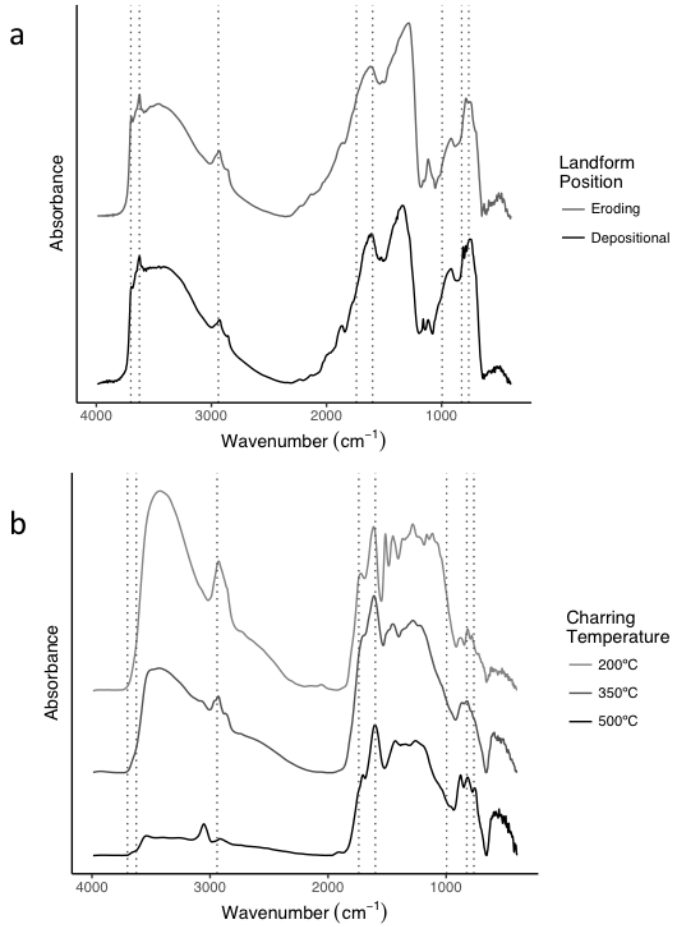

c

Absorption peaks (cm^{-1})	Peak assignment	Functional groups
765, 825	C-H, C-O	Aryl
995	C-OH, C-O-C	Ester, phenol
1600	C=C	Carboxyl
1740	C=O	Ketones, carbonyl
2940	-CH	Methyl
3625, 3700	O-H	Hydroxyl

Figure 5-5. FTIR spectra of the soil sample from eroding and depositional landform positions (a) and of the bark charred at three different temperatures (b). Absorption peak assignments (c) were adapted from Araya et al. (2017).

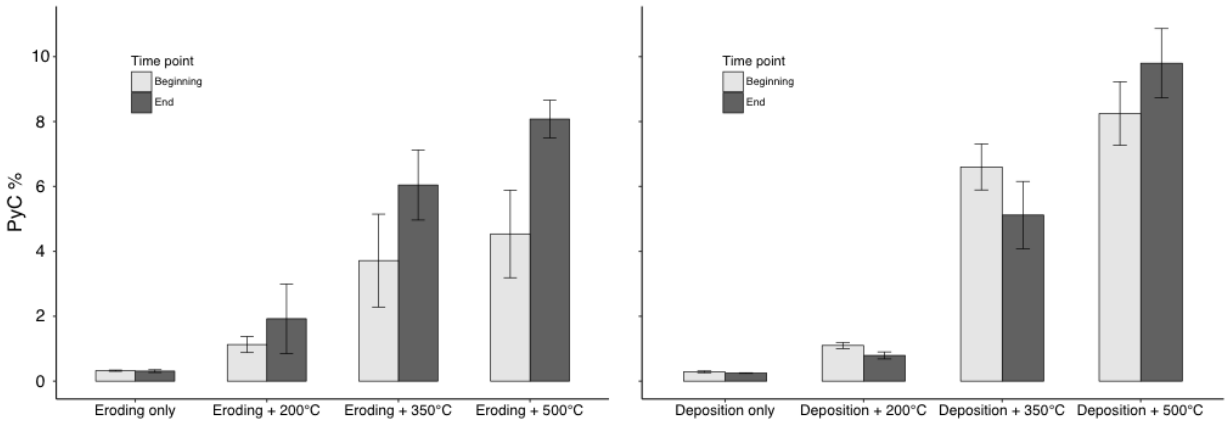

Figure 5-6. PyC content of the eroding (a) and depositional (b) soil and char mixtures was analyzed at the beginning and end time points of the incubation using Kurth MacKenzie Deluca method (Kurth et al. 2006). Error bars indicate standard error with n=4.

TABLES

Table 5-1. Chemical properties of charred bark prior to incubation. Concentration of PyC was determined using the Kurth Mackenzie Deluca approach, and the pH was measured in a 1:2 char to water ratio. Means are presented here with standard error in parentheses (n=3).

Charring temperature	**pH**	**%C**	**%N**	**δ^{13}C (‰)**	**δ^{15}N (‰)**	**PyC %**
200°C	3.52 (0.00)	54.62 (1.67)	0.14 (0.01)	-24.88 (0.04)	-13.20 (0.33)	11.1
350°C	5.03 (0.41)	72.33 (0.08)	0.20 (0.00)	-25.23 (0.03)	-8.50 (0.58)	17.7
500°C	7.78 (0.17)	85.15 (0.14)	0.19 (0.00)	-25.53 (0.01)	-9.34 (0.59)	67.0

Table 5-2. Pre-incubation soil chemical and physical properties. Means are presented here with standard error in parentheses (n=3).

Landform position	pH	Field capacity GWC %	%C	%N	δ^{15}N ‰	δ^{13}C ‰	Sand %	Silt %	Clay %
Eroding	6.44 (0.04)	8.31 (0.12)	1.95 (0.12)	0.05 (0.00)	1.18 (0.18)	-26.07 (0.02)	92.05 (0.39)	5.81 (0.46)	2.12 (0.66)
Depositional	6.41 (0.00)	20.06 (0.14)	2.40 (0.08)	0.09 (0.00)	2.59 (0.13)	-24.55 (0.04)	84.65 (0.39)	10.46 (0.48)	4.88 (0.09)

Table 5-3. Cumulative CO_2 flux for first two weeks and six months of incubation. Cumulative flux was calculated by summing flux measurements. Standard error for the estimation is presented in parentheses (n=12 for first two weeks and n=4 for six months).

	Cumulative CO_2 flux for first two weeks		**Cumulative CO_2 flux for entire incubation (six months)**	
Treatment group	**mg CO_2-C/kg C**	**mg CO_2-C/kg soil**	**mg CO_2-C/kg C**	**mg CO_2-C/kg soil**
Eroding soil only	975 (106)	19 (2)	2164 (150)	42 (2)
Eroding + 200°C char	1253 (59)	85 (4)	2445 (100)	161 (5)
Eroding + 350°C char	538 (28)	44 (2)	854 (62)	72 (4)
Eroding + 500°C char	335 (15)	31 (1)	566 (30)	51 (3)
Depositional soil only	2324 (105)	55 (2)	4718 (387)	113 (9)
Depositional + 200°C char	2855 (68)	199 (4)	4451 (209)	308 (12)
Depositional + 350°C char	897 (24)	78 (1)	1407 (58)	124 (3)
Depositional + 500°C char	595 (11)	59 (1)	1002 (26)	99 (2)

Table 5-4. Single and double pool exponential decay models (Equations 1 and 2, respectively) were fitted to cumulative respiration per g carbon data from each treatment group (standard error in parentheses, n=16). In the single pool model, C_0 is the initial C pool (µg C) and k is the day^{-1} loss constant. In the double pool model, C_0 and C_1 are the initial fast and slow cycling pools (µg C), and k_0 and k_1 are the day^{-1} constants for the fast and slow pools, respectively. Adjusted r^2 were calculated for each model, and * indicate non-significant parameters in the model ($p>0.05$). Akaike information criterion (AIC) was used to compare fit between the two models on each treatment group.

	Single pool model				**Double pool model**					
Treatment group	**C_0**	**k**	**Adj r^2**	**AIC**	**C_0**	**k_0**	**C_1**	**k_1**	**Adj r^2**	**AIC**
Depositional soil only	3920 (114)	0.005 (0.060)	0.58	1364	2025 (272)	0.197 (0.040)	3320 (550)	0.009 (0.004)	0.89	1323
Depositional + 200°C char	3731 (71)	0.137 (0.009)	0.84	1317	2453 (140)	0.296 (0.029)	2128 (162)	0.015 (0.003)	0.94	1231
Depositional + 350°C char	1191 (23)	0.126 (0.008)	0.84	1118	755 (52)	0.284 (0.033)	682 (51)	0.016 (0.004)	0.93	1043
Depositional + 500°C char	803 (16)	0.144 (0.010)	0.79	1066	486 (17)	0.406 (0.033)	546 (25)	0.014 (0.002)	0.96	903
Eroding soil only	1877 (85)	0.056 (0.007)	0.63	1303	598 (13)	0.570 (0.312)	1633 (168)	0.018 (0.006)	0.73	1277
Eroding + 200°C char	2018 (51)	0.081 (0.006)	0.82	1208	935 (84)	0.350 (0.058)	1551 (94)	0.016 (0.003)	0.93	1126
Eroding + 350°C char	672 (17)	0.182 (0.017)	0.67	1081	473 (33)	0.380 (0.058)	444 (99)	0.010 (0.005)*	0.81	1035
Eroding + 500°C char	419 (42)	0.194 (0.021)	0.57	1023	285 (18)	0.472 (0.077)	381 (115)	0.007 (0.004)*	0.79	962

CHAPTER 6: CONCLUSION

SUMMARY

This dissertation has demonstrated how erosion and fire can interactively control the soil carbon (C) cycle overall, and specifically soil C storage in fire-prone ecosystems in the Sierra Nevada. While elevated erosion rates have been widely reported post-fire (Pierson *et al.* 2008), rates of pyrogenic carbon (PyC) erosion are generally unknown. The subject of whether PyC is likely to be preferentially eroded after fires has been a topic of interest in the biogeochemistry community (Boot *et al.* 2015, Cotrufo *et al.* 2016, Nguyen *et al.* 2008, Rumpel *et al.* 2009, Rumpel *et al.* 2006). My dissertation research demonstrates that fire and erosive conditions play a major role in controlling the amount and timing of PyC erosion. The research presented here has identified charring temperature and precipitation timing as major controls of post-fire erosion of PyC. Furthermore, the location that the PyC is deposited after erosion can significantly control its stabilization or eventual breakdown in soil. Overall, I found that the interaction of combustion intensity and landform position is a critical control of the persistence of PyC in soil.

Below, I briefly summarize the main take away messages from each of my dissertation chapters.

Chapter 1: *Pyrogenic carbon erosion: implications for persistence of pyrogenic carbon in the soil system*

In the first chapter, loss processes of PyC from soil were collected into a global box model, which demonstrated that by ignoring the role of erosion and burial of PyC, we are missing a considerable source and sink of PyC in the soil system. By using a single-pool exponential decay model to test the effect of including erosion in loss constants as both a loss (erosion) and gain (deposition) from soil, there was a 200 g/m^2 difference in PyC stock after 100 years between eroding and depositional landform positions. This model was further tested to assess the impact of including erosion as a loss factor into turnover time calculations. Accounting for erosional loss and depositional input of PyC into different landform positions led to a difference in 150 years in turnover time of PyC at eroding vs. depositional landform positions. The chapter concluded that erosion is a critical variable that controls PyC cycling in soil.

Chapter 2: *Wildfire and post-fire erosion in mountainous terrain lead to rapid and major redistribution of soil organic carbon fractions*

The Gondola Fire was a moderate severity wildfire that burned a hillslope near South Lake Tahoe, NV. Two weeks after the fire, a major precipitation event instigated an ash flow that transported 7.5 Mg C and 2 Mg PyC from the eroding hillslope into a downslope depositional landform position. The upslope soils did not lose significant proportions of any of the soil organic carbon (SOC) components one- or ten-years post-fire. However, there was stable isotope (i.e., ^{13}C and ^{15}N) evidence for leaching of fresh SOC down into the soil profile of the burned hillslope.

In the depositional landform position, the input of SOC fractions and PyC after the initial erosion events increased the concentration of C in particulate, humic, and resistant organic C fractions (representing fresh particulate, decomposed, and charred OC) one-year post-fire. However, ten-years post-fire, the concentrations of SOC in all fractions was lower than pre-fire concentrations. The eroded material that was deposited downslope appears to have been have been lost via enhanced decomposition due to high nutrient and water availability (Johnson *et al.* 2007), or buried by subsequent deposition of eroded topsoil material from the upslope positions (Berhe *et al.* 2007). This study provides evidence for the rapid mobilization of SOC fractions after the first-year post-fire into landform positions that may have considerably different decomposition conditions than those that the PyC originated. This study highlights the importance of considering erosion as a control on the distribution and persistence of PyC in a dynamic landscape.

Chapter 3: *Soil erosion controls pyrogenic carbon dynamics: the effect of fire severity and slope on pyrogenic carbon transport after the Rim Fire, Yosemite National Park*

After the Rim Fire, the rate and quality of eroded sediment from the burned hillslopes was monitored for the first four major precipitation events. The sediment eroded from high severity burn classification groups was enriched in PyC compared with source soils. However, the moderate burn severity classification group was enriched in total C and N, but not PyC. The sediments from the moderate burn severity plots had significantly more coarse fraction transport than the high burn severity plots, resulting from the post-fire needle drop in the standing vegetation. This needle drop served as a continual input of organic matter into the soil and sediments, which was reflected in spectroscopic analyses of the sediments and soils.

The selective enrichment of PyC in high burn severity treatment groups indicates that high burn severity char is more erosive than lower severity char, which may have significant implications for its environmental persistence. Over the course of this study, there was no significant change in the concentration of PyC in the eroded sediment, which also indicates that erosional transport of PyC is an ongoing process that likely serves as a significant loss pathway for PyC from soil in dynamic landscapes.

Chapter 4: *Landform position and combustion temperature control decomposition of pyrogenic organic matter*

In this laboratory study, decomposition rates were determined for bark that was charred at three temperatures and incubated in soils from both eroding and depositional landform positions. Overall, the decomposition rates were significant higher in depositional landform positions, and the 200 °C char decomposed at rates two times faster than higher temperature chars. A two-pool exponential decay model fit the respiration of the soil and char treatment groups better than a one-pool model, which was a better fit for the microbial respiration data from soil only treatment groups. The addition of char equated to the addition of a slow-cycling C pool, which was lost at a rate three orders of magnitude slower than the fast-cycling C pool. However, the breakdown of higher temperature chars was not significant in this study, in that there was no change in their concentration in soil after the six-month incubation. By illustrating the role of landform position in controlling the

decomposition of PyC on surface soils, this study demonstrated the importance of erosion as a control on PyC loss or stabilization in soil.

FUTURE DIRECTIONS

Some critical questions remain unanswered about the magnitude of loss processes controlling the persistence of PyC in soil. Firstly, what is the role of burn severity in controlling the magnitude of PyC erosion in differing landscapes and soil types? Sierra Nevada hillslopes are highly erosive, and the sites in the Gondola and Rim Fire studies were selected in backslope positions. It is likely that different landform positions and slope gradations may act to enhance or slow PyC erosion rates. Secondly, the longer-term export of PyC in individual erosion events needs further investigation. While PyC was preferentially transported in the high burn severity classification groups after the Rim Fire, this enrichment was only monitored during the first-year post-fire. It is likely that this enrichment would decline over time, as a function of both limited supply of PyC available for erosion and breakdown of PyC in eroding landform positions. Thirdly, it remains unknown if eroded PyC is more susceptible to subsequent erosion events, or what landscape-scale mechanisms act to retain PyC within a hillslope. Understanding the processes associated with the redistribution PyC throughout a landscape is necessary for quantifying stabilization of PyC, as this research demonstrated that decomposition rates of PyC differ based on the landform position.

The role of leaching of PyC within a landscape is relatively unexplored, and the current research suggests that this flux may be as small as 1% or less of the PyC at the soil surface is leached into the soil profile over the course of a year (Major *et al.* 2010). So, leaching is not likely responsible for the transfer of PyC from terrestrial to aquatic systems that could account for the documented large flux of PyC from rivers to oceans (Jaffé *et al.* 2013). So our current understanding of the connection between dissolved PyC in soil water and that in the aquatic system remains incomplete (Bird *et al.* 2015), and much of this flux is likely a product of erosional transport of PyC.

SYNTHESIS AND FINAL CONCLUSIONS

Altogether, my dissertation research highlights the importance of including erosion as a loss process of PyC and landform position as a control over the decomposition of PyC, each of which impact the fate of PyC in soil. My work shows that the interaction of fire and erosion can lead to important feedbacks in PyC cycling.

Many of the impacts of wildfire on soil, such as the addition of PyC to soil and post-fire erosion, depend on local-scale environmental conditions (Figure 1). For example, in the case of a high severity wildfire, higher rates of erosion drive transport of highly charred material, which can lead it to be deposited in downslope landform positions with considerably higher rates of decomposition. In this scenario, on the landscape scale, there may be greater transport of both particulate and dissolved PyC into the soil profile via leaching and into downslope landform positions or to the aquatic system via erosion or dissolution. Some of this vertical transport of PyC into the soil profile may be facilitated by the breakdown of the hydrophobic layer with high charring temperatures, and

breakdown of soil structure (Massman *et al.* 2010), each of which may lead to higher rates of infiltration as opposed to surface runoff.

In contrast, after low and moderate severity wildfires, post-fire erosion rates may be moderately enhanced to formation of a hydrophobic layer that can increase post-fire runoff (DeBano 2000). The higher levels of hydrophobicity post-fire may also lead to relatively little leaching of PyC down into the soil profile. In these lower severity wildfires, PyC is likely not preferentially eroded, or eroded at concentrations lower than in higher severity wildfires. The PyC in this scenario is more likely to remain where is was formed, and to decompose *in situ*. This low to moderate temperature PyC should decompose faster than the PyC formed at higher temperatures.

Between these two burn severity scenarios, the interaction of landform position and charring temperature add complexity in describing and predicting soil PyC and C stocks on the landscape scale. High burn severity PyC in depositional landform positions may breakdown at the same rate as low burn severity PyC in eroding landform positions, but this depends on whether the landform position and charring temperature interact additively or in non-linear or surprising ways. Future research should focus on the landscape-scale variation in PyC controls and the interactions between them.

While this research did not explicitly investigate the role of burial PyC persistence, the burial of PyC post-deposition is likely to change its fate as burial can act as a long-term stabilization mechanism for PyC (Chaopricha & Marín-Spiotta 2014, Marin-Spiotta *et al.* 2014), enabling PyC to persist for millennia. In environments not impacted by fire, the role of erosion and subsequent burial of C-rich material in depositional landform positions has been demonstrated to serve as a C sink of 0.72 Gt C globally (Berhe *et al.* 2007). Soils store 54-109 Gt PyC (Bird *et al.* 2015), which accounts for 2.6-5.4% of the reported 2011 Gt C in the global soils (IPCC 2013). If this is scaled to the amount of PyC buried, then there is likely 17-38 Mt of PyC buried per year during erosion events. However, the preferential erosion of PyC likely means that this is an underestimate of buried PyC. The overall longer persistence times of PyC in soil compared with non-pyrogenic C suggest that the erosional burial of PyC could serve as a very slow-cycling component of the soil C pool, that begs accurate quantification.

The burial and use of PyC in the form of biochar, or man-made PyC, has received recent attention for its potential to serve as an agricultural amendment that increases the C storage of soil (Lehmann 2007), along with increasing crop productivity, cation exchange capacity, and soil nutrient retention (Biederman & Harpole 2013, Jones *et al.* 2012, Lehmann & Joseph 2015). One of the problems associated with the use of biochar is its highly erodible nature (Rumpel *et al.* 2015), which can mean that after it is applied, it may not persist long enough in the soil to provide the intended benefits. Depending on the aims for applying biochar to soil, it may be beneficial to apply moderate or higher temperature biochar to help retain soil nutrients and enhance soil C. Although, since this material is highly erosive, measures should be taken to prevent its loss from soil and to allow it to be an effective soil amendment. Producing biochar at lower to moderate temperatures may also allow for this increased soil productivity while reducing some of the erosive properties of the biochar.

Accurate and quantitative understanding of the mechanisms that act to stabilize or mobilize PyC from the soil is critical for a broad range of stakeholders, including agricultural users, fire-impacted land managers, and soil C modelers alike. By better understanding the complex relationships between the effects of fire severity and dynamics landscapes, management strategies can be implemented to increase soil productivity and C storage.

FIGURE

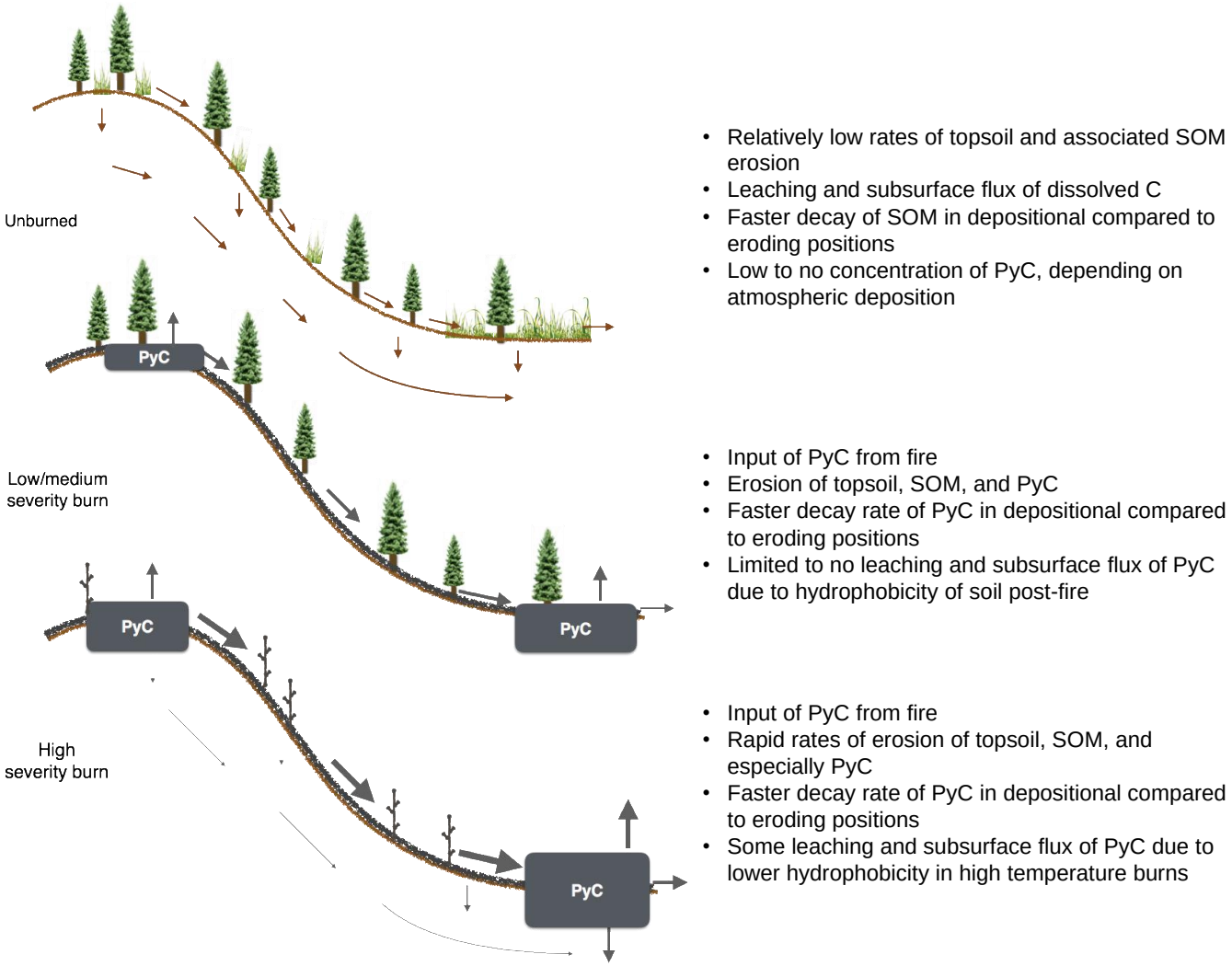

Figure 6-1. Erosion and persistence of pyrogenic carbon and soil organic matter in unburned, low/medium severity burn, and high severity burn hillslopes.

REFERENCES

Berhe AA, Harte J, Harden JW, Torn MS (2007) The Significance of Erosion-Induced Terrestrial Carbon Sink. BioScience 57(4): 337-346

Biederman LA, Harpole WS (2013) Biochar and its effects on plant productivity and nutrient cycling: a meta-analysis. GCB Bioenergy 5(2): 202-214

Bird MI, Wynn JG, Saiz G, Wurster CM, McBeath A (2015) The pyrogenic carbon cycle. Annual Review of Earth and Planetary Sciences 43: 273-298

Boot C, Haddix M, Paustian K, Cotrufo M (2015) Distribution of black carbon in ponderosa pine forest floor and soils following the High Park wildfire. Biogeosciences 12(10): 3029-3039

Chaopricha NT, Marín-Spiotta E (2014) Soil burial contributes to deep soil organic carbon storage. Soil Biology and Biochemistry 69: 251-264

Cotrufo MF, Boot CM, Kampf S, Nelson PA, Brogan DJ, Covino T, Haddix ML, MacDonald LH, Rathburn S, Ryan-Bukett S (2016) Redistribution of pyrogenic carbon from hillslopes to stream corridors following a large montane wildfire. Global Biogeochemical Cycles 30(9): 1348-1355

DeBano L (2000) The role of fire and soil heating on water repellency in wildland environments: a review. Journal of Hydrology 231: 195-206

IPCC (2013) Climate Change 2013: The Physical Science Basis, Working Group I Contribution to the Fifth Assessment Report of the Intergovernmental Panel on Climate Change. Summary for Policymakers. In: Stocker TF, Qin D, Plattner G-K, Tignor M, Allen SK, Boschung J, Nauels A, Xia Y, Bex V & Midgley PM (eds). Cambridge, United Kingdon and New York, NY, USA. p 1-30

Jaffé R, Ding Y, Niggemann J, Vähätalo AV, Stubbins A (2013) Global Charcoal Mobilization from Soils via Dissolution and Riverine Transport to the Oceans. Science:

Johnson D, Murphy J, Walker R, Glass D, Miller W (2007) Wildfire effects on forest carbon and nutrient budgets. Ecological Engineering 31(3): 183-192

Jones D, Rousk J, Edwards-Jones G (2012) Biochar-mediated changes in soil quality and plant growth in a three year field trial. Soil Biology and Biochemistry 45: 113-124

Lehmann J (2007) Bio-energy in the black. Frontiers in Ecology and the Environment 5(7): 381–387

Lehmann J, Joseph S (2015) Biochar for environmental management: science, technology and implementation. Routledge.

Major J, Lehmann J, Rondon M, Goodale C (2010) Fate of soil-applied black carbon: downward migration, leaching and soil respiration. Global Change Biology 16(4): 1366-1379

Marin-Spiotta E, Chaopricha NT, Plante AF, Diefendorf AF, Mueller CW, Grandy AS, 1–5. JAM (2014) Long-Term Stabilization of Deep Soil Carbon by Fire and Burial During Early Holocene Climate Change. Nature Geoscience 7(6): 428

Massman WJ, Frank JM, Mooney SJ (2010) Advancing investigation and physical modeling of first-order fire effects on soils. Fire Ecology 6(1): 36-54

Nguyen BT, Lehmann J, Kinyangi J, Smernik R, Riha SJ, Engelhard MH (2008) Long-term black carbon dynamics in cultivated soil. Biogeochemistry 89(3): 295-308

Pierson FB, Robichaud PR, Moffet CA, Spaeth KE, Hardegree SP, Clark PE, Williams CJ (2008) Fire effects on rangeland hydrology and erosion in a steep sagebrush-dominated landscape. Hydrological Processes 22(16): 2916-2929

Rumpel C, Ba A, Darboux F, Chaplot V, Planchon O (2009) Erosion budget and process selectivity of black carbon at meter scale. Geoderma 154(1): 131-137

Rumpel C, Chaplot V, Planchon O, Bernadou J, Valentin C, Mariotti A (2006) Preferential erosion of black carbon on steep slopes with slash and burn agriculture. CATENA 65(1): 30-40

Rumpel C, Leifeld J, Santin C, Doerr S (2015) Movement of biochar in the environment. Biochar for Environmental Management: Science, Technology and Implementation (second edition). New York: Routledge: 283-298